NTRCI

NATIONAL TRANSPORTATION RESEARCH CENTER, INCORPORATED
University Transportation Center

U26: Enhanced Finite Element Analysis Crash Model of Tractor-Trailers (Phase C)

Charles R. Miele, P.E. (Principal Investigator) – Battelle
Chuck Plaxico, Ph.D. – Roadsafe LLC
Denny Stephens, Ph.D., PMP (Program Manager) – Battelle
Srdjan Simunovic, Ph.D. – University of Tennessee

September, 2010

Technical Report Documentation Page

1. Report No.	2. Government Accession No.	3. Recipient's Catalog No.

4. Title and Subtitle	5. Report Date
U26: Enhanced Finite Element Analysis Crash Model of Tractor-Trailers (Phase C)	**September 2010**
	6. Performing Organization Code

7. Author(s)	8. Performing Organization Report No.
Charles R. Miele, P.E., Denny Stephens, Ph.D., PMP – Battelle; **Chuck Plaxico – Roadsafe LLC; Srdjan Simunovic – The University of Tennessee**	

9. Performing Organization Name and Address	10. Work Unit No. (TRAIS)
National Transportation Research Center, Inc. **University Transportation Center** **2360 Cherahala Blvd.** **Knoxville, TN 37932**	
	11. Contract or Grant No. **RITA Grant – DTRT06G-0043** **FHWA Purchase Order - DTFH61-07-P-00235**

12. Sponsoring Agency Name and Address	13. Type of Report and Period Covered
U.S. Department of Transportation **Research and Innovative Technology Administration and Federal Highway Administration** **1200 New Jersey Avenue, SE** **Washington, DC 20590**	**Final Report October 2009 – September 2010**
	14. Sponsoring Agency Code **RITA/FHWA**

15. Supplementary Notes

16. Abstract

NTRCI sponsored the research team of Battelle, Oak Ridge National Laboratory (ORNL) and the University of Tennessee at Knoxville (UTK) to conduct a three-phase investigation to enhance and refine a FE model for simulating tractor-semitrailer crash events involving roadside safety hardware such as bridge rails and median barriers. This report documents the work completed in the third phase of the project. The objective of this investigation led by Battelle was to validate and enhance computer models of a tractor-semitrailer combination for use in analysis, design, and evaluation of roadside safety hardware.

The work completed during this project phase involved:
- Continued enhancements of the tractor and semitrailer model,
- Validation of the model by comparing model results to two full-scale tractor-semitrailer crash tests, and
- Development of an interactive graphics based on-line user manual and FE model website.

The tractor-semitrailer vehicle FE model developed in this project is the most advanced of this vehicle class in terms of physical function, geometric detail and material property accuracy. The model is computationally very robust given its complexity. It has been extensively debugged and exercised hundreds of times for the cases within the range of NCHRP Report 350 TL-5 speeds and impact angles. The model is reasonably accurate and may be used by the engineering community to design and develop roadside safety hardware that will improve overall safety of the travelling public. The model is available for download at http://www.ntrci.org.

17. Key Word	18. Distribution Statement
Finite Element Model, Tractor-Semitrailer, Crash Analysis, LS-DYNA, FHWA Qualification Tests, Test Level 5, TL5, NCHRP Report 350, Model Validation, Computer Simulation	**No restrictions**

19. Security Classif. (of this report)	20. Security Classif. (of this page)	21. No. of Pages	22. Price
Unclassified	**Unclassified**	**274**	

Form DOT F 1700.7 (8-72)   Reproduction of completed page authorized

Table of Contents

List of Figures

x

List of Tables

List of Equations

Executive Summary

While many highway crashes involve vehicle-to-vehicle impacts, a substantial number of injuries and fatalities result from single vehicle impacts with roadside infrastructure such as guardrails, protective barriers, roadway signs and other fixed objects. The design and engineering of these structures strongly influence the injury-causing g-forces experienced by vehicle occupants and whether or not vehicles are redirected back into traffic.

The U.S. Department of Transportation (USDOT) and state Departments of Transportation have conducted extensive, full-scale passenger vehicle-barrier crash tests to better understand crash performance of guardrails and safety barriers and to improve their design. However, very limited work has been conducted on crash performance of barriers when impacted by medium and heavy duty trucks due to the cost and the complexity of full-scale truck testing. Substantially more data and better understanding of truck-infrastructure crashes would enable the highway community to improve barrier design, to further reduce the likelihood of vehicle-infrastructure fatalities and injuries and to reduce highway congestion resulting from severe accidents.

In collaboration with the Turner Fairbank Highway Research Center (TFHRC), the National Transportation Research Center, Inc., University Transportation Center (NTRCI) has taken an active role in enhancing industry understanding of truck-infrastructure crash behavior through funding the development and enhancement of advanced finite element (FE) computer simulation models of truck-infrastructure crashes. Recent NTRCI funded work on refinement and enhancement of models of single unit truck crashes into concrete barriers has demonstrated the ability of this advanced computer simulation technology to provide sorely needed high quality data and analysis results at substantially lower cost than full-scale crash tests. NTRCI is helping provide highway engineers with data to make better, more well-informed roadside infrastructure decisions that enhance the safety of the traveling public.

To build upon its success with single-unit truck crash simulation and analysis, NTRCI has funded the research team of Battelle, Oak Ridge National Laboratory (ORNL) and the University of Tennessee at Knoxville (UTK) to conduct a three-phase investigation to enhance and refine a FE model for simulating tractor-semitrailer crash events involving impact with roadside safety hardware such as bridge rails and median barriers. The tractor model was originally developed by the National Crash Analysis Center (NCAC) of George Washington University (GWU) and required refinement and testing before it could be used by the engineering community for infrastructure design.

The objectives of this investigation led by Battelle were to develop, enhance and validate computer models of a tractor-semitrailer combination for use in analysis, design, and evaluation of roadside safety hardware.

Phase A was completed in Year 1of the project and was documented in the Phase A Final Report[i]. Phase B was completed in Year 2 of the project and was documented in the Phase B Final Report[ii]. Phase C was completed in Year 3 of the project and the results of that effort are documented herein. The tasks completed in Phase C include:

- Continuing Enhancements to the tractor-semitrailer FE model

- Model results and qualitative evaluation of the combined tractor-semitrailer FE model by comparison of computer simulation results to full-scale tractor-semitrailer crash test results

- Quantitative evaluation of the tractor-semitrailer FE model using NCHRP 22-24 procedure

- Evaluation of the combined tractor-semitrailer FE model by the FHWA Finite Element Centers of Excellence (COE) community

- Interactive on-line user manual and FE model web site

Following is a brief summary of the research conducted in Phase C and associated results.

Continued Enhancement to the Tractor-Semitrailer FE Model

Several model enhancement tasks that were identified and recommended in Phases A and B were implemented in Phase C. These tasks included correcting model inaccuracies that may lead to numerical instabilities, testing and characterization of semitrailer air-spring, and testing and characterization of semitrailer structural components.

The tractor-semitrailer FE model has many parts that may contact each other in an impact event. Contact between parts in a numerical analysis is highly sensitive to initial geometric position, relative stiffness, and the constantly changing orientation of contacting parts during a simulation. Contact is known to be a source of run-time errors and numerical instability in crash simulations. Great care was taken during the development of the tractor-semitrailer FE model to remedy known sources of contact inaccuracies and instabilities. Nonetheless, at the end of Phase B there were still some outstanding contact issues manifested as higher-than-expected sliding (contact) energies in certain regions. These issues can affect the accuracy of results, and the numerical stability (robustness) of the analysis is highly sensitive to these non-physical energy growths.

---

[i] Plaxico, C., Kennedy, J., Simunovic, S., and Zisi, N, Enhanced Finite Element Analysis Crash Model of Tractor-Trailers (Phase A), National Transportation Research Center, Inc., Knoxville, TN, 2008.

[ii] Plaxico, C., Kennedy, J., Simunovic, S., and Zisi, N, Enhanced Finite Element Analysis Crash Model of Tractor-Trailers (Phase B), National Transportation Research Center, Inc., Knoxville, TN, 2008.

These and other contact issues were corrected by Battelle in this task. The resulting model is very robust; it has been run many times and has not shown tendency for any numerical instability issues. These models have typically been used to simulate three seconds of a crash event involving tractor-semitrailer impact into rigid barriers.

Due to the significant influence of suspension on vehicle kinematics, extensive testing and characterization was done in Phase A of this program on the tractor's front and rear suspension components, including the tractor's Airide™ suspension properties. In Phase B the semitrailer's Airide™ suspension properties were represented using the tractor's Airide™ suspension properties. In the current work, tests were conducted by Battelle to characterize the trailer's Airide™ suspension properties. The response of the Airide™ component is a function of internal pressure, deflection, and deflection rate. A test program was conducted to collect necessary data for properly characterizing the response of the component for each of these factors. Subsequent tests were conducted to verify that the models accuracy in predicting the air-springs response.

The material specifications for the parts in the Phase B semitrailer model were obtained from the open literature, from manufacturers' data, and from existing tractor FE model material data. Trailer manufacturers generally do not reveal the specific material grades used for specific parts, so the search also included aftermarket parts suppliers. Due to some uncertainty in the identification of the material makeup of several components of the semitrailer, the research team conducted physical experiments to measure material properties. Coupon samples were extracted from several key structural elements a 1990 Stoughton box trailer, and uniaxial tensile tests were performed to measure the materials' plastic stress-strain behavior. The material models for these key components of the trailer were then characterized using the test data.

Implementation of Gravity Initialization

An important factor in vehicle FE analysis is the effect of gravity on all the interacting, contacting components in the model. "Settling" (or initializing) the model under gravity will affect the response of passive (e.g., ballast) and active (e.g., suspension) components. Gravity initialization can be accomplished by simply running the FE model for a specific amount of time prior to the impact with the barrier, or by running a separate "static" gravity-only analysis and using this initial state of stress and deformation as an initial condition. In this project, the research team used both approaches. The procedures for each of these approaches are described in this report along with comments about the efficacy of each.

Tractor-Semitrailer FE Model Results and Evaluation

A primary objective of the study was to determine the overall fidelity of the tractor-semitrailer FE model by comparing simulation vehicle response with real vehicle response. Crash test data from a number of full-scale crash tests involving tractor-semitrailer impacts into roadside safety barriers were collected from the Texas Transportation Institute (TTI) and Midwest Roadside Safety Facility (MwRSF) during the first phase of the program. The data obtained from those

reports were used as a gauge to measure model fidelity. The automated dimensional adjustment program (ADAP), developed by Oak Ridge National Laboratory (ORNL) in Phase B, was used to modify the tractor and semitrailer models to represent the properties of test vehicles from two crash tests. This allowed the research team to simulate those tests to provide a broader assessment of the model's efficacy, and ultimately, provide a better quantification of the model's validity. The performance of the Phase C tractor-semitrailer FE model was assessed by comparing simulation results to:

- The results of full-scale crash test TL5CMB-2 conducted at the Midwest Roadside Safety Facility (MwRSF) in July 2007 and
- The results of full-scale crash test TTI 7069-13 conducted at TTI in July 1988.

The basic differences in these two tests were the ballasted weight of the trailer and the trailer length. The ballasted weight of the trailer was 79,705 lb (36,153 kg) for the test vehicle in test TL5CMB-2 and was 50,050 lb (22723 kg) for the test vehicle in test 7069-13. Test TL5CMB-2 involved a 48-ft trailer, while test 7069-13 involved a 45-ft trailer.

Based on a qualitative assessment of the model's results in the simulation of test TL5CMB-2, the general response of the modified FE model compared well. The analysis results replicated the basic timing and magnitudes of phenomenological events that occurred in the full-scale test. A comparison of sequential views of the test and simulation showed that the attitudes (e.g., roll and pitch) of both the tractor and the semitrailer models were also reasonably similar to the behavior of the vehicle in the full-scale crash test. The quantitative assessment also indicated that the model's results were within the range of error that would be expected between two identical crash tests, based on validation criteria defined in the NCHRP Project 22-24 report.

Based on a qualitative assessment of the model's results in the simulation of test 7069-13, the FE model did not adequately simulate the kinematic behavior of the tractor-semitrailer, nor adequately capture the timing of the basic phenomenological events that occur during impact. The overall accuracy of the results of the impact is highly dependent upon the accuracy of the trailer's attitude (roll, pitch and yaw) when the rear of the trailer "slaps" against the barrier. The current response of the model does not accurately replicate that of the test vehicle during this initial phase of impact.

Evaluation of the Combined Tractor-Semitrailer FE Model by the FHWA Finite Element Centers of Excellence (COE) Community

Following the completion of the model enhancement and preliminary validation, Battelle provided an interim version of the enhanced FEA tractor-semitrailer model to each of the other FHWA COEs in roadside safety, including the National Crash Analysis Center (NCAC), the Texas Transportation Institute (TTI), the Midwest Roadside Safety Facility (MwRSF), Worcester Polytechnic Institute (WPI), and Applied Research Associates (ARA). To date, only NCAC has

given the team any feedback on the FE models. NCAC's used the model to simulate a crash event involving a tractor-semitrailer impact with a high-tension four-cable median barrier system. The impact velocity and angle was 80 km/hr and 15 degrees, respectively. NCAC did not provide comparison of the simulation results with full-scale crash test data; however, the model did run to completion without issue.

Others have recently downloaded the model, but have not had sufficient time to provided feedback.

Interactive On-line User Manual and FE Model Web Site

An interactive graphics-based web site and User's Manual have been developed for the tractor-semitrailer FE vehicle models. The interactive graphics-based web site will be the central point of access to the tractor-semitrailer vehicle FE models for users. This web site is similar to the one that was developed for the Ford F800 Single Unit Truck vehicle FE model in 2007.

Conclusions

The tractor-semitrailer vehicle FE model is the most advanced of this vehicle class in terms of physical function, geometric detail and material property accuracy. The model is computationally very robust given its complexity. It has been extensively debugged and exercised hundreds of times for the cases within the range of NCHRP Report 350 TL-5 speeds and impact angles.

In developing the FE model, computational efficiency was considered wherever possible, but computational efficiency was considered second to fidelity. The philosophy is that today's computational resources are small relative to the next generation.

The model is reasonably accurate and may be used by the engineering community to design and develop roadside safety hardware and ultimately improve overall safety of the travelling public. The model is available for download at http://www.ntrci.org.

Although the research team considers the model to be reasonably accurate for its intended application, several enhancements have been proposed by the research team for future research that would further improve the accuracy, robustness and expand the applicability of the model.

Chapter 1 – Introduction

In recent decades, the highway community, including the U.S. Department of Transportation (USDOT), the Federal Highway Administration (FHWA), the Turner Fairbank Highway Research Center (TFHRC), and state Departments of Transportation have supported and conducted extensive full-scale passenger car-barrier crash tests to better understand crash performance of guardrails and barriers and to improve their design and to reduce the likelihood of vehicle-infrastructure crash fatalities and injuries.

Improved understanding of truck-infrastructure crashes will enable the highway community to improve barrier designs, to further reduce the likelihood of vehicle-infrastructure fatalities and injuries, and to reduce highway congestion resulting from severe accidents. In collaboration with the TFHRC, the National Transportation Research Center, Inc., University Transportation Center (NTRCI) has taken an active role in enhancing industry understanding of truck-infrastructure crash behavior through funding the development and enhancement of advanced finite element (FE) computer simulation models of truck-infrastructure crashes. NTRCI is helping provide highway engineers with data to make better, more well-informed roadside infrastructure decisions that enhance the safety of the traveling public.

NTRCI has funded the research team of Battelle, Oak Ridge National Laboratory (ORNL), and the University of Tennessee at Knoxville (UTK) to conduct a three-phase investigation to enhance and refine a FE model for simulating tractor-semitrailer crash events involving barriers and roadside safety hardware such as bridge rails and median barriers. The tractor model was originally developed by the National Crash Analysis Center (NCAC) of George Washington University (GWU) and requires refinement and testing before it can be used by the engineering community for infrastructure design.

The objective of this current investigation led by Battelle is to validate and enhance computer models of a tractor-semitrailer combination that will be used in analysis, design, and evaluation of roadside safety hardware. The research team is enhancing the overall fidelity of the tractor-semitrailer FE model by verifying vehicle failure modes from simulation against those from actual crash tests. This effort will enable the tractor-semitrailer FE model to provide more realistic predictions of crash performance and significantly reduce the need for costly full-scale truck testing. This report summarizes the results of the final phase of a three-phase program. In general terms, the three-phase plan included:

1. Phase A – Conduct an in-depth evaluation of the NCAC tractor only FE model, implement selected modifications, and develop a new trailer model.

2. Phase B – Complete preliminary modification of combined tractor-semitrailer FE models, provide them to the FHWA Center of Excellence (COE) community for beta testing, and validate them against suitable full-scale crash tests.

1

3. Phase C – Refine the combined tractor-semitrailer FE models and develop an interactive, online FE model user's website and a User's Manual document to facilitate the use of the model.

Phase A was completed in Year 1 of the project and was documented in the Phase A Final Report [1]. Phase B was completed in Year 2 of the project and was documented in the Phase B Final Report [2]. Phase C was completed in Year 3 of the project and the results of that effort are documented herein.

The intended application of the tractor-semitrailer model is to evaluate the crash performance of roadside safety features based on the crash test guidelines of National Cooperative Highway Research Program (NCHRP) Report 350 Recommended Procedures for the Safety Performance Evaluation of Highway Appurtenances for Test Level 5 [3]. In such applications, the tractor serves as a "bullet" vehicle, so model performance is judged by accuracy of load transfer of the vehicle to the barrier and accuracy in simulating the kinematic behavior of the tractor during and after impact.

Roadmap for this Report

This report covers a range of technical issues required for development and refinement of the tractor-semitrailer combination vehicle FE model. The report is organized into 8 chapters as follows.

- **Chapter 2. Continued Enhancement of the Tractor-Semitrailer FE Model** – A summary of the model enhancement tasks that were identified and recommended in Phases A and B and implemented in Phase C:

- **Chapter 3. Model Results and Qualitative Evaluation of the Tractor-Semitrailer Model** – A summary of tractor-semitrailer FE model simulations and an evaluation of the results of those simulations compared to two full-scale crash tests; TL5CMB-2 (MwRSF) and 7069-13 (TTI).

- **Chapter 4. Quantitative Evaluation NCHRP Project 22-24 Procedure** – A *quantitative* assessment of the model's results is provided based on the validation procedures recommended in the NCHRP 22-24 report titled "Recommended Procedures for the Verification and Validation of Computer Simulations used for Roadside Safety Applications"

- **Chapter 5. Summary and Discussion of Results** – A summary and discussion of the results of the evaluation of the tractor-semitrailer FE model's performance in comparison with full-scale tractor-semitrailer crash tests.

- **Chapter 6. Summary of Comments on the Tractor-Semitrailer FE Model by the FHWA Finite Element Centers of Excellence (COE) Community**

- **Chapter 7. Interactive On-line User Manual and FE Model Web Site**

- **Chapter 8. Conclusions and Recommendations for Future Research –** Summarizes the general conclusions regarding the development, model enhancements, the qualitative and quantitative validations of the tractor-semitrailer FE model and provides recommendations for additional research to further improve the accuracy, robustness, and applicability of the tractor-semitrailer FE model.

Objectives

The objective of Phase C was to complete the enhancement, evaluation and validation of the *combined* tractor-trailer model. In Phase C, Battelle collaborated with the UTK (University of Tennessee Knoxville) to generate a validated generic tractor-semitrailer model and documented modeling methodologies.[iii] The model is suitable for use in crash barrier design and evaluation according to industry best practices such as those prescribed in NCHRP Report 350.

Current Status of Model

The overall development of the FE model of a sleeper-cab tractor with a 48-foot semitrailer was completed in Phase B. That model was reasonably validated based on comparison with full-scale crash test results. The general response of that FE model replicated the basic timing and magnitudes of phenomenological events that occurred in full-scale tests of tractor-semitrailer impacts with rigid longitudinal barriers. In Phase C, more representative tractor FE models were created for comparison to the MwRSF test TL5CMB-2 and the TTI test 7069-13 which reflected more closely the geometry of the crash test vehicles. Test TL5CMB-2 used a day-cab tractor with a 129-inch wheelbase and a 48-foot semitrailer and the TTI test 7069-13 used a day-cab tractor with a 144-inch wheelbase and a 45-foot semitrailer.

The impact conditions for test TL5CMB-2 were consistent with the test requirements of National Cooperative Highway Research Program (NCHRP) Report 350 [3] Test 5-12 (e.g., impact speed and angle of 80 km/hr and 15 degrees, respectively). Based on comparison of FEA results, the research team believes that this tractor-semitrailer FE model is reasonably valid for this type of crash simulation, and that it will provide useful results in general barrier design evaluation work regarding impact loads and general vehicle-barrier interaction.

The impact conditions for test 7069-13 were consistent with the test requirements of the 1989 *Guide Specifications for Bridge Railings* (impact speed of 50 mph and angle of 15 degrees). The

---

[iii] The same staff from Battelle, ORNL and UTK that conducted Phases A and B conducted Phase C. However, the support of Dr. Srdjan Simunovic of ORNL was contracted by NTRCI through UTK.

research team believes that this tractor-semitrailer FE model can be validated for this type of crash simulation with some minor additional work. Upon final validation, it will provide useful results in general barrier design evaluation work regarding impact loads and general vehicle-barrier interaction.

Research Approach and Results

The work plan for accomplishing the objectives of Phase C included the following six tasks:

- Task 1 – Continued Enhancement of the Tractor-Semitrailer Model

- Task 2 – Continued Evaluation and Validation of the Tractor-Semitrailer Model

- Task 3 – Provide Enhanced Tractor-Semitrailer Model to COEs

- Task 4 – Interactive On-line FE Model Web Site (UTK Only)

- Task 5 – Phase C Report and User Handbook

- Task 6 – Management Reporting and Meetings.

Battelle led and conducted Tasks 1, 2, 3, 5 and 6. UTK led and conducted Task 4. A description of the work conducted for each of these tasks is presented in the following sections.

Chapter 2 – Continued Enhancement of the Tractor-Semitrailer Model

Scope

In the Phase B report, several model enhancement tasks were identified and recommended for implementation in Phase C:

- Model "robustness" – Remedy modeling inaccuracies that may lead to numerical instabilities in the analyses

- Air-spring testing and characterization for the semitrailer model

- Testing and characterization of semitrailer components.

Following is a summary of that work.

Task 1.1 – Model Robustness

The tractor-semitrailer FE model has many parts that may contact each other in an impact event. Contact between parts in a numerical analysis is highly sensitive to initial geometric position, relative stiffness, and the constantly changing orientation of contacting parts during a simulation. Contact is known to be a source of run-time errors and numerical instability in crash simulations. Great care was taken during the development of the tractor-semitrailer FE model to remedy known sources of contact inaccuracies and instabilities. Nonetheless, at the end of Phase B there were still some outstanding contact issues manifested as higher-than-expected sliding (contact) energies in certain regions. These issues can affect the accuracy of results, and the numerical stability (robustness) of the analysis is highly sensitive to these non-physical energy growths. These and other contact issues were corrected by Battelle in this task.

The energies calculated by LS-Dyna were recovered to determine whether anything numerically unstable or unreasonable was going on in the simulation. During an impact event, the initial kinetic energy of the vehicle is transformed into internal energy and sliding interface energy as the various components deform and slide over each other. Internal energy is the strain energy resulting from material deformation and is generally accumulative in crash analyses as more and more elasto-plastic parts deform. Sliding interface energy is frictional force times sliding distance for parts in contact, which can increase as sliding contact develops. Total energy is a summation of all dynamic events during a simulation. In a closed system such as this (i.e., no external energy sources), the total energy should remain constant. It may increase slightly during the analysis due to the effects of gravity, but the increase should be minimal compared to the initial kinetic energy of the striking vehicle. Other nonphysical energies are often present, such as hourglass energy, and these energies should be minimal (e.g., less than 5 percent) compared to the internal energy of the system. Figure 1 is a plot of the key energies from a typical

5

simulation. The energy check of this simulation looks reasonable: total energy does not exhibit any abrupt jumps or discontinuities, kinetic energy decreases, and sliding and internal energies are a reasonable fraction of the total energy. Hourglass energy is negligible as it should be for this vehicle simulation.
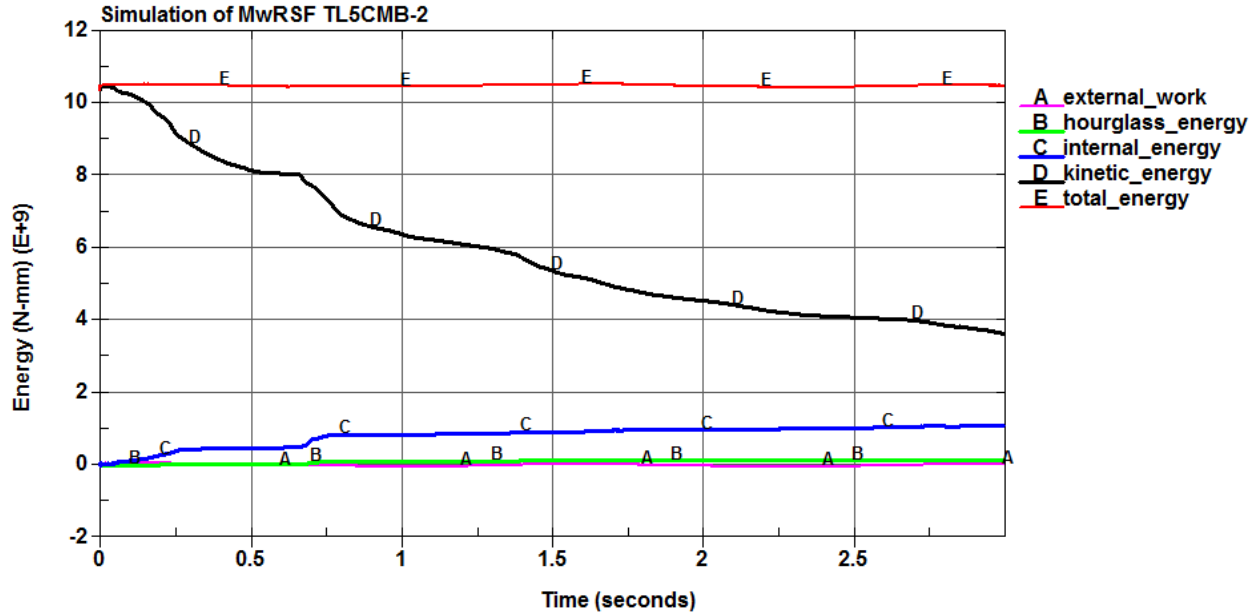
Figure 1. Chart. Energy balance for the simulation of the MwRSF test

Task 1.2 – Air-spring Testing and Characterization for the Semitrailer Model

Due to the significant influence of suspension on vehicle kinematics, extensive testing and characterization was done in Phase A of this program on the tractor's front and rear suspension components, including the tractor's Airide™ suspension properties. In Phase B, the semitrailer's Airide™ suspension properties were represented using the tractor's Airide™ suspension properties. In the current work, tests were conducted by Battelle to characterize the trailer's Airide™ suspension properties.

Figure 2 shows the semitrailer's Airide™ airbags that were removed from the semitrailer for characterization. The suspension on the 1990 Stoughton semitrailer was a Firestone Airide™ Model 1T15K-1. Because of the complexity of modeling the Airide™ suspension component in geometric detail, an idealized characterization of the component was used in the model via discrete spring and damper elements. A test program was developed and carried out in the Battelle labs to characterize the load response of the component for inclusion into the FE model. These tests were basically the same tests conducted on the tractor's Airide™ suspension in Phase A.

6

Figure 2. Photograph. Airide™ Airbag location on semitrailer

The response of the Airide™ component is a function of internal pressure, deflection, and deflection rate. The test program was designed to collect necessary data for properly characterizing the response of the component for each of these factors (Note: the response is also a function of initial height position, but this variable was not accounted for in the model). The airbags were tested quasi-statically and dynamically to quantify their response. The quasi-static and dynamic tests were conducted at several nominal pressures in the airbag's service range. The airbags were pressurized to each of the nominal pressures at their mid-stroke position, and then extended 3 inches and compressed 3 inches from the midpoint. Load vs. deflection data were recorded for a very slow (0.005 in/sec) quasi-static stroke rate and a faster (6.00 in/sec) dynamic stroke rate. Two sets of dynamic tests were run with long (2-minute) and short (5-second) dwell times at the full extension and full compression positions. Table 1 shows the test matrix for the test program. Note: The maximum dynamic stroke rate was limited by the capabilities of the load-displacement controlled test machine. The compression rate of the semitrailer suspension during impact, as calculated in the analysis, was approximately 80 in/sec. We are not aware of any load-displacement test machine that can achieve such rates in a controlled manner; however, in future studies, validation of the suspension response could be carried out by conducting dynamic impact tests in a laboratory or properly instrumenting the suspension during full-scale tests (e.g., live-driver tests over curbs or full-scale impact tests) and

then comparing the test results to those computed by the model under those same load conditions.

Table 1. Test matrix for the Airide^{TM} suspension component

Test #	Pressure (psig)	Deflection Rate (in/s)	Stroke (in)	Hold Time at +3 and -3 (sec)
TRLAB-20-qs	20	0.005	+3 to -3	0
TRLAB-40-qs	40	0.005	+3 to -3	0
TRLAB-60-qs	60	0.005	+3 to -3	0
TRLAB-20-6-SH	20	6.0	+3 to -3	5
TRLAB-40-6-SH	40	6.0	+3 to -3	5
TRLAB-60-6-SH	60	6.0	+3 to -3	5
TRLAB-20-6-LH	20	6.0	+3 to -3	120
TRLAB-40-6-LH	40	6.0	+3 to -3	120
TRLAB-60-6-LH	60	6.0	+3 to -3	120

For each test, the "zero position" of the Airide™ component was set to mid-stroke and held at this position while the internal air pressure in the component was set to the desired value. The tests were conducted under displacement control. Starting from the zero position, the displacement was ramped up 3 inches, and the displacement was held at this position for a specified period of time (e.g., 120 seconds). The displacement was then ramped down 6 inches and again held for a specified period of time. The displacement was then ramped back up 6 inches. This process was repeated for several cycles. Sequential test photos are shown in Figure 3 illustrating a typical loading cycle with annotated displacement-time history graph. The displacement-time history for each deflection rate/hold time combination is shown below in Figure 4, Figure 5 and Figure 6, respectively. A representative force-time history plot from a test is shown in Figure 7.
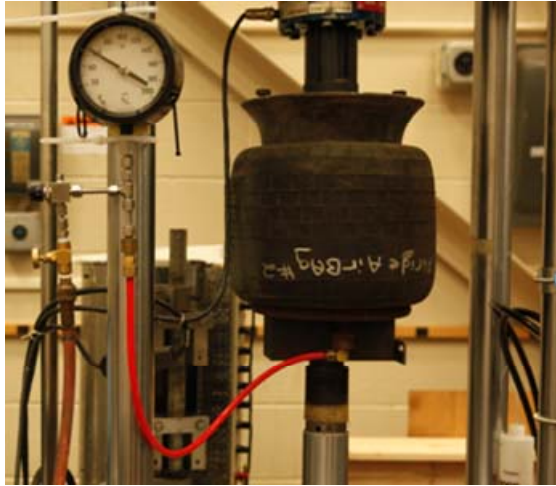
Zero Position ⓪
Spring height =
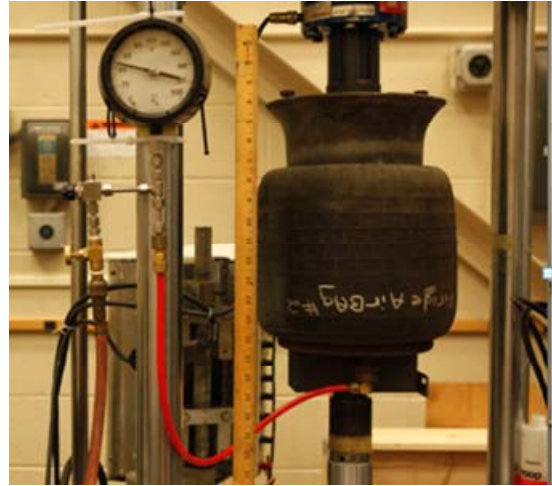
Max Extension ① ③
Spring height =
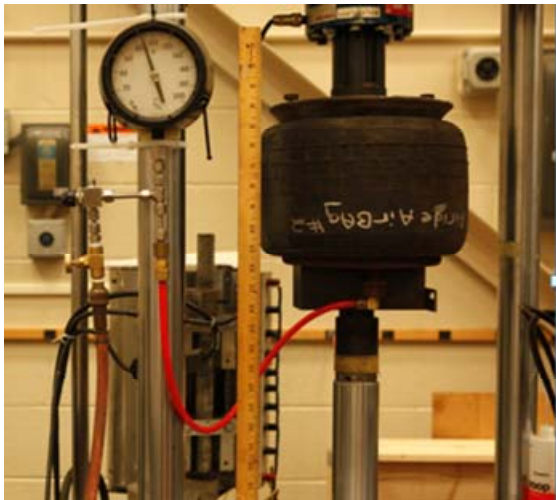
Max Compression ②
Spring height =
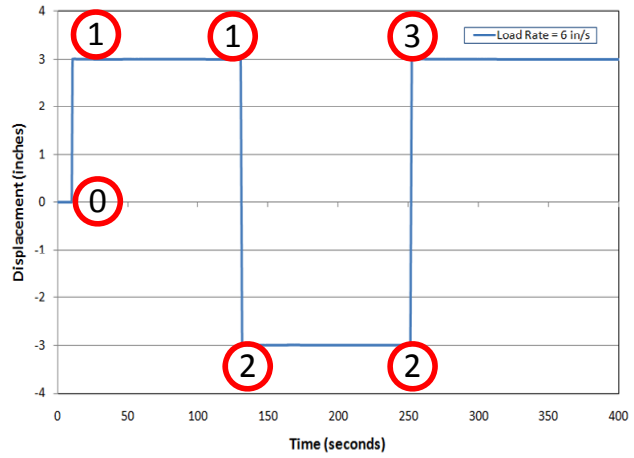
Figure 3. Photograph/Chart. Sequential views of Airide^{TM} suspension component in laboratory test
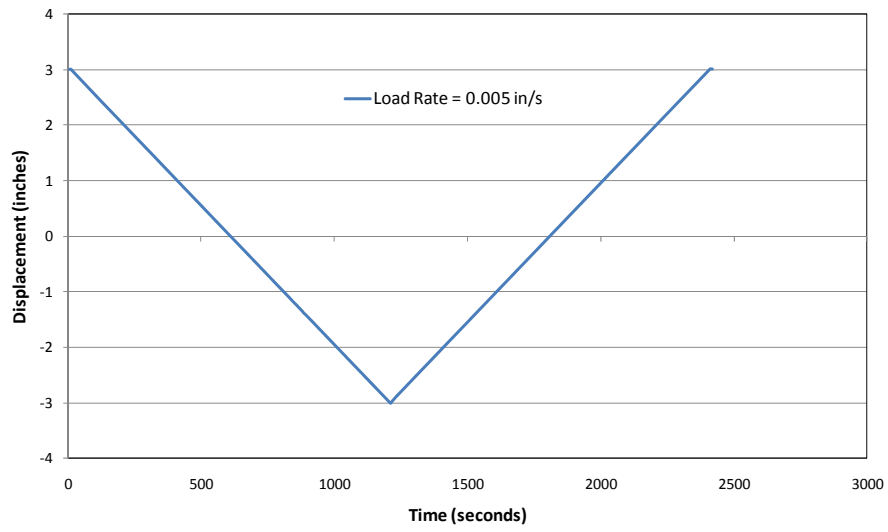
Figure 4. Chart. Displacement-time history of hydraulic ram for quasi-static load rate of 0.005 in/sec
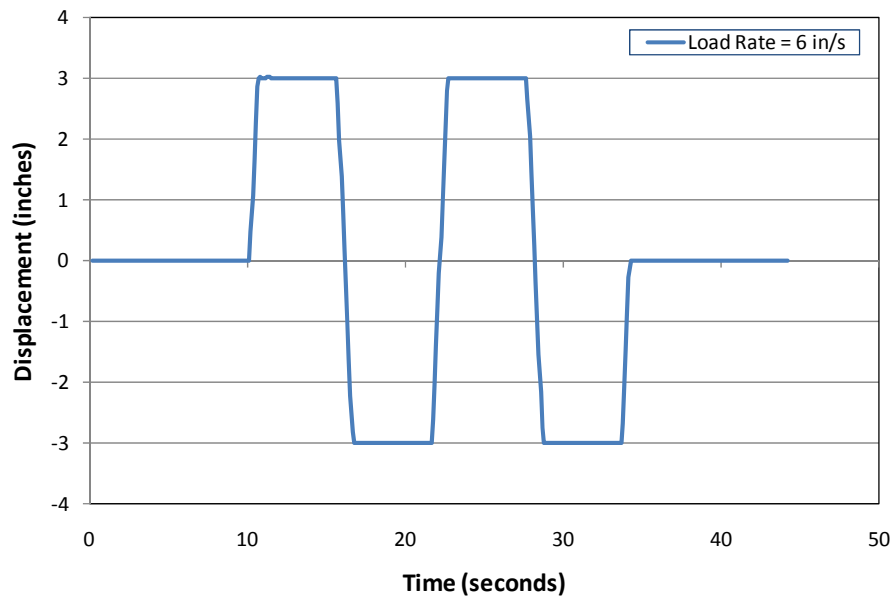
Figure 5. Chart. Displacement-time history of hydraulic ram for dynamic load rate of 6 in/sec with hold-time of 5 seconds

10
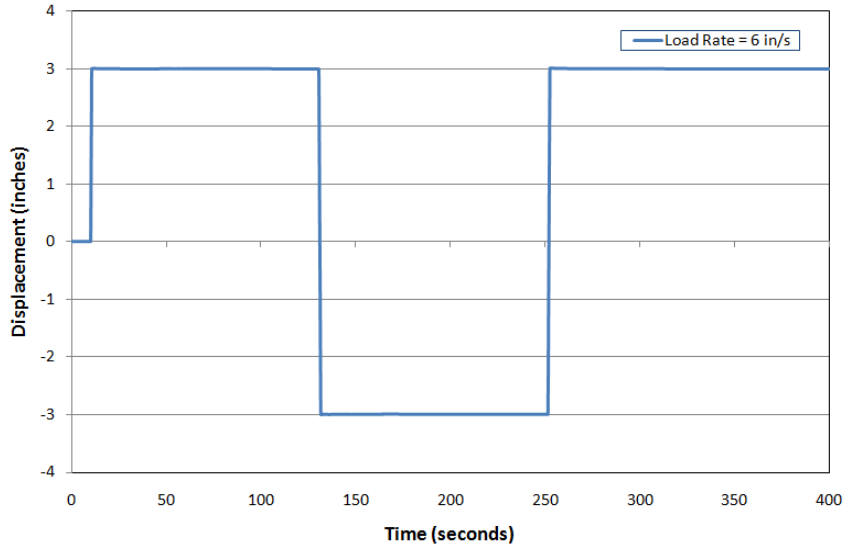
Figure 6. Chart. Displacement-time history of hydraulic ram for dynamic load rate of 6 in/sec with hold-time of 120 seconds
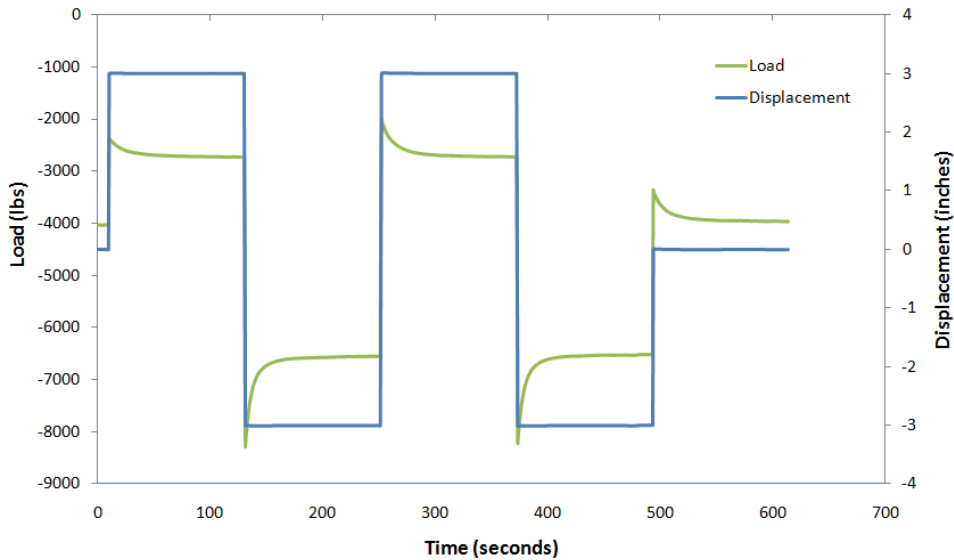
Figure 7. Chart. Force-time history and displacement-time history of Airide^{TM} component at bag pressure of 20 psig at displacement rate 1.2 in/s

Quasi-static load-deflection data from the laboratory tests conducted at 20 psig, 40 psig and 60 psig bag pressures are shown in Figure 8. Figure 9 shows a comparison of the Airide^{TM} component response at 60 psig under quasi-static loading and the 6 in/s load rate case, which clearly shows that for a given bag pressure the response is nonlinear and rate dependent. It also shows that the response is considerably different in compression than it is in extension.

11
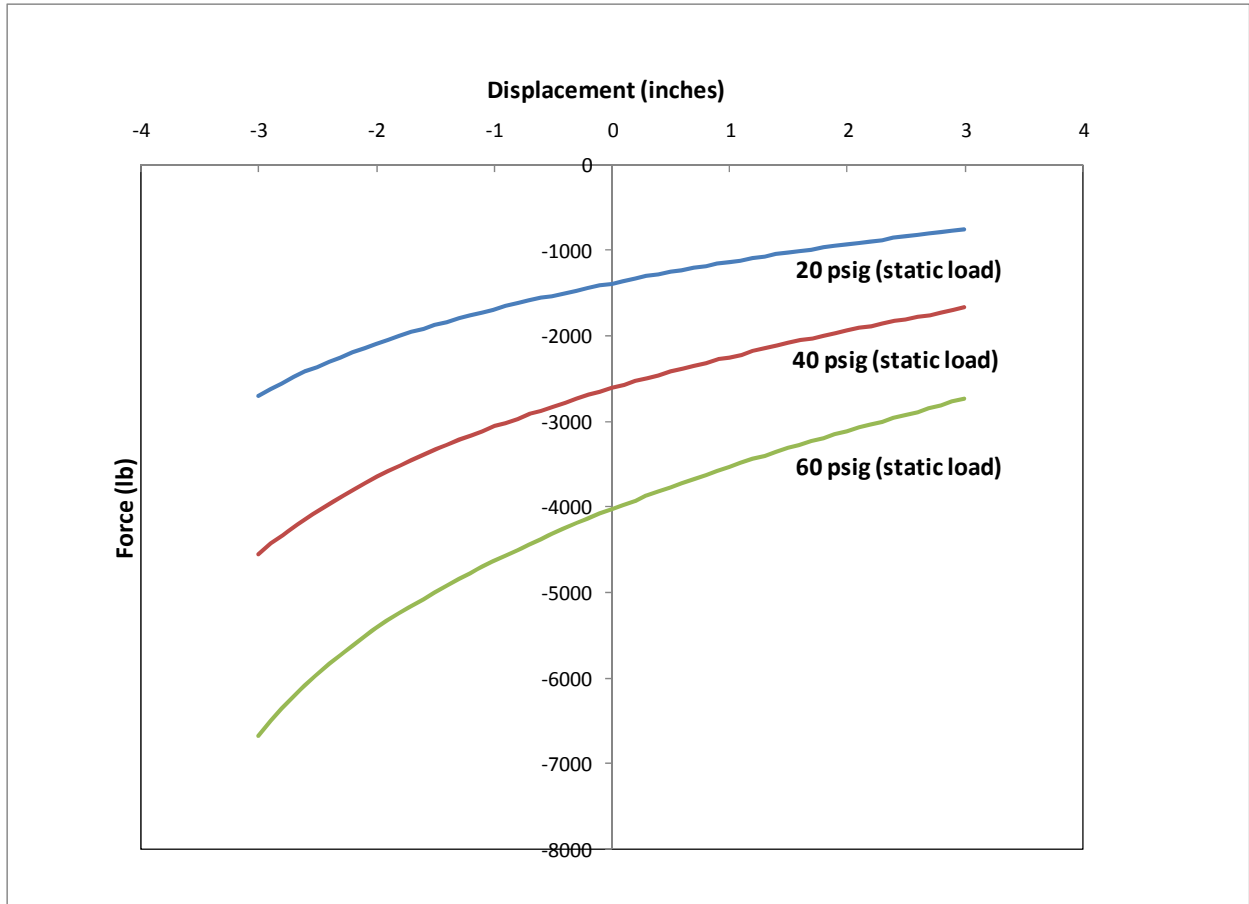
Figure 8. Chart. Quasi-static load-deflection data for Airide^{TM} component at 20, 40 and 60 psig
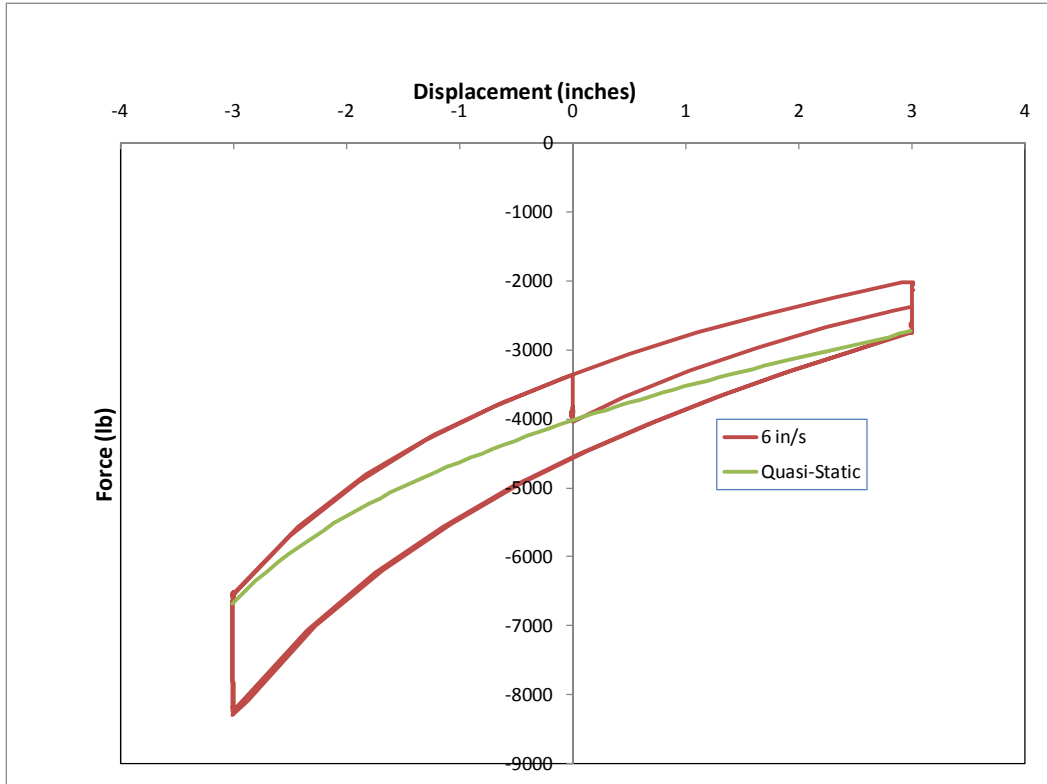
Figure 9. Chart. Load-deflection data for Airide^{TM} component at 60 psig pressure

The response of the suspension is an important factor in the overall kinematic response of the semitrailer during a redirectional impact, such as in the case of a tractor-semitrailer impacting a longitudinal barrier at a shallow angle. The test results showed that the response of the Airide^{TM} suspension is very nonlinear (e.g., nonlinear quasi-static response, dynamic response is different for extension and compression loading, sensitive to initial spring height, etc.) and cannot be accurately characterized using a simple discrete element material model. However, it was determined that the Airide^{TM} suspension response could be *reasonably approximated* by a three-parameter Maxwell model, as illustrated in Figure 10.
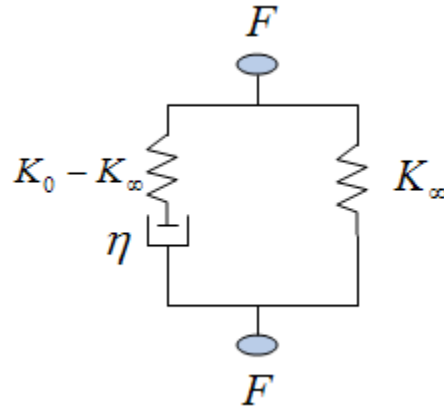
Figure 10. Illustration. Three parameter Maxwell model

The behavior of this model can be described by:

$$F = F_\infty + (F_0 - F_\infty)e^{-\beta t}$$

Equation 1. Equation for three parameter Maxwell model

When the component is given a prescribed displacement, d, and held at that position, the immediate load response is defined by $F_0 = K_0*d$, and the long-term equilibrium response is defined by $F_\infty = K_\infty*d$. The parameter $\beta = K_0/\eta$ corresponds to a time decay constant that governs the rate of force relaxation.

The material model library in LS-Dyna includes a three-parameter Maxwell model called *MAT_SPRING_MAXWELL. The input parameters for this model are given as constant coefficients for K_0, K_∞, β. To partially account for the nonlinear response, the Airide[TM] component was modeled using two discrete elements, as shown in the sketch in Figure 11. One of the elements is characterized by the *MAT_SPRING_MAXWELL material model and the other is characterized with *MAT_SPRING_NONLINEAR_ELASTIC. The parameter, K_∞, in the Maxwell model was set to zero, and the quasi-static (e.g., long-term) response was modeled using a non-linear elastic spring (K_{ne} in Figure 11) characterized by a force-deflection curve obtained from laboratory tests on the Airide[TM] suspension at a "quasi-static" rate (0.005 in/s).
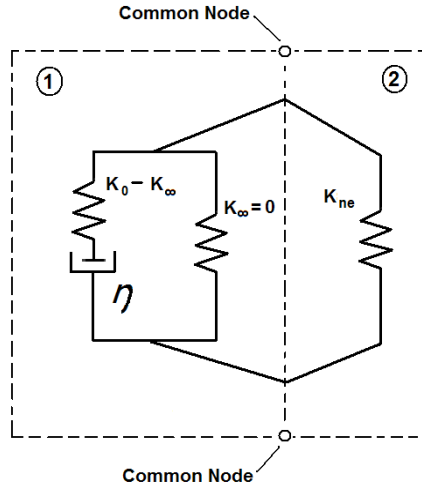
Figure 11. Illustration. Sketch of the two-element model used for modeling

With the K_∞ in the Maxwell model set to zero, the *MAT_SPRING_MAXWELL model simplifies to a linear spring and damper in series. A portion of the force-time plot corresponding to relaxation of the component under fixed displacement (see Figure 7) was used to define the spring and damper constants for the *MAT_SPRING_MAXWELL model. As seen in Figure 7, the relaxation response is different for extension and compression. It was decided that the compression response of the air spring would have a greater influence on the overall response of the trailer than the extension of the air spring; thus the compression response was used to calibrate the model.

A summary of the material models and their associated inputs for bag pressures of 20, 40 and 60 psig is shown in Table 2. These values correspond to static wheel loads of 1390 lb, 2610 lb and 4025 lb, respectively (refer to Figure 8). When static suspension (wheel) loads differ from those provided here (e.g., different ballast mass or ballast shifted fore/aft in the trailer), it is suggested that interpolation be used to determine the appropriate values. Plots of k_0 and β vs. Airide^{TM} bag pressure are shown in Figure 12. The position and attachment of the discrete element models of the air spring suspension in the semitrailer FE model is shown in Figure 13.

15

Table 2. Summary of the Airide^{TM} suspension material model and input parameters

Static Wheel Load = (20 psig bag pressure)				
Discrete Element	**Material Model**	**Material Parameters**		
		K_0 (lb/in)	K_∞ (lb/in)	β (s^{-1})
Element 1	*MAT_SPRING_MAXWELL	155	5.7E-4	0.27
Element 2	*MAT_SPRING_NONLINEAR	Load curve (see Figure 7)		

(40 psig bag pressure)				
Discrete Element	**Material Model**	**Material Parameters**		
		K_0 (lb/in)	K_∞ (lb/in)	β (s^{-1})
Element 1	*MAT_SPRING_MAXWELL	238	5.7E-4	0.17
Element 2	*MAT_SPRING_NONLINEAR	Load curve (see Figure 7)		

(60 psig bag pressure)				
Discrete Element	**Material Model**	**Material Parameters**		
		K_0 (lb/in)	K_∞ (lb/in)	β (s^{-1})
Element 1	*MAT_SPRING_MAXWELL	290	5.7E-4	0.15
Element 2	*MAT_SPRING_NONLINEAR	Load curve (see Figure 7)		

(a) Spring Constant, k_0

	20 psi	40 psi	60 psi
Values	155	238	290

(b) Decay Parameter, β

	20 psi	40 psi	60 psi
Values	0.268	0.172	0.15
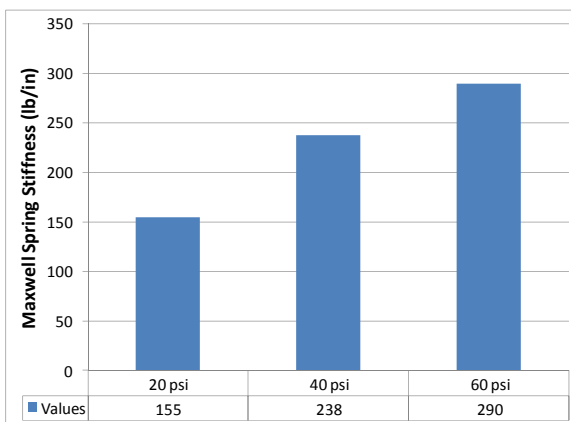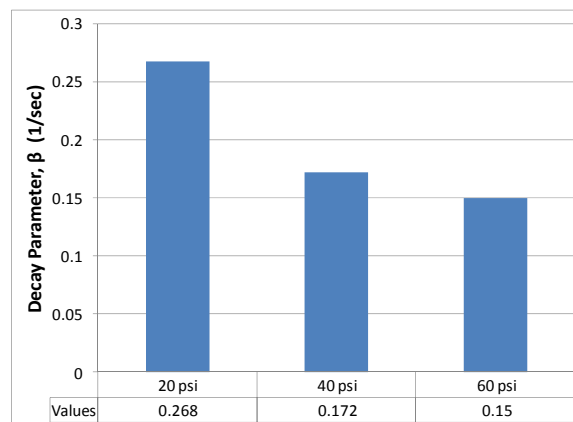
Figure 12. Chart. Plots of Maxwell spring constants k0 and β vs. Airide^{TM} bag pressure
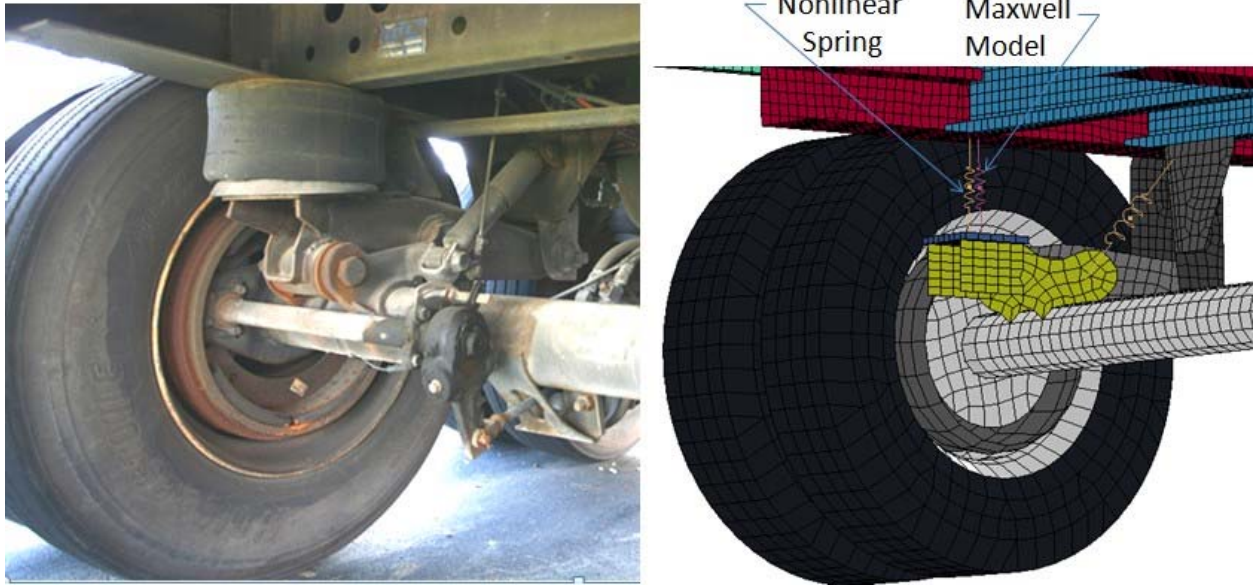
Figure 13. Photograph/Illustration. Airide^{TM} suspension component on Freightliner FLD tractor

Figure 14 through Figure 19 show the model's response compared with the test data for verification that the model was calibrated properly. The model replicates the test response very well in compression (which is the data used to calibrate the model), but does not accurately capture the rate behavior in extension. This is because the *MAT_SPRING_MAXWELL model in LS-Dyna is a linear viscoelastic model and can only simulate symmetric behavior in extension and compression. In order to accurately characterize the behavior in both loading directions, a User Material Subroutine would need to be developed, which was outside the scope of this project. However, considering the application of the semitrailer model (e.g., crash analysis), it was concluded that the compression behavior of the suspension was more important than the extension and thus the model response was considered acceptable.
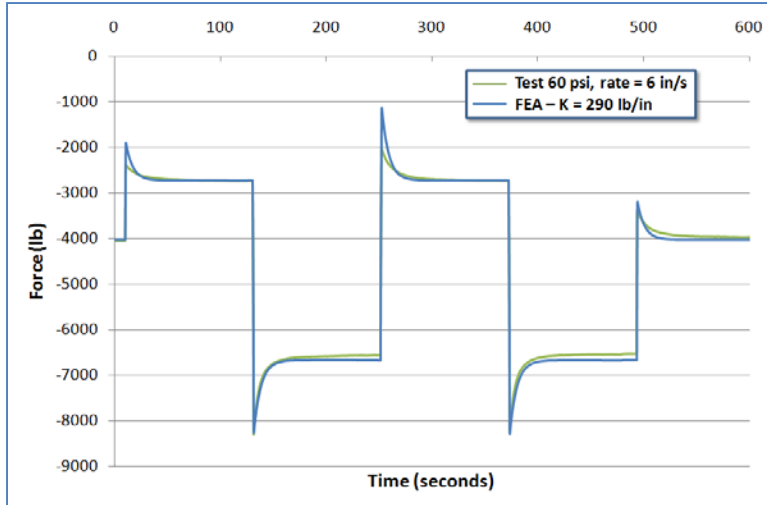
**Figure 14. Chart. FE model's response compared with the test data
for bag pressure of 60 psig and displacement rate of 6 in/s**
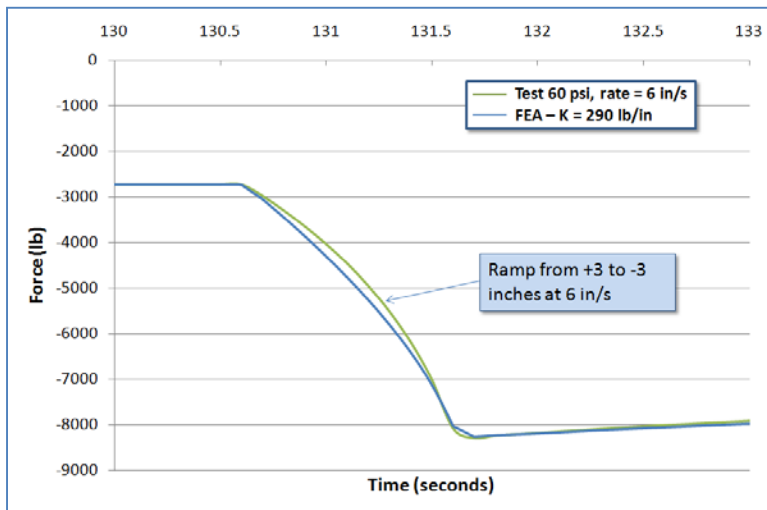
**Figure 15. Chart. FE model's response compared with the test data
for bag pressure of 60 psig and displacement rate of 6 in/s at first ramp from +3 to -3 inches**
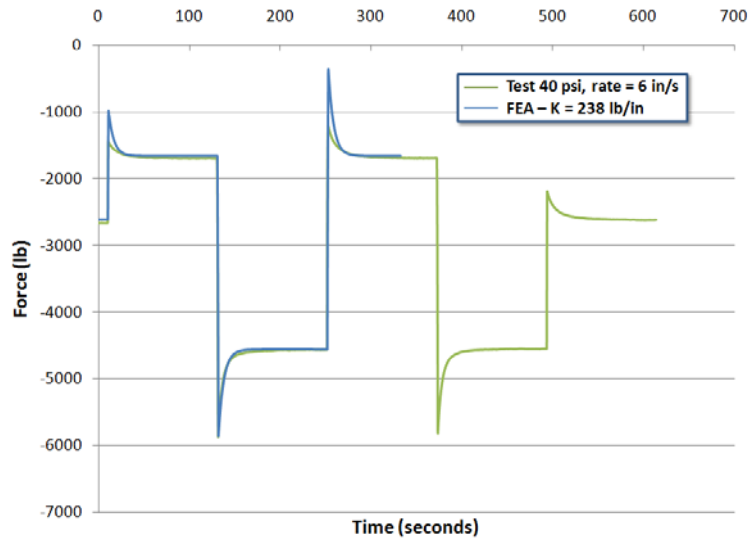
Figure 16. Chart. FE model's response compared with the test data for bag pressure of 40 psig and displacement rate of 6 in/s
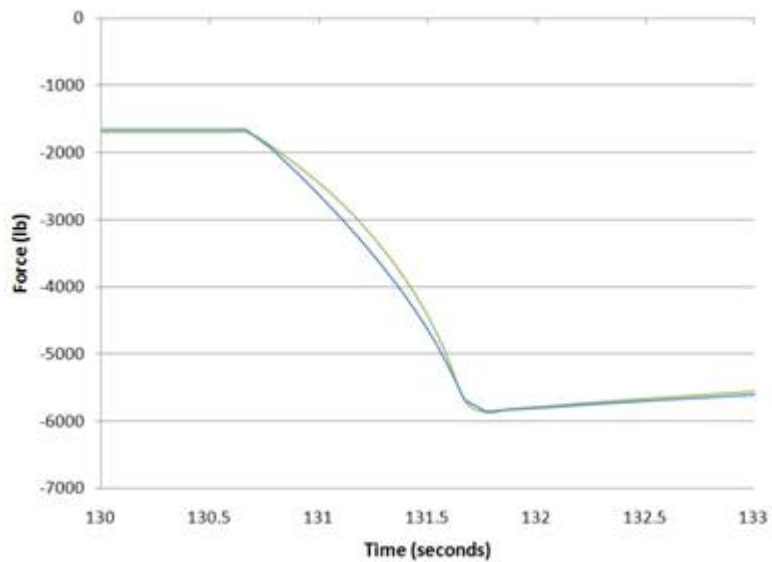
Figure 17. Chart. FE model's response compared with the test data for bag pressure of 40 psig and displacement rate of 6 in/s at first ramp from +3 to -3 inches

19
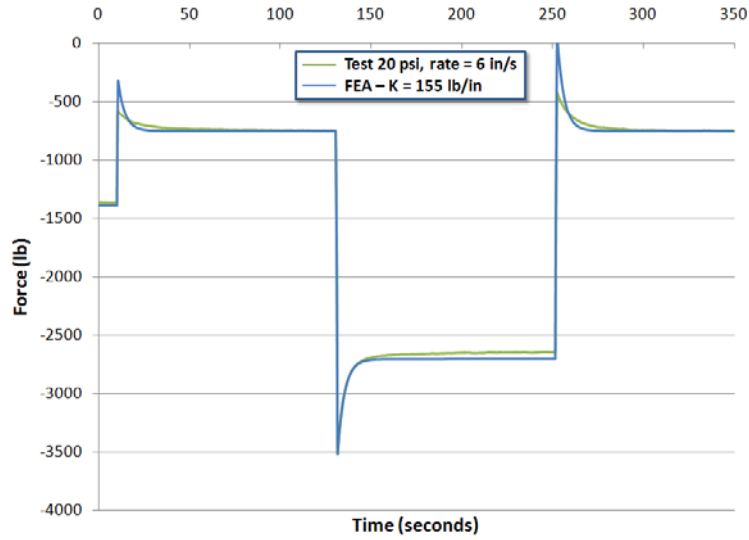
Figure 18. Chart. FE model's response compared with the test data for bag pressure of 20 psig and displacement rate of 6 in/s at first ramp from +3 to -3 inches
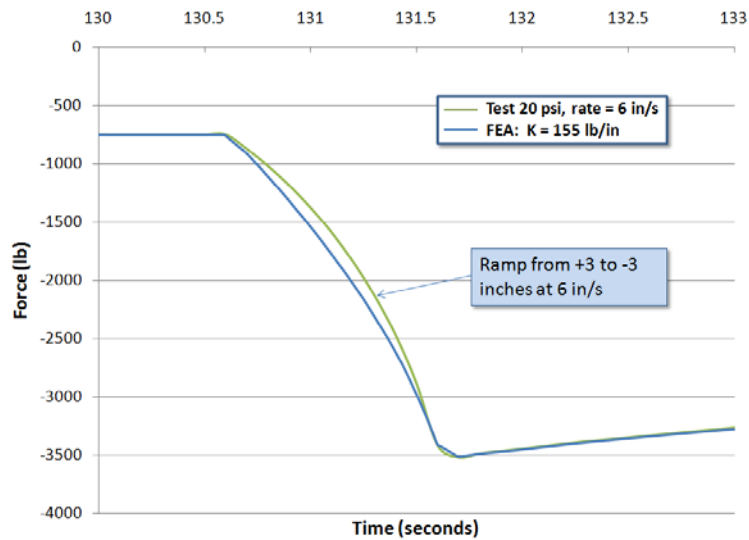
Figure 19. Chart. FE model's response compared with the test data for bag pressure of 20 psig and displacement rate of 6 in/s at first ramp from +3 to -3 inches

To use these Airide™ suspension properties in the semitrailer FE model for the simulation of the MwRSF TL-5 test, the static equilibrium forces on the semitrailer suspension had to be determined for the particular loading corresponding to the gross static mass of the vehicle under the ballasted load. To do this, a "gravity-only" run was made that included only the stationary tractor and trailer FE models. This simulation was run to a little over 2.0 seconds to dynamically settle the suspension. The resulting spring loads from this simulation were 4,833 lb per spring

20

set. The estimated wheel loads reported in the Phase B final report were 8,041 lb per wheel set. Figure 20 shows the free-body diagram for those wheel forces.
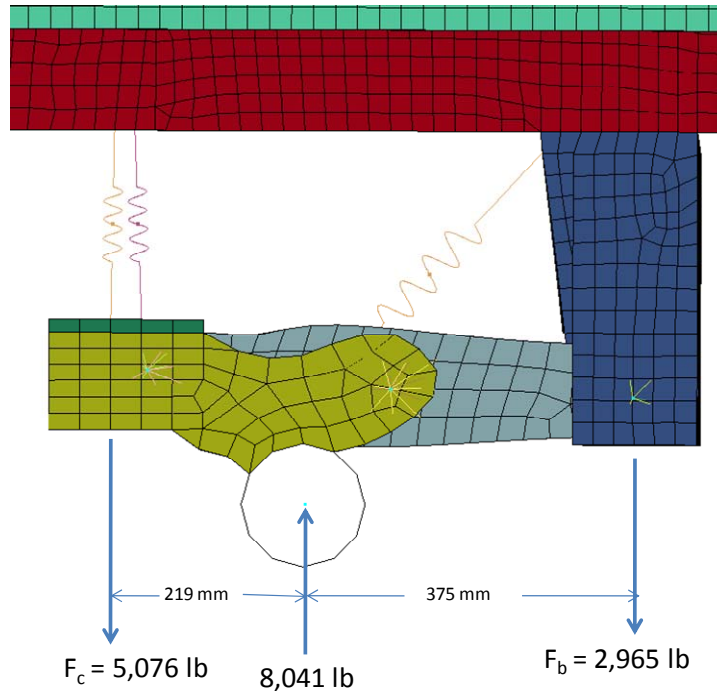
Figure 20. Illustration. Free-body diagram for semitrailer rear suspension

The 5,076 lb spring set force is within 5% of the spring load estimated from the deforc file from the ls-dyna output data. The value of 5,000 lb was used for calibrating/extrapolating the air bag spring properties. The non-linear spring force-deflection properties from the 60 psi pressure tests were scaled by 5000/4026 to derive equivalent suspension model input parameters for this loading. Figure 21 shows the air spring static load vs. pressure from the test.
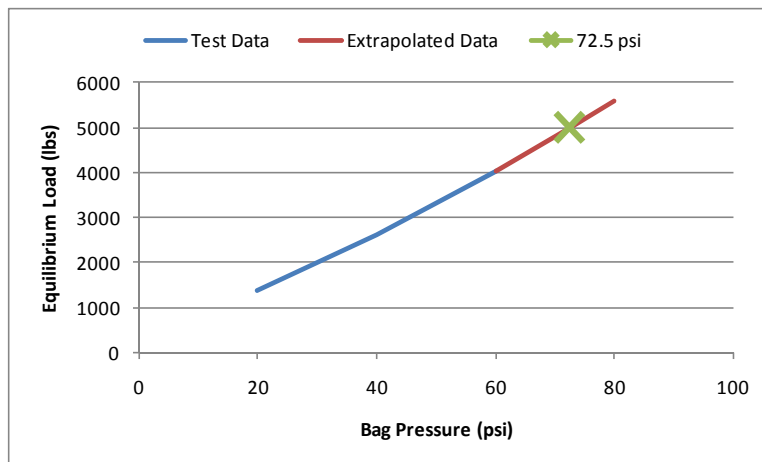
Figure 21. Chart. Air spring static load vs. pressure for the trailer's Airide^{TM} suspension

Figure 22 shows the general shape of the curve from the three test data points. The curve can be extrapolated to 80 psi with some confidence. The point on the extrapolated curve that corresponds to 5000 lb is approximately 72.5 psi. Figure 22 shows the extrapolation of the spring constant for the Maxwell model that was approximated from the test data. The mark at 72.5 psi corresponds to a spring constant of 55 N/mm.
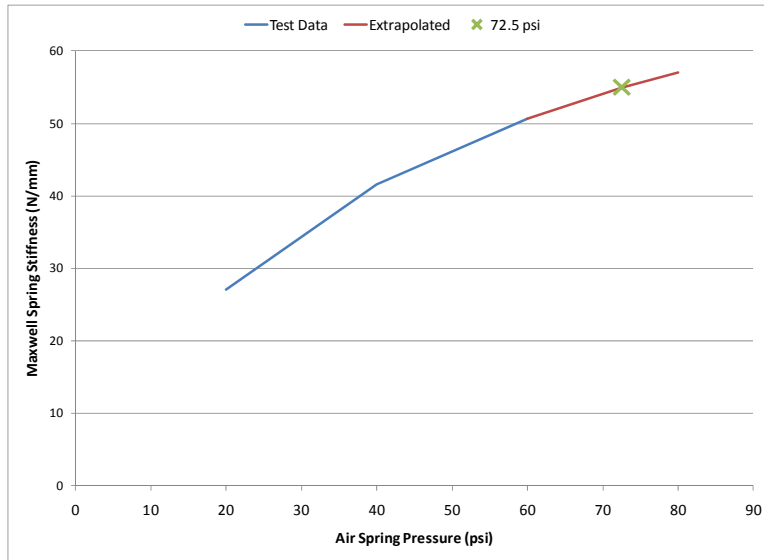
Figure 22. Chart. Extrapolated values for the Maxwell spring stiffness vs. air spring pressure

Figure 23 shows the extrapolation of the decay constant at 72.5 psi air spring pressure to be 0.144 1/s. Table 3 presents a summary of the Airide^{TM} suspension material model input parameters for the trailer model used in the simulation of the MwRSF test.
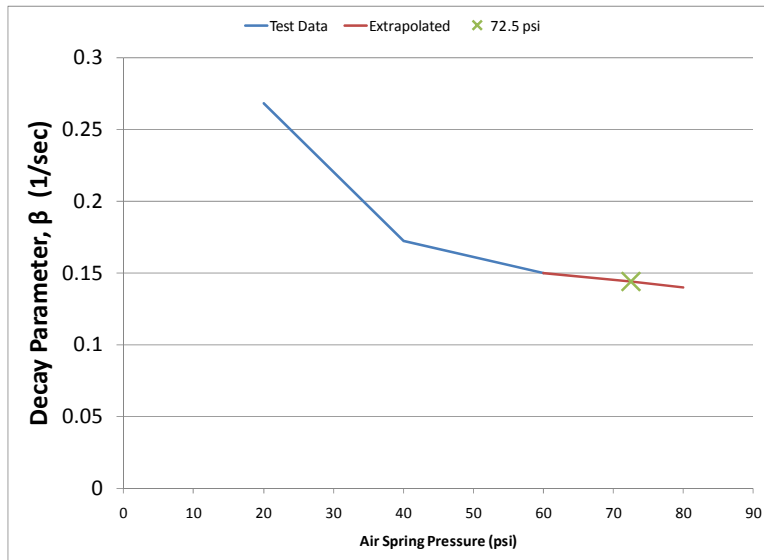
Figure 23. Chart. Extrapolated values for the Maxwell decay constant vs. air spring pressure

Trailer Suspension Properties Calculations for 45-Foot Trailer

For the simulation of the TTI test no. 7069-13 a day cab tractor with 45-foot trailer was developed by modifying the geometry of the existing day cab tractor and the existing (MwRSF model) 48-foot trailer to match the vehicle data in the 7069-13 test report. A ballast model was also created for this simulation that represented the ballast mass and CG location from TTI's 7069-13 crash test. An air bag pressure of 45 psi was estimated based on interpolation of the trailer suspension property data. The procedure for interpolating the original 20, 40, and 60 psi air bag data is similar to the extrapolation procedure just described for the 48-foot trailer.

Table 3. Summary of the Airide^{TM} suspension material model and input parameters for the trailer model used in the simulation of the MwRSF test

80,000-lb tractor-trailer Combination (EXTRAPOLATED 72.5 psig bag pressure data)					
		Material Parameters			
Discrete Element	**Material Model**	**K$_0$ (lb/in)**	**K$_\infty$ (lb/in)**	**β (s^{-1})**	
Element 1	*MAT_SPRING_MAXWELL	314	5.7E-4	0.144	
Element 2	*MAT_SPRING_NONLINEAR	Scale 60 psi curve *1.24			

Task 1.3 – Testing and Characterization of Semitrailer Components

The material specifications for the parts in the Phase B semitrailer model were obtained from the open literature, from manufacturers' data, and from existing tractor FE model material data. Trailer manufacturers generally do not reveal the specific material grades used for specific parts, so the search also included aftermarket parts suppliers. The details regarding the original material assignments and corresponding material properties are discussed in the Phase B final report.

Due to some uncertainty in the identification of the material makeup of several components of the semitrailer, the research team decided to conduct physical experiments to measure properties. Coupon samples were extracted from several key structural elements of the 1990 Stoughton box trailer that was purchased in Phase B, and uniaxial tensile tests were performed to measure the materials' plastic stress-strain behavior. Battelle performed tests on the following components to provide better material characterization in these areas:

- King Pin Box

- Lateral I-Beams

- Wheelset (Bogie)

    o Main Frame Rails

- Main Cross-members

- Cargo-box Longitudinal Slider Rails

- Suspension Pivot Vertical Support

- Suspension Pivot Arm

- Axle Tube

- Rear Bumper

- Rear Bumper Gusset

- Upper (aluminum extrusion) Longitudinal Side Rail

- Lower (aluminum extrusion) Longitudinal Side Rail.

Figure 24 through Figure 31 show the locations of these components.
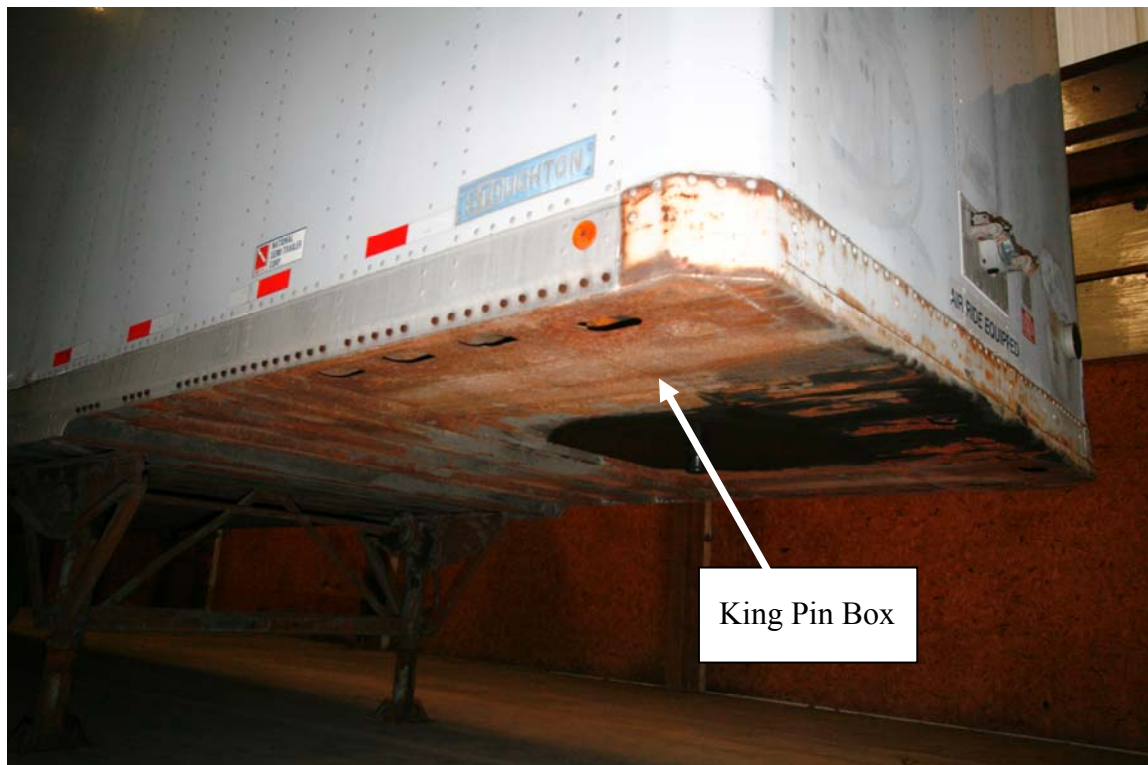
Figure 24. Photograph. Kingpin box location on semitrailer
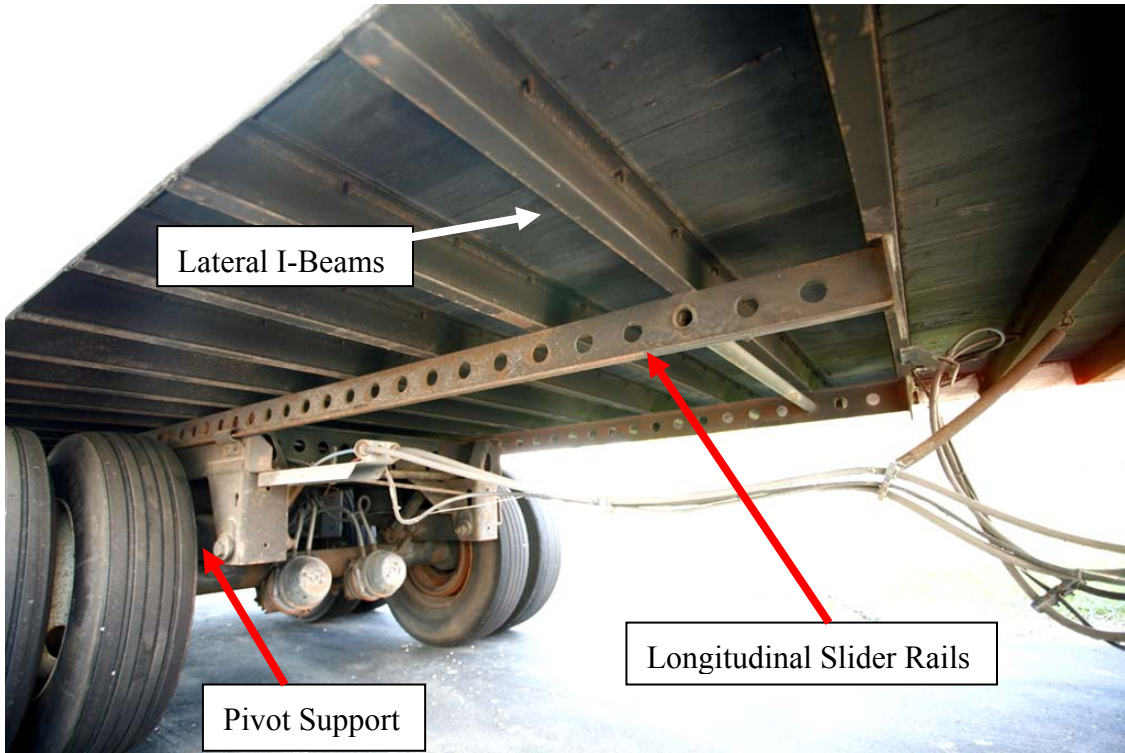
Figure 25. Photograph. Lateral I-beams, slider rail and vertical pivot support locations on semitrailer

Figure 26. Photograph. Bogie main frame rails location on semitrailer
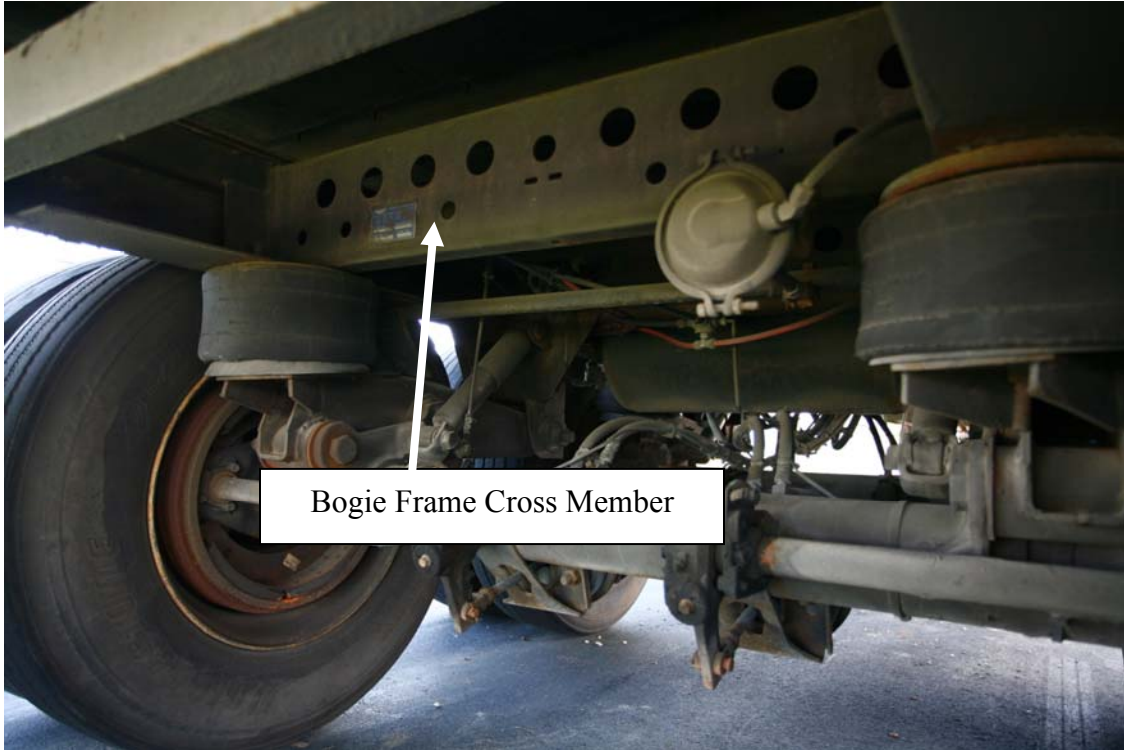
Figure 27. Photograph. Bogie frame cross-member location on semitrailer
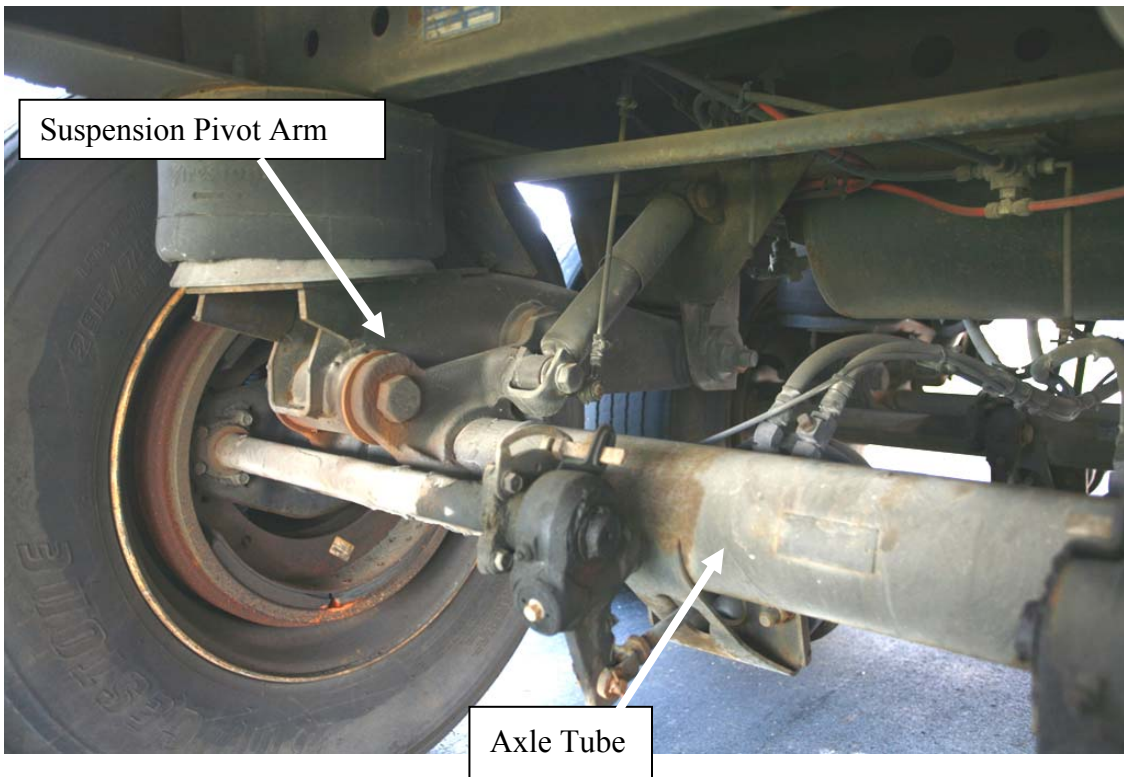
Figure 28. Photograph. Suspension pivot arm and axle tube locations on semitrailer

26

Figure 29. Photograph. Rear bumper and rear bumper gusset locations on semitrailer

Figure 30. Photograph. Lower side rail location on semitrailer

Figure 31. Photograph. Upper side rail location on semitrailer

In the tests of the lateral I-beams, bogie frame rail, pivot support and suspension pivot arm, a single extensometer was used. This 1-inch gauge length extensometer is a high precision instrument, but its displacement range is limited to the elastic strain regime. The information collected in these tests included elastic stress-strain data, yield stress, ultimate load, percent elongation of the failed sample and the reduction in cross-sectional area (R.A.) of the failed sample.

To develop adequate characterization of the trailer's materials for crash analyses, the stress-strain data should encompass as much of the material's behavior as possible up to failure. Since the range of stress-strain data collected in these tests was not sufficient to completely characterize the material response, the information from the tests was used (e.g., yield and ultimate tensile strength) together with information gathered from the literature in Phase B to determine the most probable material classification of the materials.

The tests of the lateral I-beams and bogie frame slider rails showed a yield stress of about 64 ksi (440 MPa) and a maximum stress of about 85 ksi (590 MPa). HSLA steels that generally correspond to these values of yield and ultimate strength (and elongation) are hot formed steel HF T590. The piecewise linear stress-strain values for this steel were used for material specification for the trailer's lateral I-beams and bogie frame slider rails. The tested values of the trailer's pivot support and suspension pivot arm are similar to steels HF 40Y50T and HFY

28

350, respectively. The piecewise linear stress-strain values for those steels were used for material specification for the trailer's pivot support and suspension pivot arm.

In the tests of the kingpin box, bogie frame cross member, bogie main frames, axle tubes, aluminum upper and lower rails, and rear bumper the samples were instrumented with an additional extensometer that was capable of recording displacement through failure of the material. From these tests, sufficient data were available for developing the complete stress vs. strain behavior of the materials to failure.

The following sections of this report discuss the testing procedure and the methodology used in characterizing the materials from the data collected in the tests, followed by a summary of the material characterization.

Test Procedure

Tensile tests were performed on various materials following ASTM E 8 – Standard Test Methods for Tension Testing of Metallic Materials. Specimens were machined using the sheet-type 0.500-inch wide by 2.000-inch gage length standard specimen shown in the ASTM standard. Each specimen was identified by the location from which it was removed from the trailer and placed in labeled bags. Specimen layout was based on best fit and material condition of the available samples.

Testing was done using a 25 Kip MTS hydraulic load frame with a Teststar II digital controller and hydraulic plate grips. MTS 408.21 DC signal conditioners were used for the extensometers. The 1.00-inch gage length high-resolution extensometer (MTS 632.17E-20, s/n 162) was calibrated at 0.0025inch/volt. The full range, 2.00-inch extensometer (MTS 632.25B-20, s/n 553) was calibrated at 0.100 inch/volt.

The 1.00-inch, high resolution extensometer was used in the first set of tests on the cross beams, bogie frame rail, pivot support and suspension pivot arm. A full range, 2.00-inch extensometer was added to the second group of tests on the kingpin box, bogie frame cross member, bogie main frame, axle tube, aluminum upper and lower rails, and rear bumper to capture more detailed data in the plastic strain regime.

The tests were run in displacement control using a ramp-rate of 0.040 inch/min. Data were collected at 0.1 Hertz for the first group of tests and 10 Hertz for the second group. Data channels recorded included time, load, and displacement.

Average area measurements were taken and 2-inch gage length punch marks were added before testing. After testing, the punch marks and final area were measured again to record elongation and reduction of area.

Data Reduction and Material Characterization

Uniaxial tensile tests were conducted in the Battelle laboratories to measure the load-deflection characteristics of the various semitrailer materials. When possible, these data were used to compute the stress-strain relationship for each material. The engineering stress and engineering strain were calculated using the following definitions:

$$\sigma = \frac{load}{A_0}$$

Equation 2. Equation for engineering stress

$$\epsilon = \frac{Displacement}{L_0}$$

Equation 3. Equation for engineering strain

where A_0 is the initial cross-sectional area and L_0 is the initial gauge length of the specimen, respectively.

Figure 32 and Figure 33 show the engineering stress vs. strain plots for the steel components and the aluminum components, respectively. Table 4 provides a summary of the test results including yield stress, maximum engineering stress, percent elongation at failure, and reduction in cross-sectional area at failure (R.A.).
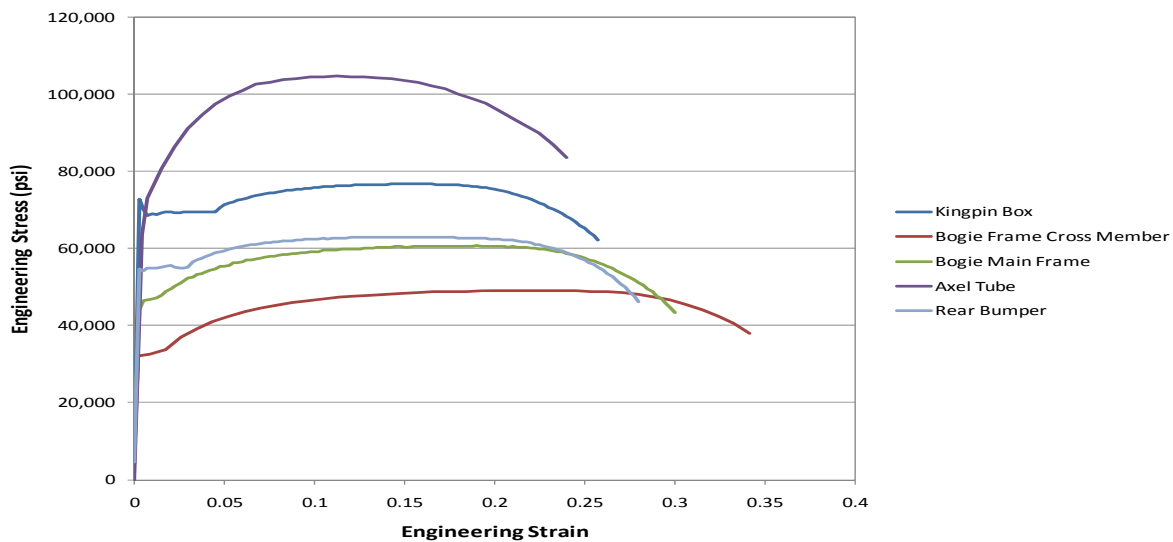
Figure 32. Chart. Engineering stress vs. engineering strain from test results (steel components)

30
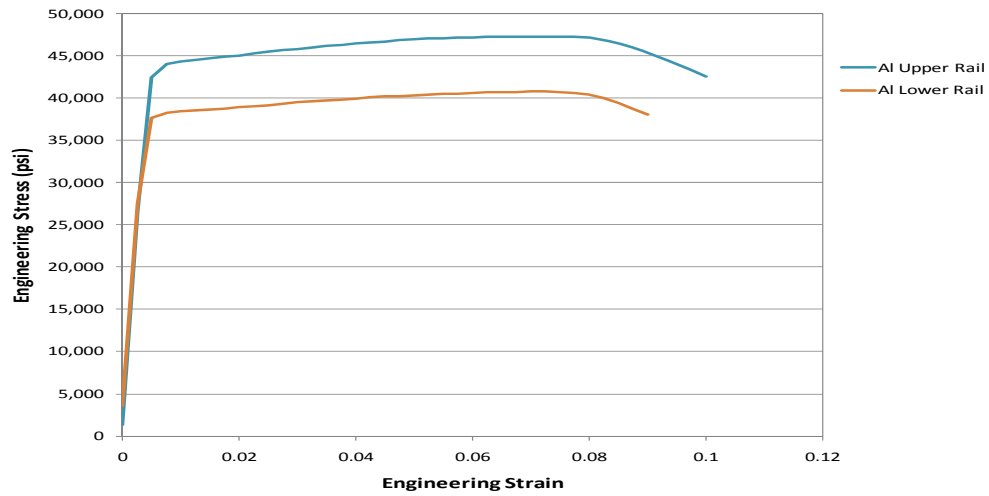
Figure 33. Chart. Engineering stress vs. engineering strain from test results (aluminum components)

Table 4. Summary of trailer materials test results

Part Description	Assumed Material Type	FE Model Part No.	Material No.	Yield Stress (psi)	Ultimate Engineering Stress (psi)	Elongation (%)	R.A.	True Failure Strain
Kingpin Box	Steel	354-358	61	73,047	76,777	27	0.61	0.94
Bogie Frame Cross Member	Steel	31	62	34,551	49,152	35	0.7	1.2
Bogie Main Frame	Steel	30	63	46,508	60,771	30	0.7	1.2
Axle Tube	Steel	2	64	63,508	104,762	26	0.6	0.92
Rear Bumper	Steel	9 and 10	67	55,439	62,978	28	0.65	1.0
Al Upper Rail	Aluminum	351-353	65	43,712	47,344	12	0.33	0.4
Al Lower Rail	Aluminum	48, 71, 72	66	37,900	40,856	11	0.23	0.26
Pivot Support	HF 40Y50T	7	69	42,260	58,072	27	0.66	1.1
Suspension Pivot Arm	HFY 350	12 and 14	8	60,000	71,429	17	0.7	1.2
Bogie Slider Rails	HDGA-HFT 590	29	68	64,400	69,235	18	0.66	1.1
Lateral I-Beam	HDGA-HFT 590	1	68	68,000	90,016	N.R.	0.5	0.69

True Stress – True Strain Characterization

At low levels of strain (e.g., up to three times the yield strain for metals) the material behavior can effectively be characterized using engineering stress-strain. As strains increase, material response must be characterized using the true definitions of stress and strain. In crash events, materials may undergo very large strains; so for crash models it is necessary to develop a representation for the entire stress-strain curve of the material to failure. The definitions for true stress and true strain are:

$$\tilde{\sigma} = \frac{Load}{A}$$

Equation 4. Equation for true stress

$$\tilde{\varepsilon} = \ln(1 + \epsilon)$$

Equation 5. Equation for true strain

where $\tilde{\sigma}$ is true stress, $\tilde{\varepsilon}$ is true strain, A is the actual area during deformation, and ϵ is the engineering strain.

Because it is difficult to accurately measure the area of the specimen during deformation, it is necessary to simplify the equation for true stress using the assumption that during plastic deformation, metals deform at constant volume, i.e., $L_0 A_0 = LA$, where L is the deformed length. Substituting into the expression for $\tilde{\sigma}$ and noting that $(1 + \epsilon) = \frac{L}{L_0}$, the true stress can simply be expressed in terms of the engineering stress-strain values as:

$$\tilde{\sigma} = \sigma(1 + \epsilon)$$

Equation 6. Equation to compute true stress from engineering stress and strain

These definitions are valid for characterizing materials using uniaxial tensile test data up to the onset of necking. After necking begins, strain is no longer uniform over the gauge length of the specimen and can no longer be approximated as an average strain over the gauge length. To accurately determine the strain in the necked region, it is necessary to measure the reduction of area as a function of load during the test and compute strain based on the relationship:

$$\tilde{\varepsilon} = \ln\frac{A}{A_0}$$

Equation 7. Equation to compute true strain from reduction in area

As mentioned previously, it is difficult to accurately measure the area of the specimen during deformation; this is particularly true after necking begins. This creates a problem for defining the stress-strain behavior after the onset of necking.

The approach taken in this project to develop the stress-strain representation of the material through necking and out to material failure was to assume that the plastic flow of the material follows the *Power Law* behavior, expressed as:

$$\tilde{\sigma} = K\tilde{\varepsilon}^n$$

Equation 8. Equation for true stress and true strain power law model

where *K* is the strength coefficient and *n* is the strain-hardening exponent.

This relationship was developed based on the *linear characteristic* of the *log stress* vs. *log strain* curve from experimental data. For example, plotting the true stress-strain curve using Equations 2 and 3 on a log-log scale will result in a curve similar to the curve illustrated in Figure 34, where the curve is linear until the start of necking. The sudden decrease in slope at necking is reflective of using load vs. displacement (i.e., average displacement over gauge length) data rather than load vs. reduction-in-area to compute stress and strain. It is usually assumed that the hardening slope leading up to necking is maintained through necking and continues until failure of the material. This assumption was necessary to develop the true stress-strain curve beyond necking, since only load-displacement data were collected in the tests.
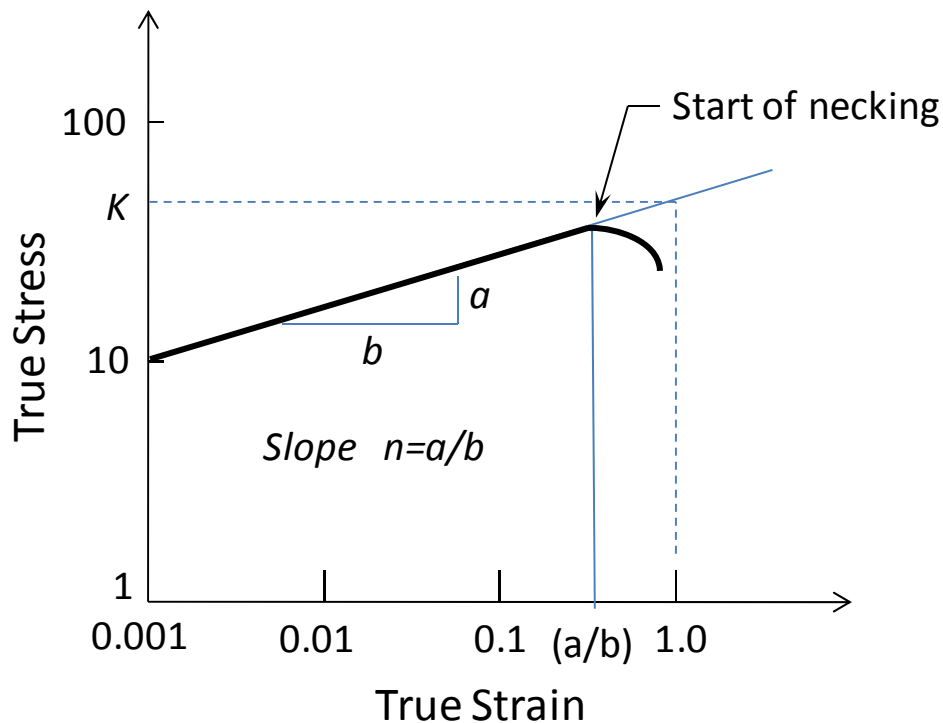
Figure 34. Illustration. Typical illustration of true stress-strain plotted on log-log scale

In many cases, the plots will be bi-linear because the hardening slope just after yielding is softer than the subsequent slope. For example, in Figure 32, all the materials would be expected to

33

display a bi-linear hardening curve except for the axle tube material. Figure 35 shows the test results (the green curve) for the axle tube material and the bogie main frame material plotted on a log-log plot. The blue curves in Figure 71 show the projection of the test data based on the assumption that the hardening slope remains constant through necking until failure. The projected log-log curves were then used to develop the true stress-strain characterization of the materials.

(a)   (b)
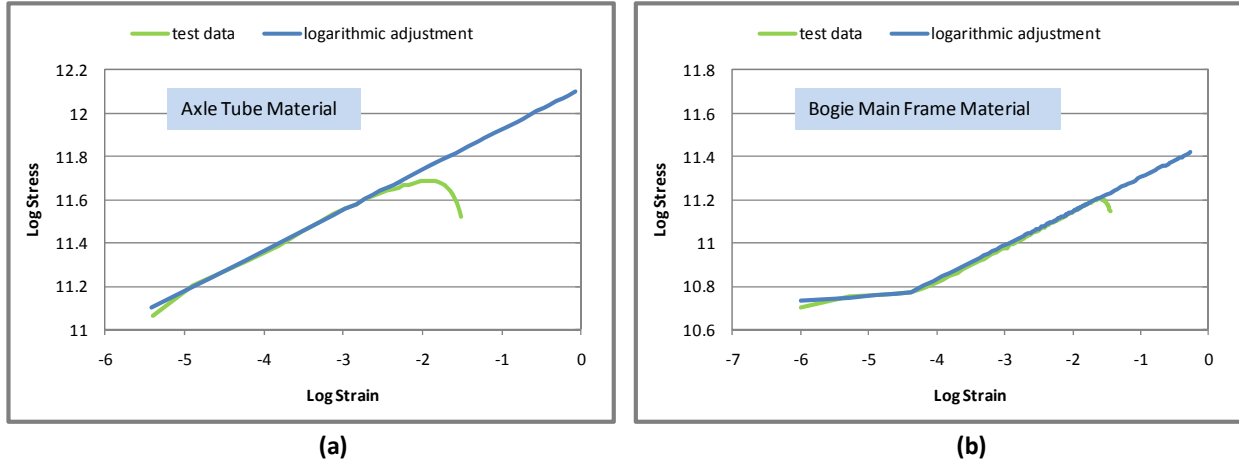
Figure 35. Chart. Log-log plot of stress vs. strain for (a) axle tube and (b) bogie main frame

The Ls-Dyna Piecewise-Linear-Plasticity model (MAT 24) was used to model the material response. This material model requires true stress vs. true *plastic* strain data. The true plastic strain is computed by subtracting the elastic strain from the true strain values:

$$\tilde{\varepsilon}_p = \tilde{\varepsilon} - \frac{\tilde{\sigma}}{E}$$

Equation 9. Equation for true plastic strain

Where $\tilde{\varepsilon}_p$ is the true plastic strain and E is Young's modulus.

The resulting true stress vs. true plastic strain curves for the material are shown in Figure 36 and Figure 37 for the steel materials and aluminum materials, respectively.

Another important characteristic of the materials is the true fracture ductility, which is often referred to simply as failure strain. The failure strain is defined by:

$$\tilde{\varepsilon}_f = ln\left(\frac{A_0}{A_f}\right) = ln\frac{1}{1 - RA}$$

Equation 10. Equation for failure strain

Where *RA* is the reduction in area, defined by:

$$RA = \frac{A_0 - A_f}{A_0}$$

Equation 11. Equation for reduction in area

Table 4 (above) provides the failure strain values computed for each material using the above relationships.
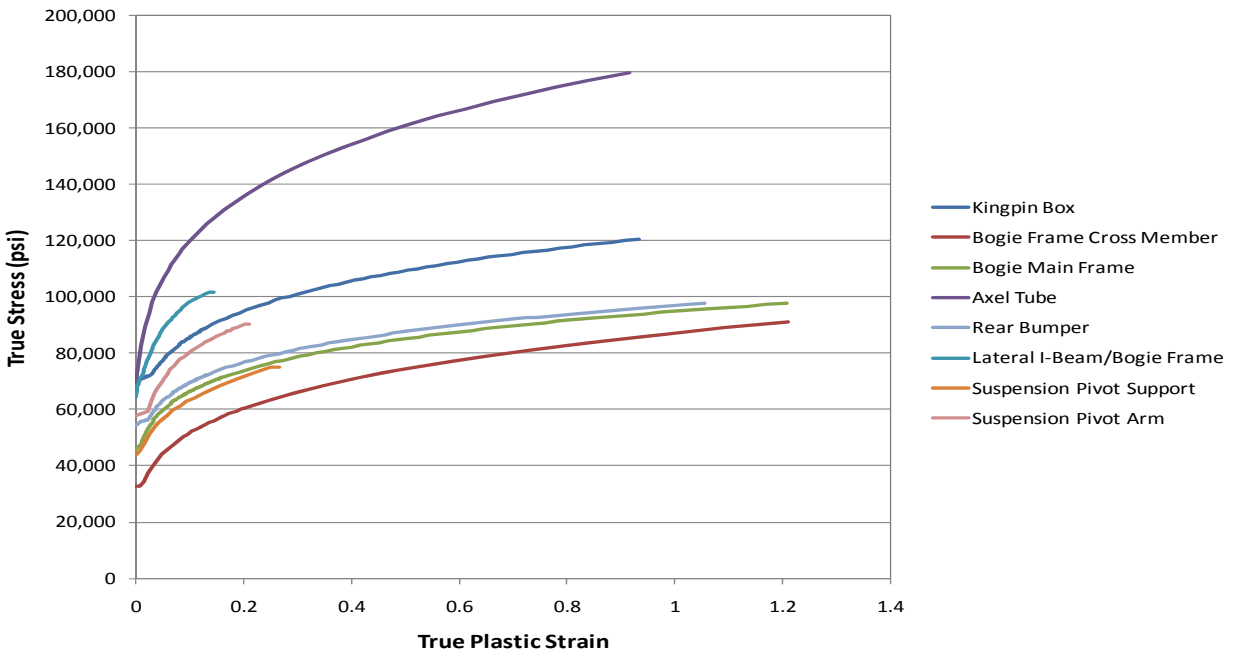
Figure 36. Chart. True stress vs. true plastic strain (steel components)
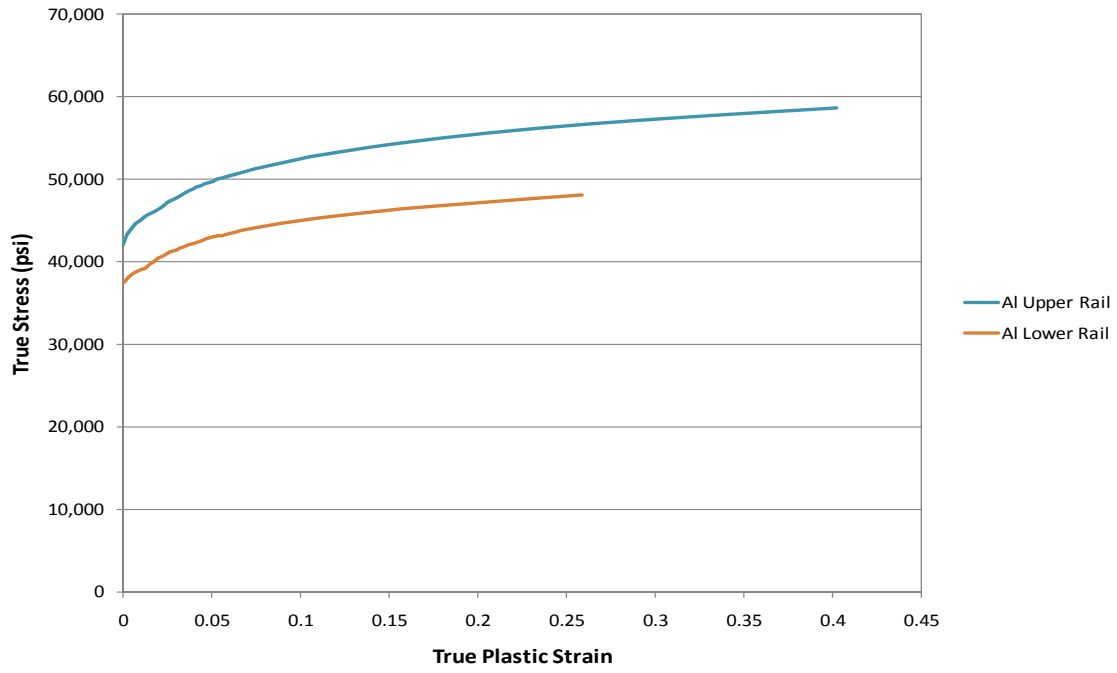
Figure 37. Chart. True stress vs. true plastic strain (aluminum components)

Chapter 3 – Model Results and Qualitative Evaluation of the Tractor-Semitrailer Model

Introduction

Scope

The scope of this task was to continue to validate the tractor-semitrailer FE model performance by comparison of the computer simulation results with full-scale tractor-semitrailer crash tests results. These comparisons were conducted according to the new verification and validation procedures for using computer simulations in roadside safety applications being developed in NCHRP Project 22-24 [4].

Approach

A primary objective of the study is to determine the overall fidelity of the tractor-semitrailer FE model by comparing simulation vehicle response with real vehicle response. Crash test data from a number of full-scale crash tests involving tractor-semitrailer impacts into roadside safety barriers were collected from the Texas Transportation Institute (TTI) and Midwest Roadside Safety Facility (MwRSF) during the first phase of the program. The data obtained from these reports were used as a gauge to further measure model fidelity.

The automated dimensional adjustment program (ADAP), developed by Oak Ridge National Laboratory (ORNL) in Phase B, was used to modify the tractor and semitrailer models to represent the properties of test vehicles from two crash tests. This allowed the research team to simulate those tests to provide a broader assessment of the model's efficacy, and ultimately, provide a better quantification of the model's validity. The team assessed the results generated by the model by comparing the kinematic behavior and failure modes of the combined tractor-semitrailer model to the behavior and failure modes of the test vehicle in the full-scale tractor-semitrailer crash tests. Based on this assessment, any deficiencies in the model that are deemed critical for accurately simulating vehicle response in impacts with roadside safety hardware were identified, and corrections to the model were implemented within the available program budget.

Validation is a comparison of the simulation and experiment to determine the degree to which a model is an accurate representation of the real world from the perspective of its intended use. Currently, there are no specific guidelines for validation of numerical models. Models commonly used in crash analyses of roadside safety barriers are typically validated only through a "qualitative" evaluation of simulation results compared to test results. Battelle teamed with researchers from WPI and Polytechnico Di Milano to conduct a study sponsored by the NCHRP (Project 22-24) that developed verification and validation procedures for using computer simulations in roadside safety applications. The NCHRP 22-24 project final report was submitted in March 2010 and is currently in review by the project panel members.

The performance of the Phase C tractor-semitrailer FE model (which includes the improvements described in the earlier sections of this report) was assessed by comparing simulation results to:

- The results of full-scale crash test TL5CMB-2 conducted at the Midwest Roadside Safety Facility (MwRSF) in July 2007 [5] and
- The results of full-scale crash test TTI 7069-13 conducted at TTI in July 1988 [6].

The basic differences in these two tests were the ballasted weight of the trailer and the trailer length. The ballasted weight for the test vehicle in test TL5CMB-2 was 79,705 lb (36,153 kg) and the ballasted weight for the test vehicle in test 7069-13 was 50,050 lb (22723 kg). Test TL5CMB-2 involved a 48-ft trailer, while test 7069-13 involved a 45-ft trailer.

The following sections present a summary of the tractor-semitrailer FE model and an evaluation of the results of the model compared to the full-scale crash tests. This chapter is organized under the following topic headings:

- Overview of the MwRSF Crash Test TL5CMB-2

- FE Model for TL5CMB-2 Simulation

- Qualitative Comparison of Simulation Results with Test TL5CMB-2

- Overview of the TTI Crash Test 7069-13

- FE Model for Simulation of Test 7069-13

- Qualitative Comparison of Simulation Results with Test

Overview of the MwRSF Crash Test TL5CMB-2

Test TL5CMB-2 was conducted by MwRSF to evaluate the crash performance of a new concrete median barrier design according to the testing guidelines of NCHRP Report 350 for Test Level 5 impact conditions. The test involved a 79,705-lb (36,153-kg) tractor-semitrailer vehicle impacting a concrete median barrier at 52.7 mph (84.9 km/hr) and impact angle of 15.4 degrees. The test vehicle was a 1991 White GMC tractor with a 1988 Pines 48-ft (14.6-m) semitrailer. The test article was a 42 inch (1.067 m) tall concrete median barrier with an installation length of 200 ft (60.9 m). Figure 38 shows the test vehicle and barrier with dimensions labeled. The geometric dimensions and mass inertial measurements of the test vehicle are provided in Figure 39.

The acceleration data from the test were collected using triaxial piezoresistive accelerometers, and the angular velocities were collected using Analog Systems 3-axis rate transducer. The Electronic Recording Devices (ERDs) were mounted at two locations: 1) the primary ERD set was mounted to the trailer floor on the inside of the trailer near the tandem axles of the trailer

and 2) the secondary ERD set was mounted near the tractor tandem axles. Unfortunately, data were not recorded for the secondary ERD set due to a premature triggering of the ERD. Four AOS high-speed video cameras with recording speeds of 500 frames/sec and six digital video cameras with recording speeds of approximately 30 frames per second were used to film the crash test.

(a) Test Vehicle

(b) Test Article

Figure 38. Photograph. (a) Tractor-semitrailer vehicle and (b) 1.067 m tall concrete median barrier used in MwRSF Test No. TL5CMB-2

Date:	7/12/2007		Test Number:	MwRSF Test No. TL5CMB-2

Tractor:
VIN No,:	4V1JLBJEGMR810558	Make:	White/GMC	Model:	WG65T
Year:	1991	Odometer:	137548		

Trailer:
VIN No,:	1p10748254jka29485	Make:	Pines 48'	Model:	48' Van
Year:	1988				

*All Measurements Refer to Impacting Side
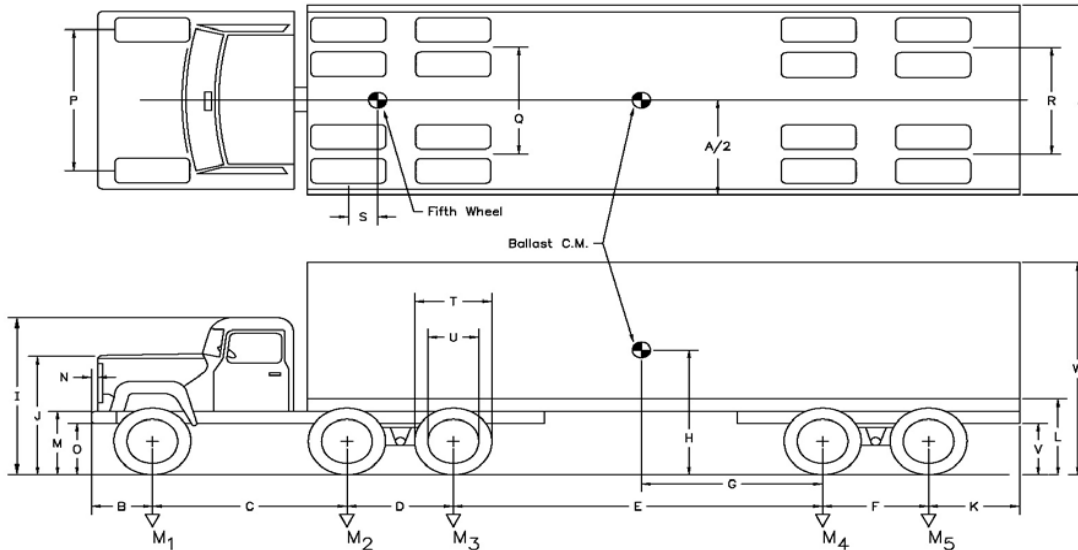
Vehicle Geomerty -mm (in)

A	2,604	(102.5)	G	5,906	(232.5)	N	0	(0.0)	T	1,016	(40.0)
B	1,314	(51.7)	H	1,831	(72.1)	O	584	(23.0)	U	597	(23.5)
C	3,270	(128.7)	J	1,746	(68.7)	P	2,007	(79.0)	V	781	(30.7)
D	1,334	(52.5)	K	1,575	(62.0)	Q	1,842	(72.5)	W	4,064	(160.0)
E	10,185	(401.0)	L	1,156	(45.5)	R	1,981	(78.0)	X	NA	
F	1,257	(49.5)	M	902	(35.5)	S	533	(21.0)			

Mass -Properties

		Curb		Test Inertial		Gross Static	
M_1	kg (lb)	3,973	(8,759)	4,441	(9,791)	4,441	(9,791)
$M_2 + M_3$	kg (lb)	5,144	(11,341)	17,017	(37,516)	17,017	(37,516)
$M_4 + M_5$	kg (lb)	3,955	(8,719)	14,696	(32,399)	14,696	(32,399)
M_{Total}	kg (lb)	13,073	(28,821)	36,154	(79,706)	36,154	(79,706)
I_{11}	kg - m^2 (lb-ft^2)		(0)		(0)		(0)
I_{22}	kg - m^2 (lb-ft^2)		(0)		(0)		(0)
I_{33}	kg - m^2 (lb-ft^2)		(0)		(0)		(0)

Figure 39. Illustration. Dimensions of the MwRSF Test No. TL5CMB-2 test vehicle

40

FE Model for TL5CMB-2 Simulation

The geometry of the tractor FE model was modified such that the wheelbase of the model was the same as the wheelbase of the test vehicle used in MwRSF Test No. TL5CMB-2. FE analysis was conducted simulating this test using the tractor-semitrailer FE model (model versions tractor_10-0520 and trailer_10-0521). The friction between the tractor and barrier was set to 0.2, and the friction between the tires and the barrier was set to 0.65. The dimensions of the barrier model were the same as those of the barrier in MwRSF Test No. TL5CMB-2 shown in Figure 38. Since there was negligible deflection of the barrier in the full-scale test, the barrier was modeled as a rigid material with rigid fixity to the ground. The impact conditions for the FE simulation were consistent with those reported in the full-scale crash test (i.e., 52.7 mph (84.9 km/hr) at an impact angle of 15.4 degrees).

The ADAP program (described previously) was used to aid in the modification of overall vehicle model size and shape parameters (e.g., wheelbase, trailer length). These scripts were designed to operate on the FE model input file directly and were used to modify the tractor model geometry.

The ADAP scripts were used to: 1) make the sleeper-cab tractor a day-cab style tractor by removing the sleeper section of the cabin and 2) adjust the wheelbase length of the tractor by removing a section of the frame rails (along with other components in this section of the model). Figure 40 shows a visual comparison between the tractor FE model and the test tractor. The geometric and mass/inertial properties of the modified tractor-semitrailer model are shown in Figure 41. A comparison of the dimensions of the FE model to the test vehicle is shown in Figure 42.

The most notable differences between the test vehicle and modified FE model are:

Length dimensions – The length dimensions of the FE model were all within 2% of the test vehicle dimensions, except for the distance from the front bumper to the center of the front wheel (e.g., dimension "B" in
- Figure 42), which was 13.5% shorter in the FE model.

- *Trailer box dimensions* – The trailer floor in the FE mo*del was 5.8 inches (14*8 mm) higher than the test vehicle (e.g., dimension "L" in Figure 42), and the top of the trailer in the FE model was 6.7 inches (169 mm) lower than the test vehicle (e.g., dimension "W" in Figure 42).

- *Ballast center of gravity (c.g.)* – The c.g. of the ballast in the FE model was located 23.6 inches (600 mm) rearward of and 4.6 inches (188 mm) higher than the c.g. location of the ballast in the test vehicle.

- *Trailer suspension* – The suspension system on the FE trailer model was the Airide™ design, and the suspension on the trailer test vehicle was a leaf-spring design.
- *Propulsion – The te*st vehicle was under engine power with drive-train engaged for the duration of the impact event. The analysis model was not.

(a) Test Vehicle
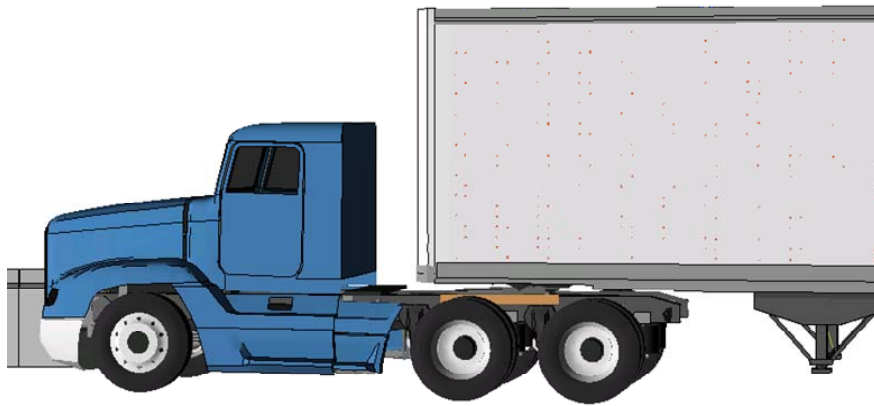
(b) FE Model

Figure 40. Photograph / Illustration. (a) Tractor test vehicle and (b) Tractor FE model

Date: 5/20/2009 Test Number: Battelle Simulation No. TT090518

Tractor:
  Model: __01a_Trac_Day_v1a_0900506.k__ Make: ____Freightliner____ Model: ____FLD120____
  Year:

Trailer:
  Model: 02b_SemiTrailer48_09-0520.k Make: ____Stoughton____ Model: __48-ft Box Trailer__
  Year: ____1990____

*All Measurements Refer to Impacting Side
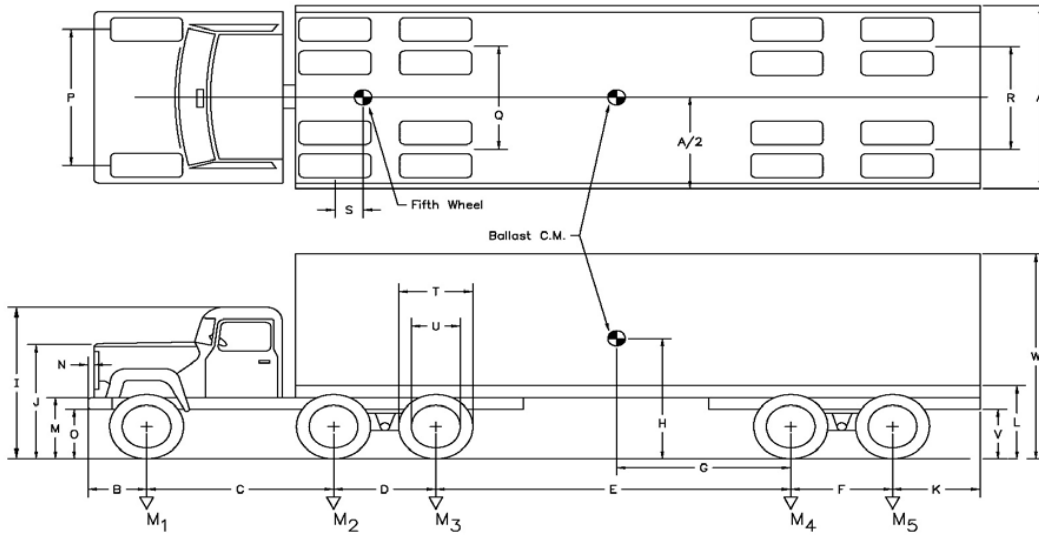
Vehicle Geomerty -mm (in)

A	2,636	(103.8)	G	5,307	(208.9)	N			T	1,004	(39.5)
B	1,136	(44.7)	H	1,949	(76.7)	O	518	(20.4)	U	592	(23.3)
C	3,280	(129.1)	J	1,734	(68.3)	P	1,929	(75.9)	V	926	(36.5)
D	1,265	(49.8)	K	1,552	(61.1)	Q	1,906	(75.0)	W	3,895	(153.3)
E	10,188	(401.1)	L	1,304	(51.3)	R	2,045	(80.5)			
F	1,245	(49.0)	M	726	(28.6)	S	460	(18.1)			

Mass -Properties

		Curb		Test Inertial		Gross Static	
M_1	kg (lb)		(0)	4,040	(8,907)	4,040	(8,907)
$M_2 + M_3$	kg (lb)		(0)	17,570	(38,735)	17,570	(38,735)
$M_4 + M_5$	kg (lb)		(0)	14,590	(32,165)	14,590	(32,165)
M_{Total}	kg (lb)	13,100	(28,881)	36,200	(79,807)	36,200	(79,807)
I_{11}	kg - m^2 (lb-ft^2)	16,020	(115,870)	31420	(227,256)	31420	(227,256)
I_{22}	kg - m^2 (lb-ft^2)	474,300	(3,430,541)	863,200	(6,243,396)	863,200	(6,243,396)
I_{33}	kg - m^2 (lb-ft^2)	473,800	(3,426,924)	866,300	(6,265,818)	866,300	(6,265,818)

Figure 41. Illustration. Dimensions of the tractor-semitrailer FE vehicle model

43
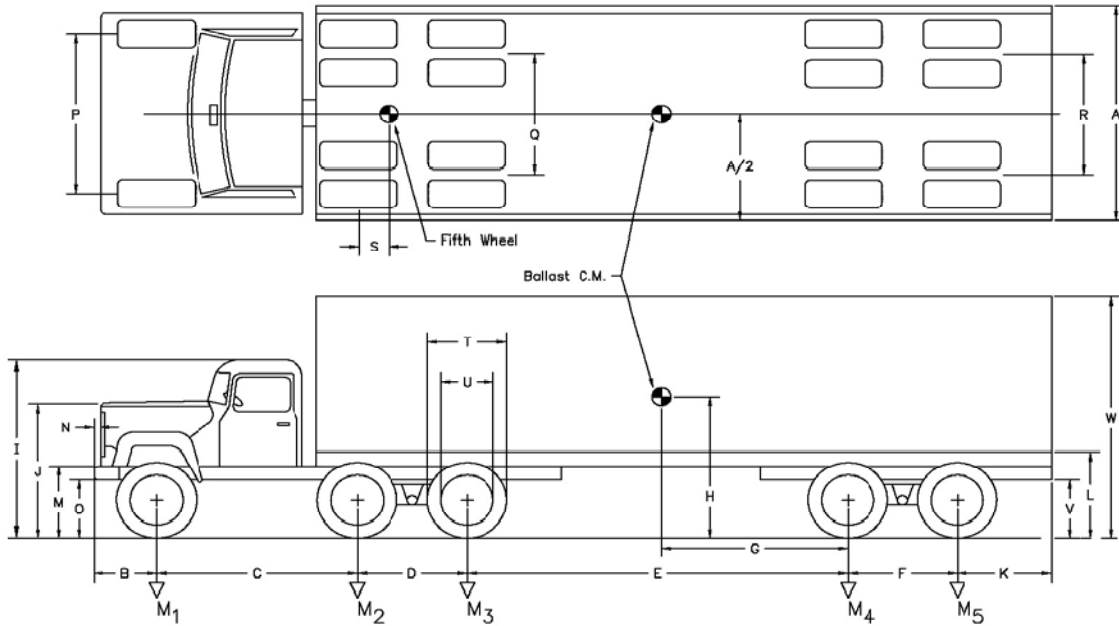
Vehicle Geomerty (inches)

	Test Vehicle	FE Model	Error %		Test Vehicle	FE Model	Error %		Test Vehicle	FE Model	Error %		Test Vehicle	FE Model	Error %
A	102.5	103.8	1.2	G	232.5	208.9	-10.1	N				T	40.0	39.5	-1.2
B	51.7	44.7	-13.5	H	72.1	76.7	6.4	O	23.0	20.4	-11.3	U	23.5	23.3	-0.8
C	128.7	129.1	0.3	J	68.7	68.3	-0.7	P	79.0	75.9	-3.9	V	30.7	36.5	18.6
D	52.5	49.8	-5.2	K	62.0	61.1	-1.5	Q	72.5	75.0	3.5	W	160.0	153.3	-4.2
E	401.0	401.1	0.0	L	45.5	51.3	12.8	R	78.0	80.5	3.2				
F	49.5	49.0	-1.0	M	35.5	28.6	-19.5	S	21.0	18.1	-13.7				

Mass -Properties

		Curb			Test Inertial			Gross Static		
		Test Vehicle	FE Model	Error %	Test Vehicle	FE Model	Error %	Test Vehicle	FE Model	Error %
M_1	(lbf)	8,759	-	-	9,791	8,907	-9.0	21,584	19,635	-9.0
$M_2 + M_3$	(lbf)	11,340	-	-	37,516	38,735	3.2	82,707	85,395	3.2
$M_4 + M_5$	(lbf)	8,719	-	-	32,399	32,165	-0.7	71,426	70,911	-0.7
M_{Total}	(lbf)	28,821	28,880	0.2	79,705	79,807	0.1	175,718	175,941	0.1
I_{11}	(kg - m^2)	-	16,020	-	-	31420	-	-	31420	-
I_{22}	(kg - m^2)	-	474,300	-	-	863,200	-	-	863,200	-
I_{33}	(kg - m^2)	-	473,800	-	-	866,300	-	-	866,300	-

Figure 42. Illustration. Comparison of FE vehicle model dimensions to those of the test vehicle

Although the mass of the test tractor was not reported, it was estimated to be 15,526 lb (7,043 kg) by considering that the total gross static mass of the test vehicle was 28,819 lb (13,073 kg) and that the typical mass of a 48-ft (14.6-m) semitrailer is approximately 13,300 lb (6,030 kg). For comparison, the mass of the FE tractor model was 15,271 lb (6,927 kg). The axle loads of the FE model were within 10% of the axle loads measured on the test vehicle. The total mass of the FE tractor-semitrailer model was 79,807 lb (36,200 kg), which was 0.1% higher than the total mass of the test vehicle.

The analysis was conducted with a time-step of 1.20 microseconds for a time period of 3.0 seconds. The suspension systems on the tractor and trailer models were initialized based on the weight of the model; however, the model was not at steady state at the beginning of the analysis. The tractor-semitrailer model was positioned at 15.4 ft (4.7 m) upstream of the impact point at the start of the analysis to allow 0.2 seconds for gravity to sufficiently load the suspension of the tractor and trailer prior to impact. The trailer's response is somewhat affected by the additional vertical dynamics associated with the sudden 'drop' of the ballast under gravity, which will be discussed in more detail in the Chapter 5 – Summary and Discussion of Results section.

Summary of Key Phenomenological Events from the Tractor-Trailer FE Model Simulation

The exact timing of phenomenological events was not possible because simulation results were only collected at 0.01 second intervals throughout the FE analysis. Therefore, a 0.01 second time window corresponding to range of time for which the event could have occurred in the analysis was reported.

The tractor began to yaw between 0.02 seconds and 0.03 seconds. The left front tires of the tractor lifted off the ground between 0.09 and 0.10 seconds. The right front corner of the trailer was vertically coincident with the front face of the barrier between 0.17 and 0.18 seconds. At 0.24 to 0.25 seconds, the trailer visibly started to roll toward the barrier. The left rear tires of the tractor were lifted off the ground between 0.22 and 0.23 seconds. Both rear trailer tires were lifted off the ground between 0.34 and 0.35 seconds. Between 0.27 and 0.28 seconds the right front corner was vertically coincident with the back face of the barrier.

The tractor became parallel to the barrier between 0.29 and 0.30 seconds. The tractor reached a peak roll angle at 0.29 and 0.3 seconds. The left front tractor tires returned to the roadway surface between 0.31 and 0.32 seconds.

The trailer was parallel to the barrier between 0.63 and 0.64 seconds. The rear trailer tandem wheels impacted the barrier between 0.65 and 0.66 seconds. Between 0.75 and 0.76 seconds the tractor rolled back to level position. The tractor started to roll back toward the barrier between 0.81 and 0.82 seconds.

At 1.1 seconds, the trailer reached maximum roll angle of 40.2 degrees (computed from the accelerometer at the trailer tandem). A maximum roll angle of 42 degrees was measured from the full-scale crash test video. The tractor reached another peak roll angle of 20.1 degrees between 1.16 and 1.17 seconds, compared to approximately 19 degrees measured from the full-scale crash test video. The tractor front-left wheel returned to the roadway surface between 1.45 and 1.46 seconds. The tractor left-side tandem wheels returned to the roadway surface between 1.50 and 1.51 seconds. The trailer tandems returned to the roadway surface between 1.78 and 1.80 seconds.

At 1.8 seconds the trailer was rolled back to level position and continued its counterclockwise roll. At 1.9 seconds the right-side trailer tandems started to rub against and ride up the barrier. At 2.1 seconds the trailer reached a maximum counter-clockwise roll angle of 8.35 degrees. The right-side trailer tandems returned to the roadway between 2.55 and 2.6 seconds. The analysis ended at 3.0 seconds, at which time:

- The trailer was rolling back toward the barrier with a roll angle of 1.8 degrees

- The tractor and trailer were approximately parallel to the barrier and still in contact

- The forward velocity of the tractor was 27.24 mph (43.84 km/hr).

Qualitative Comparison of Simulation Results with Test TL5CMB-2

Phenomenological Events

A qualitative assessment was made by comparing sequential snapshots of the full-scale crash test with the results of the simulation to verify vehicle kinematic response, as well as sequence and timing of key phenomenological events. Figure 43, Figure 44 and Figure 45 show sequential snapshots of the impact event from a downstream viewpoint, an upstream viewpoint, and from an oblique (downstream and behind the barrier) viewpoint, respectively. These figures show still images clipped from the test video next to a screen snapshot from the FE simulation at the corresponding time. Note that the test video images were only available through 1.7 seconds.

The FE model simulates the basic kinematic behavior of the tractor-semitrailer reasonably well, and adequately captures the basic phenomenological events that occur during impact. Table 5 provides a list of phenomenological events and their time of occurrence for both the full-scale crash test and the FE simulation.

a. Time = 0.000

b. Time = 0.1 second

c. Time = 0.2 second

Figure 43. Photograph / Illustration. Sequential views of MwRSF Test TL5CMB-2 and FE model simulation from a downstream viewpoint

47

d. Time = 0.3 second
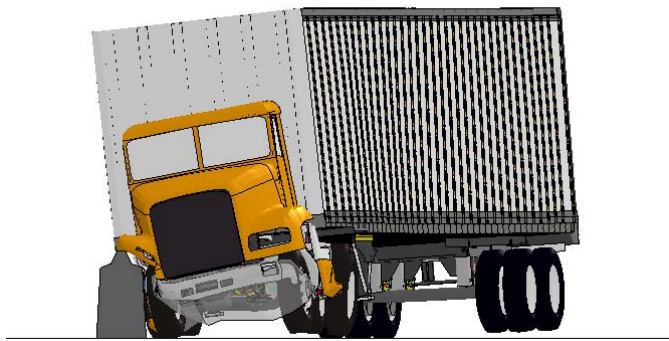
e. Time = 0.4 second
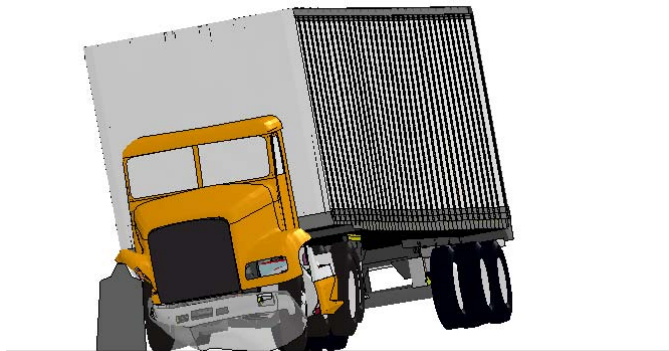
f. Time = 0.5 second
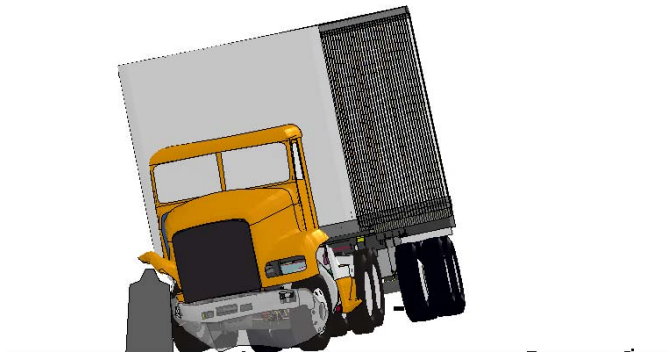
Figure 43. [CONTINUED] Photograph / Illustration. Sequential views of MwRSF Test TL5CMB-2 and FE model simulation from a downstream viewpoint

g. Time = 0.6 second

h. Time = 0.7 second

i. Time = 0.8 second
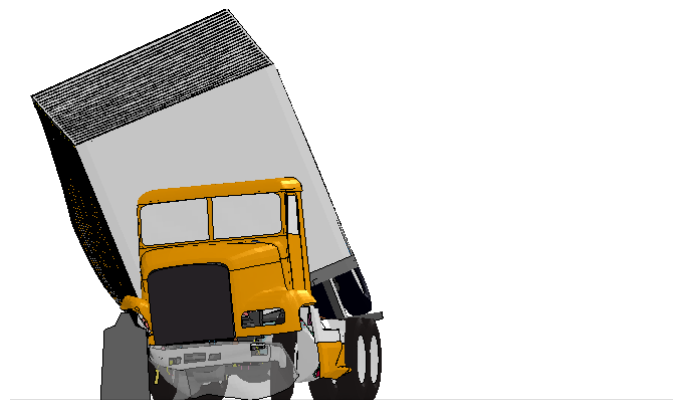
Figure 43. [CONTINUED] Photograph / Illustration. Sequential views of MwRSF Test TL5CMB-2 and FE model simulation from a downstream viewpoint

j.   Time = 0.9 second

k.   Time = 1.0 second

l.   Time = 1.1 second

Figure 43. [CONTINUED] Photograph / Illustration. Sequential views of MwRSF Test TL5CMB-2 and FE model simulation from a downstream viewpoint

m. Time = 1.2 second
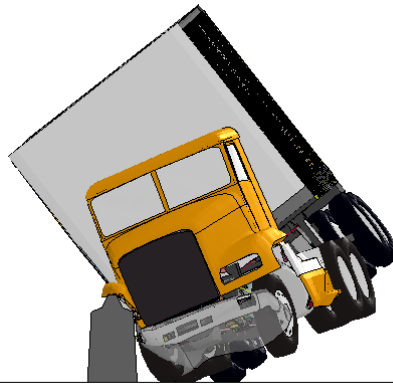
n. Time = 1.3 second
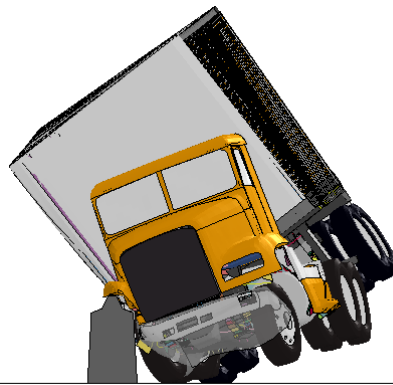
o. Time = 1.4 second

Figure 43. [CONTINUED] Photograph / Illustration. Sequential views of MwRSF Test TL5CMB-2 and FE model simulation from a downstream viewpoint

51

p. Time = 1.5 second
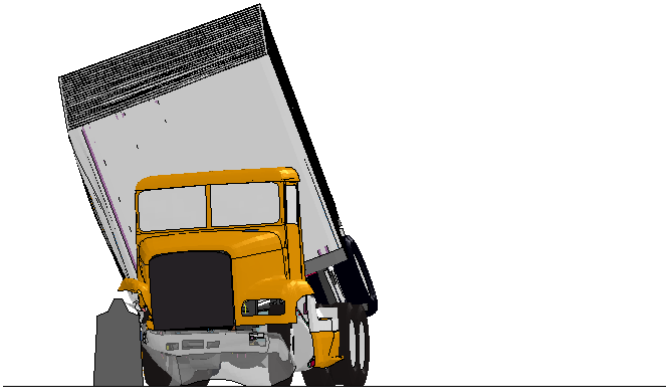
q. Time = 1.6 second

r. Time = 1.7 second

Figure 43. [CONTINUED] Photograph / Illustration. Sequential views of MwRSF Test TL5CMB-2 and FE model simulation from a downstream viewpoint

52
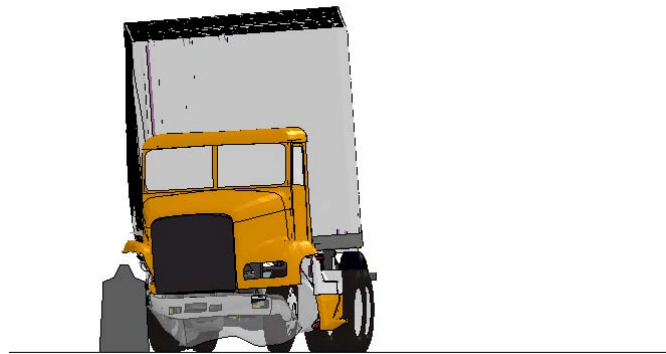
s. Time = 1.8 second

t. Time = 1.9 second

u. Time = 2.0 second

Figure 43. [CONTINUED] Illustration. Sequential views of MwRSF Test TL5CMB-2 and FE model simulation from a downstream viewpoint

v.   Time = 2.3 second

Figure 43. [CONTINUED] Illustration. Sequential views of MwRSF Test TL5CMB-2 and FE model simulation from a downstream viewpoint

a. Time = 0.000

b. Time = 0.1 second

c. Time = 0.2 second

**Figure 44. Photograph / Illustration. Sequential views of MwRSF Test TL5CMB-2 and
FE model simulation from an upstream viewpoint**

d. Time = 0.3 second
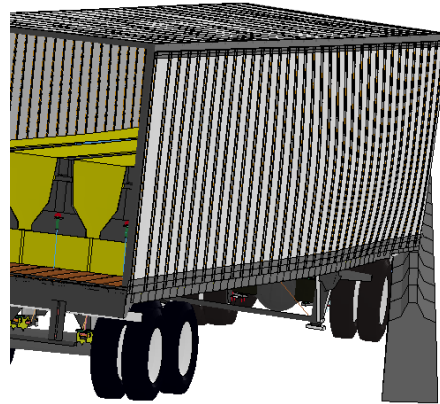
e. Time = 0.4 second
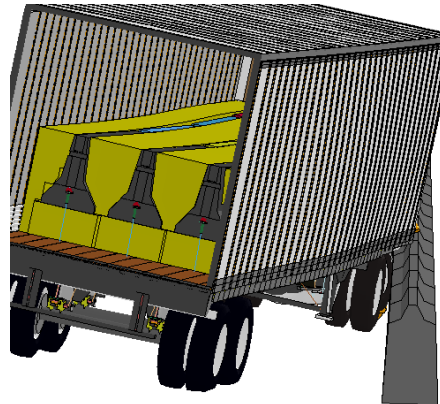
f. Time = 0.5 second
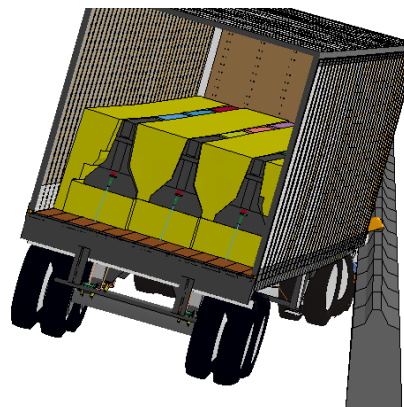
Figure 44. [CONTINUED] Photograph / Illustration. Sequential views of MwRSF Test TL5CMB-2 and FE Model simulation from an upstream viewpoint

g. Time = 0.6 second
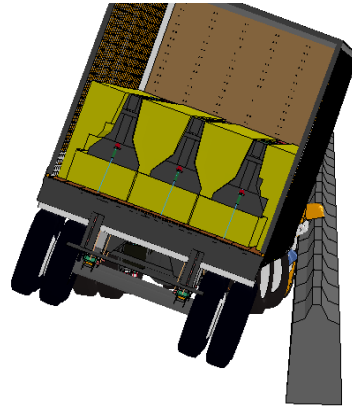
h. Time = 0.7 second
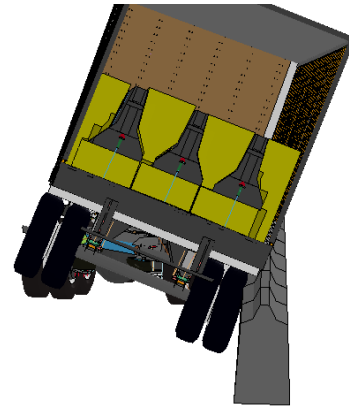
i. Time = 0.8 second
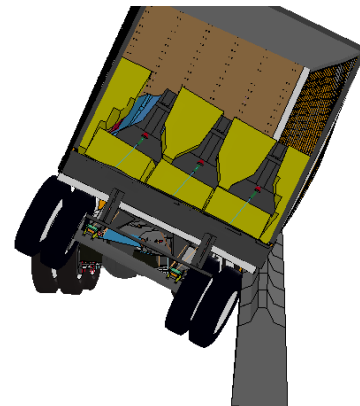
Figure 44. [CONTINUED] Photograph / Illustration. Sequential views of MwRSF Test TL5CMB-2 and FE Model simulation from an upstream viewpoint

j. Time = 0.9 second

k. Time = 1.0 second

l. Time = 1.1 second

Figure 44. [CONTINUED] Photograph / Illustration. Sequential views of MwRSF Test TL5CMB-2 and FE Model simulation from an upstream viewpoint

58

m. Time = 1.2 second
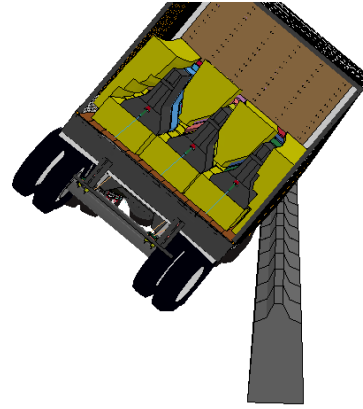
n. Time = 1.3 second
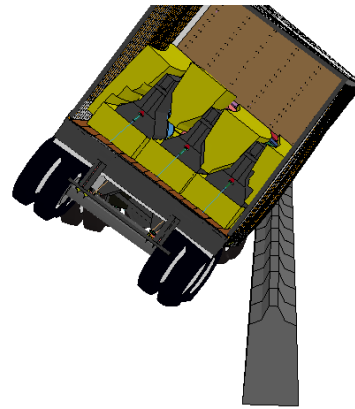
o. Time = 1.4 second
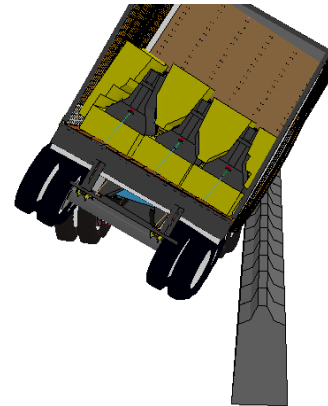
Figure 44. [CONTINUED] Photograph / Illustration. Sequential views of MwRSF Test TL5CMB-2 and FE Model simulation from an upstream viewpoint

p. Time = 1.5 second
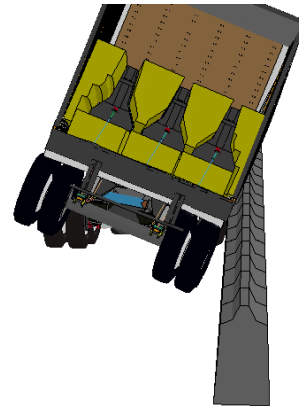
q. Time = 1.6 second
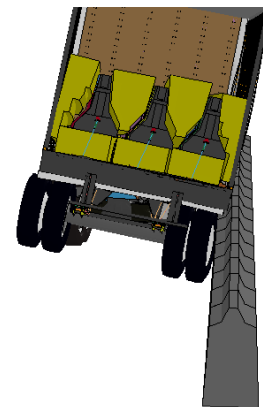
r. Time = 1.7 second

Figure 44. [CONTINUED] Photograph / Illustration. Sequential views of MwRSF Test TL5CMB-2 and FE Model simulation from an upstream viewpoint

60
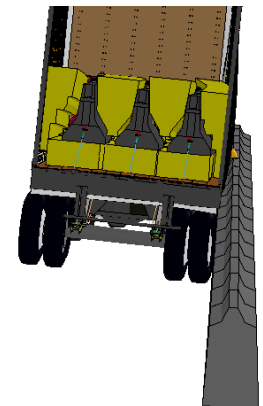
s.   Time = 1.8 second

t.   Time = 1.9 second

u.   Time = 2.0 second

Figure 44. [CONTINUED] Illustration. Sequential views of MwRSF Test TL5CMB-2 and FE Model simulation from an upstream viewpoint

v.   Time = 2.3 second

w.   Time = 2.6 second
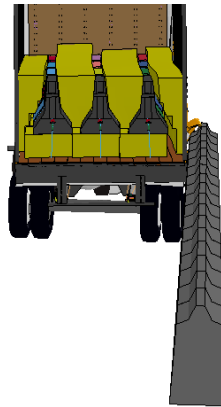
Figure 44. [CONTINUED] Illustration. Sequential views of MwRSF Test TL5CMB-2 and FE Model simulation from an upstream viewpoint

a. Time = 0.000

b. Time = 0.1 second

c. Time = 0.2 second
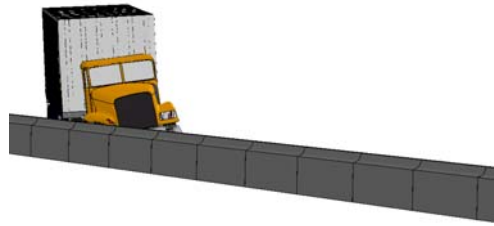
d. Time = 0.3 second
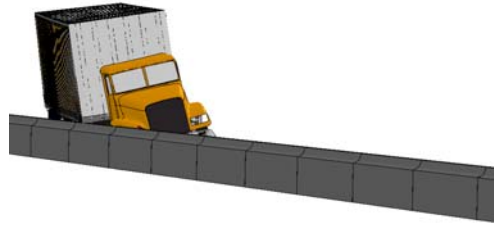
e. Time = 0.4 second
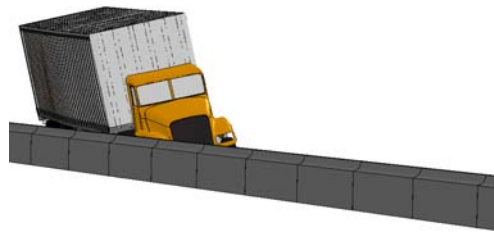
Figure 45. Photograph / Illustration. Sequential views of MwRSF Test TL5CMB-2 and FE model simulation from an isometric viewpoint

63

f. Time = 0.5 second
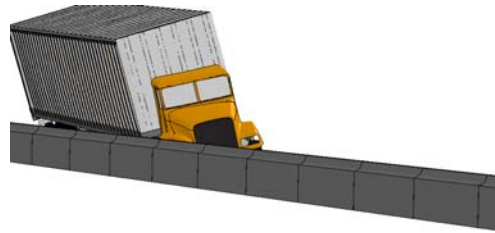
g. Time = 0.6 second
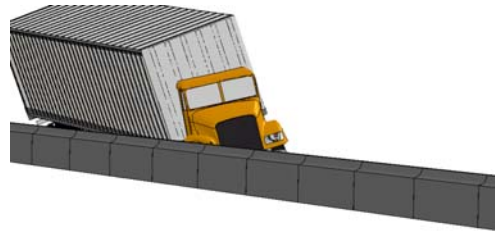
h. Time = 0.7 second
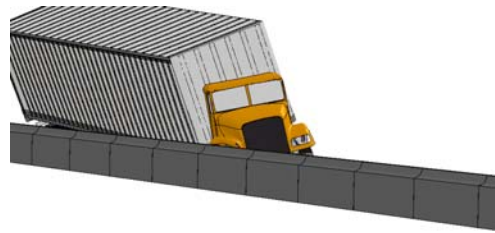
i. Time = 0.8 second
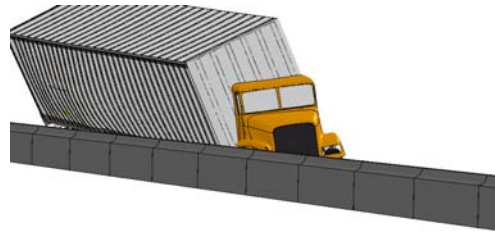
j. Time = 0.9 second
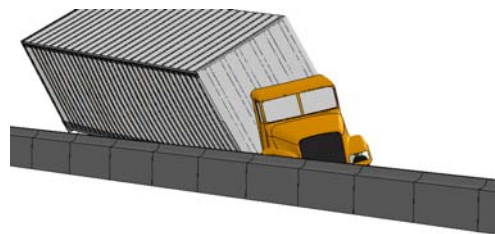
Figure 45. [CONTINUED] Photograph / Illustration. Sequential views of MwRSF Test TL5CMB-2 and FE model simulation from an isometric viewpoint

k. Time = 1.0 second

l. Time = 1.1 second
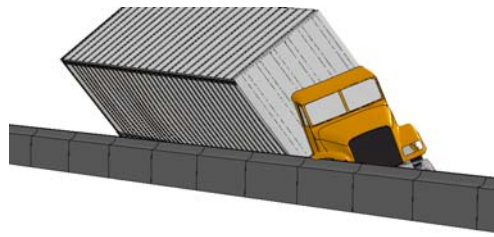
m. Time = 1.2 second
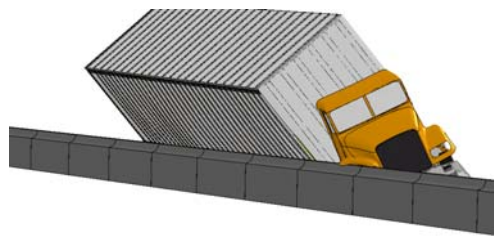
n. Time = 1.3 second
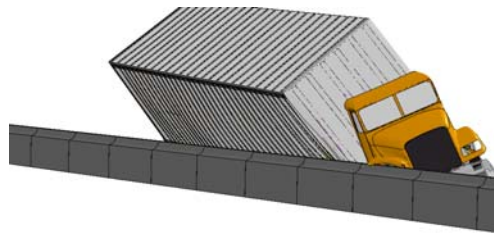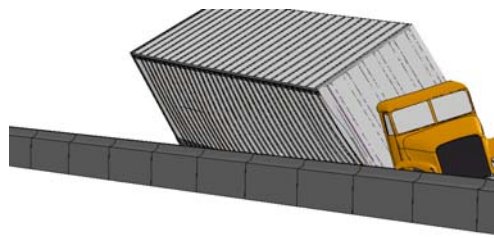
o. Time = 1.4 second

Figure 45. [CONTINUED] Photograph / Illustration. Sequential views of MwRSF Test TL5CMB-2 and FE model simulation from an isometric viewpoint

65

p.   Time = 1.5 second
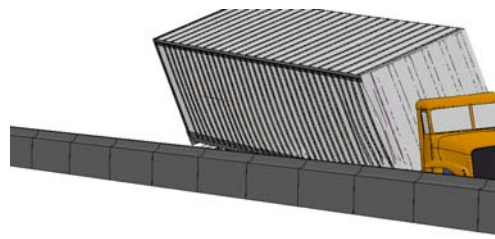
q.   Time = 1.6 second
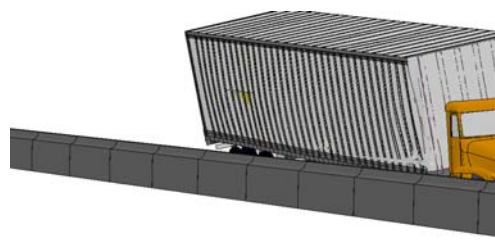
r.   Time = 1.7 second
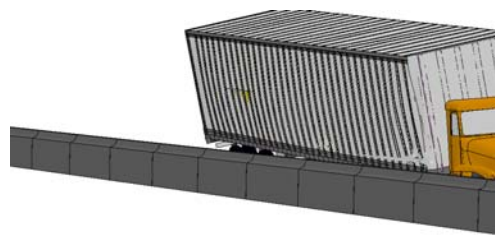
Figure 45. [CONTINUED] Photograph / Illustration. Sequential views of MwRSF Test TL5CMB-2 and FE model simulation from an isometric viewpoint

Table 5. Summary of phenomenological events that occurred during full-scale test and FE model simulation

Event	Test (TL5CMB-2) Time (seconds)	FE model Time (seconds)
Tractor begins to yaw	0.024	0.02 – 0.03
U-bolt connecting front axle to right-side leaf spring broke	unknown	0.09 – 0.1
Left-front tire lifts off pavement	0.144	0.09 – 0.10
Right-front corner of trailer contacted the top protrusion of the barrier	0.186	0.17 – 0.18
Trailer started to roll toward the barrier	0.19	0.24 – 0.25
Left-rear tires were lifted off the ground	0.2	0.22 – 0.23
The right front corner of the trailer was vertically coincident with the back face of the barrier	0.26	0.27 – 0.28
Both left-rear trailer tires were lifted off the ground	0.356	0.24 – 0.35
Tractor was parallel to barrier	0.394	0.29 – 0.30
Tractor reached peak roll and began to roll back from the barrier	0.290 – 0.364	0.29 – 0.30
Left-front tractor tires returned to roadway surface	0.468	0.31 – 0.32
Trailer was parallel to barrier	0.648	0.63 – 0.64
Tractor rolled back to level position	0.650	0.75 – 0.76
Rear trailer tandem contacts barrier	0.656	0.65 – 0.66
Time of maximum impact force between trailer tandem and barrier (i.e., trailer 'slap')	0.72	0.71 – 0.72
Tractor started to roll toward the barrier	0.776	0.81 – 0.82
Tractor left-front tire again lifted from the roadway	0.956	0.97 – 0.98
Trailer reached maximum roll and began to roll back from the barrier All left side tires were off the ground	1.150 (≈42 deg.)	1.11 – 1.12 (40.2 deg.)
Tractor again reached peak (maximum) roll angle	0.994 (≈19 deg.)	1.16 – 1.17 (20.1 deg.)
Left-front tire returned to the roadway surface	1.294	1.45 – 1.46
Tractor left side tandems returned to roadway surface	1.652	1.50 – 1.51
Trailer left side tires returned to roadway surface	1.800	1.78 – 1.80

Comparison of Time-History Data

The tractor-semitrailer FE model included 16 accelerometers, three of which were positioned at locations where accelerometers are typically mounted in full-scale crash tests. In particular:

- Accelerometer 14 was placed near the center of gravity of the tractor inside the tractor cabin on the cabin floor (e.g., tractor cabin position in full-scale crash test summary section)

- Accelerometer 15 was placed near the fifth-wheel on the cross-beam support for the frame rails at 0.225 m aft of the kingpin

- Accelerometer 16 was placed near the center of the trailer tandem axle inside the trailer box on the floor.

The locations of these accelerometers are shown schematically in Figure 46.
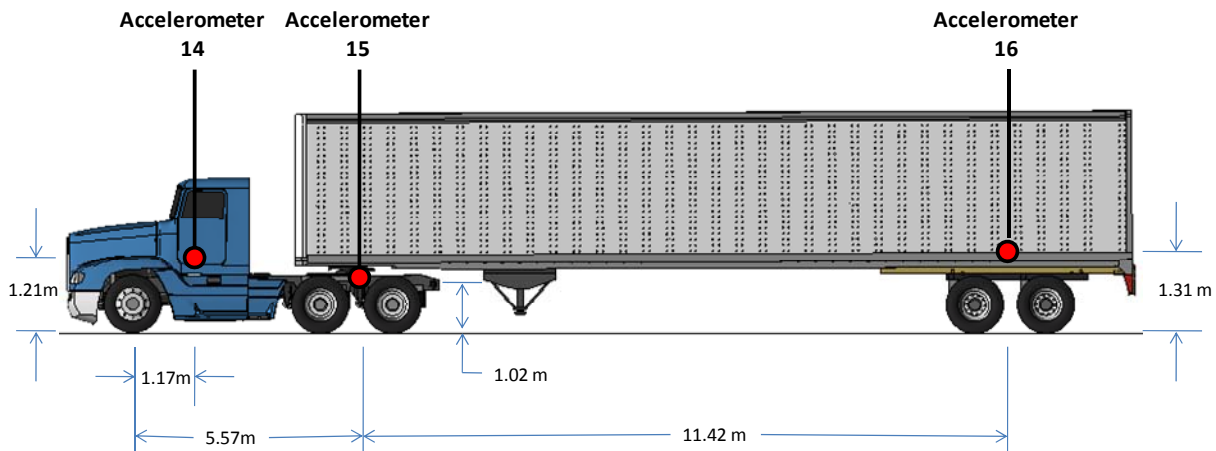
Figure 46. Illustration. Pertinent accelerometer locations in the FE model

Acceleration-time histories and angular rate-time histories were collected in the FE model using the *ELEMENT_SEATBELT_ACCELEROMETER option in LS-Dyna, which is the preferred method suggested by LS-Dyna for collecting acceleration data [7]. The accelerometers were connected to the tractor-semitrailer model using constrained nodal rigid bodies (CNRBs). The time-history data were collected from each accelerometer in a local reference coordinate system that rotates with the accelerometer in the same way that test data are collected from physical accelerometers. The data were collected at a frequency of 30 kHz, which was adequate for preventing aliasing of the data collected from the accelerometers located on the tractor model; however, the collection rate was not sufficient to prevent aliasing of the data collected from the accelerometer on the trailer model. To obtain accurate acceleration data from the trailer accelerometer, the velocity-time history for each channel was collected and differentiated to compute acceleration. These acceleration-time histories were then filtered using the SAE 180 Hz filter in LS-PrePost before post-processing.

Figures 47, 48, and 49 show the longitudinal, transverse, and vertical acceleration-time histories, respectively, computed from accelerometer 15 located at the tractor fifth-wheel. Figure 50 shows the roll, pitch, and yaw angles computed at the accelerometer 15 location.

Figures 51, 52, and 53 show the x-, y-, and z-acceleration-time histories, respectively, computed from accelerometer 16 located at the trailer axle. Figure 54 shows the rotation about x-, y-, and z-axis computed at the accelerometer 16 location.
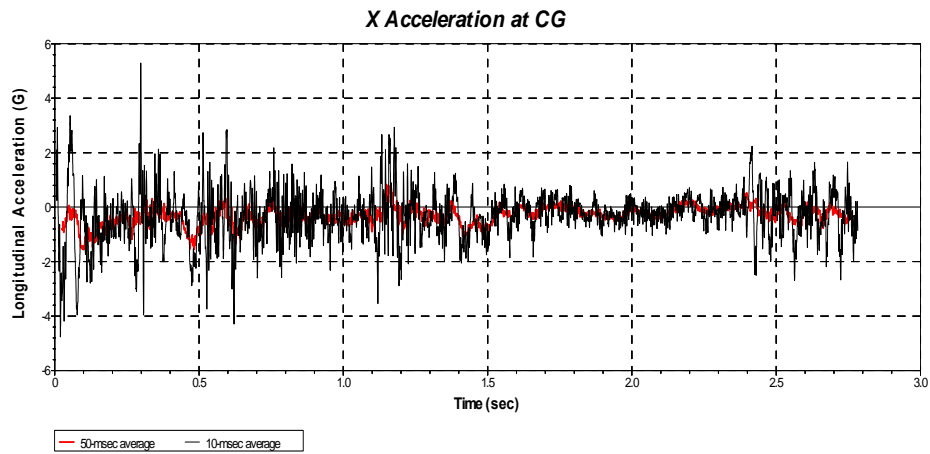
Figure 47. Chart. Longitudinal acceleration-time history plot from *accelerometer 15* near the tractor fifth-wheel (10-millisecond and 50-millisecond moving averages)
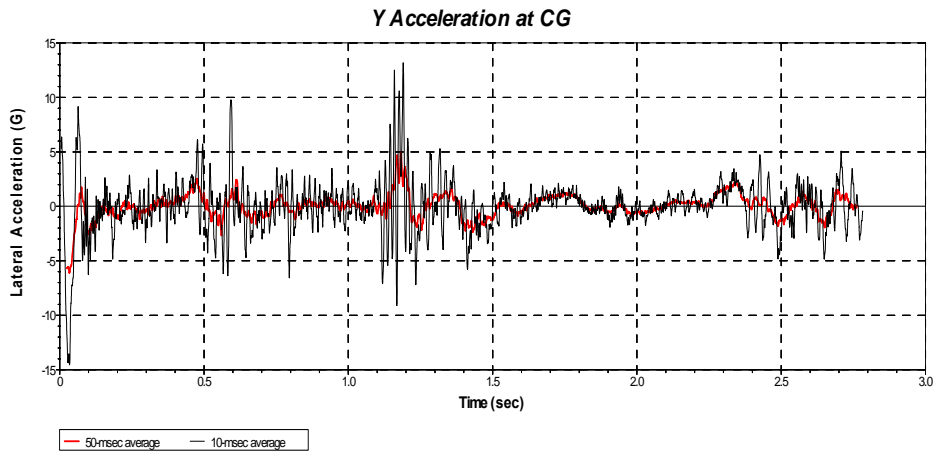
Figure 48. Chart. Transverse acceleration-time history plot from *accelerometer 15* near the tractor fifth-wheel (10-millisecond and 50-millisecond moving averages)

69
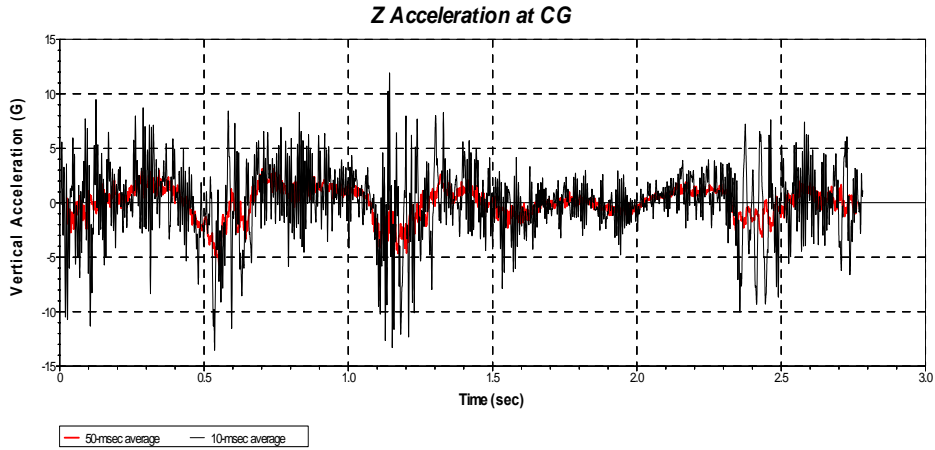
Figure 49. Chart. Vertical acceleration-time history plot from *accelerometer 15* near the tractor fifth-wheel (10-millisecond and 50-millisecond moving averages)
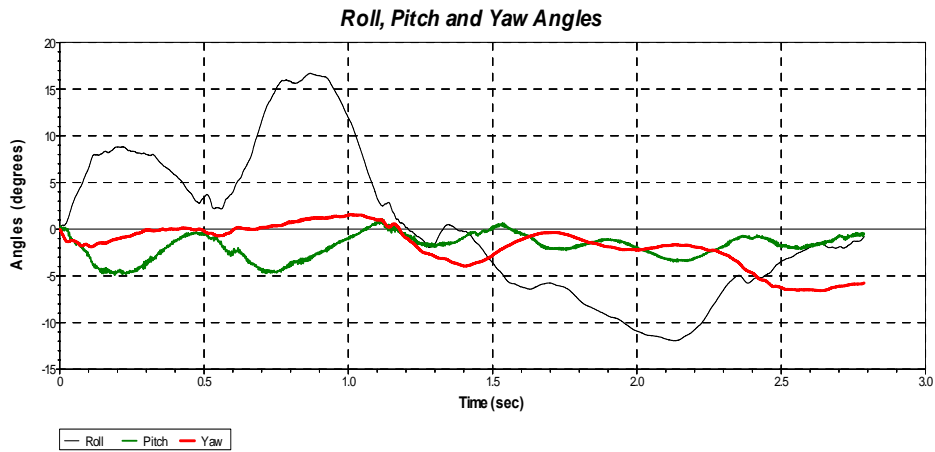
Figure 50. Chart. Roll, pitch and yaw-time history plot from *accelerometer 15* near the tractor fifth-wheel
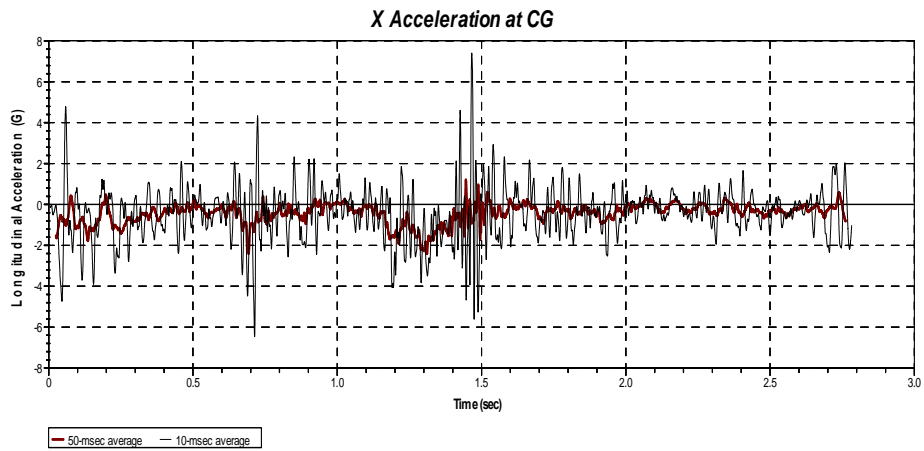
Figure 51. Chart. X-acceleration-time history plot from *accelerometer 16* near the trailer tandem axle (10-millisecond and 50-millisecond moving averages)

70
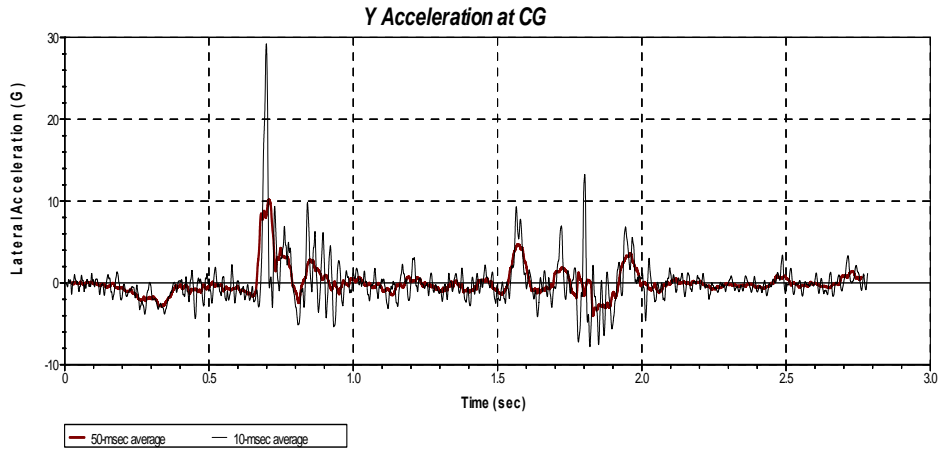
Figure 52. Chart. Y-acceleration-time history plot from *accelerometer 16* near the trailer tandem axle (10-millisecond and 50-millisecond moving averages)
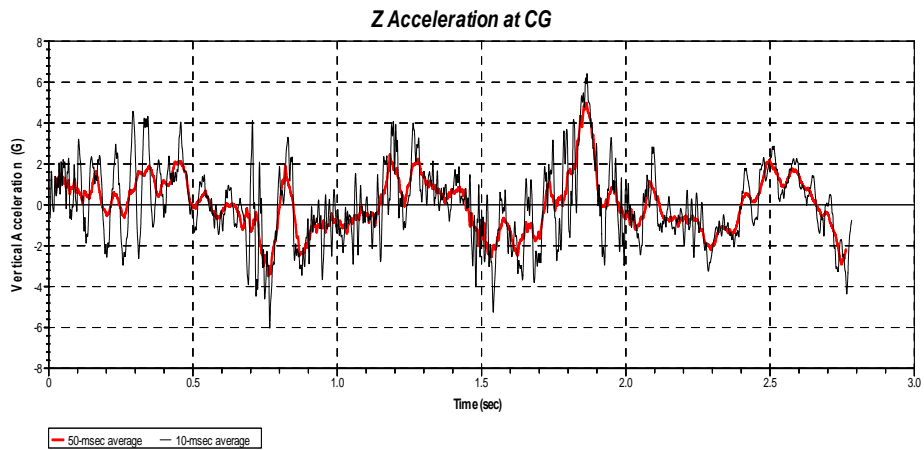
Figure 53. Chart. Z-acceleration-time history plot from *accelerometer 16* near the trailer tandem axle (10-millisecond and 50-millisecond moving averages)
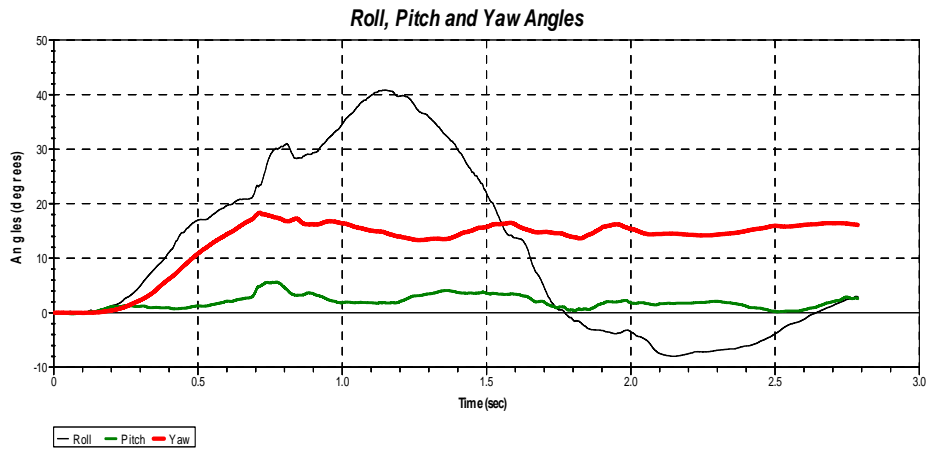
Figure 54. Chart. Angular time history plot of rotation about x-axis, y-axis and z-axis from *accelerometer 16* near the trailer tandem axle

71

Figures 55, 56, and 57 show the comparison of the 50-millisecond moving average of the longitudinal, transverse, and vertical acceleration-time histories between the FE analysis results and full-scale test TL5CMB-2. Figure 58 shows the resultant acceleration-time histories from the accelerometer located at the rear of the trailer over the trailer axle comparing the FE analysis results with full-scale test TL5CMB-2.
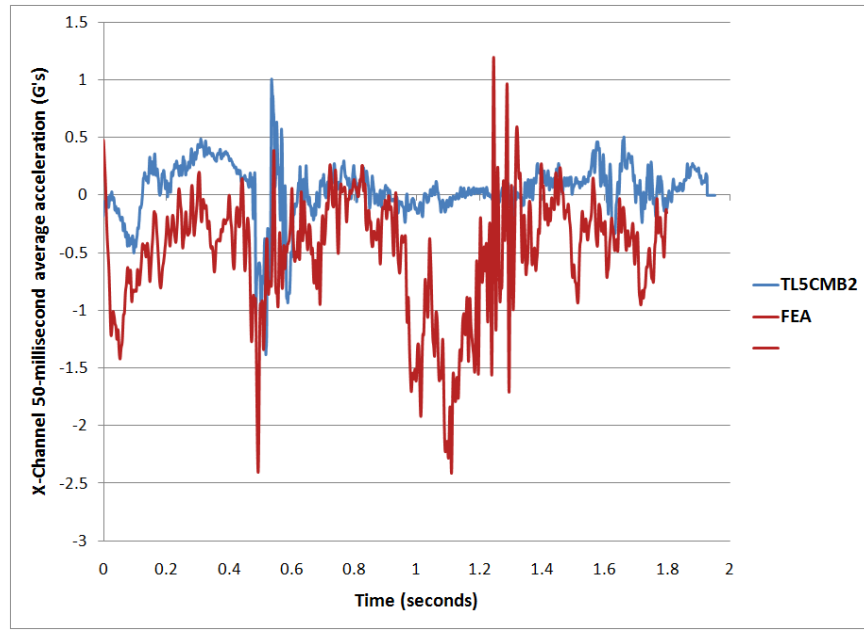
Figure 55. Chart. 50-millisecond moving average of the longitudinal acceleration-time history plot at rear of trailer comparing FE results to Test TL5CMB2
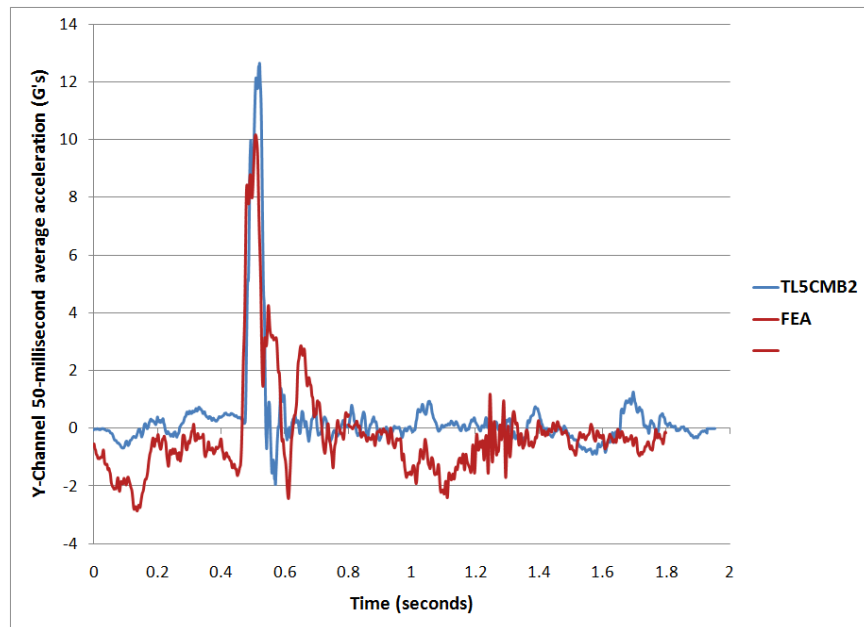
Figure 56. Chart. 50-millisecond moving average of the lateral acceleration-time history plot at rear of trailer comparing FE results to Test TL5CMB2

72
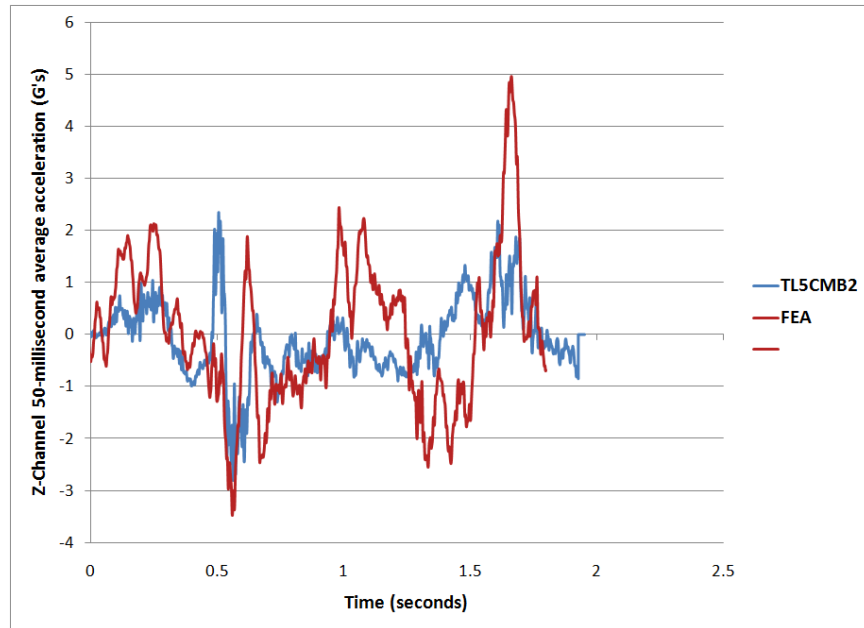
Figure 57. Chart. 50-millisecond moving average of the vertical acceleration-time history plot at rear of trailer comparing FE results to Test TL5CMB2
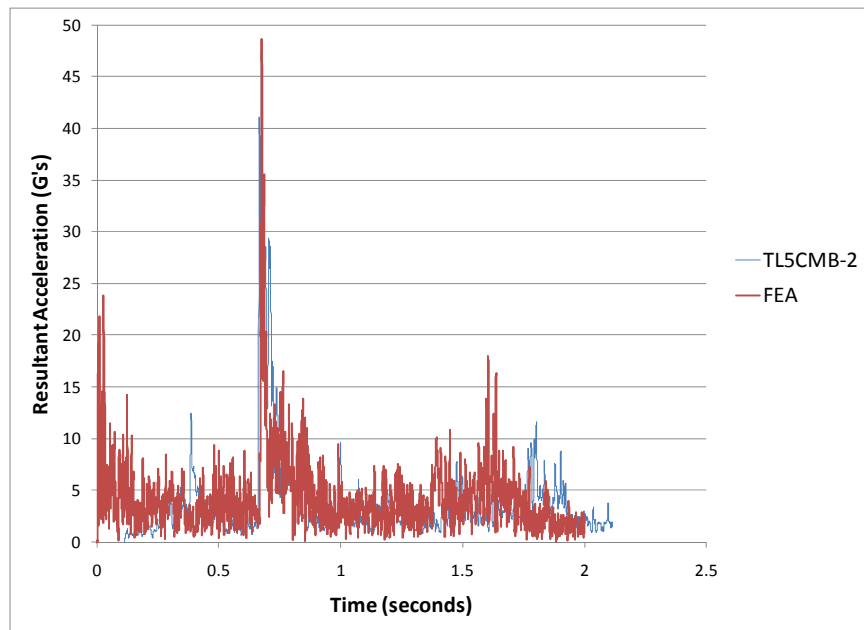
Figure 58. Chart. Resultant acceleration-time history plot from the FE simulation and Test

Angular-rate data were not collected in test TL5CMB-2; however, the high-speed videos, TL-5 CMB-2 aos3.avi and TL-5 CMB-2 aos-4.avi, from the full-scale test were used to measure the approximate roll-time history of the trailer at time intervals of 0.2 seconds. The roll-time history of the trailer from the simulation compares reasonably well to the roll-time history measured from the high-speed test video, regarding both timing and magnitude, as shown in Figure 59.

73

The magnitude of peak roll angle in the simulation was slightly less than the roll angle of the test vehicle (e.g., 40.8 degrees and 42 degrees, respectively), which affected subsequent kinematics of the vehicle. For example, the lower magnitude in peak roll angle in the analysis resulted in the vehicle rotating back to level position approximately 0.1 seconds sooner than the test vehicle. It also affected the magnitude and timing of the subsequent peak negative roll angle. The analysis was stopped at 3.0 seconds of the impact event.
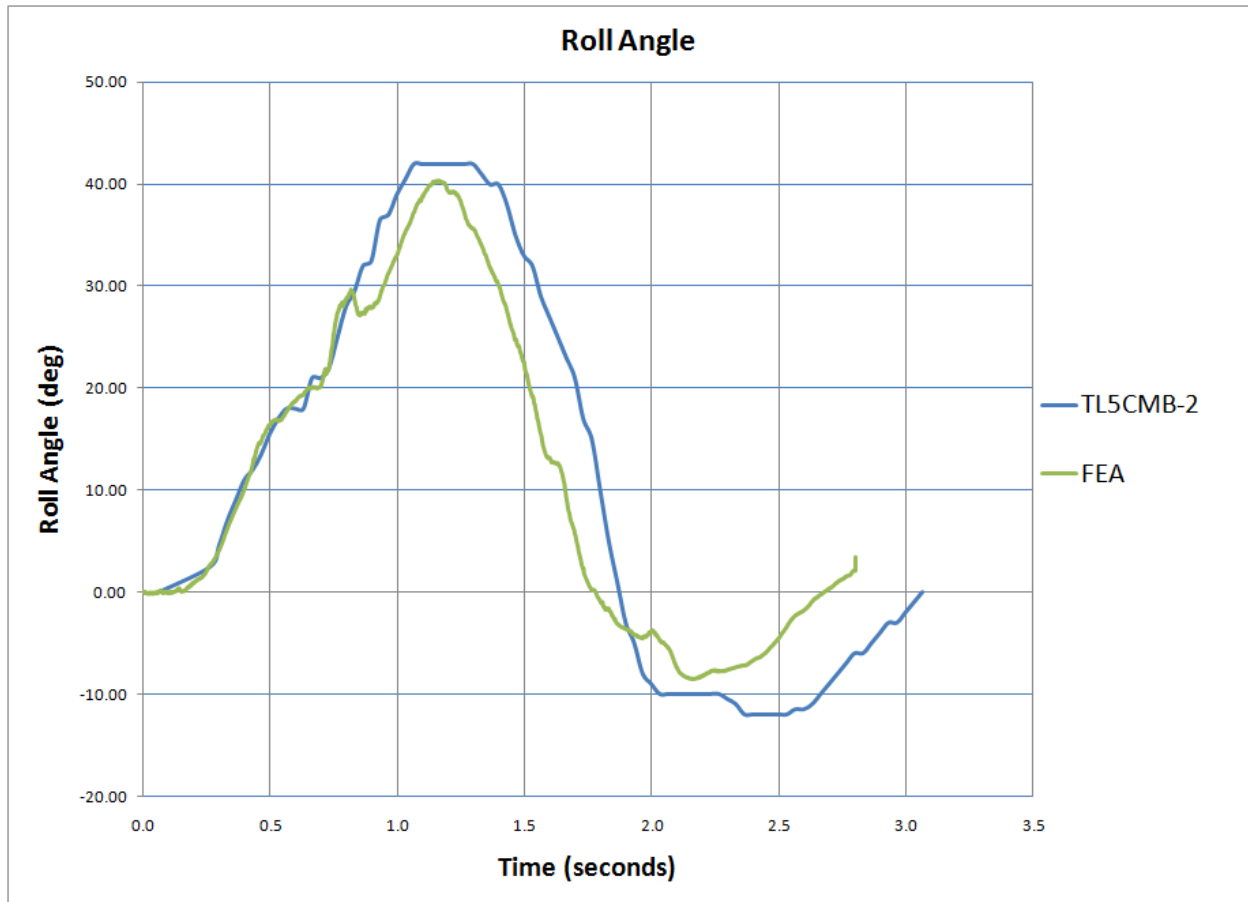
Figure 59. Chart. Roll angle-time history plot of the rear section of the trailer from the FE simulation and Test TL5CMB-2

Test Vehicle Damage

The damage caused to the tractor during the impact could not be accurately assessed because of a major secondary impact that occurred after the vehicle exited the barrier system. Before the vehicle could be stopped, it impacted another barrier system at a high impact angle, which caused further damage to the tractor, as shown in Figure 60.

Figure 60. Photograph. Post test view of test vehicle illustrating excessive damage after secondary impact

The trailer had scrapes and gouges on its right side that were caused when the trailer rolled over onto the barrier. The scrapes started at the front of the trailer at 21 inches (533 mm) above the bottom and ran all the way down the trailer in a straight line to the back of the trailer to a point 9 inches (229 mm) above the bottom of the trailer. Many of the vertical "ribs" on the impact side of the trailer box were damaged. The impact side of the trailer was bowed outward due to shifting of the ballast during impact as shown in Figure 61. The lower right corner of the bracket at the back of the trailer was fractured and bent.

Figure 61. Photograph. Post test view of the trailer showing damage to sidewall and external ribs

FE Vehicle Model Damage

Figure 62 through Figure 64 show contour plots of plastic strain, which were used to identify areas of the tractor model that suffered damage during the simulated impact event. The damage to the tractor model was limited to the impact side. The most severe damage was to the front bumper, the fender, the side steps, the fuel tank, and the front-right suspension. The high plastic strains on the rear tandem wheel rims also indicate that the tires would likely have debeaded and consequently deflated during the impact, which would affect the kinematics of the vehicle.[iv] There was also moderate plastic strain in components of the support structure for the fifth-wheel.

Figure 65 through Figure 67 show contour plots of plastic strain for the trailer model. The trailer experienced plastic strains in the bottom side rails, the suspension structure and in the connection points of the trailer bogie to the lower cross-beams of the trailer box. The impact side of the trailer was bowed outward slightly due to shifting of the ballast during impact.

---

iv The development of a more realistic tire model was outside the scope of this project.
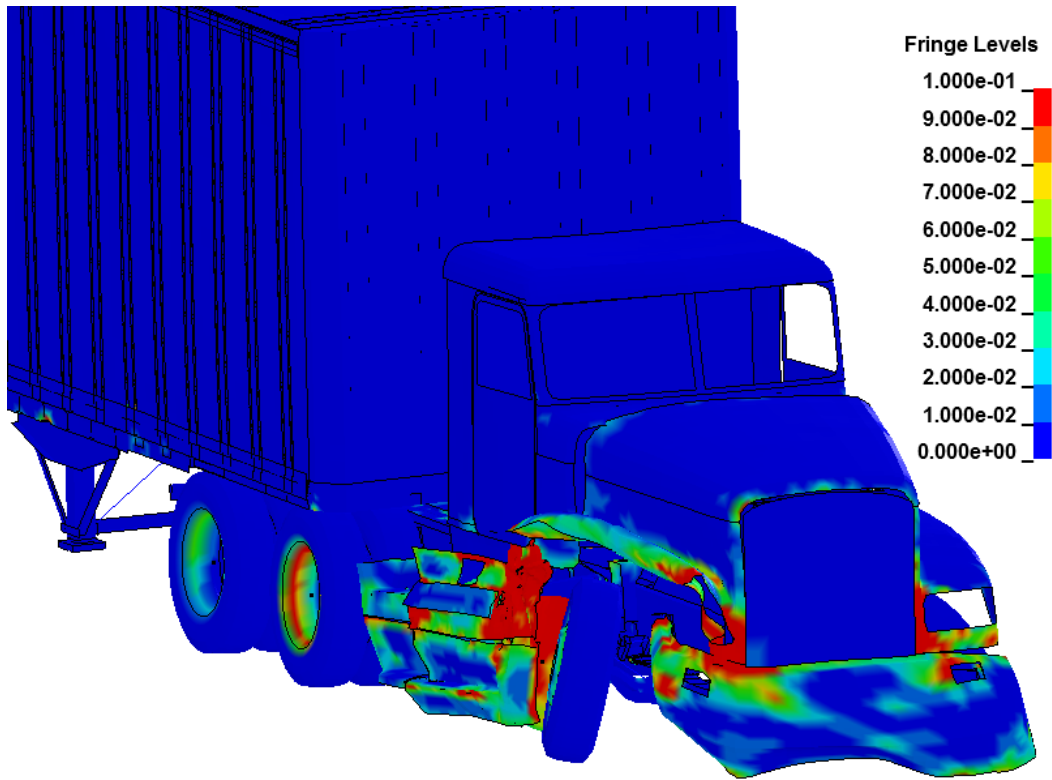
Figure 62. Illustration. Contour of effective plastic strain (with contours cut-off at 10%) used to identify areas of the tractor model that sustained damage during simulated impact
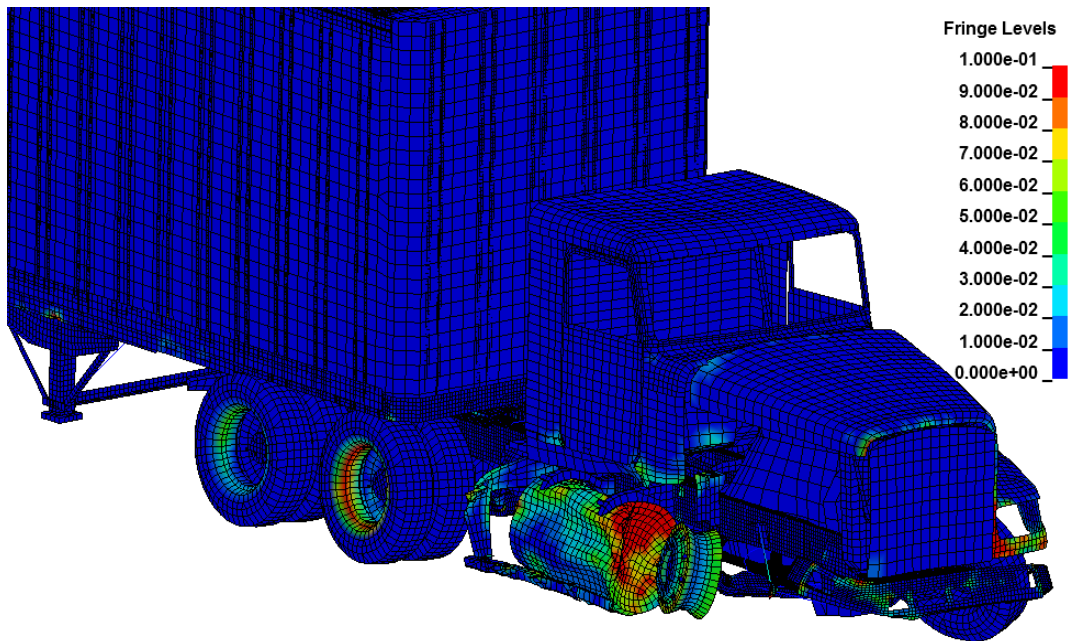
Figure 63. Illustration. Contour of effective plastic strain (with contours cut-off at 10%) used to identify areas of the tractor model that sustained damage during simulated impact
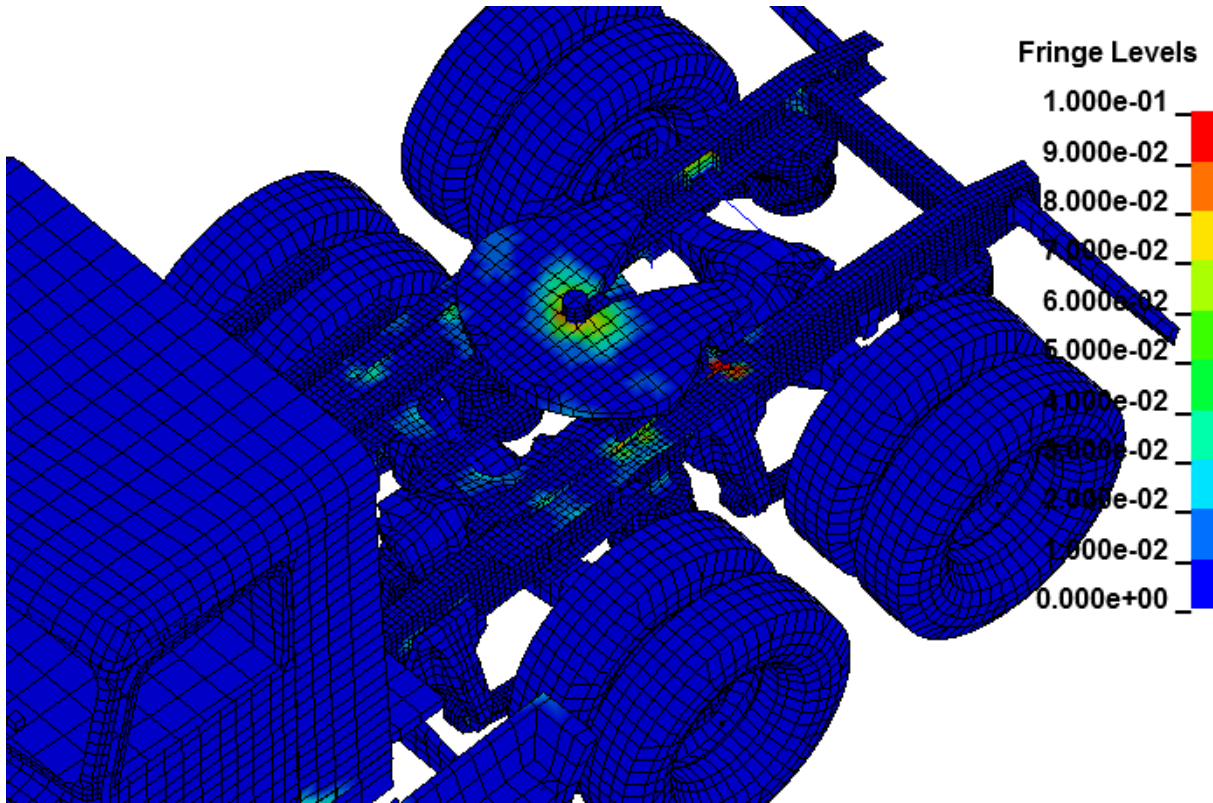
Figure 64. Illustration. Contour of effective plastic strain (with contours cut-off at 10%) used to identify areas of the tractor model that sustained damage during simulated impact
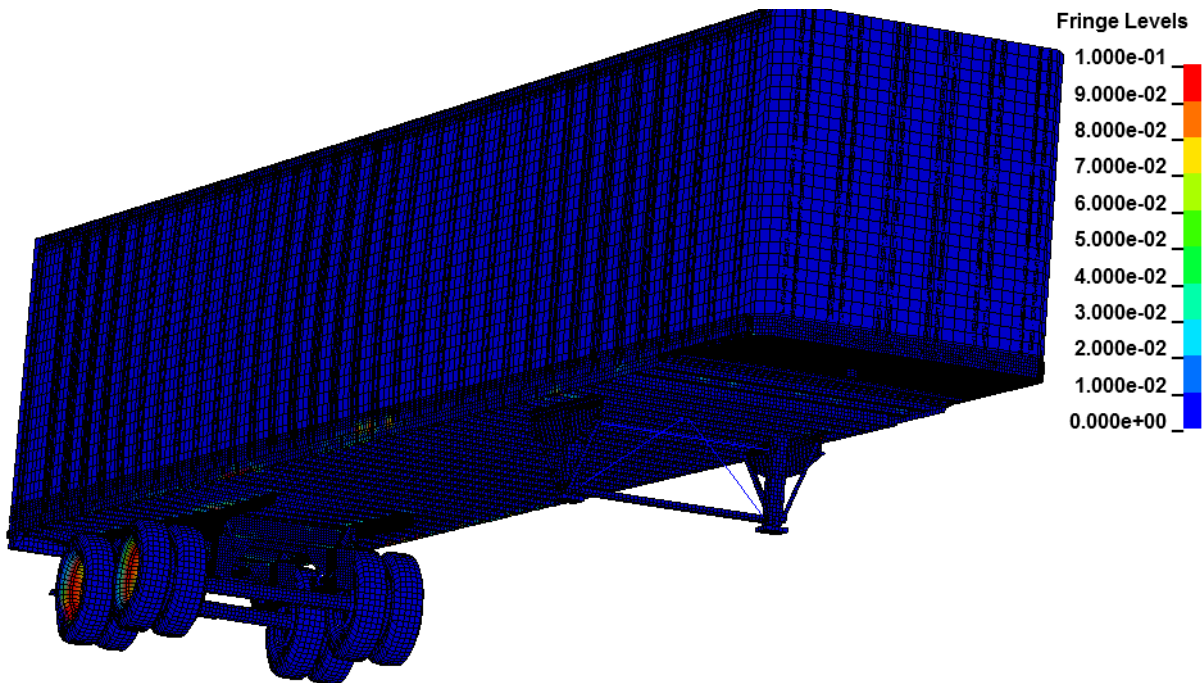
Figure 65. Illustration. Contour of effective plastic strain (with contours cut-off at 10%) used to identify areas of the trailer model that sustained damage during simulated impact
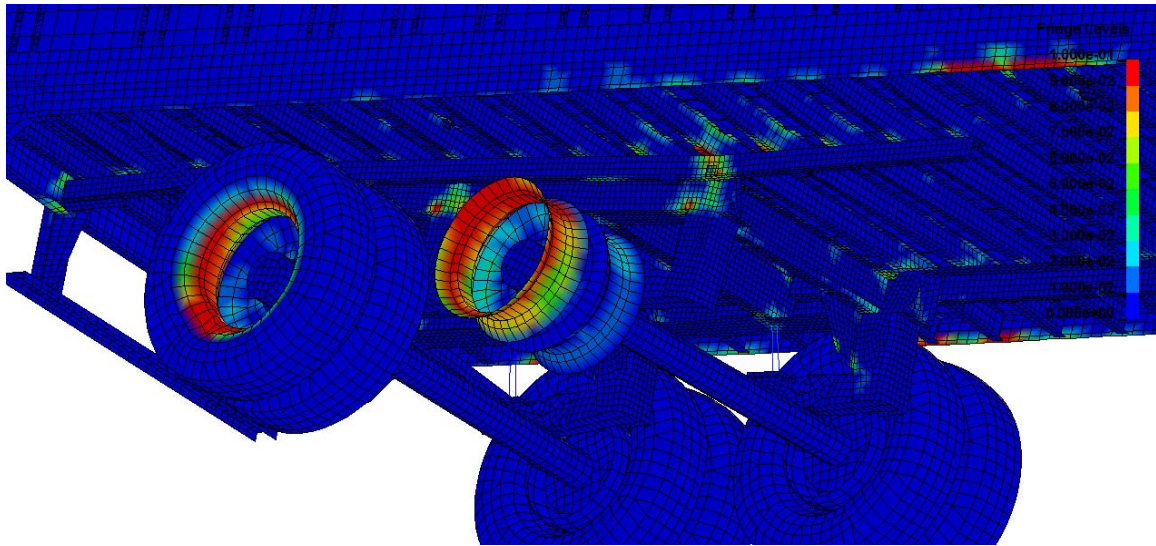
Figure 66. Illustration. Contour of effective plastic strain (with contours cut-off at 10%) used to identify areas of the trailer model that sustained damage during simulated impact
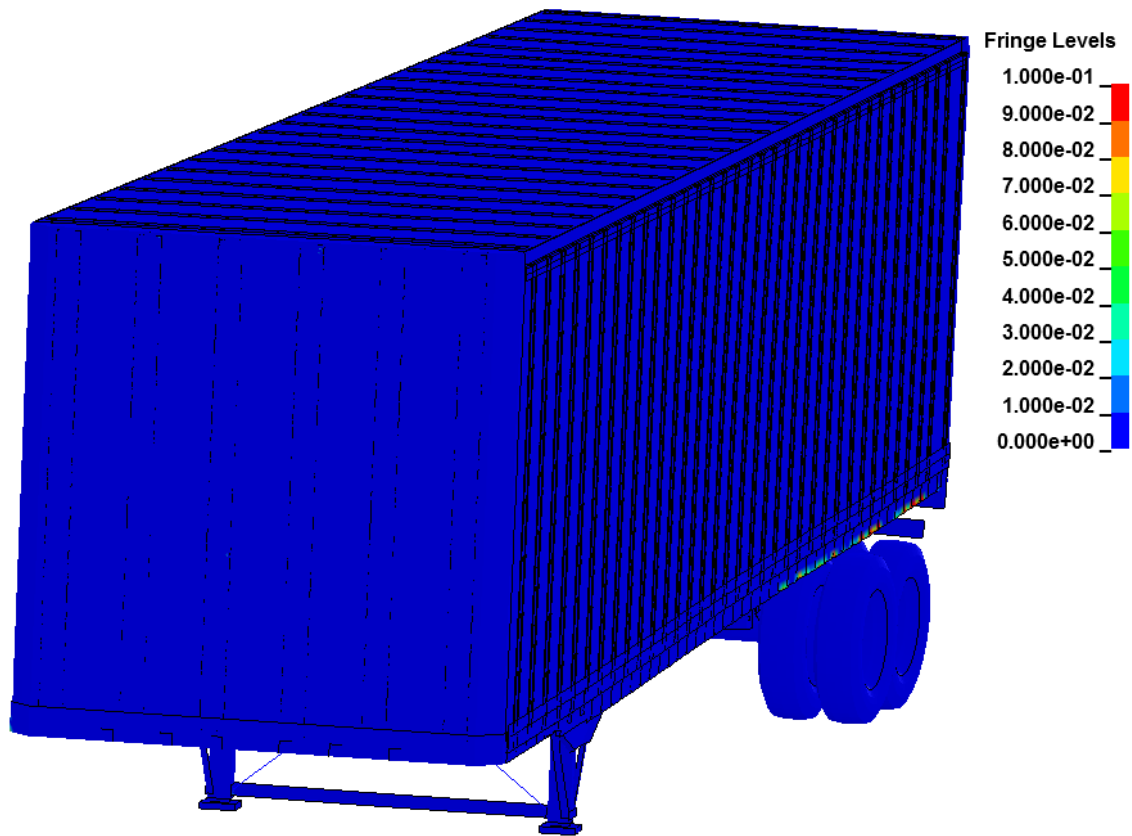
Figure 67. Illustration. Contour of effective plastic strain (with contours cut-off at 10%) used to identify areas of the trailer model that sustained damage during simulated impact

Overview of the TTI Crash Test 7069-13

Test 7069-13 was conducted by the Texas Transportation Institute (TTI), in College Station, Texas. The purpose of the test was to evaluate the strength capacity of a 42-inch (1.07-m) vertical faced concrete parapet bridge railing in accordance with the testing guidelines of the 1989 *Guide Specifications for Bridge Railings*. The test involved a 1979 International TranStar 4200 tractor with a 1977 Pullman van-trailer ballasted to 50,050 lb (22723 kg) impacting the barrier at 51.4 miles per hour (82.7 km/hr) and 16.2 degrees. The installation length of the barrier was 100 ft (30 m), and the impact point was 24 ft (7.3 m) from the upstream end. Figure 68 shows the test vehicle and barrier with the dimensions of the barrier labeled. The geometric dimensions and mass inertial measurements of the test vehicle are provided in Figure 69.

The tractor was equipped with a triaxial accelerometer block mounted near the center of gravity of the tractor and a biaxial accelerometer block mounted over the rear tractor tandems. Two biaxial accelerometer blocks were also placed inside the trailer: one set mounted toward the front near the king-pin and one set toward the rear over the trailer tandem axle. Note: there was no instrumentation to measuring angular displacement of the vehicle. Three high-speed film cameras were used to film the crash test, as shown in Figure 70:

1. Overhead camera with recording speed of 403.7 frames per second (fps),

2. Camera positioned downstream with a viewpoint longitudinal to the barrier with a recording speed of 386.3 fps, and

3. Camera positioned with a viewpoint perpendicular to the barrier with a recording speed of 398.9 fps.

Test Results

Information pertaining to vehicle trajectory and occupant risk assessment was provided in the test report as follows:

> *"Impact speed was 51.4 mi/hr (82.7 km/hr), and the angle of impact was16.2 degrees. Exit speed was not available. The vehicle trajectory path was 0 degrees. The effective coefficient of friction was 0.55. Occupant impact velocity was 10.5 ft/s (3.2 m/s) in the longitudinal direction and 12.5 ft/s (3.8 m/s) in the lateral direction. The highest 0.010-s occupant ridedown accelerations were -2.2g (longitudinal) and 4.6g (lateral). ... The maximum 0.050 –s average [accelerations] at the tractor c.g. were -3.3g (longitudinal) and 3.7g (lateral)."[6]*

A detailed description of phenomenological events was not included in the test report. The research team used the test videos to discern key phenomenological events during the crash test.

(a) Test Vehicle

12 in
(305 mm)

9 in
(229 mm)

42 in
(1,067 mm)

10 in
(254 mm)
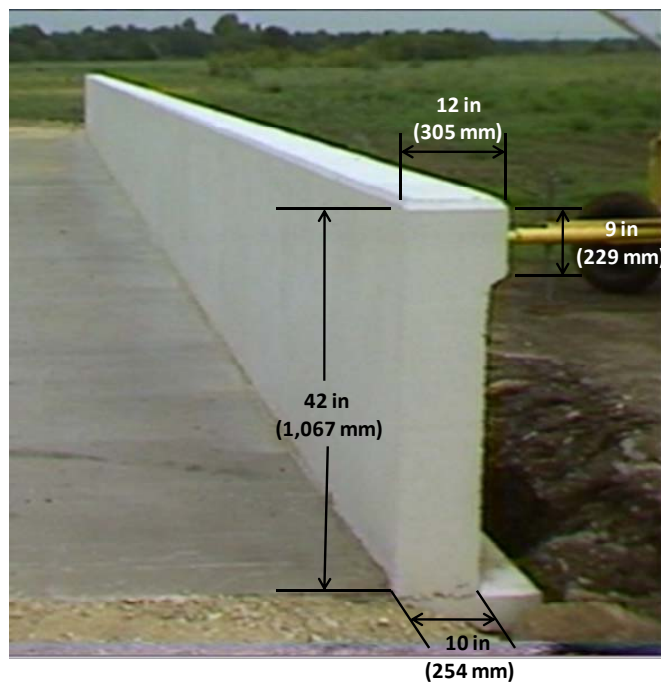
(b) Test Article

Figure 68. Photograph. (a) Tractor-semitrailer vehicle and (b) 42-inch tall concrete parapet test article from TTI Test 7069-13

Date:	7/11/1988	Test Number:	TTI 7069-13

Tractor:

VIN No,:		Make:	International	Model:	Transtar 4200
Year:	1979	Odometer:			

Trailer:

VIN No,:		Make:	Pullman	Model:	45' Van
Year:	1977				

*All Measurements Refer to Impacting Side
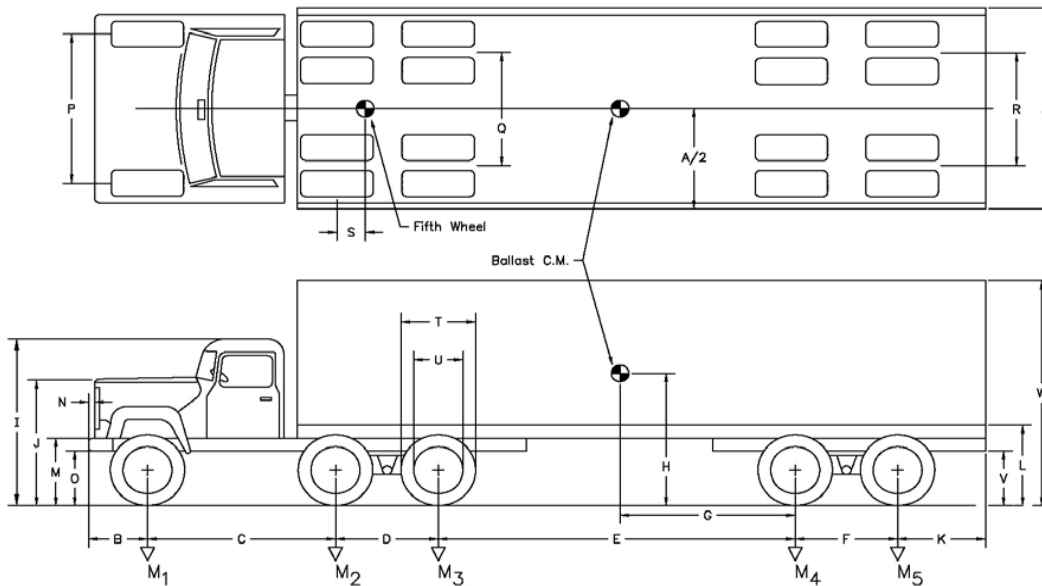
Vehicle Geomerty -in (mm)

A	-	-	G	-	-	M	31	(774.7)	S	-	-
B	31	(787.4)	H	-	-	N		(0.0)	T	-	-
C	144	(3655.1)	I	107	(2705.1)	O	21	(520.7)	U	-	-
D	50	(1276.4)	J	79	(2000.3)	P	-	-	V	-	-
E	388	(9848.9)	K	35	(885.8)	Q	-	-	W	162	(4114.8)
F	50	(1276.4)	L	48	(1219.2)	R	-	-			

Note: L is the height to the bottom of the lower rail

Mass -Properties

		Curb		Test Inertial		Gross Static	
M_1	lb (kg)	7,380	(3,348)	7,920	(3,592)	7,920	(3,592)
$M_2 + M_3$	lb (kg)	11,890	(5,393)	22,250	(10,092)	22,250	(10,092)
$M_4 + M_5$	lb (kg)	8,420	(3,819)	19,880	(9,017)	19,880	(9,017)
M_{Total}	lb (kg)	27,690	(12,560)	50,050	(22,702)	50,050	(22,702)

Figure 69. Illustration. Dimensions of the TTI Test No. 7069-13 test vehicle

| (a) Overhead view | (b) Downstream view | (c) Perpendicular view |

Figure 70. Photograph. Camera views in TTI test 7069-13

FE Model for Simulation of Test 7069-13

The geometry of the tractor FE model was modified such that the wheelbase of the model was the same as the wheelbase of the test vehicle used in TTI Test No. 7069-13. A FE analysis was conducted simulating this test using the Phase C tractor-semitrailer FE model. The friction between the tractor and barrier was set to 0.2, and the friction between the tires and the barrier was set to 0.65. The dimensions of the barrier model were the same as those of the barrier in TTI Test No. 7069-13 shown in Figure 71. Since there was negligible deflection of the barrier in the full-scale test, the barrier was modeled as a rigid material with rigid fixity to the ground. Recall that the purpose of the analysis was to verify the response of the vehicle, which is why the project team selected only full-scale tests in which barrier deflection was minimal. The impact conditions for the FE simulation were consistent with those reported in the full-scale crash test (i.e., 51.4 mph (82.7 km/hr) and 16.2 degrees).
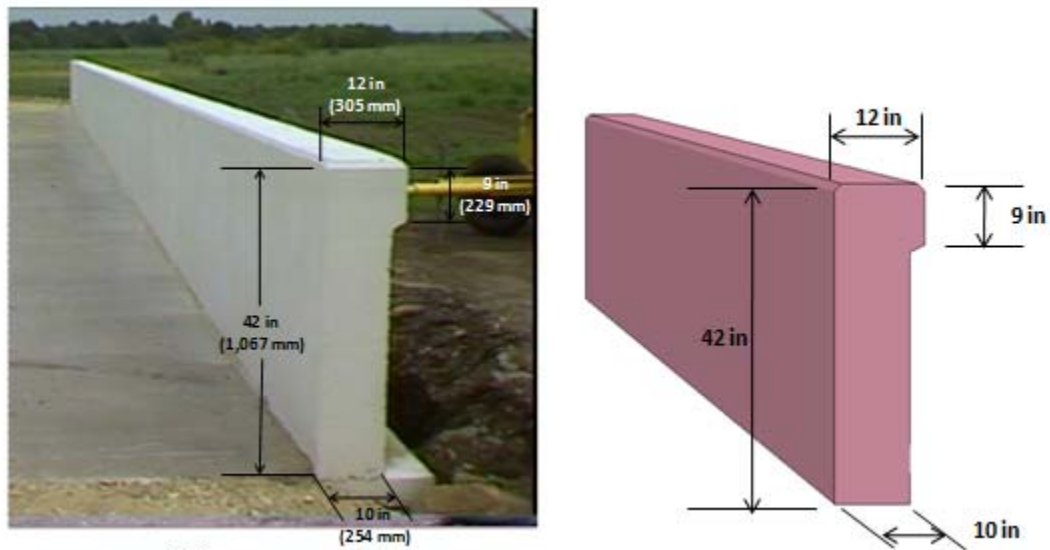
Figure 71. Photograph / Illustration. FE model of the 42-inch vertical concrete parapet

83

The ADAP program described in the Phase B final report was developed to aid in the modification of overall vehicle model size and shape parameters (e.g., tractor wheelbase and trailer length). These scripts were designed to operate on the FE model input file directly and were used in this case to modify the model's dimensions to conform to those of the test vehicle.

In particular, they were used to: 1) make the tractor a day-cab style tractor by removing the sleeper section of the cabin and 2) adjust the wheelbase length of the tractor by removing a section of the frame rails (along with other components in this section of the model). Figure 72 shows a visual comparison between the tractor FE model and the test tractor. A comparison of the dimensional properties of the FE model to the test vehicle is shown in Figure 73.

(a) Test Vehicle   (b) FE model

Figure 72. Photograph / Illustration. (a) Tractor test vehicle and (b) tractor FE model

Date: _____7/11/1988_____   Test Number: _____TTI 7069-13_____

Tractor:
  VIN No,: _____   Make: ___International___   Model: ___Transtar 4200___
  Year: _____1979_____   Odometer: _____

Trailer:
  VIN No,: _____   Make: ___Pullman___   Model: ___45' Van___
  Year: _____1977_____

*All Measurements Refer to Impacting Side

Vehicle Geomerty -mm (in)

A	-	-	G	-	-	M	31	(774.7)	S	-	-
B	31	(787.4)	H	-	-	N		(0.0)	T	-	-
C	144	(3655.1)	I	107	(2705.1)	O	21	(520.7)	U	-	-
D	50	(1276.4)	J	79	(2000.3)	P	-	-	V	-	-
E	388	(9848.9)	K	35	(885.8)	Q	-	-	W	162	(4114.8)
F	50	(1276.4)	L	48	(1219.2)	R	-	-			

Note: L is the height to the bottom of the lower rail

Mass -Properties		**Curb**		**Test Inertial**		**Gross Static**	
M_1	lb (kg)	7,380	(3,348)	7,920	(3,592)	7,920	(3,592)
$M_2 + M_3$	lb (kg)	11,890	(5,393)	22,250	(10,092)	22,250	(10,092)
$M_4 + M_5$	lb (kg)	8,420	(3,819)	19,880	(9,017)	19,880	(9,017)
M_{Total}	lb (kg)	27,690	(12,560)	50,050	(22,702)	50,050	(22,702)

Figure 73. Illustration. Comparison of FE vehicle model dimensions to those of the test vehicle used in Test 7069-13

85

The content, dimensions and restraint of the ballast were not provided in the test report; Figure 74 shows a photograph of a ballast used in an earlier TTI test (i.e., 7069-10), which consisted of a layer of sand bags on the trailer floor and two rows of hay stacked on top of the sand. The entire ballast was 'restrained' using a wooden crate, as shown in Figure 74.

Figure 74. Photo. Trailer ballast for TTI test 7069-10

Since there were not sufficient details regarding the makeup of the ballast structure in Test 7069-13, the research team used the ballast model from the MwRSF test simulation. The ballast model was modified to attain the mass of the test-ballast by removing a row of portable concrete barriers (PCB) at the rear of the trailer and reducing the density of the remaining PCB units. The resulting ballast model is shown in Figure 75.
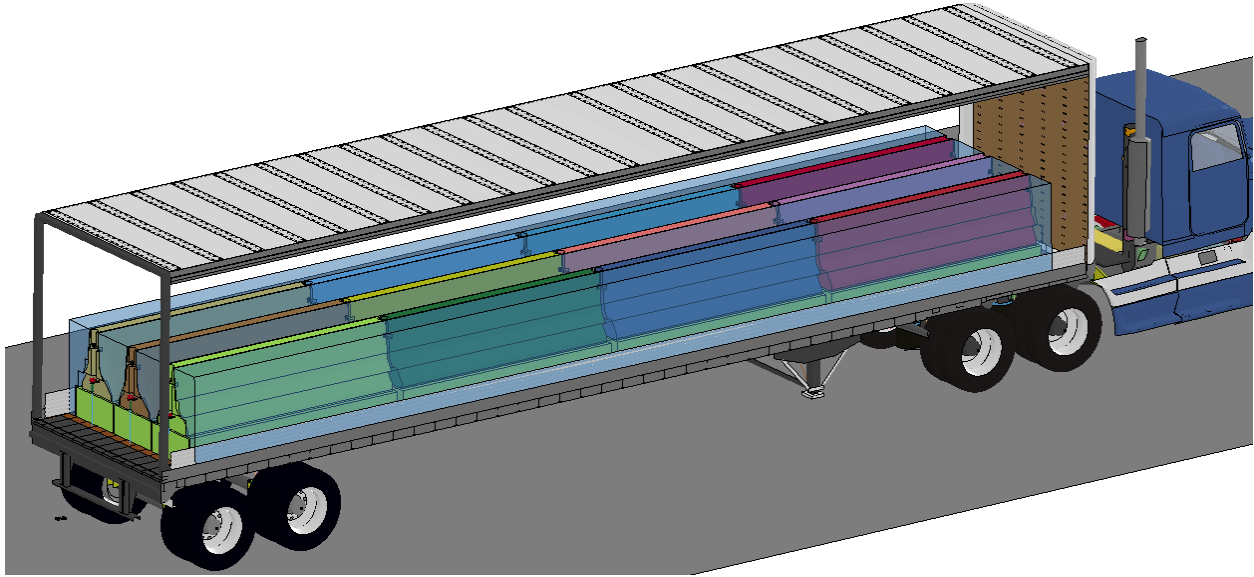
Figure 75. Ballast model used in simulation of TTI test 7069-13

The test inertial mass of the tractor was reported to be 15,010 lb (6,808 kg) and that of the 45-ft (13.7-m) semitrailer was 12,680 lb (5,752 kg). For comparison, the mass of the FE tractor model was 15,507 lb (7,034 kg) and the mass of the FE trailer model was 13,126 lb (5,954 kg). The loads on the front axle in the FE model were 13.5% higher than those of the test vehicle; the loads on the tractor tandems in the FE model were 4% less than those of the test vehicle; and the loads on the trailer tandems in the FE model were 3.5% higher than those of the test vehicle. The total mass of the FE tractor-semitrailer model including trailer ballast was 50,977 lb (23,124 kg), which was 1.85% higher than the total mass of the test vehicle, which was 50,050 lb (22,702 kg).

The most notable differences between the test vehicle and modified FE model are listed below:

- *Length dimensions* – The length dimensions of the FE model were all within 7.5% of the test vehicle dimensions, except for the distance from the front bumper to the center of the front wheel (e.g., dimension "B" in Figure 73), which was 44.2% longer in the FE model.

- *Trailer box dimensions* – The trailer floor in the FE model was 3.0 inches (76.2 mm) higher than the test vehicle (e.g., dimension "L" in Figure 73), and the top of the trailer in the FE model was 9.0 inches (228 mm) lower than the test vehicle (e.g., dimension "W" in Figure 73).

- *Trailer suspension* – The suspension system on the FE trailer model was an air-spring design, and the suspension on the trailer test vehicle was a leaf-spring design.

87

- *Tractor-Semitrailer Weight* – The FE model of the tractor was approximately 500 lbs heavier than the test tractor, and the FE model of the semitrailer was approximately 400 lbs heavier than the test semitrailer.

- *Ballast* – The properties, dimensions and restraint of the ballast were not provided in the test report; thus a modified version of the ballast model from the MwRSF test simulation was used.

- *Propulsion* – The test vehicle was under engine power with drive train engaged for the duration of the impact event. The analysis model was not.

The analysis was conducted with a time-step of 1.20 microseconds for a time period of 3.0 seconds. Prior to the analysis, the model was set at equilibrium with respect to gravity, i.e., the geometry and stresses in all parts of the tractor-trailer model were at equilibrium with gravity. The basic procedure was to 1) conduct an analysis involving the vehicle subjected to only gravity load, 2) save node and element information (e.g., nodal coordinates and element stresses) from the gravity analysis, and 3) include them in subsequent analyses as part of the initial conditions for the model.

Qualitative Comparison of Simulation Results with Test 7069-13

Phenomenological Events

A qualitative assessment was made by comparing sequential snapshots of the simulation with the results of the full-scale crash test to verify vehicle kinematic response, as well as the sequence and timing of key phenomenological events. Figure 76 shows sequential snapshots of the impact event from a downstream viewpoint. Note: the time-stamp for test 7069-13 in the sequential views of Figure 76 and in the summary of phenomenological events of Table 6 were estimated using the test video[v] and assuming a frame rate of 386.3 frames per second[vi].

The FE model simulates the basic kinematic behavior of the tractor-semitrailer reasonably well, and adequately captures the basic phenomenological events that occur during impact. The analysis ran to completion with no numerical instability problems.

---

[v] The high-speed test film was converted to DVD format which may have altered the frame-rate.

[vi] The frame rate for the overhead film camera was provided by Dr. Roger Bligh of TTI via e-mail on 2/23/2010.

a.   Time = 0.000

b.   Time = 0.1 second

c.   Time = 0.2 second

**Figure 76. Photograph / Illustration. Sequential views of TTI Test 7069-13 and
FE model simulation from a downstream viewpoint**

d.   Time = 0.3 second
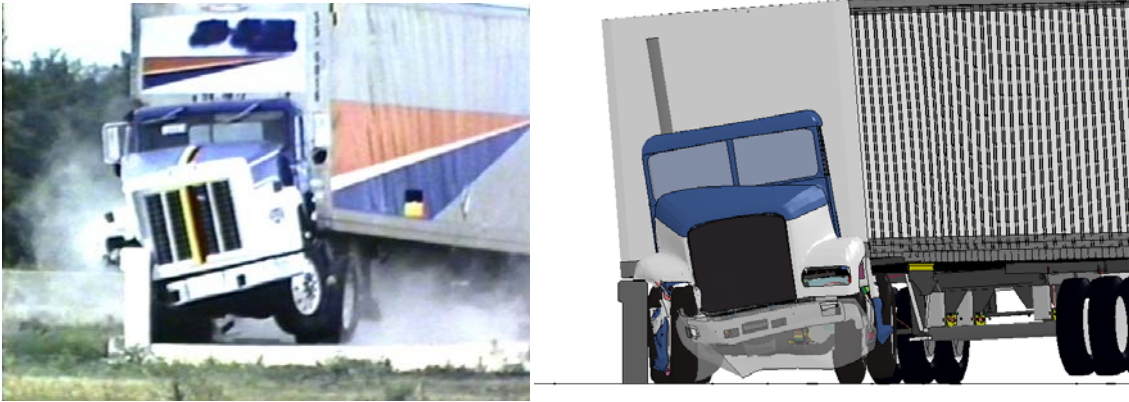
e.   Time = 0.4 second
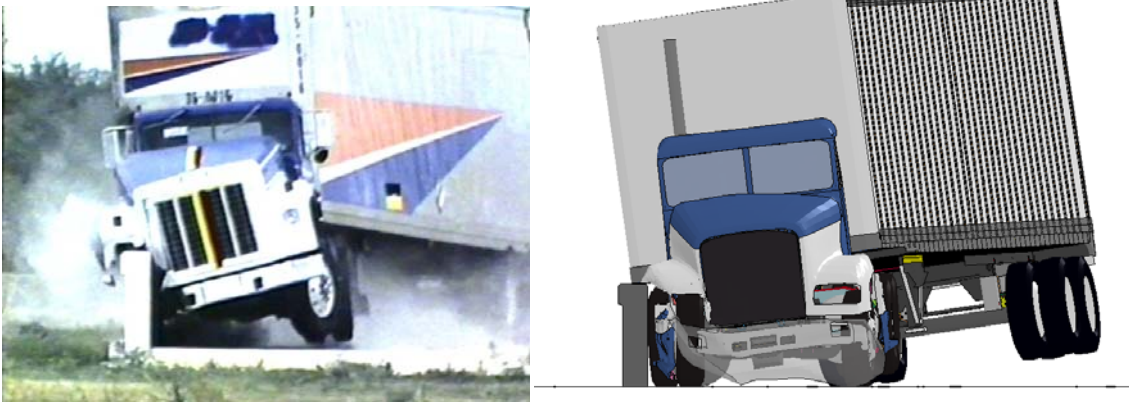
f.   Time = 0.5 second

Figure 76 . [CONTINUED] Photograph / Illustration. Sequential views of TTI Test 7069-13 and FE model simulation from a downstream viewpoint

g. Time = 0.6 second
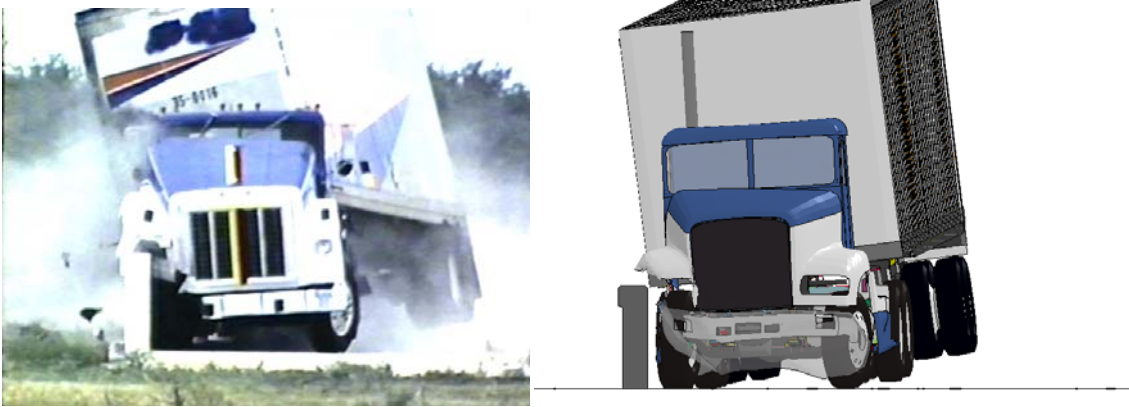
h. Time = 0.7 second
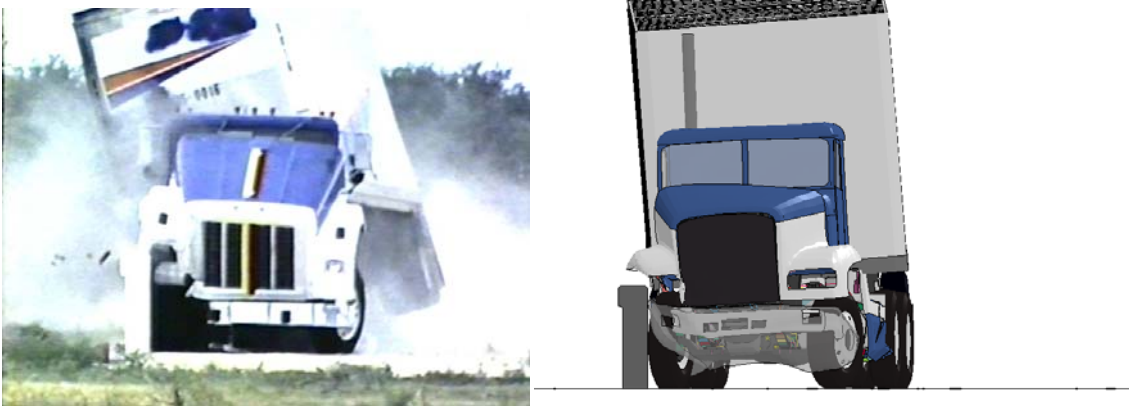
i. Time = 0.8 second
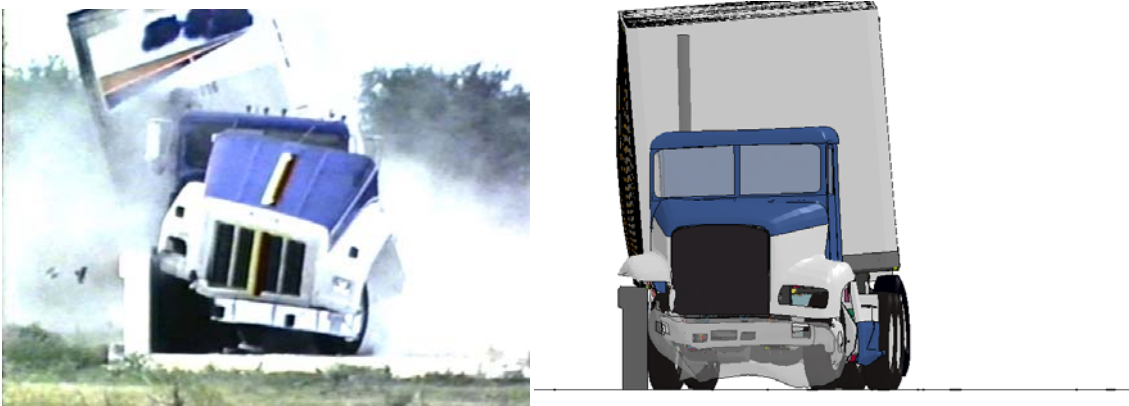
Figure 76. [CONTINUED] Photograph / Illustration. Sequential views of TTI Test 7069-13 and FE model simulation from a downstream viewpoint

j. Time = 0.9 second

k. Time = 1.0 second

l. Time = 1.1 second

Figure 76. [CONTINUED] Photograph / Illustration. Sequential views of TTI Test 7069-13 and FE model simulation from a downstream viewpoint

m. Time = 1.2 second

n. Time = 1.3 second

o. Time = 1.4 second

**Figure 76. [CONTINUED] Photograph / Illustration. Sequential views of TTI Test 7069-13 and
FE model simulation from a downstream viewpoint**

p. Time = 1.5 second

q. Time = 1.6 second

r. Time = 1.7 second

Figure 76. [CONTINUED] Photograph / Illustration. Sequential views of TTI Test 7069-13 and FE model simulation from a downstream viewpoint

s. Time = 1.8 second

t. Time = 1.9 second

u. Time = 2.0 second

Figure 76. [CONTINUED] Photograph / Illustration. Sequential views of TTI Test 7069-13 and FE model simulation from a downstream viewpoint

Table 6. Summary of Phenomenological Events that Occurred during Full-scale Test 7069-13 and FE Model Simulation

Event	Test (TL5CMB-2) Time[vii] (seconds)	FE model Time (seconds)
Tractor begins to yaw	0.024	0.02 – 0.03
U-bolt connecting front axle to right-side leaf spring broke	0.08 – 0.11[viii]	0.06 – 0.08
Left-front tire lifts off pavement	0.18 -0.19	0.17 – 0.18
Right-front corner of trailer crosses front edge of barrier	0.21 – 0.22	0.21 – 0.22
Left-rear tires were lifted off the ground	0.34 – 0.35	0.25 – 0.26
The right front corner of the trailer was vertically coincident with the back face of the barrier	0.28 – 0.30	0.26 – 0.27
Tractor was parallel to barrier	0.35 – 0.40	0.34 – 0.35
Tractor reached peak roll and began to roll back from the barrier	0.33 – 0.35	0.34 – 0.35 (12.1 deg.)
Left-front tractor tires returned to roadway surface	0.50 – 0.52	0.31 – 0.32
Tractor rolled back to level position	0.67 – 0.70	0.51 – .052
Rear trailer tandem contacts barrier	0.65 – 0.68	0.68 – 0.70
Time of maximum impact force between trailer tandem and barrier	0.72	0.71
Trailer reached maximum roll and began to roll back from the barrier. All left side tires were off the ground	1.4 – 1.5 (unknown roll angle)	0.46 – 0.47 (9 degrees)
Tractor again reached peak (maximum) roll angle	unknown	0.63 – 0.64 (5 degrees)

Comparison of Time-History Data

The tractor-semitrailer FE model was instrumented with 17 accelerometers with 3 accelerometers positioned at locations consistent with the accelerometer placement in the full-scale crash test. In particular:

- Accelerometer 14 was placed near the center of gravity of the tractor inside the tractor cabin on the cabin floor

- Accelerometer 16 was placed near the center of the trailer tandem axle inside the trailer box on the floor

- Accelerometer 17 was placed inside the trailer on the floor near the kingpin.

[vii] Estimated from DVD video

[viii] Estimated from time-history data

The locations of these accelerometers are shown schematically in Figure 77. Figure 78 shows an illustration documenting the accelerometer locations of the test vehicle (taken from page 12 of the test report) [6].
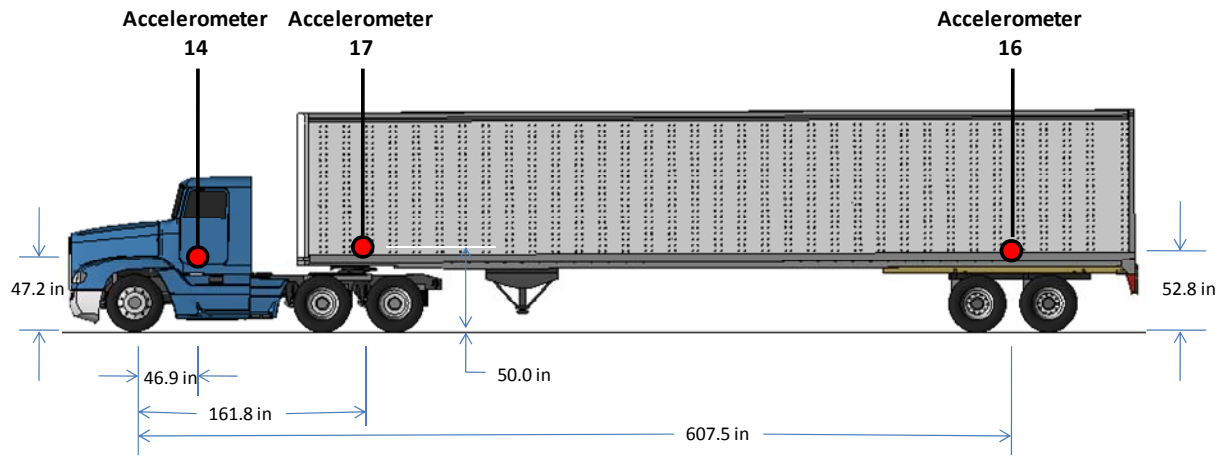
Figure 77. Illustration. Pertinent accelerometer locations in the FE model

Ax,y,z CG - Accelerometer mounted near center-of-gravity, 10 in right of centerline
Ax,y TF - Accelerometer mounted inside trailer on floor over pin
Ax,y R   - Accelerometer mounted on cross member (frame) 9 in rear of fifth wheel
Ax,y TR - Accelerometer mounted outside trailer on floor between axles

1 in = 25.4 mm
1 lb = 0.454 kg
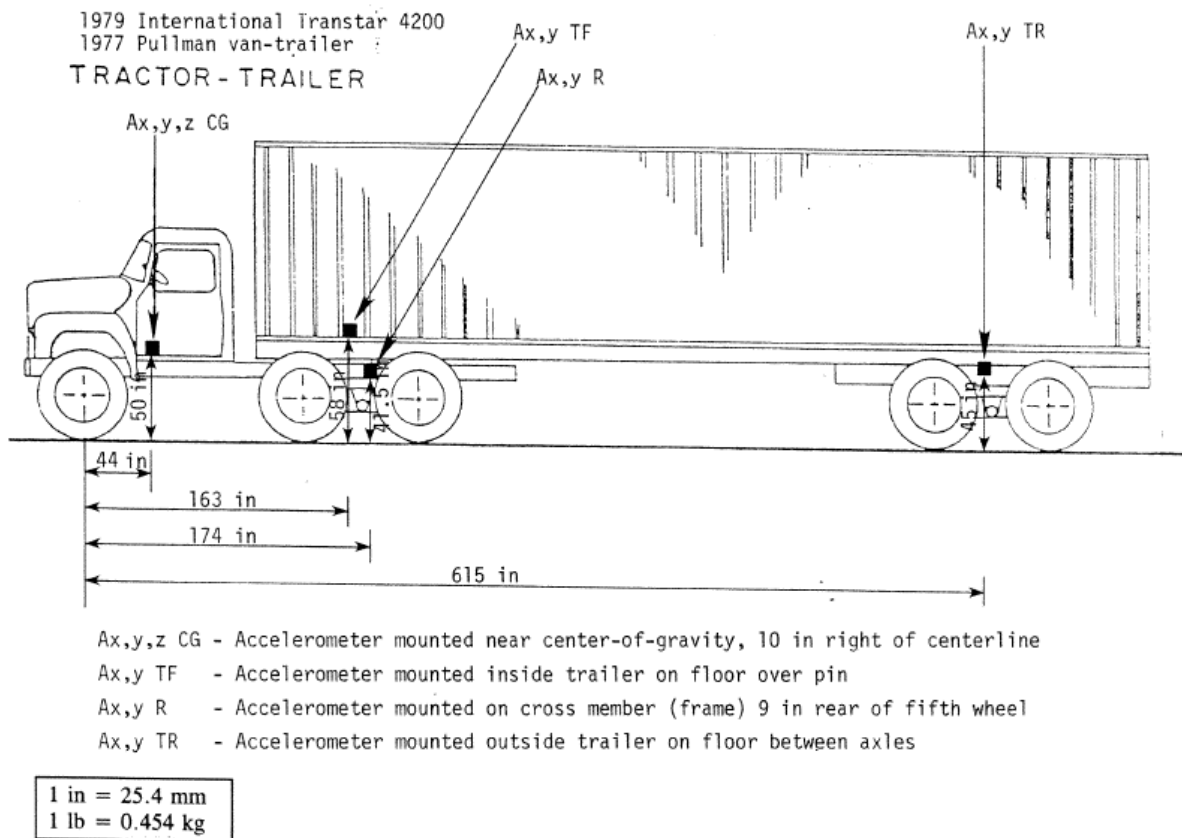
Figure 78. Illustration. Location of accelerometers for vehicle used in test 7069-13[6]

Figures 79, 80, and 81 show the longitudinal, transverse, and vertical acceleration-time histories, respectively, computed from accelerometer 14 located inside the tractor cabin. Figure 82 shows the roll, pitch, and yaw angles computed at accelerometer 14 location.

Figures 83, 84, and 85 show the longitudinal, transverse, and vertical acceleration-time histories, respectively, computed from accelerometer 16 located at the trailer tandem axle. Figure 86 shows the roll, pitch, and yaw angles computed at accelerometer 16 location.

Figures 87, 88, and 89 show the longitudinal, transverse, and vertical acceleration-time histories, respectively, computed from accelerometer 17 located at the trailer kingpin. Figure 90 shows the roll, pitch, and yaw angles computed at accelerometer 17 location.
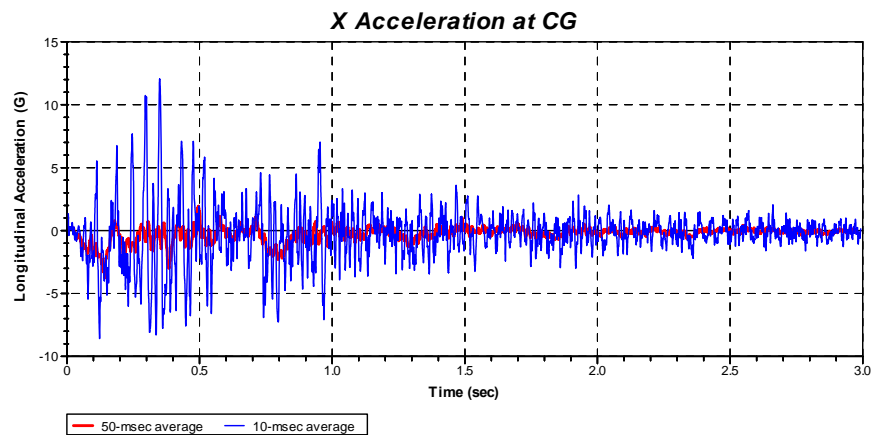
Figure 79. Chart. Longitudinal acceleration-time history plot from *accelerometer 14* inside the tractor cabin (10-millisecond and 50-millisecond moving averages)
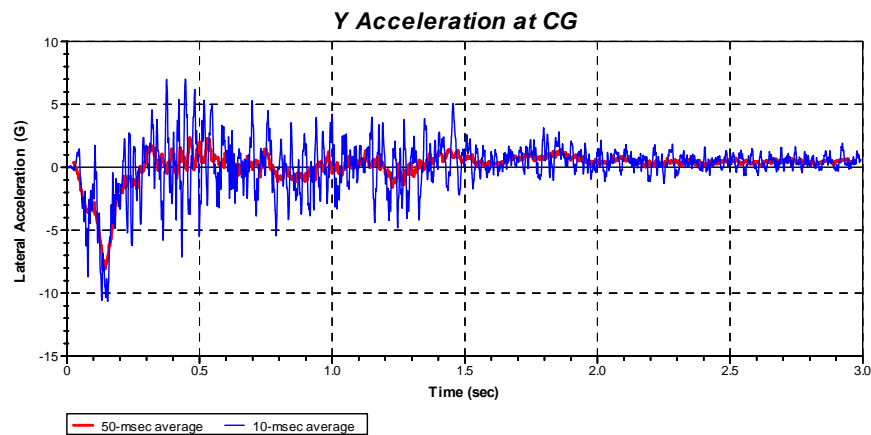
Figure 80. Chart. Transverse acceleration-time history plot from *accelerometer 14* inside the tractor cabin (10-millisecond and 50-millisecond moving averages)

Z Acceleration at CG
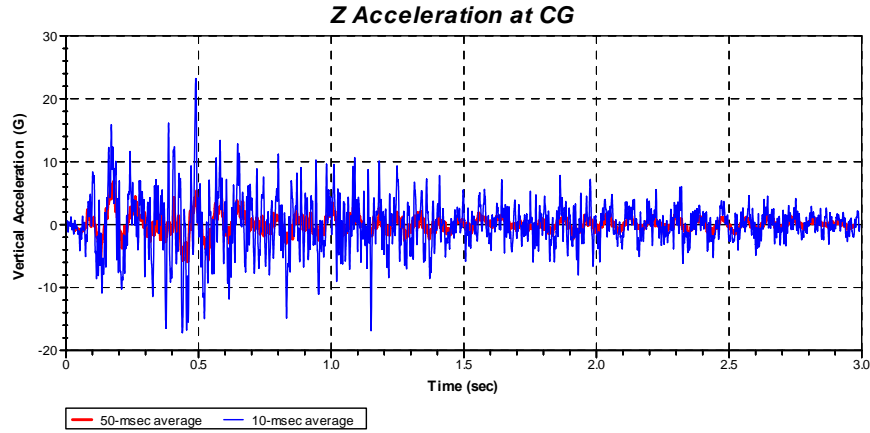
Figure 81. Chart. Vertical acceleration-time history plot from *accelerometer 14* inside the tractor cabin (10-millisecond and 50-millisecond moving averages)

Roll, Pitch and Yaw Angles
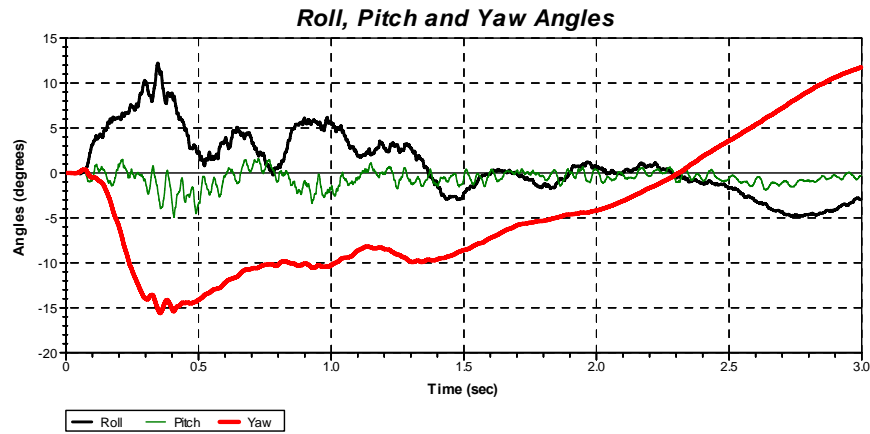
Figure 82. Chart. Roll, pitch and yaw-time history plot from *accelerometer 14* location inside the tractor cabin

X Acceleration at CG
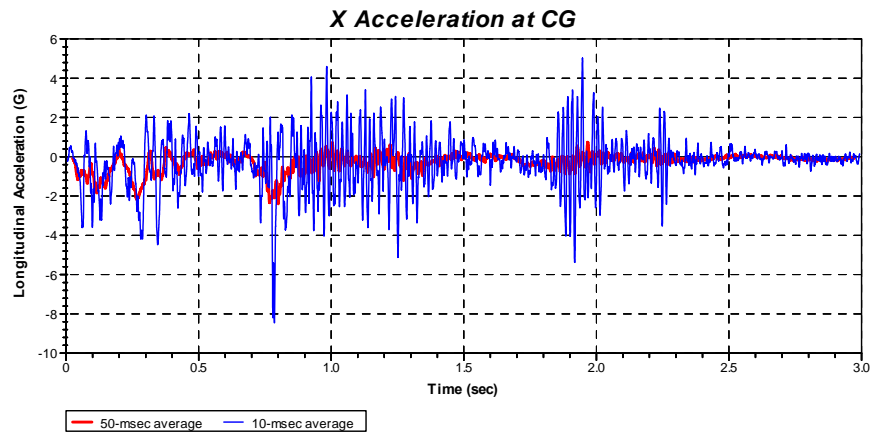
Figure 83. Chart. Longitudinal acceleration-time history plot from *accelerometer 16* near the trailer tandem axle (10-millisecond and 50-millisecond moving averages)

99
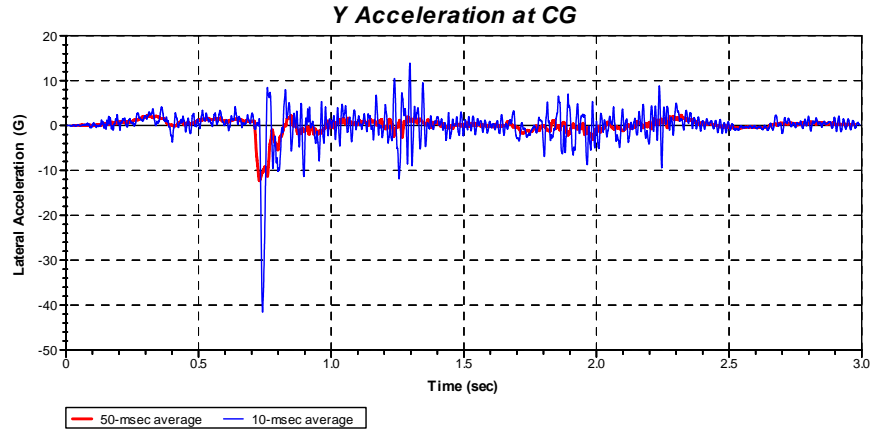
Figure 84. Chart. Transverse acceleration-time history plot from *accelerometer 16* near the trailer tandem axle (10-millisecond and 50-millisecond moving averages)
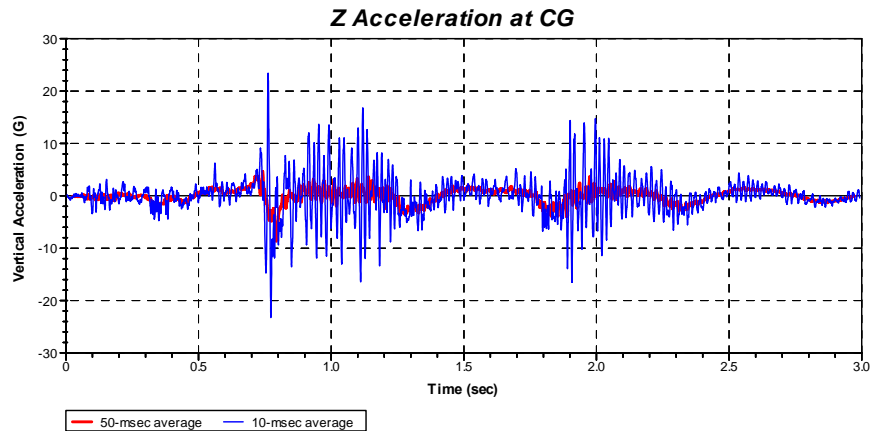
Figure 85. Chart. Vertical acceleration-time history plot from *accelerometer 16* near the trailer tandem axle (10-millisecond and 50-millisecond moving averages)
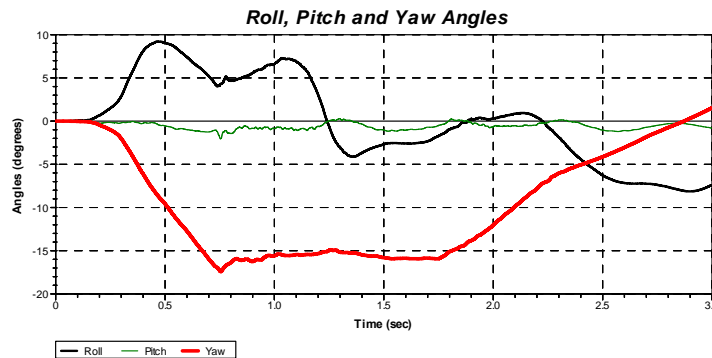
Figure 86. Chart. Roll, pitch and yaw-time history plot from *accelerometer 16* near the trailer tandem axle

100
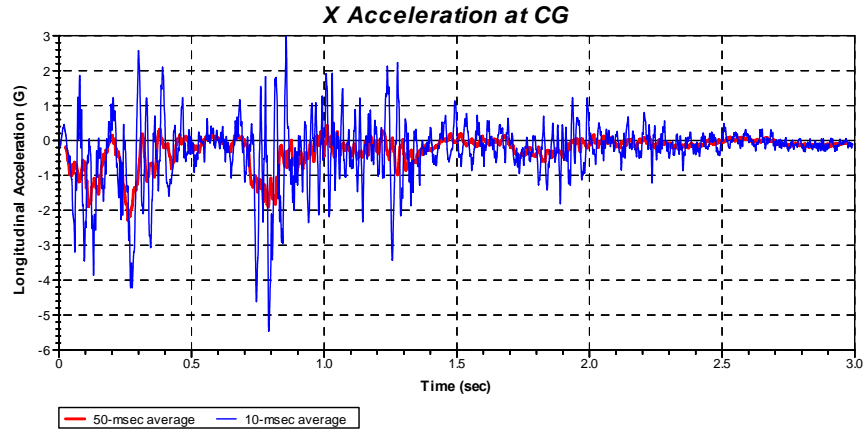
Figure 87. Chart. Longitudinal acceleration-time history plot from *accelerometer 17* near the trailer kingpin (10-millisecond and 50-millisecond moving averages)
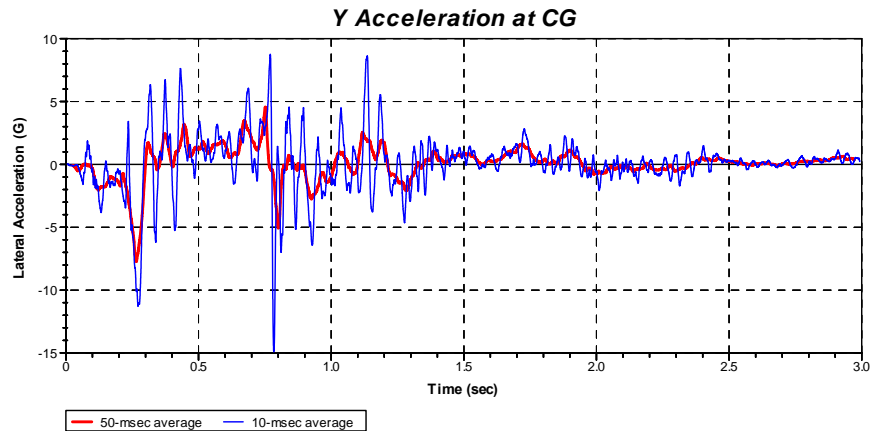
Figure 88. Chart. Transverse acceleration-time history plot from *accelerometer 17* near the trailer kingpin (10-millisecond and 50-millisecond moving averages)
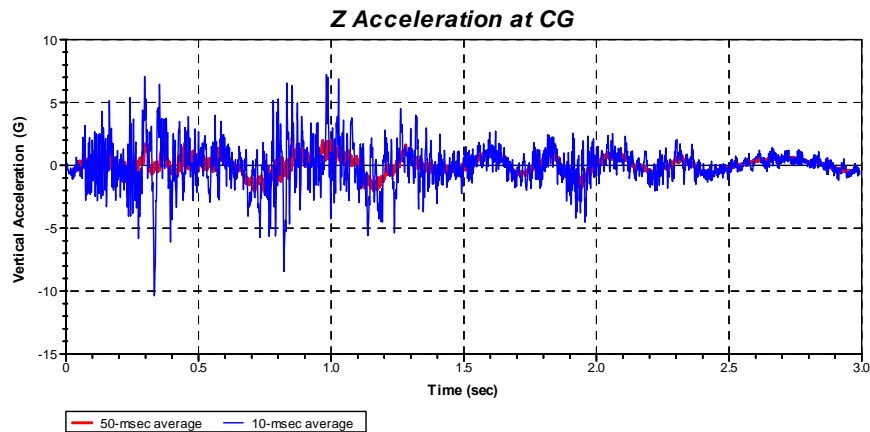
Figure 89. Chart. Transverse acceleration-time history plot from *accelerometer 17* near the trailer kingpin (10-millisecond and 50-millisecond moving averages)

101
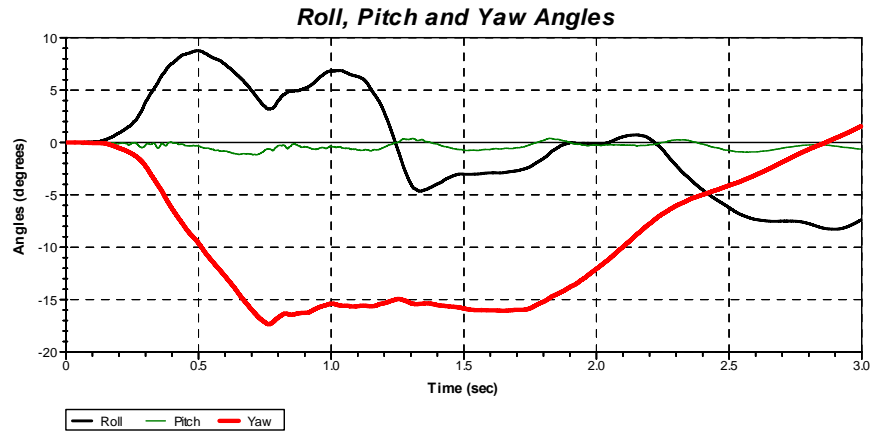
Figure 90. Chart. Roll, pitch and yaw-time history plot from *accelerometer 17* near the trailer kingpin

Figures 91, 92 and 93 show the 50-millisecond moving average of the longitudinal, transverse, and vertical acceleration-time histories, respectively, at the tractor c.g. location, comparing the FE analysis results with full-scale test, 7069-13. Figures 94 and 95 show the 50-millisecond moving average of the longitudinal and transverse acceleration-time histories, respectively, at the trailer kingpin location. Figures 96 and 97 show the 50-millisecond moving average of the longitudinal and transverse acceleration-time histories, respectively, at the trailer tandem location.

Figures 91 and 92 are annotated with phenomena from the analysis results to help understand the meaning of the peaks in acceleration at key points during the impact event. Each of these phenomena is described below:

- The first peak in acceleration occurred at approximately 0.04 to 0.06 seconds after impact and was coincident with the front impact side tire impact against the rigid barrier.

- At approximately 0.06 – 0.08 seconds the u-bolts connecting the front axle to the leaf-suspension on the impact side of the vehicle failed, allowing the wheel and front axle to push backwards relative to the vehicle.

- At 0.117 seconds the right-side wheel pushed back against the wheel-well and fuel tank resulting in the maximum longitudinal and lateral load on the tractor.

- After reaching the peak load, the tractor subsequently rebounded slightly away from the barrier resulting in a significant decrease in load, as noted by the reversal of both the longitudinal and lateral acceleration values.

- At 0.2 seconds the wheels of the tractor tandem engaged the barrier and caused the next significant peak in longitudinal acceleration.

- At 0.34 – 0.35 seconds the tractor was parallel to the barrier.

102

- At 0.38 seconds the bottom of the front, impact side of the trailer dropped onto the top of the barrier, resulting in another peak longitudinal acceleration.

- The final major peak in both longitudinal and lateral acceleration occurs at 0.75 seconds when the rear of the trailer impacted the barrier.
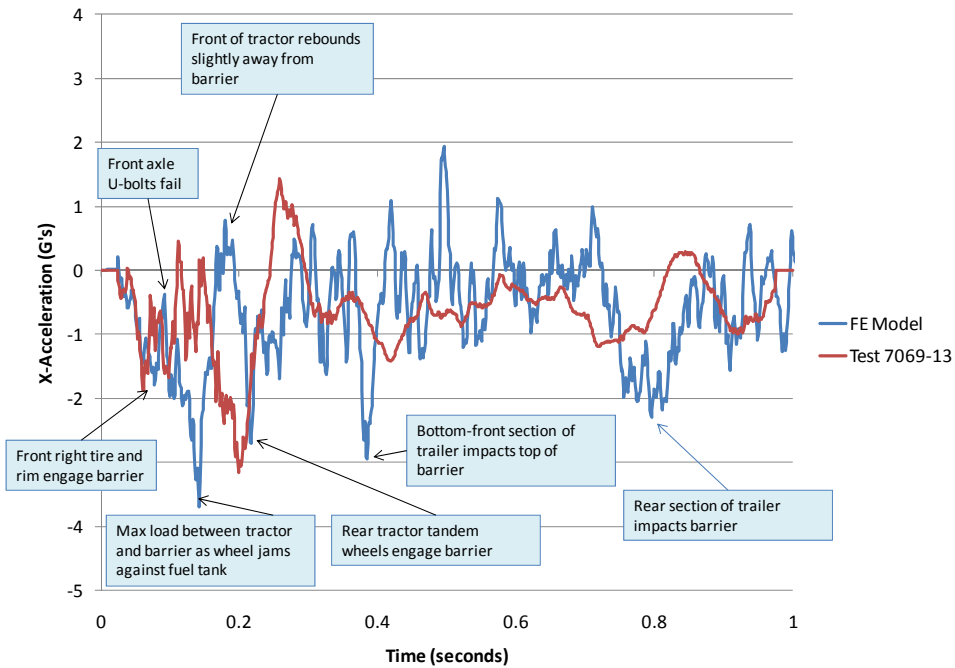
Figure 91. Chart. Longitudinal acceleration-time history plot from the FE simulation and Test 7069-13 from accelerometer at the tractor C.G. (50-millisecond moving averages)
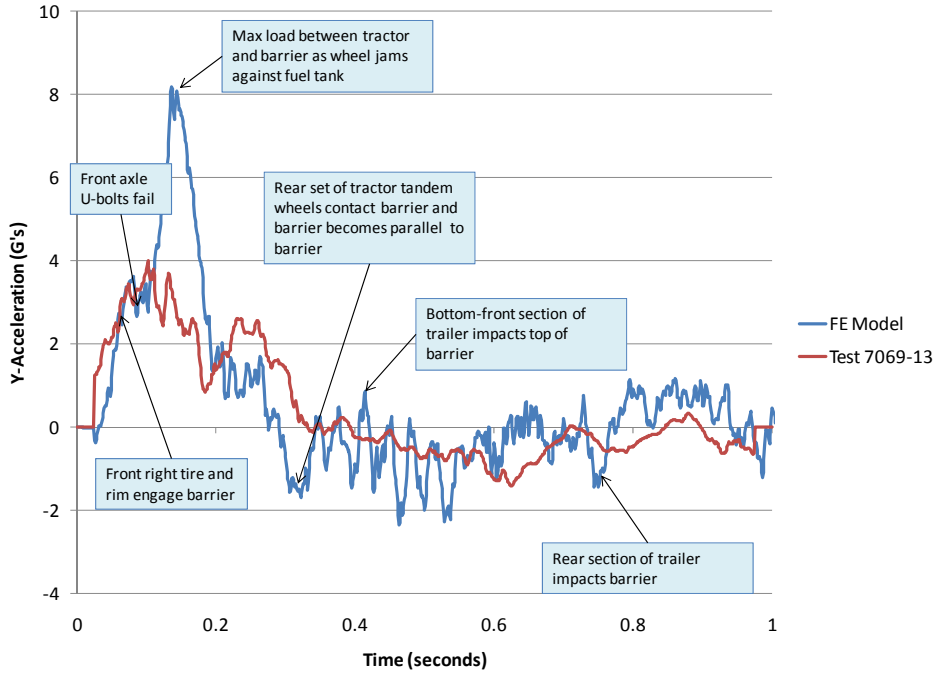
Figure 92. Chart. Lateral acceleration-time history plot from the FE simulation and Test 7069-13 from accelerometer at the tractor C.G. (50-millisecond moving averages)
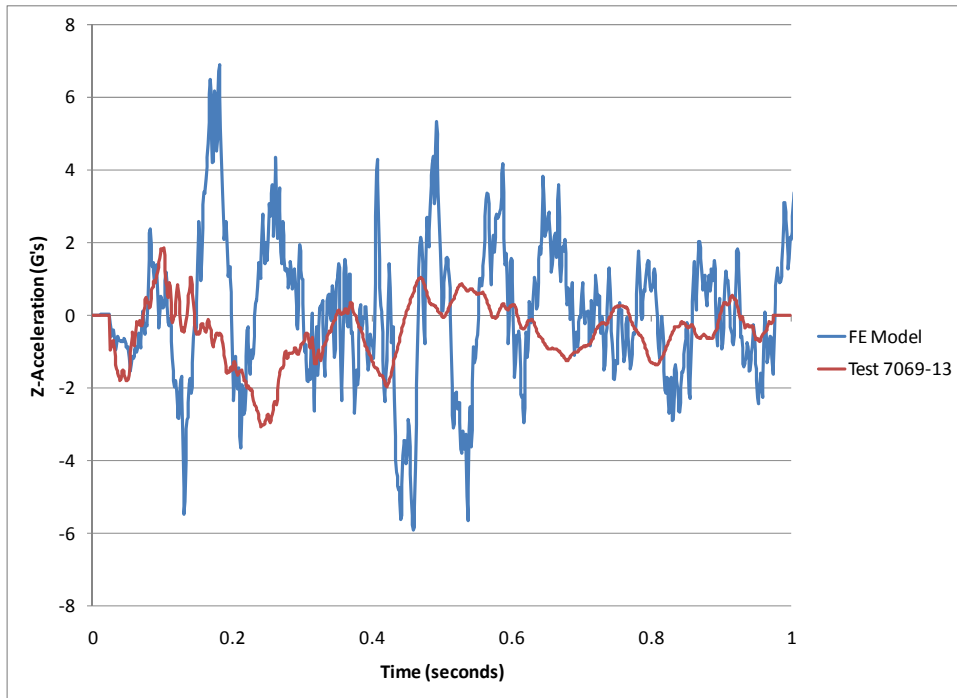
Figure 93. Chart. Vertical acceleration-time history plot from the FE simulation and Test 7069-13 from accelerometer at the tractor C.G. (50-millisecond moving averages)
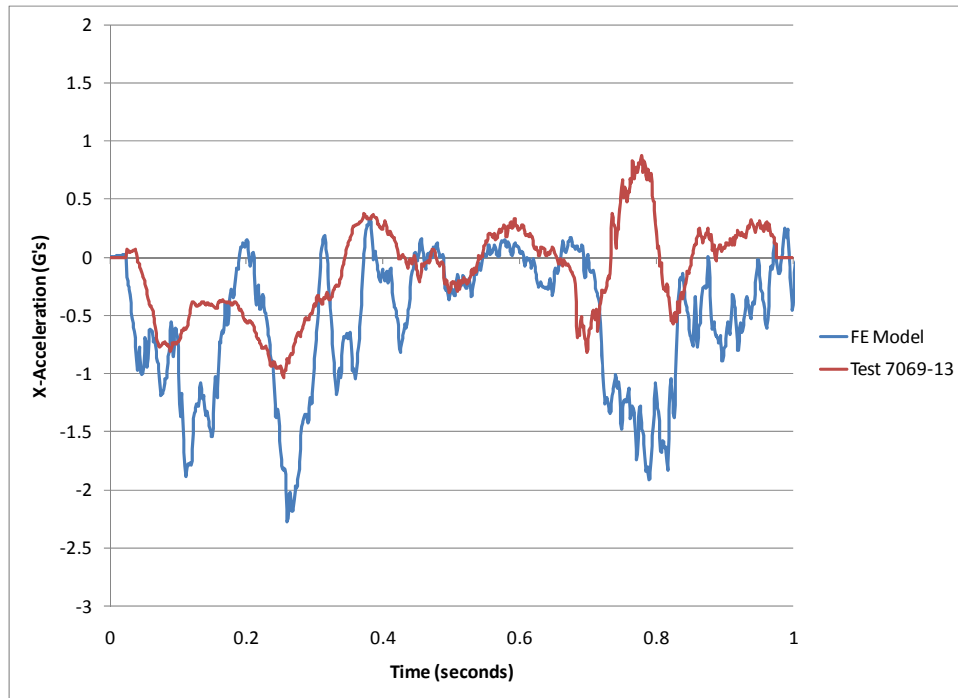
Figure 94. Chart. Longitudinal acceleration-time history plot from the FE simulation and Test 7069-13 from accelerometer at the trailer kingpin (50-millisecond moving averages)
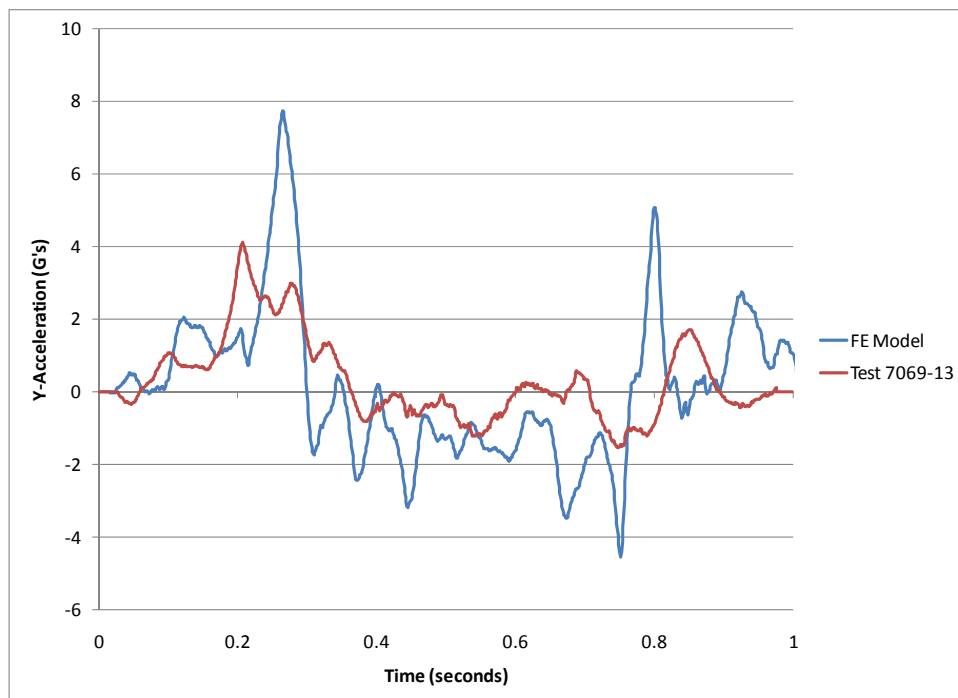
Figure 95. Chart. Lateral acceleration-time history plot from the FE simulation and Test 7069-13 from accelerometer at the trailer kingpin (50-millisecond moving averages)
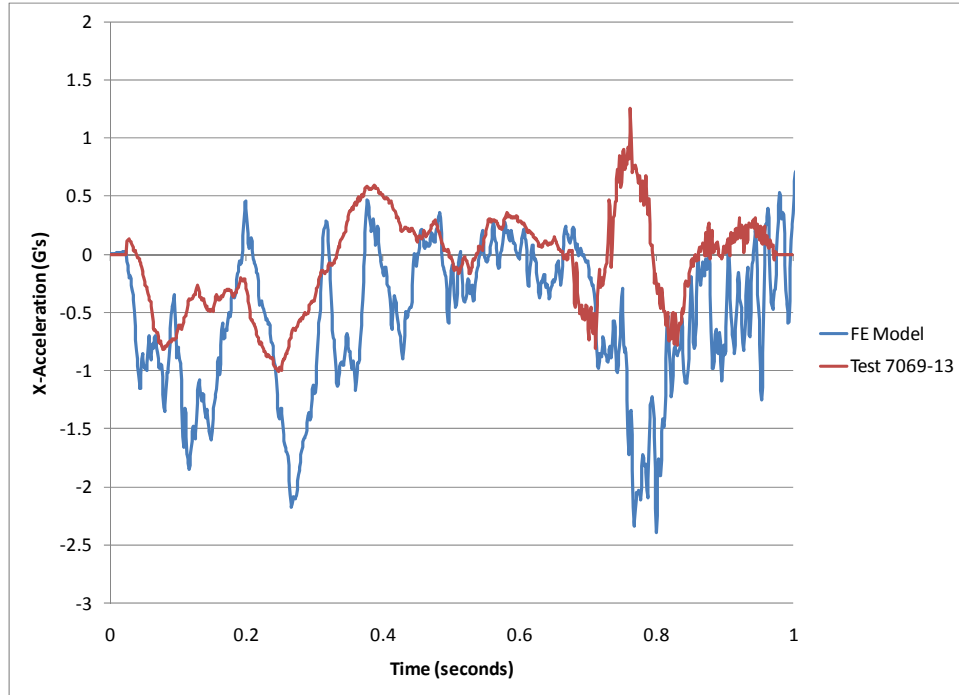
Figure 96. Chart. Longitudinal acceleration-time history plot from the FE simulation and Test 7069-13 from accelerometer at the trailer tandem (50-millisecond moving averages)
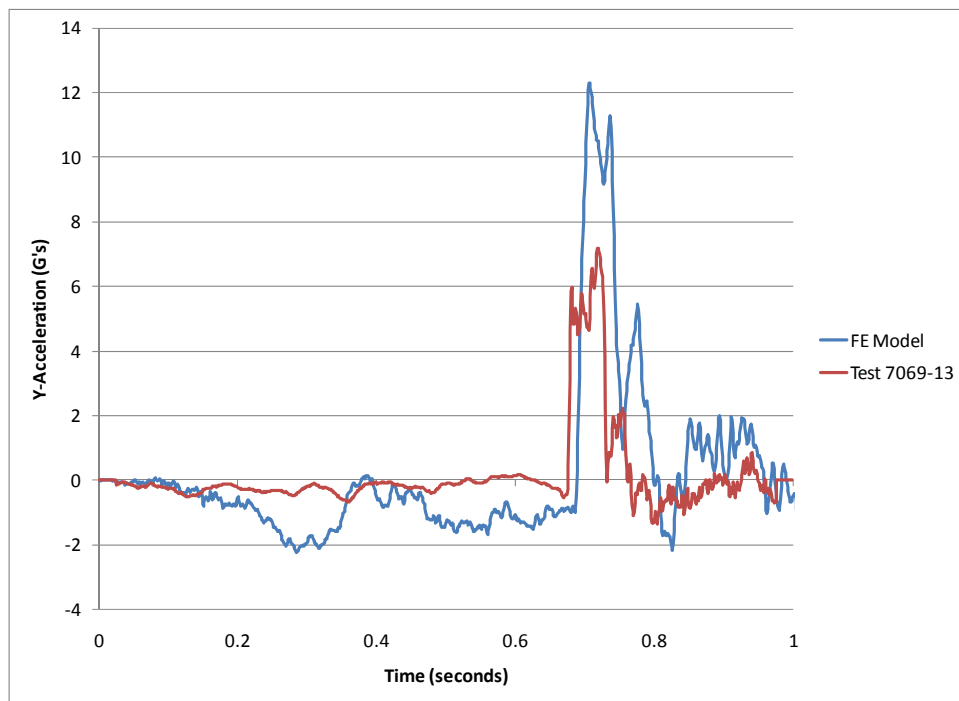
Figure 97. Chart. Lateral acceleration-time history plot from the FE simulation and Test 7069-13 from accelerometer at the trailer tandem (50-millisecond moving averages)

106

Test Vehicle Damage

The test report did not provide information regarding damage to the vehicle. The test report and test videos showed that the tractor and trailer rolled onto its side at approximately 3 seconds after impact with the barrier. The damage caused to the right side of the tractor during the impact can be seen in Figure 98. It is also apparent in Figure 98 that the front axle separated from the vehicle at some point during the test. There was additional damage to the left side of the vehicle that resulted from the vehicle rolling over onto its side, as shown in Figure 99.

Figure 98. Photograph. Post test view of test vehicle illustrating damage to tractor

Figure 99. Photograph. Post test view of test vehicle illustrating damage to tractor due to roll-over

107

FE Vehicle Model Damage

Figure 100 through Figure 103 show contour plots of plastic strain, which were used to identify areas of the tractor model that suffered damage during the simulated impact event. The damage to the tractor model was limited to the impact side. The most severe damage was to the front bumper, the fender, the side steps, the fuel tank, and the front-right suspension. There was also moderate plastic strain in components of the support structure for the fifth-wheel.

Figure 104 through 106 show contour plots of plastic strain for the trailer model. The trailer experienced plastic strains in the rear impact-side of the bumper, the suspension structure and in the connection points of the trailer bogie to the lower cross-beams of the trailer box.
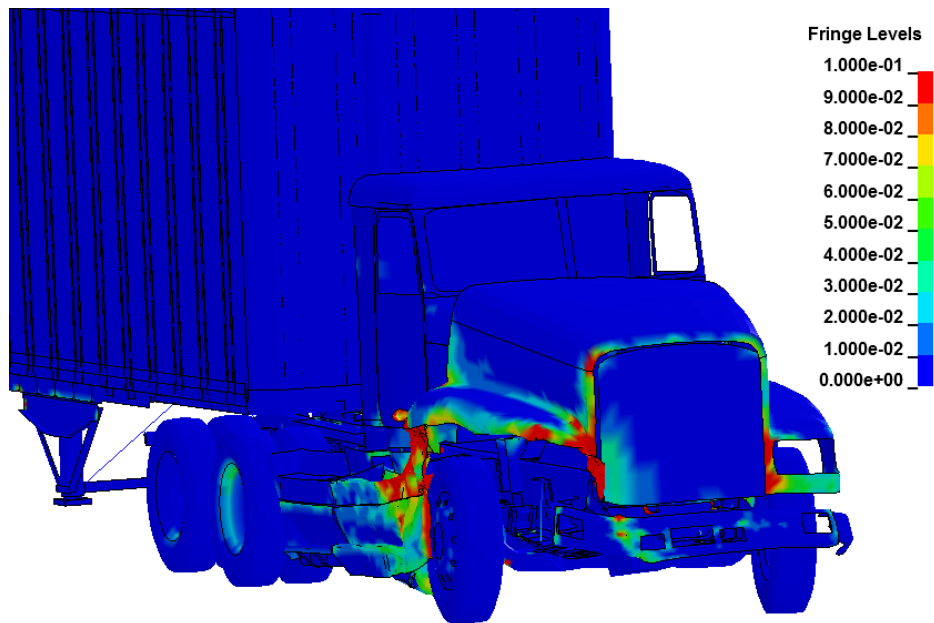
Figure 100. Illustration. Contour of effective plastic strain (with contours cut-off at 10%) used to identify areas of the tractor model that sustained damage during simulated impact
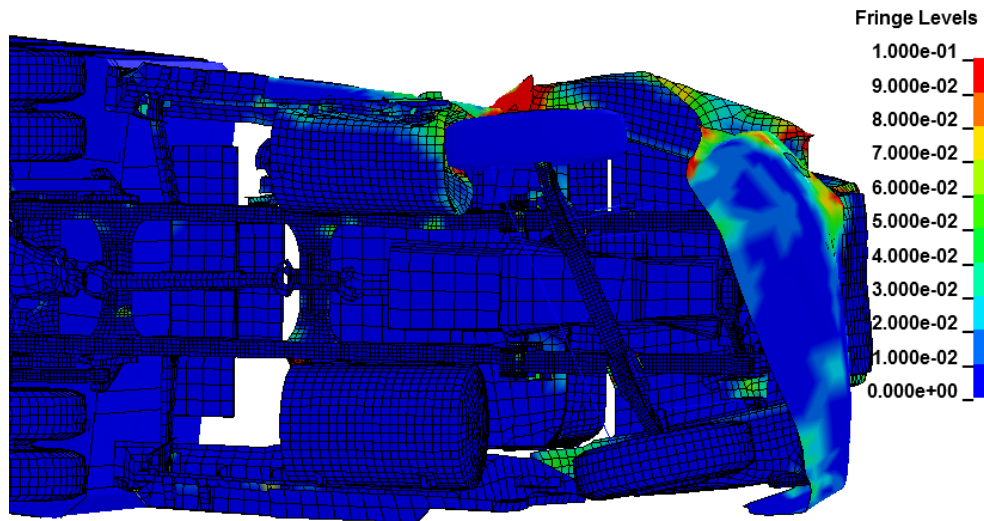
Figure 101. Illustration. Contour of effective plastic strain (with contours cut-off at 10%) used to identify areas of the tractor model that sustained damage during simulated impact
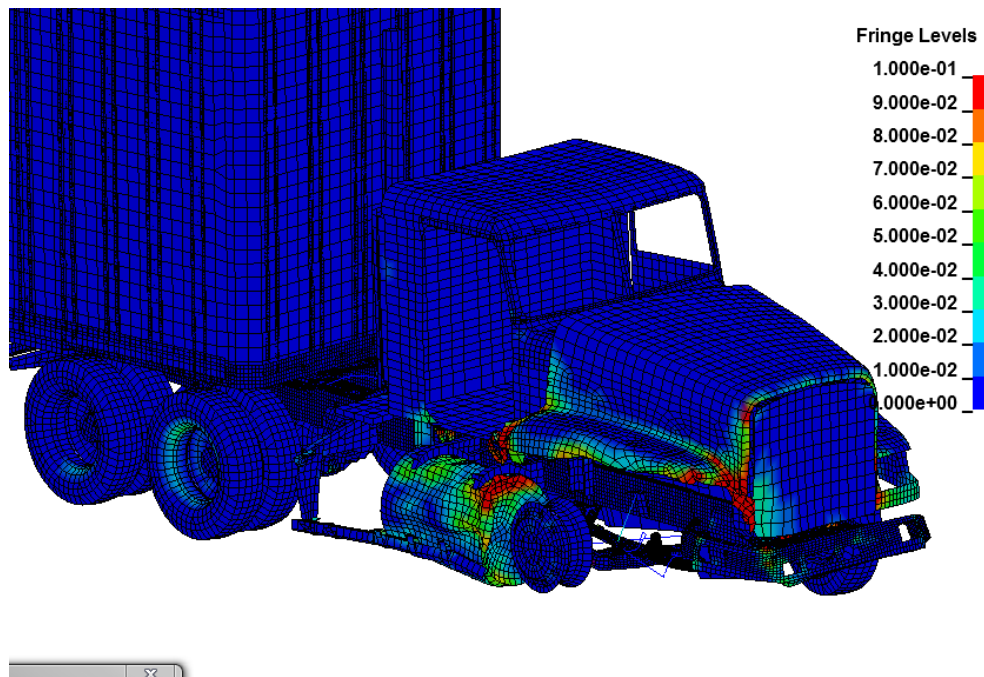
Figure 102. Illustration. Contour of effective plastic strain (with contours cut-off at 10%) used to identify areas of the tractor model that sustained damage during simulated impact
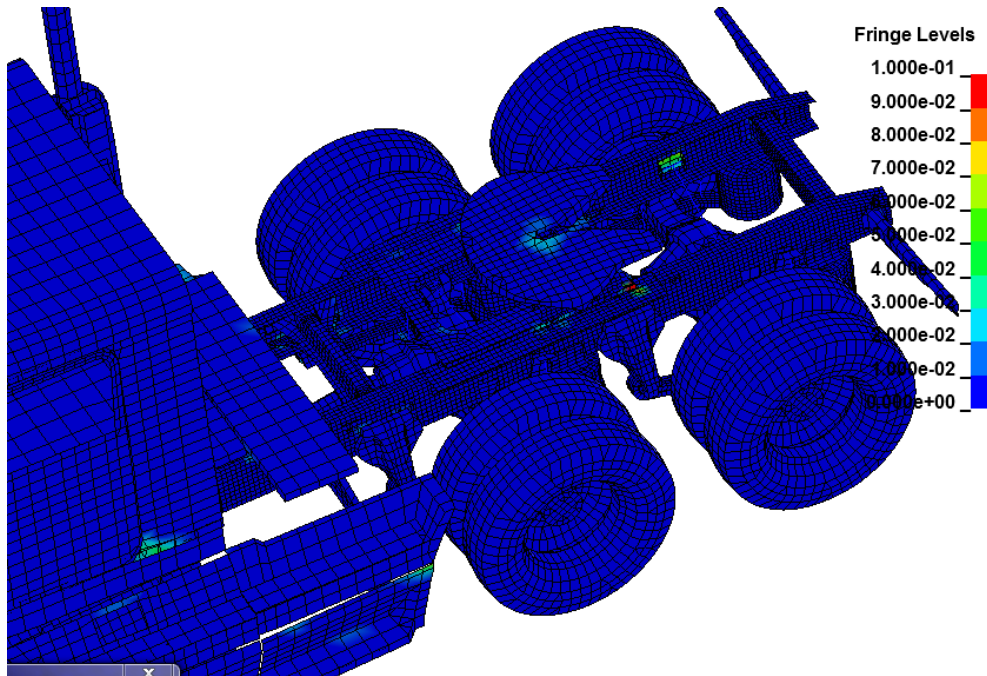
Figure 103. Illustration. Contour of effective plastic strain (with contours cut-off at 10%) used to identify areas of the tractor model that sustained damage during simulated impact
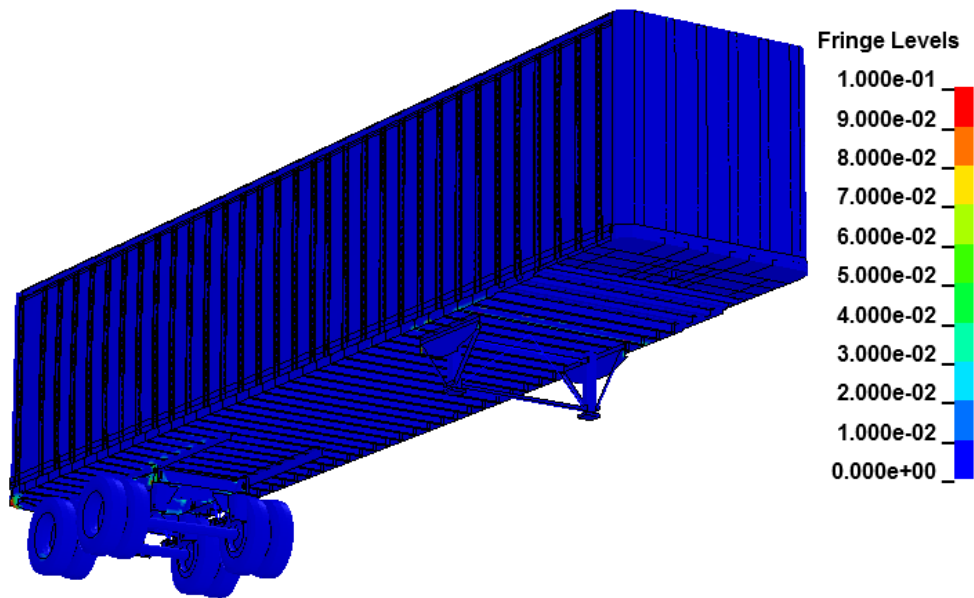
Figure 104. Illustration. Contour of effective plastic strain (with contours cut-off at 10%) used to identify areas of the trailer model that sustained damage during simulated impact
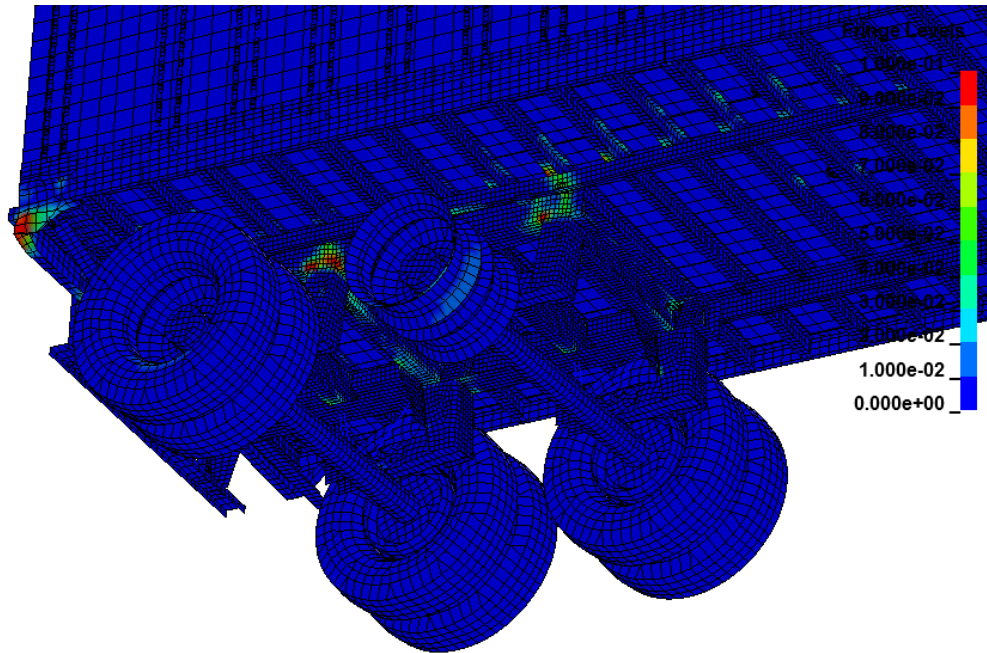
Figure 105. Illustration. Contour of effective plastic strain (with contours cut-off at 10%) used to identify areas of the trailer model that sustained damage during simulated impact
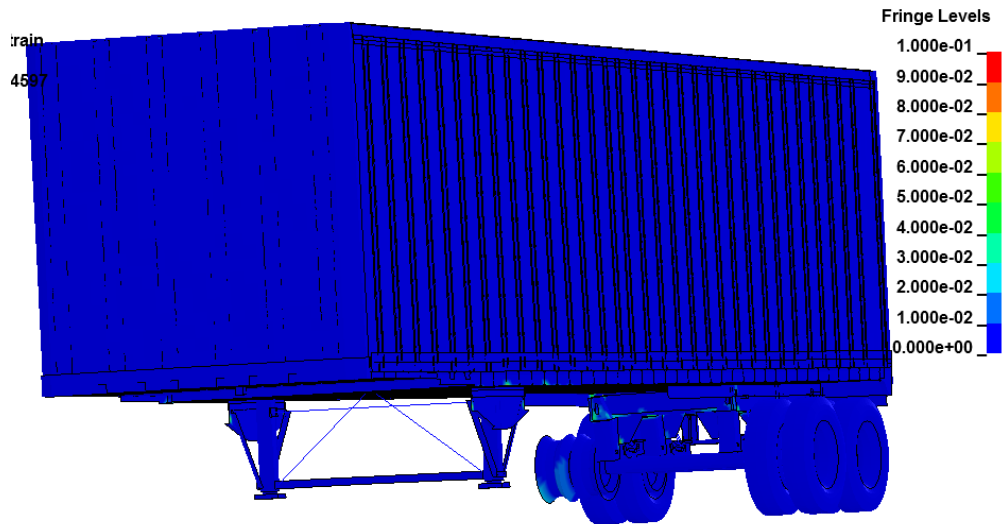
Figure 106. Illustration. Contour of effective plastic strain (with contours cut-off at 10%) used to identify areas of the trailer model that sustained damage during simulated impact

Chapter 4 – Quantitative Evaluation using NCHRP 22-24 Procedure

Quantitative Validation Approach

The *quantitative validation* assessment of the model's results was based on the recommended validation procedures that are outlined in NCHRP report 22-24 titled "Recommended Procedures for the Verification and Validation of Computer Simulations used for Roadside Safety Applications" [4]. The objective of NCHRP 22-24 is to develop guidelines for verification and validation of FE analysis models for crash simulations of roadside safety features. The focus of these guidelines is to establish accuracy, credibility, and confidence in the results of crash test simulations that are intended to support policy decisions, and to be used for approval of design modifications to roadside safety devices that were originally approved with full-scale crash testing.

The tractor-trailer FE model is one of several models that are being used as "benchmark cases" for the NCHRP 22-24 project. This quantitative validation will reflect those recommended procedures.

The validation procedure has three steps:

1. Solution verification: Indicates whether the analysis solution produced numerically stable results (ensures that basic physical laws are upheld in the model).

2. Time-history evaluation: Quantitative measure of the level of agreement of time-history data (e.g., x, y, z accelerations and roll, pitch, and yaw rates) between analysis and test.

3. Phenomena Importance Ranking Table: A table that documents the types of phenomena that a numerical model is intended to replicate and verifies that the model produces results consistent with its intended use.

Following is a discussion of the time-history evaluation metrics, their acceptance criteria, and the Phenomena Importance Ranking Table.

Time-History Evaluation

A major task in the NCHRP 22-24 project was the development of a computer program that will allow the user to select one or more validation metrics as a basis to compare results from a computational model to the results from physical tests. The validation program is called RSVVP, after the acronym for "Roadside Safety Verification and Validation Program."
The metrics computed in RSVVP provide a mathematical measure that quantifies the level of agreement between the shapes of time-history data obtained from simulations and tests such as acceleration, velocity, and displacement at specific sensor locations. There are currently 14 methods in the RSVVP software that are available for computing quantitative comparison measures. All the metrics are deterministic shape-comparison metrics and are classified into

three main categories. These are listed below and are described in detail in the Final Report for the NCHRP Report 22-24 project and in the literature [4, 8, 9, 10, 11]. The methods are"

Magnitude Phase Composite (MPC) metrics
1. Geers
2. Geers CSA
3. Sprague & Geers
4. Russell
5. Knowles & Gear

Single Value Metrics
6. Whang's inequality
7. Theil's inequality
8. Zilliacus error
9. RSS error
10. Weighted Integrated Factor
11. Regression coefficient
12. Correlation Coefficient
13. Correlation Coefficient (NARD)

Analysis of Variance (ANOVA)
14. Ray

The MPC metrics treat the magnitude and phase of the curves separately and combine them into a single value comprehensive metric. The single-value metrics give a single numerical value that represents the agreement between two curves. The ANOVA metric is a statistical assessment of whether the variance between two curves can be attributed to random error.

Another important task in the NCHRP 22-24 project included determining which of the metrics are the most effective for comparing results of roadside safety impact events and developing acceptance criteria (e.g., what value of the metric indicates that the curves are statistically the same).

The recommended metrics that were suggested by the NCHRP 22-24 project team for comparing time-history traces from full-scale crash tests and/or simulations of crash tests are the Sprague & Geers metrics and the ANOVA metrics. The Sprague & Geers metrics assess the magnitude and phase of two curves while the ANOVA examines the differences of residual errors between them. The definitions of these metrics are shown below:

Sprague & Geers

$$\text{Magnitude } (M) = \sqrt{\frac{\Sigma c_i^2}{\Sigma m_i^2} - 1}$$

$$\text{Phase } (P) = \frac{1}{\pi} \cos^{-1} \frac{\Sigma c_i m_i}{\sqrt{\Sigma c_i^2 \Sigma m_i^2}}$$

$$\text{Comprehensive } (C) = \sqrt{M^2 + P^2}$$

Equation 12. Equations for calculating the sprague & geers metrics

ANOVA

$$\text{Residual Error } (\bar{e}^r) = \frac{\Sigma(m_i - c_i)}{m_{max}} \cdot \frac{1}{n}$$

$$\text{Standard Deviation } (\sigma) = \sqrt{\frac{1}{n}\Sigma(m_i - c_i - \bar{e}^r)^2}$$

Equation 13. Equations for calculating the ANOVA metrics

Where,

c_i = calculated quantities

m_i = measured quanties

m_{max} = maximum measured experimental value

$\bar{e}^r$ = relative average residual error

σ = relative standard deviation

Time-History Evaluation Acceptance Criteria

Once a measure of comparison is obtained using a quantitative metric, it is necessary to establish an acceptance criterion for deciding if the comparison is acceptable. Because of the highly nonlinear nature of crash events, there are often considerable differences in the results of essentially identical full-scale crash tests – this was shown in the NCHRP study. Likewise, a computational model may not match "exactly" the results of a physical test, but the difference should be no greater than what is expected between physical tests. The approach taken in the NCHRP study was to determine the realistic variation in the deterministic shape comparison metrics for a set of identical physical experiments and use that variation as an acceptance criterion. For example, if a series of physical experiments result in a shape comparison metric that is within some specific range, a mathematical model of the same phenomena should fall within that same range.

The current acceptance criteria is based on the results of a quantitative comparison of ten essentially identical full-scale crash tests that were performed as part of the ROBUST project involving small car impact into a vertical rigid wall at 100 km/hr and 25 degrees [12, 13]. The

purpose of the ROBUST project was to assess the repeatability of full-scale crash tests and the consistency of data processing among different test agencies. There were two sets of tests carried out by five independent test laboratories. The first set involved the same vehicle make, model and year. The second set of tests involved a variety of vehicle makes and models, but in all cases, the test vehicle corresponded to the standard small-car test vehicle specified in the European crash test standards, EN 1317 [14]. A rigid barrier was intentionally chosen to limit the scatter of the results by isolating the energy of the event to strain energy and kinetic energy in the test vehicle. In all cases, the three components of acceleration were measured at the center of gravity of the vehicles.

The comparison metrics were used to compare the similarity of the time histories of the tests and to determine acceptance criteria based on those results. The original raw time histories from the 10 tests were filtered, re-sampled, and synchronized so they could be directly compared to each other. The statistics derived from the analysis of the residuals confirmed that the errors were normally distributed and were thus attributable to normal random experimental error. The expected error between the tests was shown to be approximately 40 percent based on the Sprague-Geers metrics. The average residual error component of the ANOVA metric was generally very close to zero for all the crash tests. The standard deviation of the residual errors was as high as 31 percent, and like all the other metrics, the standard deviation of the standard deviation of the residuals doubled in the second set of tests where the vehicles were similar but not identical.

In a much earlier study, Ray proposed an acceptance criterion of a mean residual error less than 5 percent of the peak and a standard deviation of less than 20 percent of the peak test acceleration based on an evaluation of the ANOVA metrics for a series of six identical frontal rigid pole impacts [11]. The redirection impacts in the ROBUST project resulted in greater error than this between the test data, because as discussed earlier, redirection tests are highly nonlinear. While the impact conditions may be essentially identical in redirection tests, uncontrollable variations in the experiment, such as the suspension or steering system response, can significantly affect the overall result.

A similar multi-vehicle study should be carried out to compare the results of full-scale tractor trailer tests. It is expected that a comparison of essentially identical tractor-trailer tests, where there are many aspects of the vehicle that could influence the results (e.g., suspension response, suspension failure, friction between tire and pavement, vehicle articulation), would result in higher level of expected error between tests.

Based on the results of the NCHRP 22-24 study, comparisons must be made using acceleration-time histories and/or angular rate-time histories with the following time-history acceptance criteria:

116

- Sprague & Geers
  - Magnitude should be less than 40 percent
  - Phase should be less than 40 percent
- ANOVA metrics
  - Mean residual error should be less than 5 percent
  - Standard deviation should be less than 35 percent.

Multi-channel Time-History Evaluation

In some cases, there may be one or two components of acceleration that dominate an impact event. An example might be a small sign support test where the longitudinal acceleration has a much greater influence on the results of the impact event than do the lateral or vertical accelerations. Or, a 90-degree side impact where the lateral acceleration dominates. The less important channels may not satisfy the criteria because they are essentially recording noise. The dominant channel in these examples will probably be an order of magnitude greater than some of the other less important channels and the response is essentially determined by one channel. RSVVP includes a method for accounting for different levels of importance of channels. The procedure basically uses the change in momentum represented by each channel and weights the comparison metrics by the proportion of the momentum in each channel. Then, a single set of composite metrics are computed based on the weighted average of the individual data channels.

Phenomena Importance Ranking Tables (PIRT)

FE models, like all mathematical models, are idealized representations of physical systems. The model developer must make assumptions about what is important in the model and what phenomena should be represented in the mathematical model. Unfortunately, these assumptions are generally not apparent to those reviewing the results of the model. A PIRT provides a quick way of documenting the phenomena that have been included in a mathematical model. The PIRT ranks the importance of those phenomena and assesses the overall verification and validation level of the model, so that subsequent users of the model or reviewers of the results will know what phenomena the model can reasonably be expected to represent.

Roadside safety simulations are generally patterned after the standardized tests in NCHRP Report 350. Each Report 350 test involves a test vehicle, a roadside appurtenance, and initial conditions. Each of these should be represented in a PIRT. For example, vehicle models must, at a minimum, have the correct mass distribution, correct exterior geometry, and realistic structural components. Depending on the application, the vehicle models may also require greater detail in the suspension system, the possibility of tire failure, and other refinements. The PIRT is not a static document and it should be developed based on the model's functionality.

The PIRT is patterned after the full-scale crash test evaluation criteria listed in Table 5.1 in NCHRP Report 350. The analyst is asked to report the values for the individual metrics from the

full-scale test and the computer analysis and calculate the relative difference. If the relative differences are less than 20 percent, then the phenomena are considered to be replicated.

The PIRT includes information regarding quantitative validation of individual components of the model. In the current tractor-semitrailer model for example, physical tests were performed for validating the front leaf-spring assembly for the tractor, the air-spring suspension for both the tractor and trailer, material properties for components of the trailer, shock absorbers, and suspension bump-stop for the front suspension. The simulation data was compared to the test data using the metrics in RSVVP. A PIRT validation form was included for each validated component of the model and is included as Appendix D in this report.

Quantitative Evaluation Results

FEA vs. Test TL5CMB2

<u>*Trailer Rear Accelerometers*</u>

The quantitative evaluation was based on a comparison of the acceleration-time histories collected in the model to those collected in full-scale crash test TL5CMB-2. The data was obtained from an accelerometer mounted to the floor of the semitrailer near the center of the tandem axle at the rear of the trailer. The comparison metrics were computed using RSVVP (Roadside Safety Verification and Validation Program). The results of the quantitative validation are provided in the Verification/Validation Report located in Appendix B. The quantitative evaluation showed mixed results regarding individual components of acceleration, but overall the model was in good agreement with the test, as described below.

Individual Channel Assessment

Based on the Sprague & Geers metrics, a comparison of the individual components of acceleration indicated that the simulation was in good agreement with the test regarding the y-component acceleration (i.e., lateral acceleration), but was not in agreement with the test regarding x-acceleration channel (longitudinal component) and z-acceleration channel (vertical component). However, the metrics computed for the resultant acceleration-time history were in good agreement with the test. The ANOVA metrics indicated that the simulation was in good agreement with the test regarding comparison of the individual components of acceleration, as well as the resultant acceleration-time history. Table 7 shows the Sprague & Geers metrics and the ANOVA metrics computed for the x-, y- and z-acceleration channels using the RSVVP program.

Table 7. Roadside Safety Validation Metrics Rating Table – Time History Comparisons

	Evaluation Criteria									
O	***Sprague-Geer Metrics*** List all the data channels being compared. Calculate the M and P metrics using RSVVP and enter the results. Values less than or equal to 40 are acceptable.							**Time interval** **[0 sec; 1.54 sec]**		
		RSVVP Curve Preprocessing Options								
		Filter Option	**Sync. Option**	**Shift**		**Drift**		**M**	**P**	**Pass?**
				True Curve	**Test Curve**	**True Curve**	**Test Curve**			
	X acceleration	CFC 180	Min. area of Residuals	N	N	N	N	60.6	48.8	N
	Y acceleration	CFC 180	Min. area of Residuals	N	N	N	N	17.3	35.4	Y
	Z acceleration	CFC 180	Min. area of Residuals	N	N	N	N	18.7	46.3	N
	Resultant acceleration	CFC 180	Min. area of Residuals	N	N	N	N	3.3	20	Y
P	***ANOVA Metrics*** List all the data channels being compared. Calculate the ANOVA metrics using RSVVP and enter the results. Both of the following criteria must be met: • The mean residual error must be less than five percent of the peak acceleration ($\bar{e} \leq 0.05 \cdot a_{Peak}$) and • The standard deviation of the residuals must be less than 35 percent of the peak acceleration ($\sigma \leq 0.35 \cdot a_{Peak}$)							**Mean Residual**	**Standard Deviation of Residuals**	**Pass?**
	X acceleration/Peak							0.02	0.11	Y
	Y acceleration/Peak							0.01	0.09	Y
	Z acceleration/Peak							0.0	0.13	Y
	Resultant Acceleration							0.03	0.08	Y

Multi-Channel Assessment

Since the metrics computed for the individual data channels did not all satisfy the acceptance criteria, the multi-channel option in RSVVP was used to calculate the weighted Sprague & Geers and ANOVA metrics for the three data channels.

Table 8 shows the Sprague & Geers metrics and the ANOVA metrics computed for the weighted composite of the x-, y- and z-acceleration channels using the multi-channel option in RSVVP. According to the multi-channel assessment the changes in momentum of the test vehicle during the impact were dominated by the lateral accelerations/forces, e.g., the lateral acceleration (y-channel) accounted for 70% of the changes in momentum during the event. The composite Sprague and Geers metrics indicated that the magnitude and phase of the analysis results were in agreement with the full-scale test. The ANOVA metrics also indicated that the analysis was in agreement with the test regarding the mean residual error and the standard deviation of the mean residual errors.

Table 8. Roadside Safety Validation Metrics Rating Table – Time History Comparisons

Evaluation Criteria (time interval [0 sec; 1.54 sec])				
Channels (Select which was used)				
⊠ X Acceleration		⊠ Y Acceleration	⊠ Z Acceleration	
☐ Roll rate		☐ Pitch rate	☐ Yaw rate	
Multi-Channel Weights -Area (II) Method-	X Channel – 0.111 Y Channel – 0.697 Z Channel – 0.192			

		M	P	Pass?
O	**Sprague-Geer Metrics** Values less or equal to 40 are acceptable.	22.4	39	Y

		Mean Residual	Standard Deviation of Residuals	Pass?
P	**ANOVA Metrics** Both of the following criteria must be met: • The mean residual error must be less than five percent of the peak acceleration ($\bar{e} \le 0.05 \cdot a_{Peak}$) • The standard deviation of the residuals must be less than 35 percent of the peak acceleration ($\sigma \le 0.35 \cdot a_{Peak}$)	0.01	0.10	Y

120

FEA vs. Test 7069-13

The quantitative evaluation was based on a comparison of the acceleration-time histories collected from three accelerometer locations: 1) inside the cabin near the tractor's center of gravity, 2) inside the trailer near the kingpin, and 3) inside the trailer near the trailer axles. The comparison metrics were computed using RSVVP. The results of the quantitative validation are provided in the Verification/Validation Report located in Appendix C. The quantitative evaluation indicated that the analysis results were not in good agreement with the test. A summary of the quantitative evaluation report is provided in the following sections.

Tractor C.G. Accelerometers

Individual Channel Assessment

Based on the Sprague & Geers metrics, a comparison of the individual components of acceleration indicated that the simulation was not in agreement with the test. The ANOVA metrics indicated that the mean residual error and the standard deviation of the mean residual error were in agreement with the test for the x-acceleration channel but were not in agreement for the y- and z-channels. Table 9 shows the Sprague & Geers metrics and the ANOVA metrics computed for the x-, y- and z-acceleration channels using the RSVVP program.

Multi-Channel Assessment

Since the metrics computed for the individual data channels did not all satisfy the acceptance criteria, the multi-channel option in RSVVP was used to calculate the weighted Sprague & Geers and ANOVA metrics for the three data channels.

According to the multi-channel assessment the changes in momentum of the test vehicle during the impact were most strongly influenced by the longitudinal accelerations; however, the lateral and vertical components of acceleration also showed significant influence. Table 10 shows the Sprague & Geers metrics and the ANOVA metrics computed for the weighted composite of the x-, y- and z-acceleration channels using the multi-channel option in RSVVP. The metrics confirmed that the accelerations of the tractor were not in close agreement with the full-scale test.

121

**Table 9. Roadside Safety Validation Metrics Rating Table – Time History Comparisons
(single channel option) – Tractor Cabin Accelerometer**

<table>
<tr><td colspan="9" align="center">Evaluation Criteria</td><td rowspan="2"></td></tr>
<tr><td rowspan="4">O</td><td colspan="8">Sprague-Geer Metrics
List all the data channels being compared. Calculate the M and P metrics using RSVVP and enter the results. Values less than or equal to 40 are acceptable.</td><td colspan="2" align="center">Time interval
[0 sec; 1.00 sec]</td></tr>
<tr><td rowspan="3"></td><td colspan="5" align="center">RSVVP Curve Preprocessing Options</td><td rowspan="3">M</td><td rowspan="3">P</td><td rowspan="3">Pass?</td></tr>
<tr><td rowspan="2">Filter Option</td><td rowspan="2">Sync. Option</td><td colspan="2" align="center">Shift</td><td colspan="2" align="center">Drift</td></tr>
<tr><td>True Curve</td><td>Test Curve</td><td>True Curve</td><td>Test Curve</td></tr>
<tr><td></td><td>X acceleration</td><td>CFC 180</td><td>Min. area of Residuals</td><td>N</td><td>N</td><td>N</td><td>N</td><td>135.2</td><td>47</td><td>N</td></tr>
<tr><td></td><td>Y acceleration</td><td>CFC 180</td><td>Min. area of Residuals</td><td>N</td><td>N</td><td>N</td><td>N</td><td>176.7</td><td>41.2</td><td>N</td></tr>
<tr><td></td><td>Z acceleration</td><td>CFC 180</td><td>Min. area of Residuals</td><td>N</td><td>N</td><td>N</td><td>N</td><td>344.4</td><td>48.8</td><td>N</td></tr>
<tr><td>P</td><td colspan="8">ANOVA Metrics
List all the data channels being compared. Calculate the ANOVA metrics using RSVVP and enter the results. Both of the following criteria must be met:
• The mean residual error must be less than five percent of the peak acceleration ($\bar{e} \leq 0.05 \cdot a_{Peak}$) and
• The standard deviation of the residuals must be less than 35 percent of the peak acceleration ($\sigma \leq 0.35 \cdot a_{Peak}$)</td><td>Mean Residual</td><td>Standard Deviation of Residuals</td><td>Pass?</td></tr>
<tr><td></td><td colspan="8">X acceleration/Peak</td><td>0.0</td><td>0.34</td><td>Y</td></tr>
<tr><td></td><td colspan="8">Y acceleration/Peak</td><td>0.01</td><td>0.38</td><td>N</td></tr>
<tr><td></td><td colspan="8">Z acceleration/Peak</td><td>0.05</td><td>0.93</td><td>N</td></tr>
</table>

Table 10. Roadside Safety Validation Metrics Rating Table – Time History Comparisons (multi-channel option using Area II method) – Tractor Cabin Accelerometer

Evaluation Criteria (time interval [0 sec; 1.00 sec])		
Channels (Select which was used)		
☒ **X Acceleration**	☒ **Y Acceleration**	☒ **Z Acceleration**
☐ **Roll rate**	☐ **Pitch rate**	☐ **Yaw rate**

Multi-Channel Weights -Area (II) Method-	**X Channel** – 0.423 **Y Channel** – 0.267 **Z Channel** – 0.310	

		M	P	Pass?
O	**Sprague-Geer Metrics** Values less or equal to 40 are acceptable.	211.1	46	N

		Mean Residual	Standard Deviation of Residuals	Pass?
P	**ANOVA Metrics** Both of the following criteria must be met: • The mean residual error must be less than five percent of the peak acceleration ($\bar{e} \leq 0.05 \cdot a_{Peak}$) • The standard deviation of the residuals must be less than 35 percent of the peak acceleration ($\sigma \leq 0.35 \cdot a_{Peak}$)	.01	0.53	N

Trailer Kingpin Accelerometers

Individual Channel Assessment

The electronic data recorder at the kingpin location on the test vehicle included a biaxial accelerometer block to record longitudinal (x-channel) and lateral (y-channel) accelerations. Based on the Sprague & Geers metrics computed by RSVVP, the simulation was not in agreement with the test regarding the individual components of acceleration. The ANOVA metrics (i.e., the mean residual error and the standard deviation of the mean residual error) computed by RSVVP indicated that the analysis was in agreement with the test regarding the x-acceleration channel but was not in agreement regarding the y- channel. Table 11 shows the Sprague & Geers metrics and the ANOVA metrics computed for the x-, y- and z-acceleration channels using the RSVVP program for the data collected at the trailer kingpin location.

123

Evaluation Criteria									
O **Sprague-Geer Metrics** List all the data channels being compared. Calculate the M and P metrics using RSVVP and enter the results. Values less than or equal to 40 are acceptable.							**Time interval [0 sec; 1.00 sec]**		
	RSVVP Curve Preprocessing Options								
	Filter Option	**Sync. Option**	**Shift**		**Drift**		**M**	**P**	**Pass?**
			True Curve	**Test Curve**	**True Curve**	**Test Curve**			
X acceleration	CFC 180	Min. area of Residuals	N	N	N	N	130.5	48.6	N
Y acceleration	CFC 180	Min. area of Residuals	N	N	N	N	116.8	40.1	N
P **ANOVA Metrics** List all the data channels being compared. Calculate the ANOVA metrics using RSVVP and enter the results. Both of the following criteria must be met: • The mean residual error must be less than five percent of the peak acceleration ($\bar{e} \le 0.05 \cdot a_{Peak}$) and • The standard deviation of the residuals must be less than 35 percent of the peak acceleration ($\sigma \le 0.35 \cdot a_{Peak}$)							**Mean Residual**	**Standard Deviation of Residuals**	**Pass?**
X acceleration/Peak							.07	0.33	Y
Y acceleration/Peak							0.03	0.47	N

Multi-Channel Assessment

Since the metrics computed for the individual data channels did not all satisfy the acceptance criteria, the multi-channel option in RSVVP was used to calculate the weighted Sprague & Geers and ANOVA metrics for the two data channels.

According to the multi-channel assessment the changes in momentum of the test vehicle during the impact were most strongly influenced by the lateral acceleration. Table 12 shows the Sprague & Geers metrics and the ANOVA metrics computed for the weighted composite of the x- and y- acceleration channels using the multi-channel option in RSVVP. The metrics confirmed that the accelerations of the tractor were not in close agreement with the full-scale test.

Table 12. Roadside Safety Validation Metrics Rating Table – Time History Comparisons (multi-channel option using Area II method) – Trailer Kingpin Accelerometer

Evaluation Criteria (time interval [0 sec; 1.00 sec])		
Channels (Select which was used)		
☒ X Acceleration	☒ Y Acceleration	☐ Z Acceleration
☐ Roll rate	☐ Pitch rate	☐ Yaw rate

Multi-Channel Weights -Area (II) Method-	X Channel – 0.298 Y Channel – 0.702	

	Sprague-Geer Metrics Values less or equal to 40 are acceptable.	M	P	Pass?
O		120.6	42.5	N

	ANOVA Metrics Both of the following criteria must be met: • The mean residual error must be less than five percent of the peak acceleration ($\bar{e} \leq 0.05 \cdot a_{Peak}$) • The standard deviation of the residuals must be less than 35 percent of the peak acceleration ($\sigma \leq 0.35 \cdot a_{Peak}$)	Mean Residual	Standard Deviation of Residuals	Pass?
P		.00	0.43	N

Trailer Rear Accelerometers

Individual Channel Assessment

The electronic data recorder at the trailer rear axle location on the test vehicle included a biaxial accelerometer block to record longitudinal (x-channel) and lateral (y-channel) accelerations. Based on the Sprague & Geers metrics computed by RSVVP, the simulation was in good agreement with the test regarding the y-component acceleration (i.e., lateral acceleration), but was not in agreement with the test regarding x-acceleration (longitudinal component). The ANOVA metrics computed by RSVVP indicated that the analysis was in agreement with the test regarding both the x- and y- acceleration channels. Table 13 shows the Sprague & Geers metrics and the ANOVA metrics computed for the x- and y-acceleration channels using the RSVVP program for the accelerometer located at the rear of the trailer.

Table 13. Roadside Safety Validation Metrics Rating Table – Time History Comparisons (single channel option) – Accelerometer at Rear of Trailer

	Evaluation Criteria									
O	**Sprague-Geer Metrics** List all the data channels being compared. Calculate the M and P metrics using RSVVP and enter the results. Values less than or equal to 40 are acceptable.							**Time interval [0 sec; 1.00 sec]**		
		RSVVP Curve Preprocessing Options								
				Shift		**Drift**		**M**	**P**	**Pass?**
		Filter Option	**Sync. Option**	**True Curve**	**Test Curve**	**True Curve**	**Test Curve**			
	X acceleration	CFC 180	Min. area of Residuals	N	N	N	N	200.8	45.2	N
	Y acceleration	CFC 180	Min. area of Residuals	N	N	N	N	37.4	33	Y
P	**ANOVA Metrics** List all the data channels being compared. Calculate the ANOVA metrics using RSVVP and enter the results. Both of the following criteria must be met: • The mean residual error must be less than five percent of the peak acceleration ($\bar{e} \leq 0.05 \cdot a_{Peak}$) and • The standard deviation of the residuals must be less than 35 percent of the peak acceleration ($\sigma \leq 0.35 \cdot a_{Peak}$)							**Mean Residual**	**Standard Deviation of Residuals**	**Pass?**
	X acceleration/Peak							.09	0.44	Y
	Y acceleration/Peak							0.00	0.08	Y

Multi-Channel Assessment

Since the metrics computed for the individual data channels did not all satisfy the acceptance criteria, the multi-channel option in RSVVP was used to calculate the weighted Sprague & Geers and ANOVA metrics for the two data channels.

According to the multi-channel assessment, the changes in momentum of the test vehicle during the impact were most strongly influenced by the lateral acceleration; however, the x-acceleration component also showed moderate contribution in the crash event. Table 14 shows the Sprague & Geers metrics and the ANOVA metrics computed for the weighted composite of the x- and y-acceleration channels using the multi-channel option in RSVVP. The composite Sprague and Geers metrics indicated that the magnitude of accelerations were not in agreement with the full-scale test; whereas the ANOVA metrics (i.e., the mean residual error and the standard deviation

of the mean residual error) indicated that the analysis was in agreement regarding the mean residual error and the standard deviation of the mean residual error between the simulation and test data.

Table 14. Roadside Safety Validation Metrics Rating Table – Time History Comparisons (multi-channel option using Area II method) – Accelerometer at Rear of Trailer

Evaluation Criteria (time interval [0 sec; 1.00 sec])					
Channels (Select which was used)					
☒ X Acceleration		☒ Y Acceleration		☐ Z Acceleration	
☐ Roll rate		☐ Pitch rate		☐ Yaw rate	

Multi-Channel Weights -Area (II) Method-	X Channel – 0.298 Y Channel – 0.702	

		M	P	**Pass?**
O	*Sprague-Geer Metrics* Values less or equal to 40 are acceptable.	86.2	36.7	N

		Mean Residual	Standard Deviation of Residuals	
P	*ANOVA Metrics* Both of the following criteria must be met: • The mean residual error must be less than five percent of the peak acceleration ($\bar{e} \le 0.05 \cdot a_{Peak}$) • The standard deviation of the residuals must be less than 35 percent of the peak acceleration ($\sigma \le 0.35 \cdot a_{Peak}$)			Pass?
		.00	0.19	Y

Chapter 5 – Summary and Discussion of Results

The work completed in Phase C of the project included several improvements to the tractor-semitrailer model and an evaluation of its performance by comparing computer simulation results to two full-scale tractor-trailer crash test results from the literature:

1. MwRSF test TL5CMB-2
   - Test date – 7/12/2007
   - Vehicle mass – 79,705 lb (36,153 Kg)
   - Vehicle speed – 52.7 mph (84.9 km/hr)
   - Impact angle – 15.4 degrees
   - Trailer length – 48 ft (14.6 m)
   - Overall tractor-trailer length – 62.1 (18.9 m)
   - Barrier type –concrete median barrier
   - Barrier height – 42 inches (1.067 m)
2. TTI test 7069-13
   - Test date – 7/11/1988
   - Vehicle mass – 50,050 lb (22,702 Kg)
   - Vehicle speed – 51.4 mph (82.7 km/hr)
   - Impact angle – 16.2 degrees
   - Trailer length – 45 ft (13.7 m)
   - Overall tractor-trailer length – 58.2 (17.7 m)
   - Barrier type – vertical face concrete parapet
   - Barrier height – 42 inches (1.067 m)

Figure 107. Photograph. Test TL5CMB2

Figure 108. Photograph. Test 7069-13

Model Enhancement

There were three major areas of improvement to the model during Phase C:

1. Model "robustness" – Remedy modeling inaccuracies that may lead to numerical instabilities in the analyses
2. Testing and characterization of semitrailer components
3. Air-spring testing and characterization for the semitrailer model.

Model Robustness

Contact between parts in a numerical analysis is highly sensitive to initial geometric position, relative stiffness, and the constantly changing orientation of contacting parts during a simulation. Contact is known to be a source of run-time errors and numerical instability in crash simulations. Great care was taken during the development of the tractor-semitrailer FE model to remedy known sources of contact inaccuracies and instabilities. Nonetheless, at the end of Phase B there were still some outstanding contact issues manifested as higher-than-expected sliding (contact)

energies in certain regions. These issues can affect the accuracy of results, and the numerical stability (robustness) of the analysis is highly sensitive to these non-physical energy growths. These and other contact issues were corrected in Phase C.

Testing and Characterization of Semitrailer Components

The material specifications for the parts in the Phase B semitrailer model were obtained from the open literature, from manufacturers' data, and from existing tractor FE model material data. Due to some uncertainty in the identification of the material makeup of several components of the semitrailer, physical experiments were conducted in Phase C to measure material properties. Coupon samples were extracted from several key structural elements of the 1990 Stoughton box trailer that was purchased in Phase B, and uniaxial tensile tests were performed to measure the materials' plastic stress-strain behavior. The components for which material testing and characterization was performed included: the kingpin box, lateral I-beams, trailer bogie main frame rails, trailer bogie main cross members, cargo-box longitudinal slider rails, vertical support for the suspension pivot, suspension pivot arm, axle tube, rear bumper, rear bumper gusset, upper side rail, and lower side rail.

Air-Spring Testing and Characterization

Due to the significant influence of the suspension on vehicle kinematics, extensive testing and characterization of the air spring element of the semitrailer was conducted in Phase C. The suspension on the 1990 Stoughton semitrailer was a Firestone Airide™ Model 1T15K-1. Because of the complexity of modeling the Airide™ suspension component in geometric detail, an idealized characterization of the component was used in the model via discrete spring and damper elements. The test program was designed to collect necessary data for properly characterizing the response of the component as a function of internal pressure, deflection, and deflection rate. A table of input data for the air-spring model corresponding to bag pressures of 20, 40 and 60 psig was developed. These values correspond to static wheel loads of 1390 lb, 2610 lb and 4025 lb, respectively. When static suspension (wheel) loads differ from those provided here (e.g., different ballast mass or ballast shifted fore/aft in the trailer), it is suggested that interpolation be used to determine the appropriate values.

Model Validation

Ideally, the assessment of the model would be based on comparison of the analysis results to a test involving the same vehicle that the model was based on (i.e., a 1991 Freightliner tractor pulling a 14.6-m (48-ft) Stoughton trailer). Unfortunately, no such test data are currently available. The performance of the tractor-semitrailer FE model was assessed by comparing simulation results to:

- The results of full-scale crash test TL5CMB-2 conducted at the Midwest Roadside Safety Facility (MwRSF) in July 2007 and

- The results of full-scale crash test TTI 7069-13 conducted at TTI in July 1988.

The impact conditions (e.g., vehicle dimensions, mass, velocity, and impact angle) for Test No. TL5CMB-2 were consistent with the crash testing guidelines specified in NCHRP Report 350 Test 5-12.[3] The impact conditions for Test No. 7069-13 conformed to performance level three of the 1989 *Guide Specifications for Bridge Railings*.[15] The basic differences in these two testing procedures involved the ballasted weight of the vehicle and the trailer length. For example, the ballasted weight of the vehicle in test TL5CMB-2 was 79,705 lb (36,153kg), whereas the ballasted weight of the test vehicle in test 7069-13 was 50,050 lb (22723 kg). The trailer length in Test TL5CMB-2 was 48 ft (14.6 m), whereas the trailer length in test 7069-13 was 45 ft (13.7 m).

To evaluate the model against available test data, the geometric and inertial properties of the baseline model were modified using the ADAP scripts (developed in Phase B) to match as closely as possible those of the test vehicles. However, there were still some notable differences related to the box-trailer height dimensions, ballast properties and trailer suspension type (i.e., the test vehicles had a leaf-spring suspension and the FE model was developed with an air-spring suspension). Each of these basic differences will affect the response of the vehicle in an impact to some degree.

Summary of Analysis Results from Simulation of Test TL5CMB-2

The ADAP program was used to modify the length dimensions of the tractor-semitrailer model to conform to those of the test vehicle. However, there were still several differences between the vehicle model and the test vehicle, with the most notable differences listed below:

- *Length dimensions* – The length dimensions of the FE model were all within 2% of the test vehicle dimensions, except for the distance from the front bumper to the center of the front wheel (e.g., dimension "B" in Figure 42, which was 13.5% shorter in the FE model.
- *Trailer box dimensions* – The trailer floor in the FE model was 5.8 inches (148 mm) higher than the test vehicle (e.g., dimension "L" in Figure 42, and the top of the trailer in the FE model was 6.7 inches (169 mm) lower than the test vehicle (e.g., dimension "W" in Figure 42).
- *Ballast center of gravity (c.g.)* – The c.g. of the ballast in the FE model was located 23.6 inches (600 mm) rearward of and 4.6 inches (188 mm) higher than the c.g. location of the ballast in the test vehicle.
- *Trailer suspension* – The suspension system on the FE trailer model was the Airide™ design, and the suspension on the trailer test vehicle was a leaf-spring design.
- *Propulsion* – The test vehicle was under engine power with drive train engaged for the duration of the impact event. The analysis model was not.

The analysis ran to completion with no numerical instability problems. Based on a qualitative assessment of the model's results to test TL5CMB-2, the general response of the modified FE model compared reasonably well to the full-scale test; the analysis results replicated the basic timing and magnitudes of phenomenological events that occurred in the full-scale test. A comparison of sequential views of the test and simulation showed that the attitudes (e.g., roll and pitch) of both the tractor and the semitrailer models were also reasonably similar to the behavior of the vehicle in the full-scale crash test. The quantitative assessment also indicated that the model's results were within the range of error that would be expected between two identical crash tests, based on validation criteria defined in the NCHRP Project 22-24 report [4].

Summary of Analysis Results from Simulation of Test 7069-13,

As discussed previously, the ADAP program was used to modify the length dimensions of the tractor-semitrailer model to conform to those of the test vehicle. However, there were still several differences between the vehicle model and the test vehicle, with the most notable differences listed below:

- *Length dimensions* – The length dimensions of the FE model were all within 7.5% of the test vehicle dimensions, except for the distance from the front bumper to the center of the front wheel (e.g., dimension "B" in Figure 73), which was 44.2% longer in the FE model.

- *Trailer box dimensions* – The trailer floor in the FE model was 3.0 inches (76.2 mm) higher than the test vehicle (e.g., dimension "L" in Figure 73), and the top of the trailer in the FE model was 9.0 inches (228 mm) lower than the test vehicle (e.g., dimension "W" in Figure 73).

- *Trailer suspension* – The suspension system on the FE trailer model was the Airide™ design, and the suspension on the trailer test vehicle was a leaf-spring design.

- *Ballast* – The properties, dimensions and restraint of the ballast were not provided in the test report; thus a modified version of the ballast model from the MwRSF test simulation was used.

- *Tractor-Semitrailer Weight* – The FE model of the tractor was approximately 500 lbs heavier than the test tractor, and the FE model of the semitrailer was approximately 400 lbs heavier than the test semitrailer.

- *Propulsion* – The test vehicle was under engine power with drive train engaged for the duration of the impact event. The analysis model was not.

Prior to the analysis, the model was set at equilibrium with respect to gravity, i.e., the geometry and stresses in all parts of the tractor-trailer model were at equilibrium with gravity. The basic procedure was to 1) conduct an analysis involving the vehicle subjected to only gravity load, 2) save node and element information (e.g., nodal coordinates and element stresses) from the

gravity analysis, and 3) include them in subsequent analyses as part of the initial conditions for the model.

The analysis ran to completion with no numerical instability problems; however, the FE model did not adequately simulate the kinematic behavior of the tractor-semitrailer, nor adequately capture the timing of the basic phenomenological events that occur during impact. The results of the quantitative assessment of the results confirmed that the simulation did not adequately replicate the test results.

Discussion of Model Performance

The accuracy of the model results throughout the duration of the impact analysis is greatly affected by the response of the vehicle model during the early stages of the impact event. In particular, the overall results of the impact are highly dependent upon the accuracy of the trailer's attitude (roll, pitch and yaw) when the rear of the trailer "slaps" against the barrier. The current response of the model does not accurately replicate that of the test vehicle during this initial phase of impact, especially in the simulation of test 7069-13. In the full-scale tests, the friction forces between the tires and the road surface caused the trailer to continuously increase its roll angle as the trailer yawed toward the barrier. The model accurately simulated this phenomenon up to approximately 0.4 seconds of the impact event, as shown in Figure 76, at which time the suspension on the trailer model started to rebound. At 0.52 seconds the right-side tires of the trailer left the roadway completely, as shown in Figure 109. With the tires no longer in contact with the road surface, the roll rate of the trailer reversed direction resulting in a relatively low roll angle of the trailer at the time of impact with the barrier. In the full-scale tests, the right-side tires of the trailer remained in contact with the roadway throughout this stage of the impact event.

| (a) 0.3 seconds | (b) 0.4 seconds | (c) 0.5 seconds | (d) 0.6 seconds |
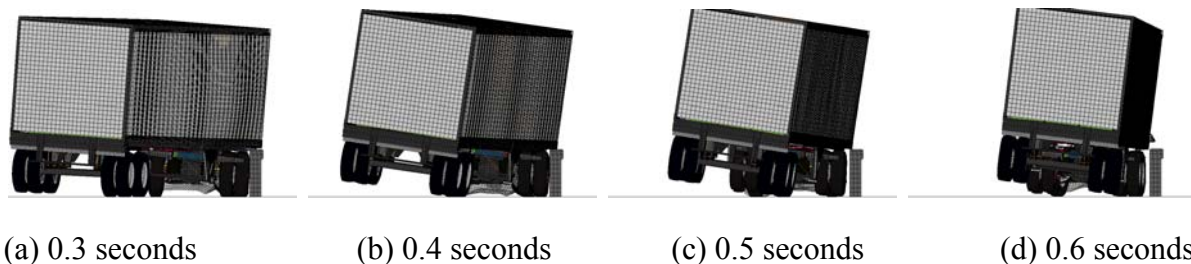
Figure 109. Illustration. Sequential views of trailer model during simulation of test 7069-13 illustrating roll angle of trailer as the trailer yaws toward the barrier

The research team investigated several potential factors that may cause the trailer to pitch as it is approaching the barrier, including: trailer suspension properties, friction between the tractor and barrier, friction between the tires and roadway, fidelity of the ballast model and gravity initialization.

Sensitivity Analysis – Trailer Suspension Properties

Sensitivity analyses were conducted to investigate the effects of the trailer suspension's stiffness and damping properties on the kinematic behavior of the trailer during the first 0.6 seconds of the impact event (details not included in this report). The properties of the suspension were increased and decreased significantly, and in all cases the attitude of the trailer was only moderately affected.

Sensitivity Analysis – Friction Forces Between Tractor and Barrier

Another consideration for the source of the unexplained pitch of the trailer was the tractor's sudden decrease in speed upon impact with the barrier. As the tractor suddenly slows, the high center of gravity of the ballasted trailer (e.g., the center of gravity of the ballasted trailer is above the kingpin connection to the tractor's fifth-wheel) may tend to cause the rear of the trailer to pitch upward. To investigate the model's sensitivity to this phenomenon, friction between the tractor and barrier was removed. The resulting trailer response was only moderately affected.

Sensitivity Analysis – Friction Forces Between Tires and Roadway

The friction coefficient between the tires and the roadway was increased to investigate its affect on the model's results. The increase in friction resulted in an increase in roll angle of the trailer, but it had little effect on the pitch behavior of the trailer.

Sensitivity Analysis – Ballast Model Fidelity

In Phase B of the project it was determined that the ballast model had a significant effect on the kinematic response of the trailer during simulation of the impact event. The initial modeling approach was to model the ballast as a simple block of solid elements with the appropriate mass and inertial properties. This had two effects on the model: 1) it effectively increased the rotational stiffness of the trailer and 2) it changed the impact dynamics of the ballast. Each of these attributes of the model has an effect on the kinematic response of the trailer during impact, especially in impacts involving significant angular displacements of the vehicle. Based on these findings, the model of the ballast for simulation of test TL5CMB-2 was developed including enough fidelity to sufficiently match the geometry, material, and restraint of the ballast used in the test vehicle. As a result, the analysis results adequately reflected the results from the full-scale test for that case.

The content, dimensions and restraint of the ballast used in test 7069-13 were not provided in the test report. It was assumed that the ballast for test 7069-13 was similar to the ballast used in test 7069-10, which consisted of a layer of sand bags on the trailer floor and two rows of hay stacked on top of the sand with the entire ballast constrained by a wooden crate. Unfortunately, the research team was not able to successfully develop an accurate model of the ballast used in test 7069-13 within the time and budget constraints of the project.

Another important factor in the analysis was the initialization of the ballast weight on the trailer due to gravity. At the start of the analysis, the air-spring suspension properties were initialized to the ballasted load of the trailer; however, the ballast itself was not at equilibrium at the start of the analysis. At time zero, the ballast is initially suspended and suddenly drops onto the trailer floor under the gravity load. This sudden loading caused the trailer suspension and tires to compress and rebound. A preliminary gravity-load-only analysis (not included in this report) showed that the semitrailer's suspension would require at least 3 to 5 seconds for the vertical oscillations of the trailer to damp sufficiently to acquire "equilibrium" under gravity.

The research team determined two possible remedies for the gravity initialization problem:

1. Set the initial position of the vehicle such that it travels for 3 seconds prior to impact with the barrier.
2. Impose equilibrium state through initial conditions – Conduct an analysis of the vehicle subjected only to gravity, save node and element information (e.g., nodal coordinates and element stresses) from the gravity analysis, and include them in subsequent analyses as part of the initial conditions for the model.

The first option would greatly increase computation time for routine analyses, since the gravity initialization phase of the analysis would be required for each analysis case. This option may also lead to divergence issues related to round-off in the calculations (e.g., a 6-second simulation conducted at a time-step of 1.2 microseconds results in 5 million sequential equilibrium calculations throughout the analysis). A variation of this option was used with reasonable success in the simulation of Test TL5CMB-2, as discussed in Chapter 3. The tractor-semitrailer model was positioned at 15.4 ft (4.7 m) upstream of the impact point at the start of the analysis so that, as the vehicle moved toward the barrier, the vertical oscillation of the trailer suspension was on the compression cycle as the trailer was starting its yaw toward the barrier. This caused the tires to remain in contact with the road surface while the trailer was yawing toward the barrier and resulted in the correct roll angle of the trailer at the time when the rear of the trailer contacted the barrier.

For routine analyses, the second option would be the preferred method for initializing gravity in the model since the gravity initialization analysis is only conducted once, and thus subsequent analyses using the same vehicle and ballast need only to read in the equilibrium conditions of the model as initial conditions.

Chapter 6 – Summary of COE Comments on the Tractor-Trailer FE Model

Following the completion of Task 1 and preliminary validation in Task 2, Battelle provided an interim version of the enhanced FEA tractor-semitrailer model to each of the other FHWA COEs in roadside safety, including NCAC, TTI, MwRSF, WPI, and ARA via the project's SharePoint site. In addition to this initial deliverable, the research team has continuously uploaded the revised tractor-semitrailer LS-Dyna models to the SharePoint site as significant revisions are made.

NCAC

NCAC ran an NCHRP Report 350 TL-5 test using the FE model of the 80,000 lb day-cab tractor and 48-ft semitrailer (36000V) into a Cable Barrier. The Cable Barrier was a high-tension four-cable system, 200 meters in length with 3-foot post spacing. The impact speed was 80 km/kr and the impact angle was 15° on flat terrain. NCAC modified the FE model file structure such that the tractor-trailer vehicle was in one file (rather than separate *INCLUDE files). NCAC also ran their analysis single (rather than double) precision due to some file storage and CPU resource limitations. Figures 77 through 88 show a sequence of the simulation. NCAC reported roll and yaw angles for the tractor and the trailer, as well as upstream and downstream anchor forces. NCAC did not provide any comparison of their simulation with full-scale crash test data.
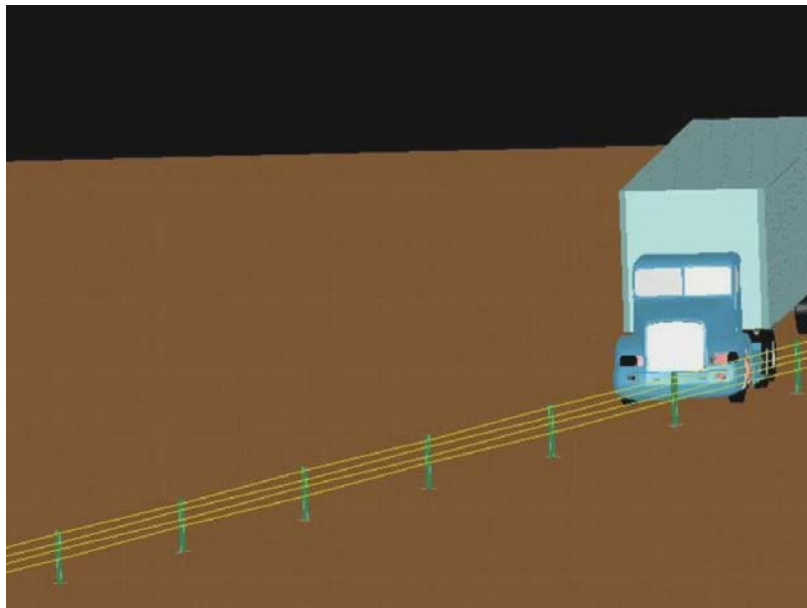
Figure 110. Illustration. NCAC run of TL5 median barrier test view 1
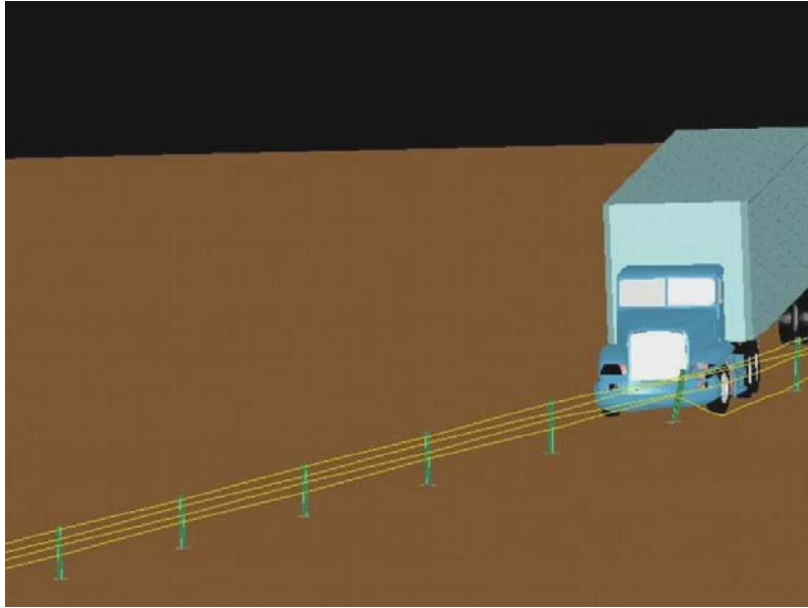
Figure 111. Illustration. NCAC run of TL5 median barrier test view 2
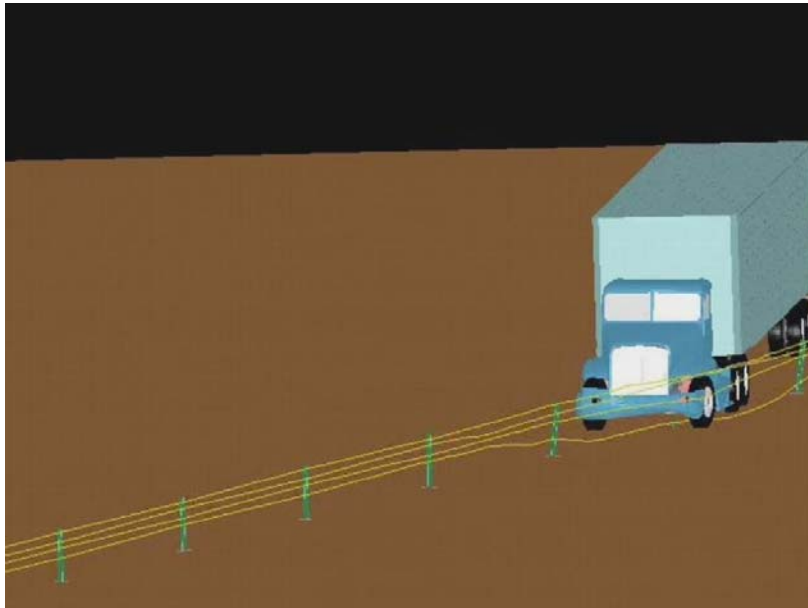
Figure 112. Illustration. NCAC run of TL5 median barrier test view 3
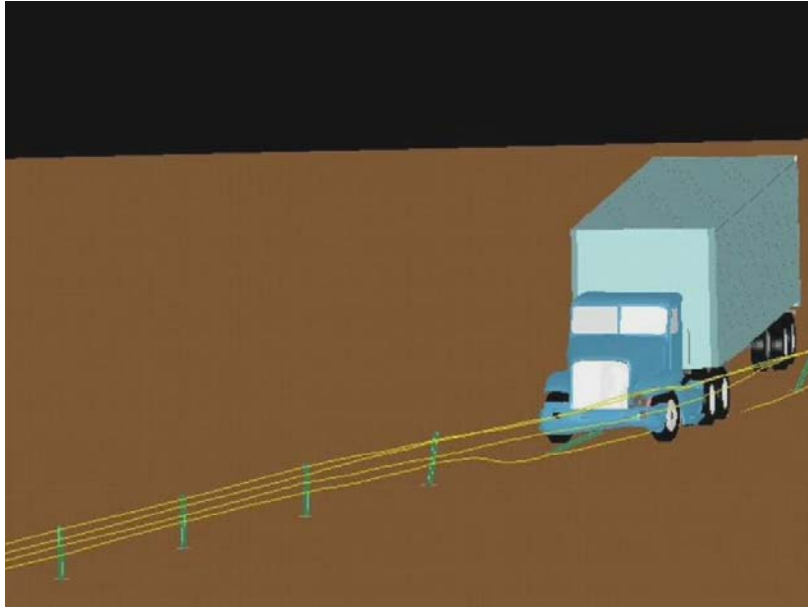
Figure 113. Illustration. NCAC run of TL5 median barrier test view 4
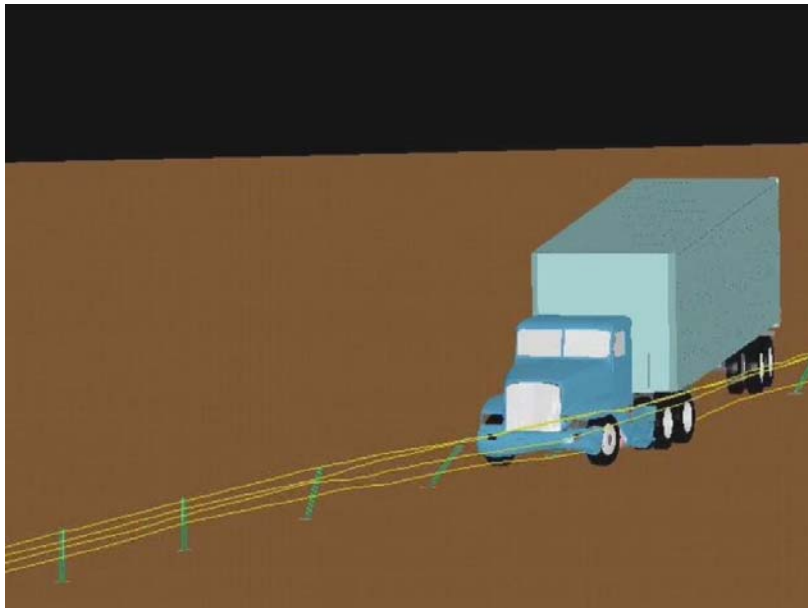
Figure 114. Illustration. NCAC run of TL5 median barrier test view 5
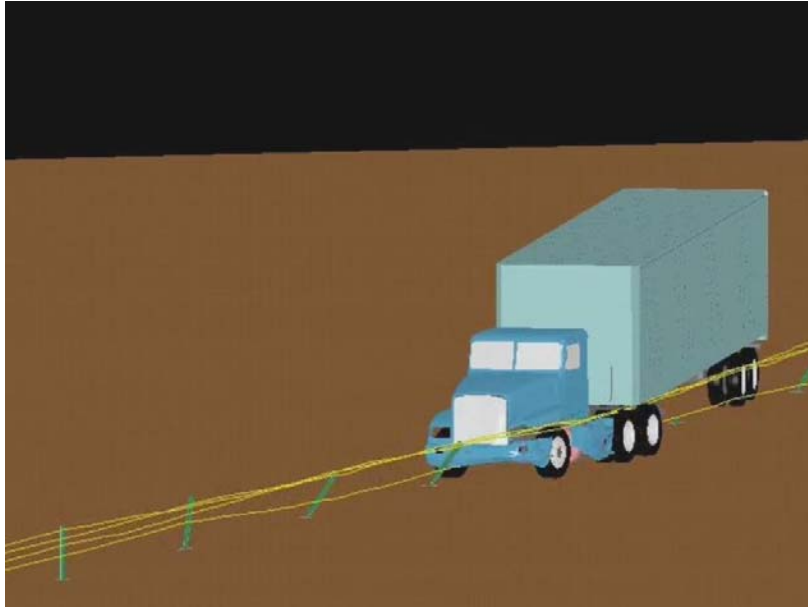
Figure 115. Illustration. NCAC run of TL5 median barrier test view 6
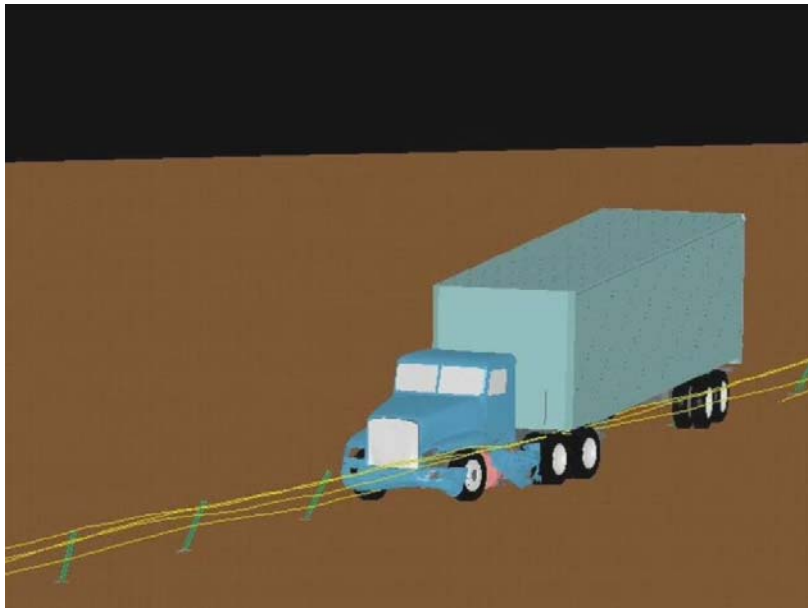
Figure 116. Illustration. NCAC run of TL5 median barrier test view 7
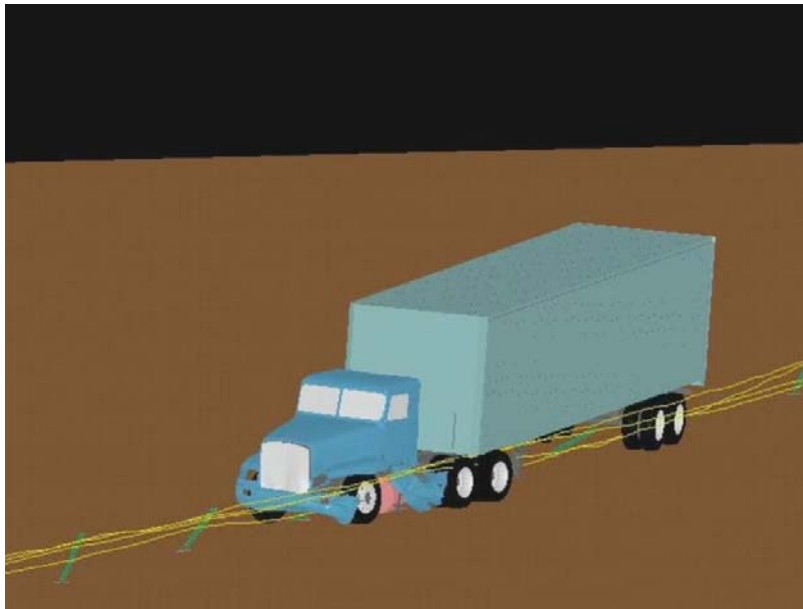
Figure 117. Illustration. NCAC run of TL5 median barrier test view 8
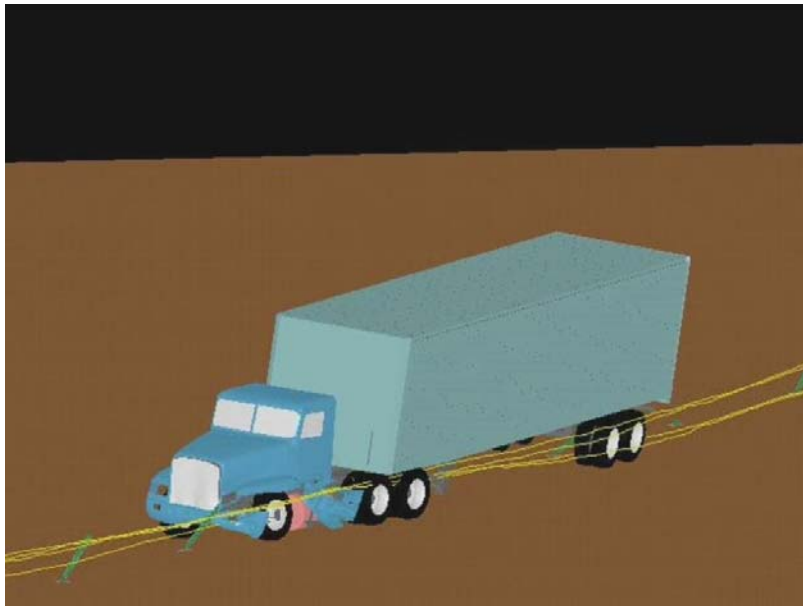
Figure 118. Illustration. NCAC run of TL5 median barrier test view 9
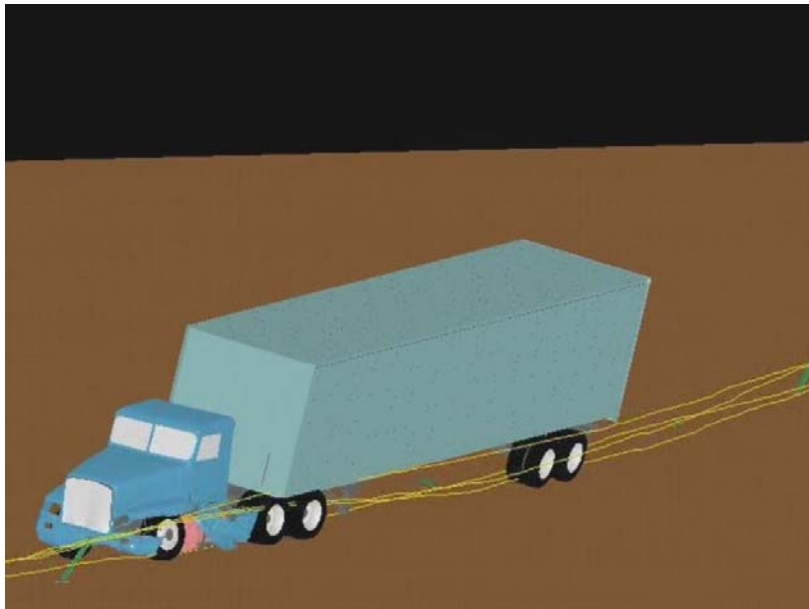
Figure 119. Illustration. NCAC run of TL5 median barrier test view 10
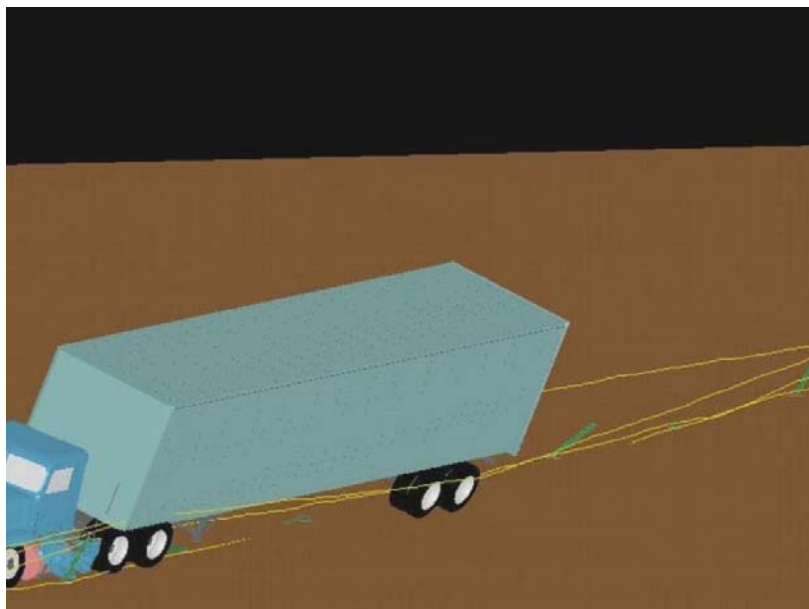
Figure 120. Illustration. NCAC run of TL5 median barrier test view 11
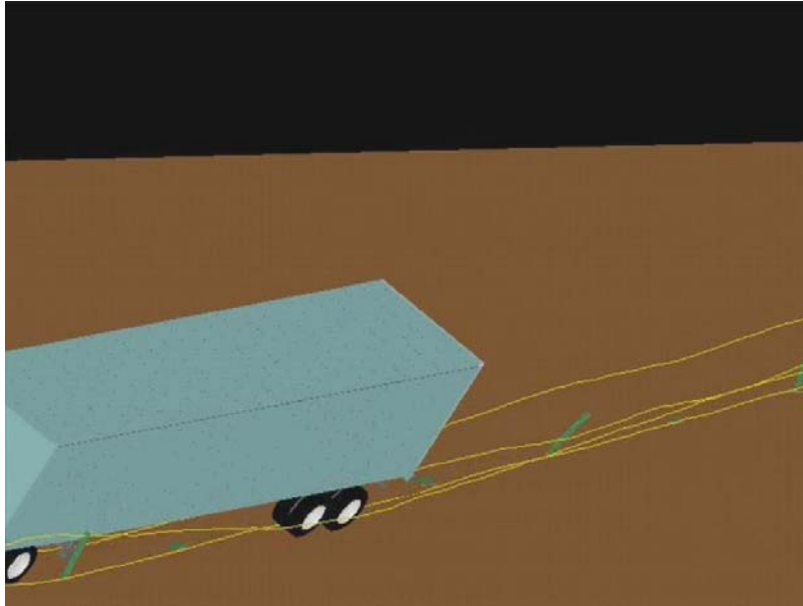
Figure 121. Illustration. NCAC run of TL5 median barrier test view 12

WPI

The 45-foot tractor-semitrailer (TTI test 7069-13) FE model was downloaded and run at Worcester Polytechnic Institute on their linux cluster where their LS-Dyna resides. Unlike the other COE's experience, and relative unfamiliarity with this FE model, the model was run by one of the research team members from this project, Dr. Chuck Plaxico rather than by WPI staff. Consequently, the feedback from this experience with the FE model is limited to comments about running this model at another institution, on a different computer platform. The FE model itself was downloaded from the Heavy Vehicles Share Point Site with no problems. The simulation using the full gravity-initialization approach was run on WPI's computers (AMD64 system) using SMP LS-Dyna version ls971d (R4.2.1) Revision 53450. The analysis ran to completion and experienced no numerical instabilities. The most important difference in the simulation on WPI's computers was that the contact between the tractor's front suspension U-bolts and its associated connection components "released", which resulted in the U-bolt penetrating the surrounding parts undetected. In effect, the front axle was not fastened to the suspension of the tractor. This led to very different post-initial-impact kinematics/behavior of the tractor-semitrailer vehicle. It is yet undetermined why the contact works correctly on the Battelle and NCAC computers running MPP LS-Dyna but does not work on the WPI computers running SMP LS-Dyna.

Chapter 7 – Interactive On-line User Manual and FE Model Web Site

Approach

Current state-of-the-art finite element crash models of vehicles are built using advanced CAD and FEM tools as a collaborative endeavor of engineers, modelers and computer specialists. The models have very detailed geometry and discretization, they contain a large of number of sub-models, parts, components, and systems with complex properties, interaction, connectivity, spatial and functional relations. Describing and documenting such a model in detail becomes an equally complex undertaking. The emerging web-based technologies provide a framework that can assist in presenting the model information and facilitate its use.

Most of the current web-based documentation of computational models is based on static information that primarily consists of document libraries, presentations, simulation results and model input files. Although they provide considerably more information than the conventional printed documents, they do not take advantage of the potential offered by the technology. One of the most powerful features of the interactive web is the ability to interlink the data in hypertext documents such that they mimic the relations that exist in the model. Navigating the interlinked data is then very similar to navigating the actual finite element model. The sequence of steps for model examination is not fixed, which gives the user a certain level of control over how to examine the information and acquire the knowledge.

The focus of the interactive documentation system is how to effectively use the technology and find the correct balance of simplicity necessary for a wide use and ability for in-depth inquiry into the model demanded by expert users. Ideally, the system will provide an ability to configure access to match the level of the user's expertise. It should also be able to support the model development process such that the evolving changes to the model are documented and controlled - similar to software development systems. Such capabilities are outside the scope of this project but are planned for future work.

The web-based manual developed during this project is an attempt to develop a comprehensive documentation system for several models of tractors and semitrailers, which can be combined as-required for crash simulations.

The original approach for a web-based documentation system was based on the interactive manual developed for the Single Unit Truck finite element model. That system was developed using direct generation of the content and presentation programs. This approach required a large effort and will scale proportionately to the number of the models to be processed. As the models change during the course of their development, detecting, updating and tracking the differences becomes quite tedious and time-consuming. To deal with an increased number of models and their variations, we have decided to develop a system that can accommodate these requirements and can process the models in relatively short time. In doing so, we took a path towards a more general system for finite element model documentation that is relatively independent of the models under consideration.

The web documentation system developed in this project consists of three major components. The first component is the underlying *data model* and *relational database* that describe the finite element model information and relations within the model. One of the possible approaches is to work directly with the LS-Dyna model files and dynamically extract content as queried by a user. One drawback is the size of the models - which will grow as the model becomes more sophisticated. Therefore, some underlying condensation of information and simplification of the model is necessary for a system to be reasonably fast. The second component is the *multi-media content generation* software used for presenting the characteristics of the model and relations within it. The last component is a *web-based interface* for querying and displaying the information. In the web-based manual for the SUT model, all of these web documentation system components were interwoven into one and would operate primarily on the static information, but that system was not easily extendable. In this new web documentation system, adding a new finite element model to the documentation system does not require any modification of the display system, it only requires generation of the model data and media, images, Virtual Reality Modeling Language (VRML) (http://www.web3d.org/), movies, etc., and their entry into the data system. The content is disassociated with the presentation engine and the two can be developed separately. These three web documentation system components are described in detail below. The web documentation system is available for download at http://www.ntrci.org

Data Model and Relational Database

The most detailed and direct examination of the tractor-semitrailer LS-Dyna models is accomplished via LSTC's software; LS-PrePost. This limits the models' interpretation to an expert group of users. Large-scale finite element models are usually developed as proprietary products for specific application and are not meant for wide distribution. Finite element models developed by academia and government institutions are usually in the public domain and their target audience is intentionally wide.

Web technologies such as Extensible Markup Language (XML) (http://www.w3.org/XML/), and related tools can be adapted to the documentation of finite element models. Fortunately, the syntax of finite element models' (formatted numerical sequence) file input format is compatible with these markup languages. While some idiosyncrasies remain in the finite element model syntax (likely to be eliminated in new versions of the codes), the transformation from the current finite element model formats, such as LS-Dyna's "keyword" format, are relatively simple.

Once a transformation from a finite element input file format to XML form is made, we have a convenient basis for manipulating and transforming data. The relations that exist in the finite element model are encoded in the XML form and a relational database for the model is created. Data transformations are performed by a series of programs that extract the pertinent data from the finite element model file, process that data, build cross-link references and links to media content (images and interactive 3D files), and finally store all that information in XML files. These files represent a relational database stored in a format that can be viewed and edited in any text/word processor. This database is then used for various queries defined in the user interface.

Multi-Media Content Generation

User's multi-media expectations have grown in proportion to increased communication bandwidth and capability of computer hardware. The amount of media that needs to be generated and presented is an order of magnitude larger than what was common just few years ago.

Spatial relationships within a finite element model are best described by images and 3D renderings, ideally to be manipulated by the model user. We have developed computer programs to create image libraries and interactive 3D files for selected finite element model components. The parts or part sets of a finite element model can be grouped together by their physical association to a certain model component, specific material, section, or contact type.

A series of scripts were written to generate images for the documentation. The programs use freeware programs capture images of finite element model entities from different points of view and in different orientations. The user is able to display images of a selected entity of interest individually, or as a part highlighted in the overall model showing exactly where it fits in the model. Another set of programs extracts the finite element model data for creating the interactive 3D views. "Level of Detail" algorithms are used to optimize the number of polygons necessary for the 3D display. X-Y graph presentation of material and other "curve" data has been implemented (using public domain software) to correlate visual and tabular representation of data to their location in the finite element model input file.

Data retrieval and web display

The tractor-semitrailer web server was built on a CGI interface that receives and processes user requests, interacts with the XML database type files and serves the requested content. This web server system is continuously updated as new versions of the FE model evolve. Enhanced display and inquiry options can be implemented based on user demand, if warranted by a future project.

The content is organized into six sections:

The "Home" section contains a summary of the project and excerpts of all chapters in the final report.

The "FE Model" section offers model selection and includes briefs for the following LS-Dyna keywords: *PART, *SECTION_ . . , *MAT_ . . , *DEFINE_ . . , *CONSTRAINED_ . . , *AIRBAG_ . . , *CONTACT_ . . , and *SET_ . . . This subset of keywords was selected because it describes the essence of the model.

Typically, the user selects the model to query from the available database of models. Queries of data in the selected model are done by selecting options and links in the browser window. The presented data is stored in tables and cross-linked appropriately. For example, the user can view all the parts that are modeled with a selected material, or view parts that share a common section property, etc.

For additional information, the user can:
- Launch a popup window to view the excerpt of the FE model file that served as an information source;
- View a series of static entity images (applicable for parts, sections, materials, contacts and airbags);
- Use an interactive 3D application to get a more detailed model view (applicable for parts, sections, materials, contacts and airbags;
- Launch a popup window to get curve graphs (applicable for tables and curves);
- Launch a popup window to view the section in the LS-Dyna manual for a particular keyword.

The "Simulation" section offers movies showing FE model simulations performed with individual tractors or tractor-semitrailer combinations. Cross-links offer a connection to the "Download" section.

The "Test" section contains video recordings of actual crash tests performed with tractors and tractor-semitrailer vehicles.

The "Download" section offers links to tractor and tractor-semitrailer FE models. Cross-links enable connections to the "Simulations" section.

The "About" section contains general information about the project and people that designed the web based interface as well as links to the web sites of the institutions that participated in, and funded this project.

Chapter 8 – Conclusions and Recommendations for Future Research

Conclusions

These tractor-semitrailer vehicle FE models are the best "36000V" class vehicle FE models currently available to the roadside safety research community. As of this writing they are the most advanced FE models available of this vehicle in terms of physical function, geometric detail and material property accuracy.

These models are computationally quite robust given their complexity. They have been extensively debugged and exercised hundreds of times for the cases within the range of NCHRP Report 350 TL-5 speeds and impact angles.

In developing these FE models, computational efficiency is considered wherever possible, but computational efficiency is considered second to fidelity. The philosophy is that today's computational resources are small relative to the next generation.

These FE models fulfill their intended application for evaluating the crash performance of roadside safety features based on the crash test guidelines of National Cooperative Highway Research Program (NCHRP) Report 350 Recommended Procedures for the Safety Performance Evaluation of Highway Appurtenances for Test Level 5 [16]. In such applications, these tractor-semitrailer models serve as "bullet" vehicles, whose purpose is to accurately simulate the load transfer from the vehicle to the barrier during and after impact.

In Phase C of this project, more representative tractor FE models were created for comparison to the MwRSF test TL5CMB-2 and the TTI test 7069-13 which reflected more closely the geometry of the crash test vehicles. These FE models were validated using the verification and validation procedures of NCHRP Project 22-24. Based on the metrics used in these verification and validation procedures, the simulation of the MwRSF test TL5CMB-2 compared very well with the crash test data and is considered a validated FE model. Based on these same metrics, the simulation of the TTI test 7069-13 did not compare very well with the crash test data, and cannot yet be considered a validated FE model. The procedures used and the results of the quantitative validations of both simulations to their respective tests are described in detail in chapters 3, 4 and 5. By studying these cases, the reader can see a real-world example of a well-validated and a non-validated FE simulation performed according to the objective criteria set forth in the validation procedures.

Recommendations for Future Work

The following sections describe additional research that would further improve the accuracy, robustness, and applicability of the tractor-semitrailer FE model. These tasks are not listed in priority order.

Continue Work with Daycab Tractor – 45-foot Semitrailer FE Model to Obtain Validation

Time and funding did not permit the complete validation of the Daycab – 45-foot semitrailer FE model with the TTI test 7069-13 by the conclusion of Phase C. The research team recommends that work be continued on this effort to a successful level of validation for this FE model.

Model Evaluation for Other Impact Conditions

Impact events other than the redirective type have not yet been run with these tractor-semitrailer FE models for the purpose of model validation. All validation so far on this tractor-semitrailer FE model has been done by comparison to redirective impact type crash tests into rigid barriers, e.g., NCHRP Report 350 Test 5-12 through about 3.00 seconds of the impact event. The research team believes that this tractor-semitrailer FE model is reasonably valid for this type of crash simulation, and that it will provide useful results in general barrier design evaluation work regarding impact loads and general vehicle-barrier interaction. However, the model has not been assessed for use in other applications, such as high-energy impacts (e.g., full frontal impact with bridge pier), vehicle dynamics (e.g., vehicle response due to steer maneuvers), or vehicle-to-vehicle impacts to name a few.

Whether full-scale crash data for another impact scenario can be obtained or not, it would be valuable to use the FE model in a different impact condition to investigate the general level of performance and robustness of the FE model.

Leaf Spring Suspension for Semitrailer Model

The current tractor and semitrailer FE models both have Airide™ airbag type suspension systems on their rear tandems. Some older tractors and semitrailers used for crash testing have leaf-spring type suspension systems. To be more compatible and comparable with crash test data, it is recommended that this these suspensions be added to provide the option in the FE model to specify either type of suspension system.

Improved Tire Model for Tractor FEM

When a vehicle impacts an object such as a roadside safety barrier, one or more of its tires may deflate or "blowout" as the tire(s) interacts with the object. Tire deflation affects the dynamics of a vehicle during impact because it alters the magnitude of forces and the mechanism of how those forces are transferred between various vehicle components. For example, as shown in Figure 122 during full-scale, low-angle impacts with longitudinal concrete barriers, the front; impact side tire of a vehicle often gets pushed back into the wheel housing. If the tire remains inflated during this event, the wheel will wedge more severely against adjacent parts and impose significant forces on its surroundings. The magnitude of these forces may be sufficient to cause deformation or failure of critical components (e.g., frame-rail or suspension), which will affect subsequent kinematic behavior of the vehicle.

Figure 122. Illustration / Photo. Initial tire impact interaction with barrier

The tires of the tractor and semitrailer models are represented by a single part constructed of isotropic thin shell elements with constant thickness for all regions of the tire, including side wall and tread. The air pressure inside the tire is simulated using the simple airbag option in LS-Dyna and cannot accurately simulate proper tire response. This method of modeling tires has been shown to produce unrealistic deformation and response of the tire during impact.

The development of a computationally efficient tire model that incorporates the critical parts of a tire structure such as the bead coils, radial fibers, rubber sidewall, under-belt radial fibers, steel belt, and tire tread simulation is considered important to model accuracy, but was beyond the scope of work in this project.

Currently, tire-blowout can be simulated and incorporated into an LS-Dyna vehicle simulation using the approach developed by Orengo, et. al. in 2003 [17]. This approach involves monitoring the contact between the tire and the wheel rim, and stopping and restarting the simulation. When LS-Dyna senses that the contact is lost at the contact between the tire and the wheel rim, the simulation is terminated. The simulation is then "manually" restarted with a zero tire pressure. The latest release of LS-Dyna Version 971 has some more advanced "sensor" technology that might be developed into a more automatic tire-blowout simulation. Some work would need to be done to implement this feature in the model.

Improved Steering Linkage Model and Passive Steering Response Characterization

When a vehicle impacts a roadside safety barrier at an oblique angle the front tires are the first to experience the brunt of the impact force. The response of the wheel as it interacts with the barrier can have a significant influence on the impact event. For example, it may create the potential for wheel snag, affect vehicle redirection, and may alter load path and magnitude to the barrier.

The response of the impact-side wheel is of course governed by *all* of the components that make up the wheel assembly. One aspect of the wheel assembly that may have notable influence but is

151

often overlooked in models is the steering assembly – in particular, the steering linkage and steering resistance response. When a tire impacts a barrier, the wheels will tend to steer either along the longitudinal direction of the barrier or perpendicular to it. The direction of steer and the rate of steer are primarily influenced by three factors: friction between the tire and barrier, "back-driving" of the steering linkage with hydraulic steering pump reaction, and (to some degree) rotational inertial effects. Figure 123 shows a detail of the steering linkage and the connections from the steering box to the spindle where a simulated.
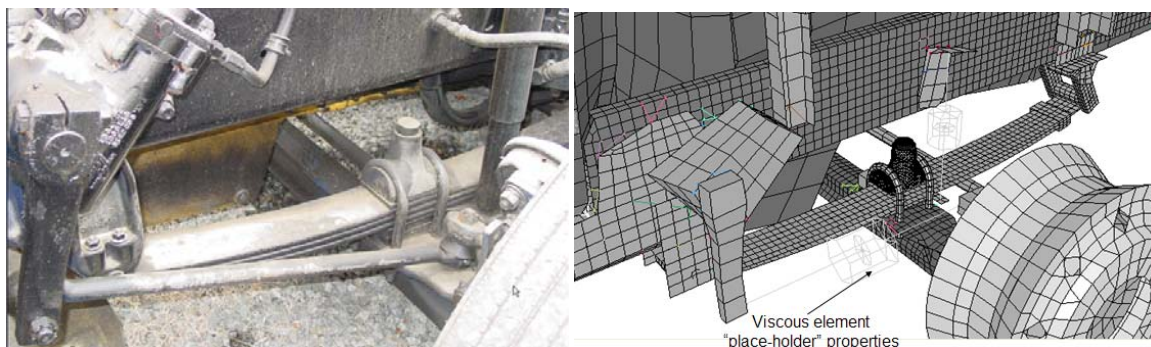
Figure 123. Photograph / Illustration. Tractor steering linkage detail

Standard Trailer Lengths

A suite of standard-length trailer FE models would be valuable for researchers. Most semitrailers used in crash tests are specific standard lengths such as 45-feet, 48-feet, 50-feet, and 53-feet. It is recommended that ADAP scripts be developed and applied to create ready-to-run LS-Dyna FE models of several different common-length semitrailers.

More Extensive Literature Review

The synthesis of the full-scale crash tests provided very valuable information regarding the kinematic behavior and impact response of tractor-semitrailer vehicles during impact with roadside safety barriers. Unfortunately, the synthesis is largely incomplete due to the inaccessibility of much of the crash test data. These tests were conducted over a span of 26 years starting in 1981 and the data storage devices that some of the data were recorded on are incompatible with our current data reading devices. Of the 12 crash tests that were identified in the literature, crash data was available for only 6. It is possible that these test data can be found (in a compatible format) in the NCAC crash test repository. It is our understanding that the data in this repository is available to the public for a nominal fee; however, we expect that this fee may be waived when the data is to be used for government-sponsored projects.

A more extensive literature assessment is recommended to provide more additional meaningful crash test data for the program and for assessing the response the model. This effort would also provide very useful information to the roadside safety community in general for use in design of roadside safety barriers.

Conduct Full Scale Crash Test for FE Model Validation

This program would benefit significantly from conducting a full-scale crash test for FE model validation. A test specifically designed for this purpose would be more beneficial than validating the model only against prior tests. There are two approaches to performing this task. One is to conduct a full-scale crash test of a tractor-semitrailer of the *same* (or very similar) make and model as the current tractor-semitrailer FE models into a rigid barrier for the specific purpose of obtaining validation data for the FE model. The second approach would be to participate in a scheduled full-scale crash test of a tractor-semitrailer being conducted elsewhere during the performance period of Phase C. This project could request and potentially provide additional funding to the other testing agency's budget to support 1) the purchase of a specific make and model tractor and/or semitrailer that would closely match the current FE model, and 2) the implementation of additional electronic data recording devices at points of interest to the FE model validation.

Increased Fidelity of the Trailer Model and the Trailer-to-Tractor Connection

The current trailer FE model was conceived as a "bullet" model along the same lines as the tractor FE model. The current trailer model is designed with the intent of being compatible primarily with redirective type of impacts with roadside safety hardware. In particular, the connection of the trailer to the tractor is a fairly simple kinematic revolute joint with no failure specified. Other kinds of tractor-trailer impact scenarios that users might desire to simulate could be non-redirective – i.e., head-on impacts with walls, bridge piers, security perimeters, etc. The current tractor model would need to be upgraded and validated for these kinds of impact scenarios.

The tractor FE model would need to be remeshed in areas that would sustain damage in a more frontal impact. For example, the mesh of the frame-rails and cross-members would need to be refined so they could more realistically capture buckling-type modes of failure. The connections of major components to the frame rails would need to be re-evaluated for their ability to simulate failure as appropriate. Similarly, the cab-to-frame connections would need to be evaluated for their ability to simulate failure. Also, more structural detail would need to be added to the cab and cab interior to account for more structural impact energy absorption.

Accommodating a non-redirective impact would also require a more accurate model of the tractor-to-trailer connection region. The fifth-wheel and kingpin mechanisms, and the structure/weldment surrounding the kingpin would need to be modeled in more detail, and laboratory tests would need to be run to characterize the materials and failure mechanisms.

The current trailer FE model was built based on our survey of the existing semi trailers that were available to us to photograph and measure. Most of the trailers we observed were equipped with Air-Ride (airbag) type suspensions rather than leaf-spring suspensions. Consequently, the current trailer FE model has an Air-Ride type suspension. We believe that, in general, this was a

reasonable choice because the model will be more representative of current and future semi trailers. The down-side of this choice is that much of the existing full scale crash data for tractor-trailers is from past years when most of the trailers had leaf-spring type suspensions. To best validate the tractor-trailer FE model against this existing crash data we would need to add a leaf-spring suspension option to the trailer FE model. The leaf-spring suspension model could be adapted to the current trailer FE model and modularized in such a way that the user could choose either suspension option.

Model Sensitivity Analysis and Uncertainty Quantification

The current tractor-trailer model is a complex assembly of parts, materials, FE formulations, and modeling approaches. The model will be used by other researchers in combination with equally complex structure models to simulate impact events. Basic questions need to be answered for the model to be widely adopted by prospective users, such as:

- Range of model validity and application

- Identification of the model's crucial factors/parameters and the how they affect key output metrics

- Determination of the model's parameters that best match experimental data, etc.

Sensitivity analysis tools such as parameter studies, design and analysis of computer experiments, and general sampling methods are used in these studies in combination with High Performance Computing resources that are necessary to investigate a wide range of parameters and design space. Uncertainty analysis and quantification based on uncertain inputs can help 1) determine variance of outputs and probabilities of outcomes that identify parameter correlations/local sensitivities, 2) identify inputs whose variances contribute most to output variance (global sensitivity analysis) and 3) quantify uncertainty when using the calibrated model to predict outcomes outside the domain of calibration. The above methods were extensively developed in the U.S. Department of Energy weapons programs and can be applied to the current vehicle models from DOT.

Appendix A – User Handbook and Release Notes

Tractor-Semitrailer FE Model
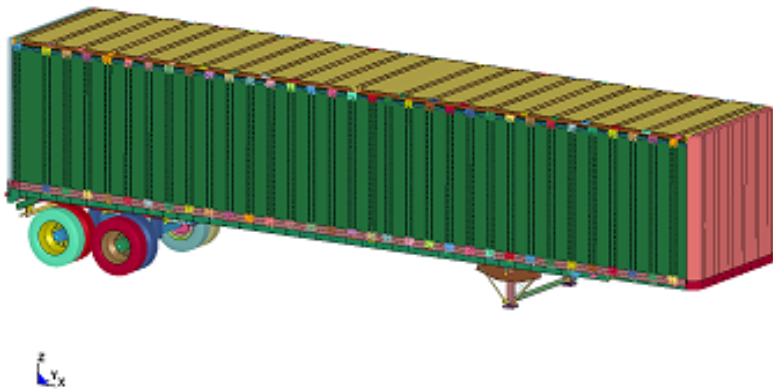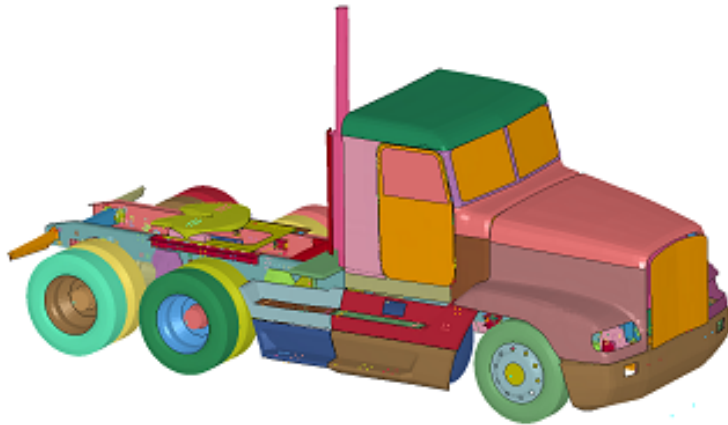
User's Manual / Release Notes

Charles R. Miele, P.E.

Chuck A. Plaxico, PhD

Battelle Memorial Institute

Tractor-Semitrailer FE Model User's Manual and Release Notes
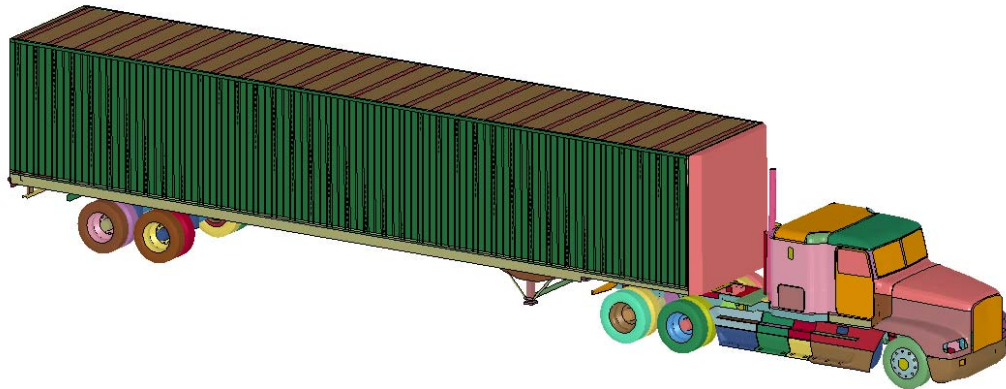
Introduction

This Tractor-Semitrailer vehicle FE model is the product of three year's work. Many hours of research were spent to determine the best and most accurate material property definitions, critical components were characterized and validated by experimental testing and countless simulations were run and rerun to test, validate and debug this vehicle model. The main focus of this work was to validate the FE model for redirective type impact scenarios which are the most prevalent use of vehicle FE simulation. Markedly different impact scenarios such as head-on, rollover, or rear impact would need similar specific validation work.

There were several versions of the tractor and the trailer FE models developed throughout the course of this work. The level of development of each of the FE models is tied directly to availability of full scale crash test data. A long wheelbase sleeper cab tractor was developed from NCAC's original tractor-only FE model. This tractor model was modified to reflect NCAC's full scale tractor-only crash test (No.03008) and validated against that test. To date the accuracy of the combined tractor-semitrailer model has been assessed by comparing analysis results against two full scale crash tests: MwRSF Test TL5CMB2 and TTI Test 7069-13. In each case, the baseline models of the tractor and semitrailer were modified to be similar to the test vehicles' length dimensions and mass properties.

Test TL5CMB-2 involved a 79,705-lb (36,153-kg) tractor-semitrailer vehicle impacting a concrete median barrier at 52.7 mph (84.9 km/hr) and impact angle of 15.4 degrees. The test vehicle was a 1991 White GMC tractor with a 1988 Pines 48-ft (14.6-m) semitrailer. The test

article was a 42 inch (1.067 m) tall concrete median barrier with an installation length of 200 ft (60.9 m).

Test 7069-13 involved a 1979 International TranStar 4200 tractor with a 1977 Pullman van-trailer ballasted to 50,050 lb (22723 kg) impacting the barrier at 51.4 miles per hour (82.7 km/hr) and 16.2 degrees. The installation length of the barrier was 100 ft (30 m), and the impact point was 24 ft (7.3 m) from the upstream end.

All assessments of the models' results have so far been done by comparison to redirective type impacts with longitudinal rigid barriers (e.g., impact speed and angle of 80 km/hr and 15 degrees, respectively). The simulation results have indicated that this tractor-semitrailer FE model is *reasonably* valid for this type of crash simulation and that it will provide useful results in general barrier design evaluation work, regarding impact loads and general vehicle-barrier interaction. The model has not, however, been assessed for use in other applications, such as high-energy impacts (e.g., full frontal impact with bridge pier), general vehicle dynamics (e.g., vehicle response due to steer maneuvers) or vehicle-to-vehicle impacts, to name a few.

The information in this manual is generally applicable to all the tractor and trailer FE Models. Specific details are best found in the LS-Dyna keyword input files or through the online user's guide. The link to the SharePoint site where the FE models reside is: http://websps1.battelle.org/heavyfem/home/Models/Shared%20Documents/Forms/AllItems.aspx

The link to the Tractor-Trailer web site and On Line User's Guide is available for download at:

http://www.ntrci.org

User Notes

From the experienced-user's perspective, there are some basic model-usage issues, and model-specific practical considerations that users of this FE model should be aware of:

The tractor-semitrailer FE model used for simulating the MwRSF test TL5CMB-2 needs about 300 milliseconds (0.300 seconds) pre-impact time to stabilize and settle under gravity. The front suspension's oscillations damp out almost immediately. The rear suspension seems to take longer for the oscillations to damp out. Another approach taken by the research team was to "time" the rear suspension's oscillations such that the rear tires were most firmly pressed against the ground at the time of rear wheelset impact with the barrier, similar to the rear wheelset action in the video of the actual crash test. This resulted in a starting position of the tractor-semitrailer at 4.7 meters from the impact point of the barrier. This strategy also resulted in a good correlation of the simulation results with the crash test data. This initial offset distance takes less computation time than the 300 millisecond pre-impact time stabilization approach.

The tractor-semitrailer FE model used for simulating the TTI test 7069-13 includes additional input files (i.e., nodesin.k and dynain.k) that contain necessary node and element information for "full" gravity initialization of the model prior to start of the analysis. One important note about the "nodesin.k" file is that this file **replaces all node definitions in all the input *.k files** when the gravity initialization approach is used. The original node definitions are still in the input files; they are defined at the end of the files, and are "commented out" by the insertion of a *END right before the node definitions. This provides the user an easy way to reinstate the original node definitions in any input file by removing the *END line before the node definitions if the user desires to run a simulation using this model without gravity initialization.

Orienting vehicle and barrier models for a particular simulation **should not be done "manually"** by moving nodes/elements in a pre-processor. Use the *DEFINE_TRANSFORMATION and the *INCLUDE_TRANSFORM options in LS-Dyna (in the 00Main.k file) **only** for any re-orientation of the vehicle or the barrier. The reasons for this are: 1) There are several inertias defined that are not exactly orthogonal to the global coordinate system, but they are defined in the global coordinate system. 2) The shell element stress tensors defined for the front suspension preload are defined relative to each element's local coordinate system. Changing the orientation of the tractor or the trailer with a pre-processor may not properly account for the correct orientation of specified inertias and initial stress information. Transformations and orientations that are done "within" LS-Dyna using *DEFINE_TRANSFORMATION and *INCLUDE_TRANSFORM will guarantee that stresses and inertias are accounted for properly.

The tractor and trailer models are oriented orthogonal to the global coordinate system such that X is forward, Y is to the left, and Z is up. Barriers or other targets can then be oriented relative to the vehicle (global) coordinate system.

All the various tractor and trailer FE models, the Airide™ suspension models, and to some extent the ballast FE models are designed to be modular and can be interchanged relatively easily to facilitate other combinations of tractors and trailers. This is most easily done using the *INCLUDE and *TRANSFORM options via a "00Main.k" file.

A minor bug in LS-PrePost when writing an FE model that has the *MAT_SIMPLIFIED_RUBBER_WITH_DAMAGE option is that the unloading load curve number is written in scientific notation to 4 significant digits rather than as an integer. This creates an error condition when LS-Dyna tries to read the keyword file because LS-Dyna is expecting an integer.

Contact Us

Please submit questions and comments on the model to Chuck Miele at Battelle by telephone at (614) 424-4023 or by e-mail at miele@battelle.org. The Program Team will respond as quickly as possible to resolve issues identified.

Basic FE Model Statistics

An example of the FE model information summary that is generated directly by LS-PrePost is shown in Figures A-1 and A-2. These model statistics are for reference only, and are approximate. They are based on the original long-wheelbase tractor model and the 48-foot semitrailer model. The actual count of parts, mass, CG locations, etc. are best found by generating them from the most current FE model via the online user's guide.
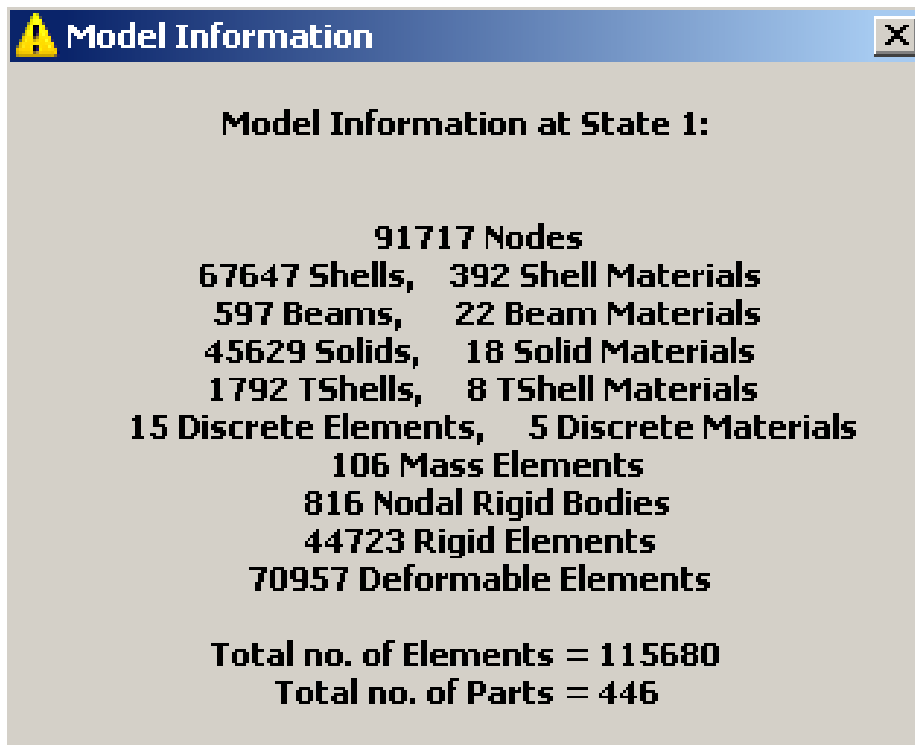
Figure A-1. Illustration. Sleeper cab tractor model information window from LS-PrePost
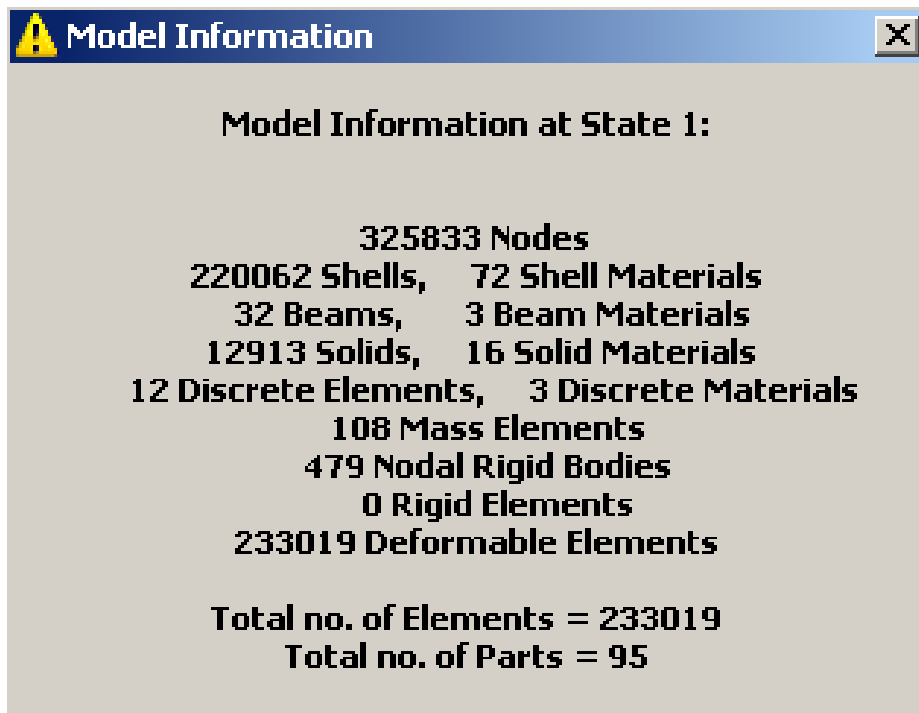
Figure A-2. Illustration. 48-foot semitrailer model information window from LS-PrePost

Table A-1. FE Model Masses

Long Wheelbase Tractor	**17,110 Lbs (7,762 Kg)**
Short Wheelbase Daycab Tractor	**15,506 Lbs (7,703 Kg)**
48-foot Semitrailer	**13,626 Lbs (6,181 Kg)**
45-foot Semitrailer	**13,125 Lbs (5,954 Kg)**
Ballast for MwRSF Test	**50,920 Lbs (23,098 Kg)**
Ballast for TTI Test 7069-13	**22,360 Lbs (10,134 Kg)**

The mass values shown in Table A-1 and the CG locations shown in Figure A-3 are for scale and perspective only.
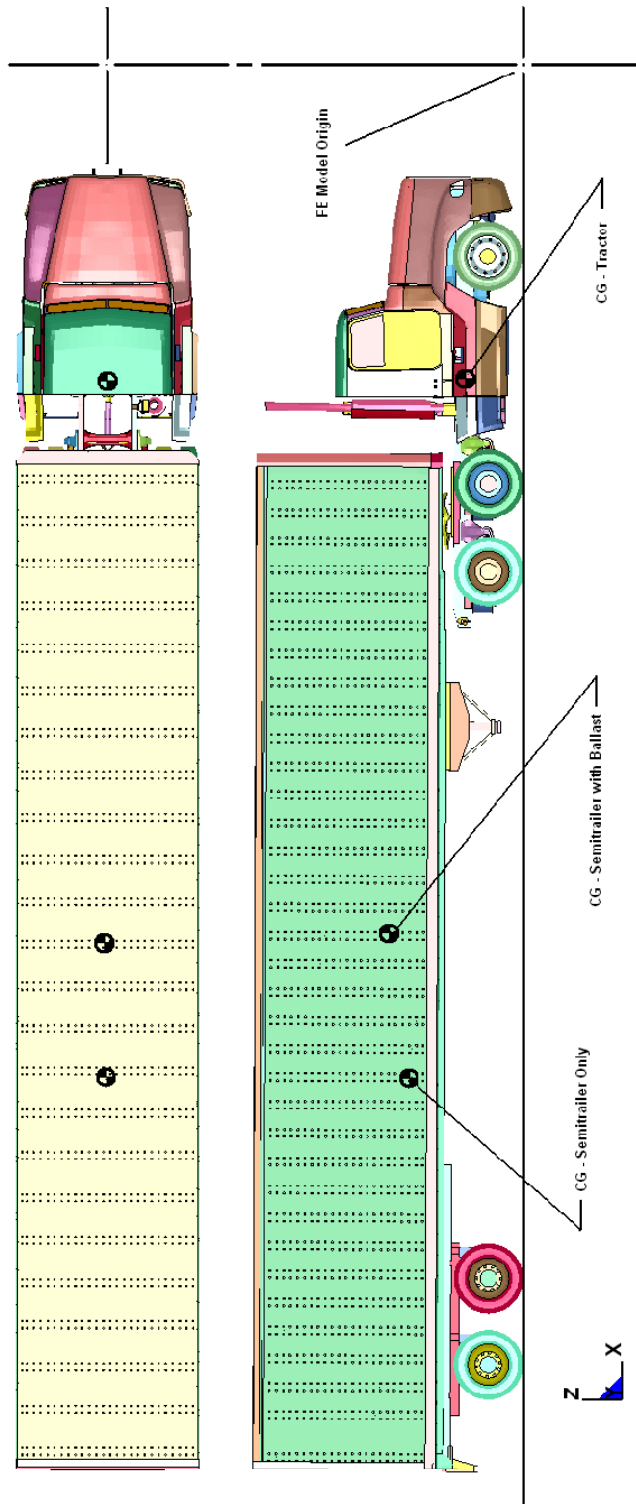
Figure A-3. Illustration. FE model CG locations and origin

Actual FE model Vehicle Masses and C.G. Locations

Figure A-3 is a schematic showing the approximate locations of a tractor's and a semitrailer's CGs. Use LS-PrePost to obtain the values and locations for a specific FE model. Go to the "Measure" command in Panel 1, Item: Inertia. Select and display the desired part or parts, check "Active Elements Only", and "All", highlight "X-cg", then click on "Apply". Figure A-4 shows a screen snapshot of this operation for a tractor FE model.
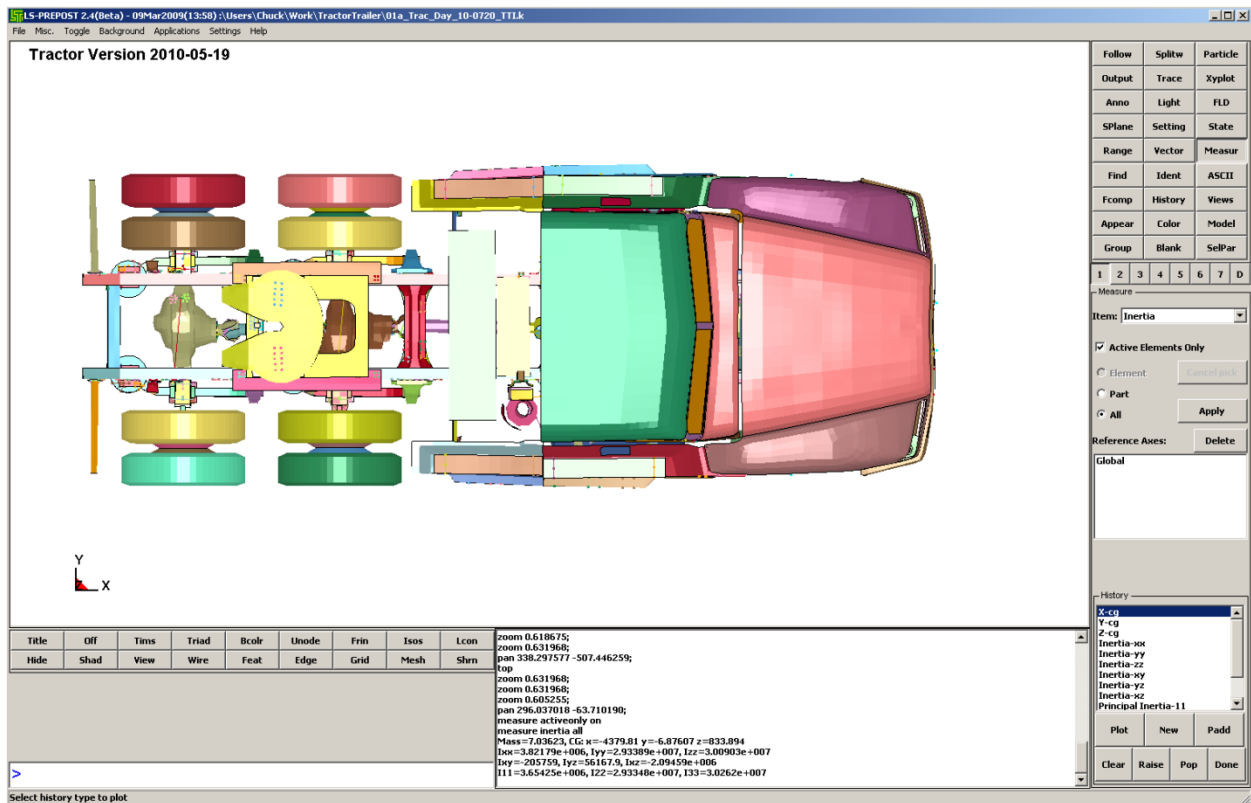
Figure A-4. Illustration. Finding CG information in LS-PrePost

FE Model File Organization

Quick-Start Overview of FE Models on SharePoint Site

List of Files on the Share Site:

📁 **Phase A Final Report and Simulation Videos**

📁 **Phase B Final Report and Simulation Videos**

📁 **Phase C Final Report and Simulation Videos**

📁 **Tractor-Trailer Models**

📄 **TTUserManual**

The four directories' names are self-explanatory. The Tractor-Trailer Models directory contains three subdirectories where the LS-Dyna keyword input files reside for the two simulations used to compare to crash tests TL5CMB2 and 7069-13, and a directory containing the original sleeper cab tractor FE model. The FE models of the TL5CMB2 and 7069-13 test simulations are the most recent and more debugged than the FE models in the original sleeper cab directory. The larger keyword input files are also provided as zipped files for a more convenient download size.

The LS-Dyna d3plot and binout results files are available for download for the two crash test simulations in subdirectories called "d3plots-binouts" directly under the keyword file directories.

The Word document "TTUserManual2010" is the printable written-document User's Manual for the Tractor-Semitrailer FE Vehicle models.

The following lists the names and a brief description of the input files that are available on the SharePoint Site as of this writing. A more detailed description of each file follows in the next section.

General Description of Input Files for the Day Cab Tractor + 45-foot Trailer Model

1. **00MainGravInit.k**: This is the input file that is submitted to LS-Dyna for analysis. It uses the *INCLUDE command to combine all the input files for the model.

2. **01a_Trac_Day_10-0621_TTI.k**: The finite element model of a Freightliner FLD120 tractor geometrically modified to be the Day Cab tractor from the TTI test 7069-13. All nodes, elements, materials, connections, etc. for the tractor are included in this file.

3. **01b_Intial-stress_Tractor.k**: File containing initial stress state for the front leaf springs of the tractor to account for equilibrium load on the leaf spring components under gravity loading. Without this file, the tractor would displace significantly under gravity load, altering the center of gravity and bumper height.

4. **01c_AirRide20psi.k**: Part, Section and Material definition for the discrete element model of the Airide suspension with properties corresponding to 20 psi internal pressure for a tractor-only simulation.

5. **01c_AirRideTractor45psi.k**: Part, Section and Material definition for the discrete element model of the Airide suspension with properties corresponding to 45 psi internal pressure. Used in tractor-semitrailer model for trailer ballasted to 50,000 lbs (22,700 kg).

6. **02a_SemiTrailer45_10-0621_TTI7069-13.k**: The finite element model of 45-ft Stoughton semitrailer. All nodes, elements, connections, etc. for the trailer are included in this file.

7. **02c_AirRideTrailer20psi.k**: Part, Section and Material definition for the discrete element model of the Airide suspension with properties corresponding to 20 psi internal pressure for an empty trailer.

8. **02c_AirRideTrailer45psi.k**: Part, Section and Material definition for the discrete element model of the Airide suspension with properties corresponding to 45 psi internal pressure.

9. **02b_TrailerMaterials_2010-0217.k**: Material database for the semitrailer

10. **03Tractor2Trailer_connection.k**: Creates a spherical joint connection between the trailer kingpin and the tractor fifth-wheel. Also, defines contact between the kingpin box and fifth-wheel.

11. **05NJB-Ballast2-foam11b.k**: Ballast for the trailer model with mass of 10,134 kg

12. **05Contact11.k**: Tie contact between ballast bolts and trailer floor, the ballast parts with the trailer and ballast self-contact.

13. **15TL-3_7069-13_Bridge_Parapet_Elastic2.k**: Impacted bridge parapet barrier

14. **15contact-tractor2010-0323.k**: Contact between tractor and median barrier

15. **15contact-trailer2.k**: Contact between trailer and median barrier

16. **20control1.k**: Defines *CONTROL, *DATABASE, *CONTACT_INTERIOR for the entire model. This file is always read in last and overrides any previous definitions of these parameters from the earlier input files.

17. **dynain.k**: Gravity-initialized stresses for the entire FE model

18. **nodesin.k**: Gravity-initialized nodal locations for the entire FE model

General Description of Input Files for the Day Cab Tractor + 48-foot Trailer Model

19. **00Main2.k**: This is the input file that is submitted to LS-Dyna for analysis. It uses the *INCLUDE command to combine all the input files for the model.

20. **00MainBackedUp.k**: This is the input file that is submitted to LS-Dyna for analysis with the tractor-semitrailer backed up 4.7 meters from the barrier. It uses the *INCLUDE command to combine all the input files for the model.

21. **01a_Trac_Day_2010-0520.k**: The finite element model of a Freightliner FLD120 tractor geometrically modified to be a Day Cab tractor. All nodes, elements, materials, connections, etc. for the tractor are included in this file.

22. **01b_Intial-stress.k**: File containing initial stress state for the front leaf springs of the tractor to account for equilibrium load on the leaf spring components under gravity loading. Without this file, the tractor would displace significantly under gravity load, altering the center of gravity and bumper height.

23. **01c_Airide_60psi.k**: Part, Section and Material definition for the discrete element model of the tractor Airide^TM suspension with properties corresponding to 60 psi internal pressure. Used in tractor-semitrailer model for trailer ballasted to 80,000 lbs (36,000 kg).

24. **02a_semitrailer48_10-0521.k**: The finite element model of 45-ft Stoughton semitrailer. All nodes, elements, connections, etc. for the trailer are included in this file.

25. **02b_AirRideTrailer72p5psi.k**: Part, Section and Material definition for the discrete element model of the Airide^TM suspension with properties corresponding to 72.5 psi internal pressure. Used in tractor-semitrailer model for trailer ballasted to 80,000 lbs (36,000 kg).

26. **02b_TrailerMaterials_2010-0217.k**: Material database for the semitrailer.

27. **03Tractor2Trailer_09-0206.k**: Creates a spherical joint connection between the trailer kingpin and the tractor fifth-wheel. Also, defines contact between the kingpin box and fifth-wheel.

28. **05NJB-Ballast-foam11b.k**: Ballast for the trailer model

29. **05contact11.k**: Defines contact between the ballast parts and the trailer.

30. **15TL-5_Median_Barrier_Elastic.k**: Impacted bridge parapet barrier

31. **15contact-tractor2010-0323.k**: Contact between tractor and median barrier

32. **15contact-trailer2.k**: Contact between trailer and median barrier

33. **20control1.k**: Defines *CONTROL, *DATABASE, *CONTACT_INTERIOR for the entire model. This file is always read in last and overrides any previous definitions of these parameters from the earlier input files.

General Description of Sleeper Cab Tractor + 48-Foot Trailer Model and Miscellaneous Input Files

34. **00Main500x.k**: This is the input file that is submitted to LS-Dyna for analysis. It uses the *INCLUDE command to combine all the input files for the model for analysis with the tractor-semitrailer 0.50 meters from the barrier.

35. **00MainAtBarrier.k**: This is the input file that is submitted to LS-Dyna for analysis with the tractor-semitrailer at the barrier. It uses the *INCLUDE command to combine all the input files for the model.

36. **01a_Trac_Sleepr_10-0308.k**: The finite element model of a Freightliner FLD120 Sleeper Cab tractor. All nodes, elements, materials, connections, etc. for the tractor are included in this file.

37. **01b_Intial-stress.k**: File containing initial stress state for the front leaf springs of the tractor to account for equilibrium load on the leaf spring components under gravity loading. Without this file, the tractor would displace significantly under gravity load, altering the center of gravity and bumper height.

38. **01c_Airide_60psi.k**: Part, Section and Material definition for the discrete element model of the tractor Airide^{TM} suspension with properties corresponding to 60 psi internal pressure. Used in tractor-semitrailer model for trailer ballasted to 80,000 lbs (36,000 kg).

39. **02a_semitrailer48_10-0521.k**: The finite element model of 45-ft Stoughton semitrailer. All nodes, elements, connections, etc. for the trailer are included in this file.

40. **02b_AirRideTrailer72p5psi.k**: Part, Section and Material definition for the discrete element model of the Airide^{TM} suspension with properties corresponding to 72.5 psi internal pressure. Used in tractor-semitrailer model for trailer ballasted to 80,000 lbs (36,000 kg).

41. **02b_TrailerMaterials_2010-0217.k**: Material database for the semitrailer.

42. **03Tractor2Trailer_09-0206.k**: Creates a spherical joint connection between the trailer kingpin and the tractor fifth-wheel. Also, defines contact between the kingpin box and fifth-wheel.
43. **05NJB-Ballast-foam11b.k**: Ballast for the trailer model

44. **05contact11.k**: Defines contact between the ballast parts and the trailer.

45. **15TL-5_Median_Barrier_Elastic.k**: Impacted bridge parapet barrier

46. **15contact-tractor2010-0323.k**: Contact between tractor and median barrier

47. **15contact-trailer2.k**: Contact between trailer and median barrier

48. **20control1.k**: Defines *CONTROL, *DATABASE, *CONTACT_INTERIOR for the entire model. This file is always read in last and overrides any previous definitions of these parameters from the earlier input files.

More Detailed Description of File Organization and Content

The LS-Dyna FE model of the tractor-semitrailer vehicle is organized using the *INCLUDE options in LS-Dyna. This organizational strategy allows users to easily reconfigure the simulated crash vehicle and the simulated crash-test device. All of the model input files required for a particular simulation are brought together in a "main" file. This main file is typically named 00Main.k. The intent of the leading zeros are to place the main file at the top of the file list in the directory. One advantage of using the LS-Dyna *INCLUDE file option is that entire (keyword file) models can be positioned via the *TRANSFORM option and can also be conveniently renumbered into ranges that are meaningful and useful to the analyst. Figures A-5 and A-6 show an example of a "00Main.k" file annotated with explanations of the *INCLUDE command inputs. This assumes the standard analysis-file organization "convention" for LS-Dyna/Linux environments of creating a separate directory for each simulation.

The baseline tractor vehicle FE Model is based on the original NCAC-developed FE model of a sleeper-cab style tractor with a 242-inch wheelbase. Variations on this baseline FE model are accomplished using the ADAP scripts developed by ORNL. Variations include a day-cab style model and various (shorter) wheelbases. Completed variations are available for the day cab tractors used in MwRSF and TTI crash tests TL5CMB2 and 7069-13.

Note that the position of the semitrailer rear wheelset assembly (bogey) is adjustable (fore-aft) by the user for any cargo box length and bogey position. Some care must be taken when doing this. In the FE model, the part of the bogey frame that adjusts its relative position on the trailer longitudinal rails is connected using *MAT_SPOTWELD (solid) elements. These elements are a type of tied contact, so they do not have to be "manually" disconnected and reconnected when the bogey position is adjusted. The bogey and these *MAT_SPOTWELD elements are selected and then translated using LS-PrePost. The direction of this fore-aft motion is not *exactly* along the global X direction because the trailer is angled 2° downward from the rear wheels to the kingpin. Given this, the actual translation should be done by choosing the appropriate "N1-to-N2" reference nodes in the translation utility in LS-PrePost. Also, when the wheels are moved, the locations of the wheel rotation *JOINTs and the rotation centers for the *INITIAL_VELOCITY option must be updated by the user. If the user needs to make this adjustment for several different cases, separating the bogey assembly into its own keyword file with specific joint and initial velocity definitions may be preferable. The user can call this separate bogey k file into the 00Main file using the *INCLUDE_TRANSFORM option.

Many of the keyword files themselves contain comment lines with information about the content of the particular file as well as comments about revisions and modifications to the content.

```
*KEYWORD
$
$ -------------------- Tractor ----------------
$
*DEFINE_TRANSFORMATION
101                                                    ——— ID to associate origin, translation, rotation, etc.
TRANSL, 0, 0, 0                                         ——— Type and actual magnitude
$
*INCLUDE_TRANSFORM                                      ——— Include the file with a transformation
Trac_Day_Cut_v6.k                                      ——— File to operate on
0, 0, 0, 0, 0, 0, 0 ⎞
0,                  ⎟                                   Numbering offsets for nodes, elements, parts,
0, 0,0, 0, 0        ⎠                                   materials, properties, etc.
101                                                    ——— Transformation ID
*INCLUDE                                               ——— Include the file without a transformation
01b_Initial-stress.k
*INCLUDE
01c_Airide_60psi.k
$
$ ----------------- Semi-Trailer --------------
$
*INCLUDE_TRANSFORM
02a_SemiTrailer48_09-0725.k
0, 0, 0, 0, 0, 0, 0
0,
0, 0,0, 0, 0
101
*INCLUDE
02b_AirRideTrailer60psi.k
*INCLUDE
02c_TrailerMaterials_09-0413.k
*INCLUDE_TRANSFORM
03Tractor2Trailer_09-0206.k
0, 0, 0, 0, 0, 0, 0
0,
0, 0,0, 0, 0
101
$
```

Figure A-5. Illustration. Main keyword input file – 00Main.k

```
$
$ ------------------- Ballast ----------------
$
*DEFINE_TRANSFORMATION
1
TRANSL,  1600.0,  0, -6
*INCLUDE_TRANSFORM
05NJB-Ballast-foam11.k
1000000, 1000000, 1000000, 1000000, 1000000, 1000000, 1000000
1000000,
0, 0,0, 0, 0
1
*INCLUDE
05contact11.k
$
$ ------------------- Barrier ----------------
$
*DEFINE_TRANSFORMATION
15
ROTATE 0, 0, 1, -152.435, -1120.61, 806.027, 0.5000
TRANSL,  4716.6, 410, 0
$ velocity = 23583.000 mm/s
*INCLUDE_TRANSFORM
15TL-5_Median_Barrier_R10.k
0,0,0,0,0,0,0
0,
0, 0,0, 0, 0
15
*INCLUDE
15contact-tractor.k
*INCLUDE
15contact-trailer.k
$
$ ----------------- Control Cards -------------
$
*INCLUDE
20control.k
*END
```

Figure A-6. Illustration. Main keyword input file – 00Main.k

Figure A-7 shows a typical listing of LS-Dyna input files and a brief description of each file's purpose. The file names are generally meant to be self-explanatory of their contents. More detailed descriptions of some of these files are provided below where their content/purpose is not obvious from their names or description in the figure.

```
00Main.k ─────────────────── Main file for creating a simulation
01a_Trac_Day_v1a_090506.k ─────── Tractor FE Model
01b_Initial-stress.k ──────────── Tractor front leaf spring initial load stresses
01c_Airide_20psi.k ⎫
01c_Airide_60psi.k ⎭ ──────────── Tractor rear suspension for loaded and unloaded cases
02a_SemiTrailer48_09-0725.k ───── Semitrailer FE Model
02b_AirRideTrailer20psi.k ⎫
02b_AirRideTrailer60psi.k ⎭ ───── Semitrailer rear suspension for loaded and unloaded cases
02c_TrailerMaterials_09-0413.k ── Semitrailer materials input
03Tractor2Trailer_09-0206.k ───── Tractor-to-semitrailer interface - contacts, joints, etc.
05contact11.k ─────────────── Ballast to semitrailer contact definitions
05NJB-Ballast-foam11.k ───────── Semitrailer ballast
15contact-tractor.k ──────────── Tractor to barrier contact definition
15contact-trailer.k ──────────── Semitrailer to barrier contact definition
15TL-5_Median_Barrier_R10.k ───── Barrier FE Model
20control.k ─────────────── LS-Dyna *CONTROL options
Trac_Day_Cut_v6.k ───────────── Tractor FE Model
```

Figure A-7. Illustration. Example input file listing

00MainGravInit.k

This "00Main" file contains all the *INCLUDE file specifications for every FE model component for the simulations of the TTI test 7069-13. It also includes the special gravity initialization – initial stress and initial node location – dynain.k and nodesin.k files for the entire tractor-semitrailer FE model.

00MainBackedUp.k

This "00Main" file contains all the *INCLUDE file specifications for every FE model component for the simulations of the MwRSF test TL5CMB2. It is configured such that the tractor-semitrailer starts the simulation initially positioned 4.7 meters from the barrier impact point. This was done to allow (simulation) time for gravity initialization of the FE model.

01b_Initial-stress_Tractor.k

This file contains a set of stresses that provide the preloaded, prestressed state of the front leaf springs, at the geometric shape representing their equilibrium position (shown in Figure A-8) under gravity loading. The front leaf spring suspension is supporting approximately 4,845 lb (21,550 N) under gravity load.

To obtain this set of initial stress, an analysis was conducted to compress the leaf-spring model into its proper equilibrium position. The nodal coordinates of the suspension in this deformed state were extracted and put back into the leaf-spring suspension model. The element stresses at this position were also obtained from the analysis (via *INTERFACE_SPRINGBACK option in LS-Dyna) and were used to apply pre-stress to the leaf-spring elements (via the

*INITIAL_STRESS_SHELL card in LS-Dyna). Figure A-10 shows the equilibrium position of the tractor model under gravity load with the pre-stressed leaf-spring model.
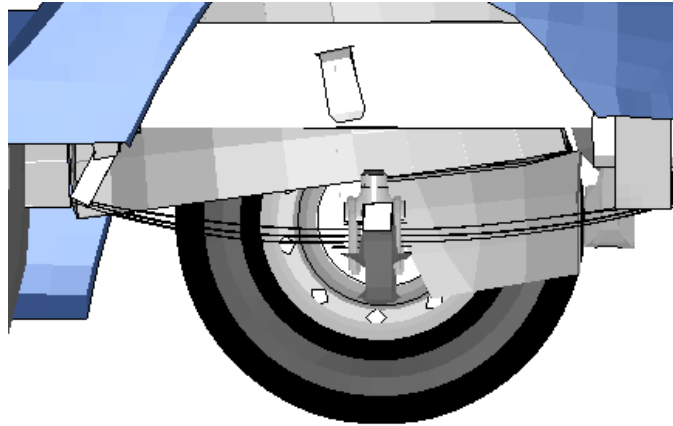
Figure A-8. Illustration. Equilibrium position of the tractor model with pre-stressed leaf-spring model

01c_Airide_20psi.k , 01c_Airide_45psi.k and 01c_Airide_60psi.k

These files are the three currently available options for the tractor's rear suspension stiffness. The 20 psi option is to be used to simulate the rear suspension (Airide™) stiffness associated with a simulation that has either no semitrailer, or an unloaded semitrailer. The 45 psi and 60 psi options are used to simulate the rear suspension (Airide™) stiffness associated with a simulation has a partially or fully loaded semitrailer. Figure A-9 shows a view of the actual tractor Airide™ rear suspension system and a view of this rear suspension as modeled.
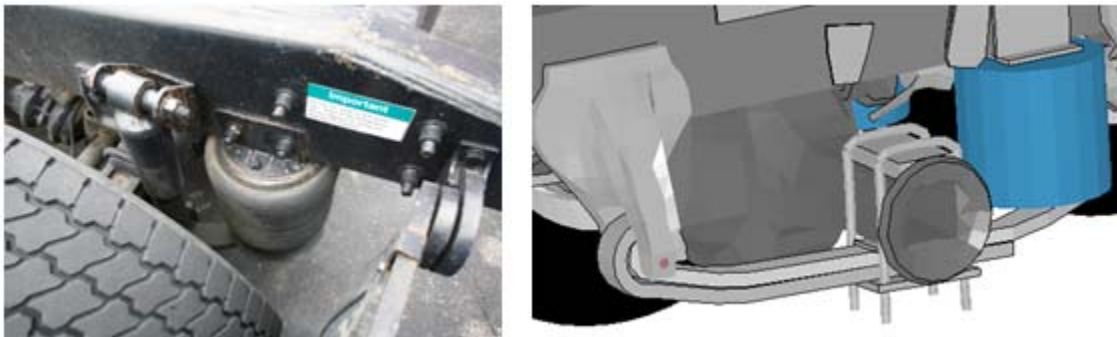
Figure A-9. Photograph / Illustration. Tractor Airide™ rear suspension

Static load-deflection data from laboratory tests conducted at 20 psig and 60 psig bag pressures are shown in Figure A-10.
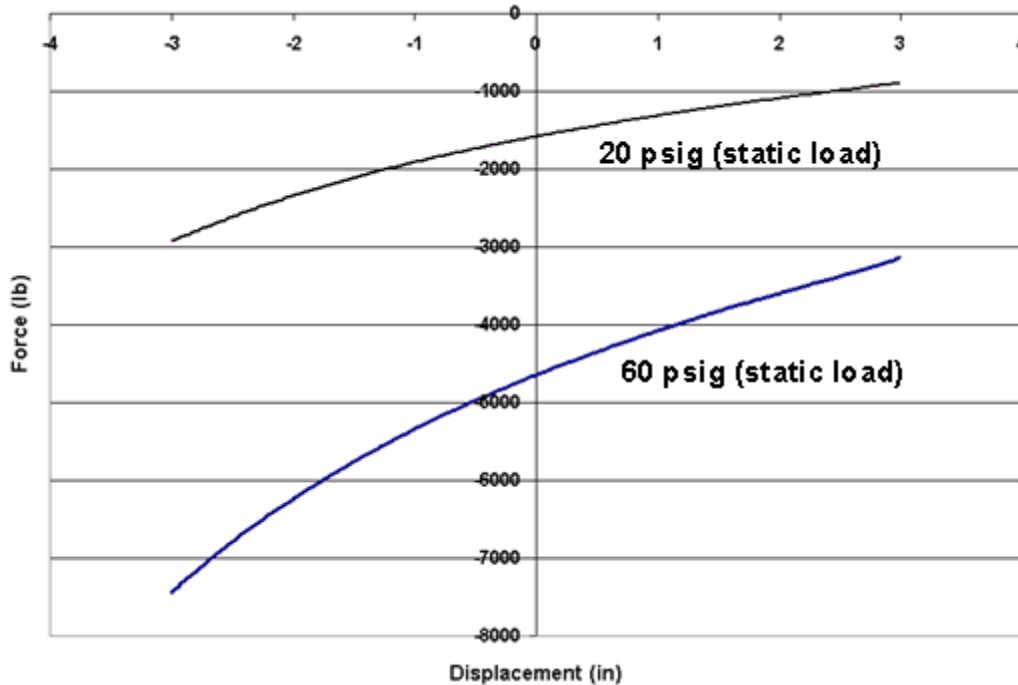
Figure A-10. Chart. Load-deflection data for AirideTM component at 20 and 60 psig pressure

02b_AirRideTrailer20psi.k, 02b_AirRideTrailer60psi.k and 02b_AirRideTrailer72p5psi.k

These files are the currently available options for the semitrailer's rear suspension stiffness. The 20 psi option is to be used to simulate the rear suspension (Airide™) stiffness associated with a simulation that has an unloaded semitrailer. The 60 and 72.5 psi options are used to simulate the rear suspension (Airide™) stiffness associated with a simulation has a partially or fully loaded semitrailer. The suspension stiffness properties included in the 60 psi files are the original data from the trailer airide suspension tests the suspension stiffness properties included in the 72.5 psi files were created by extrapolation for the fully loaded 48-foot semitrailer.

02_TrailerMaterials_2010-0217.k

This file contains all the material data for the LS-Dyna material models used in both the 45 and 48-foot trailers. Various material models are used, including elastic, elastic-plastic, Johnson-Cook, and wood. The majority of the metallic materials are specified as piecewise-linear plasticity with an initial elastic modulus.

03Tractor2Trailer_connection.k

This file contains the *JOINT and *CONTACT definitions for the tractor fifth-wheel interface with the trailer kingpin area. This connection is explained further in the next section.

05NJB-Ballast-foam11.k

This file contains the specific semitrailer ballast used in the MwRSF crash test TL5CMB-2. This same ballast model with modified mass is used in the TTI crash test 7069-13.

05contact11.k

This file contains the contact definitions for ballast self contact and ballast to trailer.

15contact-trailer2.k and 15contact-tractor2010_0304.k

These files contain the tractor-to-barrier contacts and the trailer-to-barrier contacts. Contact (and friction) can be specifically defined for the tires and wheels to the barrier and for the tractor or trailer body to barrier.

Tractor to Trailer Connection

The tractor is connected kinematically to the semitrailer via three spherical joints and contact between the Fifth Wheel and the King Pin Box. Figure A-11 shows the locations of the spherical joints, and Figure A-12 indicates the two parts that are in contact. This is the simplest mechanical connection that provides the correct functionality. This connection typically does not fail in redirective-type crash tests, so no failure mechanism has been specified for this connection.
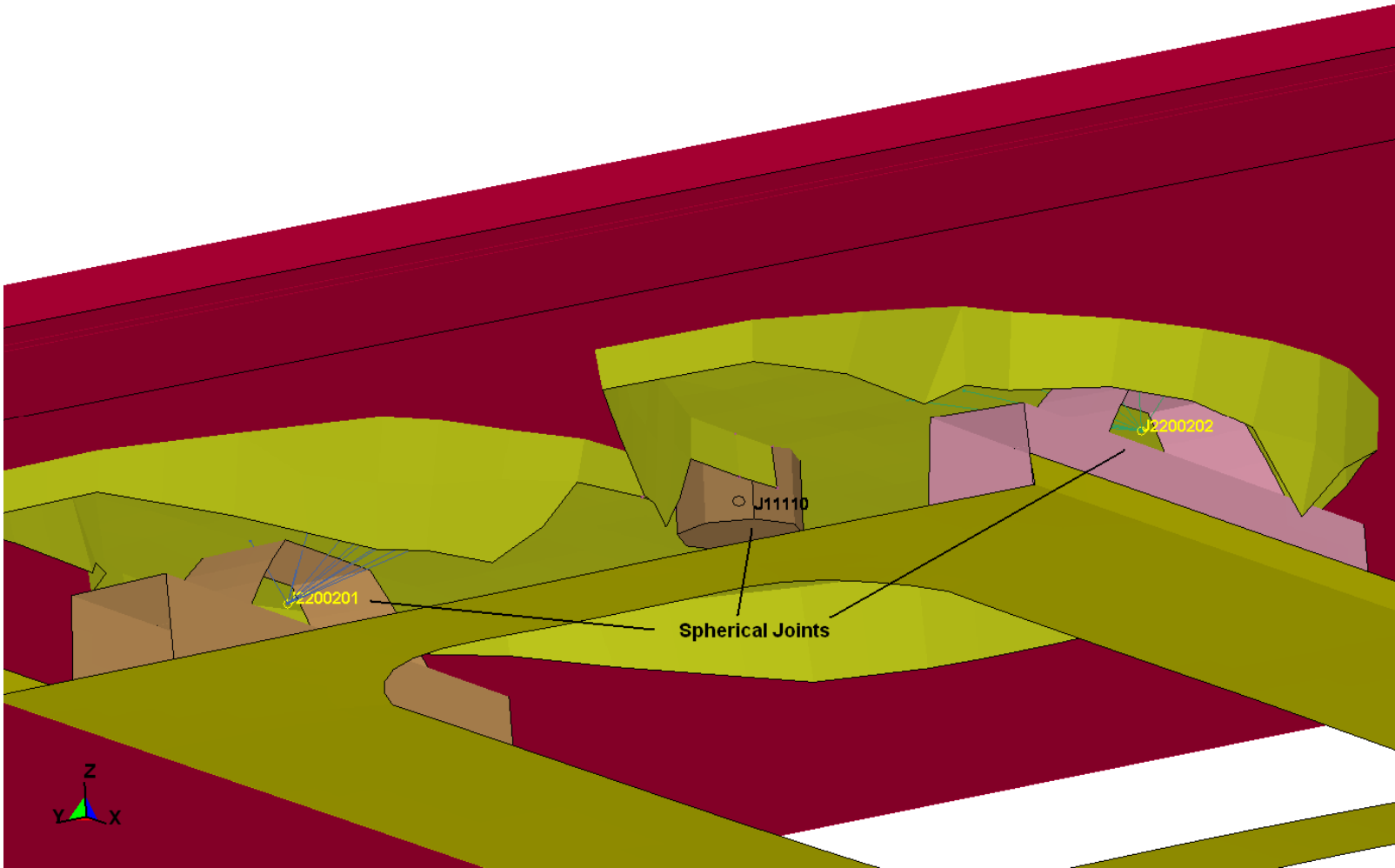
Figure A-11. Illustration. Spherical joints for tractor to semi-trailer connection

King Pin Box

Fifth Wheel
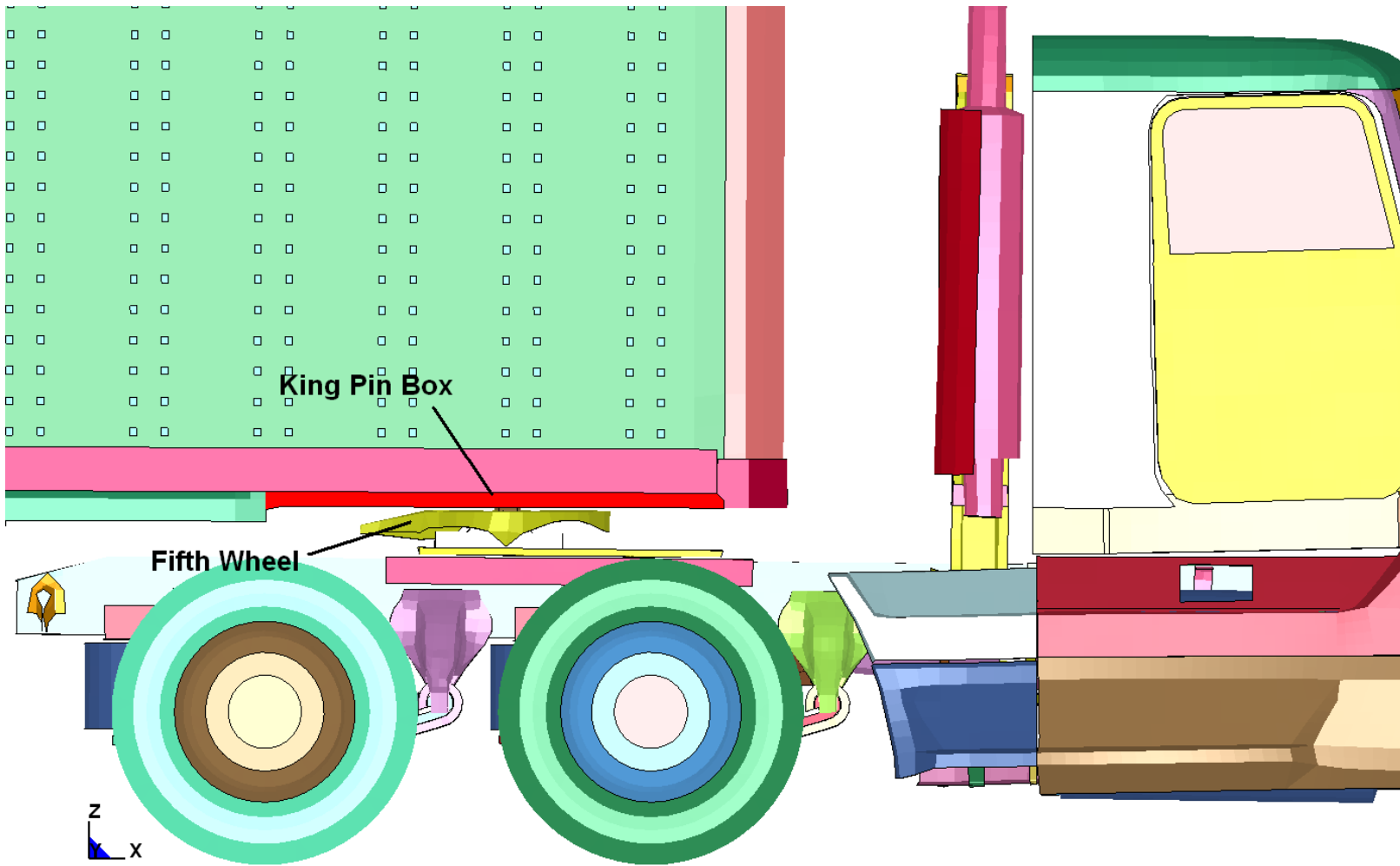
Figure A-12. Illustration. Parts in contact for tractor to semi-trailer connection

Accelerometer Locations

This FE model uses the LS-Dyna option: *ELEMENT_SEATBELT_ACCELEROMETER to define accelerometer locations and orientations. The baseline tractor vehicle FE model has 15 of these accelerometers defined. The baseline semitrailer vehicle FE model has one accelerometer defined. Figures A-13 and A-14 show the locations of the origin-node of these accelerometers. All these accelerometers are oriented with their local X-directions (initially) in the global X direction.
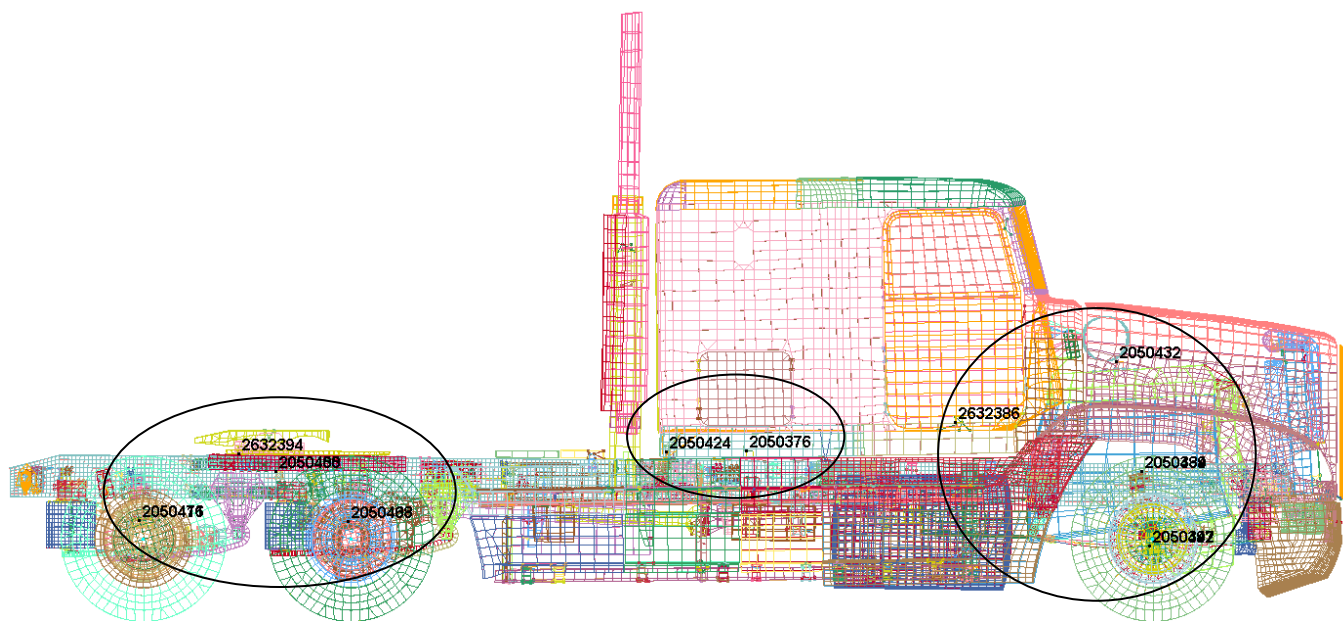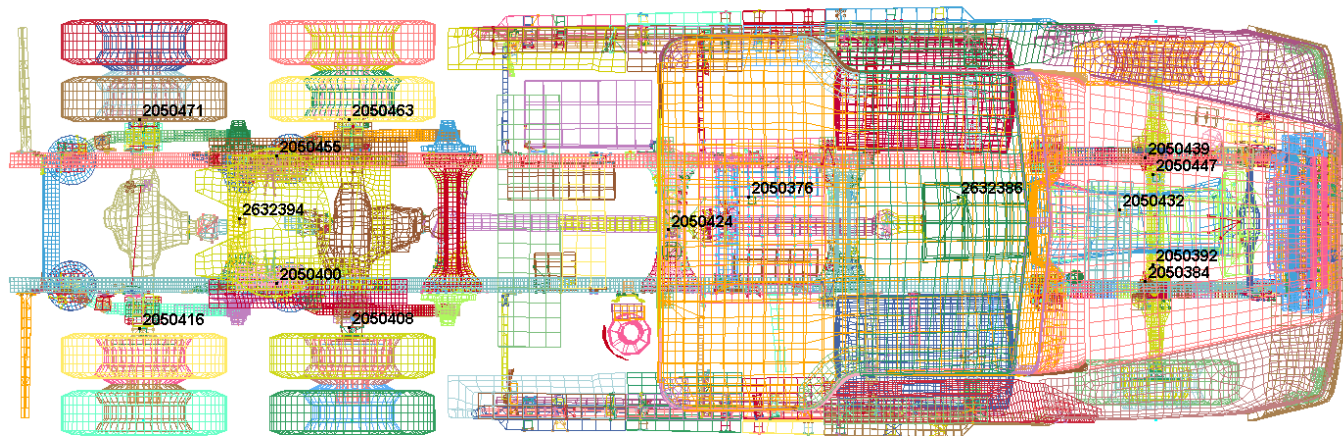
Figure A-13. Illustration. Accelerometer locations in long wheelbase tractor
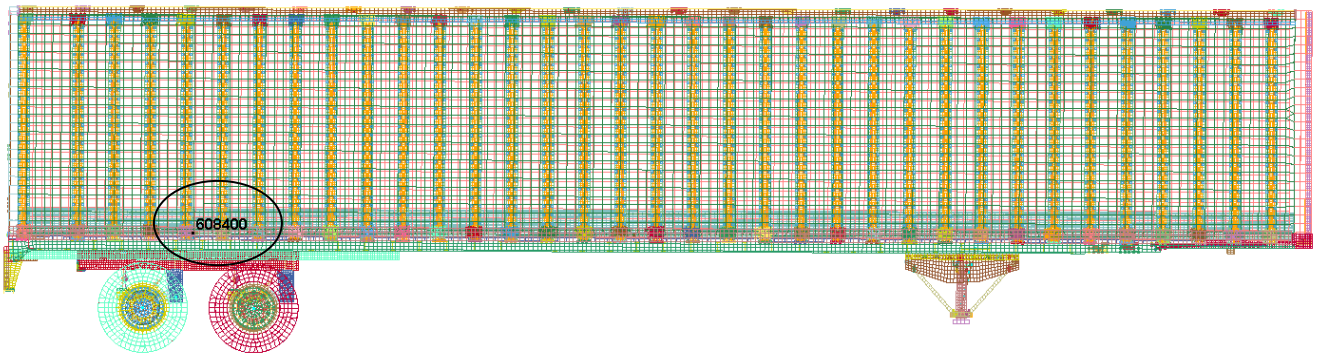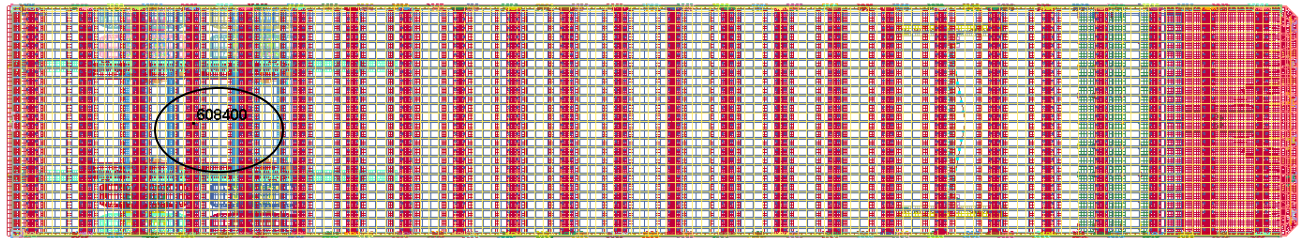
Figure A-14. Illustration. Accelerometer location in 48-foot semi-trailer

Initial Velocity Control

The vehicle model is given an initial translational velocity at every node along its longitudinal (X) axis using the *INITIAL_VELOCITY_GENERATION option in LS-Dyna. Figure A-15 shows a typical example of this from an LS-Dyna input file. In addition to this initial translational velocity, each node on every tire, wheel, and associated rotating component is given an initial rotation about its rotational axis. The user should ensure that these rotations are positioned exactly collinear with the center of the wheel-set and are proportional to, and consistent with the O.D. of the tire.

```
*INITIAL_VELOCITY_GENERATION
$#nsid/pid      styp      omega         vx         vy        vz
    2000001        1 46.866699 23583.000
$#      xc       yc         zc         nx         ny        nz     phase
-1162.5800    0.000 501.82800      0.000   1.000000
    2000002        1 46.866699 23583.000
-6043.5801    0.000 501.82800      0.000   1.000000
    2000003        1 46.866699 23583.000
-7308.0801    0.000 501.82800      0.000   1.000000
    2000004        1     0.000 23583.000
     0.000    0.000     0.000      0.000   1.000000
```

Figure A-15. Illustration. LS-Dyna input for initial velocity

There is a specific initial velocity specification for each keyword-file defined model that has motion associated with it, rather than one overall initial velocity specification for everything in one file. There is also a specific initial velocity specification used for the TTI test 7069-13 simulation with gravity initialization that reflects the gravity-deflected nodal positions in that model.

Element Types Used

Throughout the tractor and semitrailer FE models, shell elements are specified and type 2 and 16. These are fairly efficient, robust fully integrated shell-formulations. Type 16 elements will also accommodate some warping. Shell elements in areas that were expected to see significant bending were assigned 5 integration points through the thickness. Shell elements in other areas were assigned the default 3 integration points through the thickness.

Solid element type 2, fully integrated/selectively-reduced integration elements, was used to model deformable or geometrically complex solid parts. Solid element type 1, single-integration-point elements, was used for less structurally detailed parts such as spotwelds, and accelerometer elements, or rigid elements.

Connection Schemes Used

In the many areas of the FE model where parts needed to be connected, various methods were used to implement the connections:

Common-Node: Wherever possible, intersecting and adjoining plates were modeled with simple common-node connections that required no further complication.

Constrained Nodal Rigid Bodies (CNRB): CNRB's were used to connect parts that were more-or-less permanently connected and were not likely to be modified by the user.

CNRBs were used to connect adjoining parts that had mesh-dissimilarities such as different mesh size or element type (shell-to-solid, shell-to-beam, etc.).

Tied Contact: In many areas of the model, parts are connected using the *CONTACT_TIED option in LS-Dyna. Care must be taken when using this option to avoid possible conflicts with other constraints, such as CNRBs. The advantage of using this constraint method is that the associated parts can be remeshed without having to redefine the constraints.

Moveable Wheelset (Bogie)

The semitrailer FE model has a moveable wheelset (bogey) with fore-aft position adjustment just like actual semitrailers. The wheelset is attached to the cargo box via a sliding connection to allow for positioning of the trailer's wheels fore-aft for various loading conditions. This sliding connection is the (nested) interface of the wheelset's subframe (Z-channel) members with the cargo box main longitudinal frame (Z-channel) members. Figures A-16 and A-17 show the actual semitrailer and the FE model wheelset respectively.

LS-Dyna *MAT_SPOTWELD elements were used to model the connection components of the wheelset subframe to main longitudinal cargo box frame. The *CONTACT_TIED option in LS-Dyna was used to constrain the *MAT_SPOTWELD elements to both the subframe and main cargo box frame. This connection method allows the user to reposition the moveable assembly of the wheelset to any fore-aft position without the need for remeshing, reconnection or redefinition of connection elements. To adjust the bogey position *MAT_SPOTWELD elements are selected and then translated using LS-PrePost. The direction of this fore-aft motion is not *exactly* along the global X direction because the trailer is angled 2° downward from the rear wheels to the kingpin. Given this, the actual translation should be done by choosing the appropriate "N1-to-N2" reference nodes in the translation utility in LS-PrePost. Also, when the wheels are moved, the locations of the wheel rotation *JOINTs and the rotation centers for the *INITIAL_VELOCITY option must be updated by the user. If the user needs to make this adjustment for several different cases, separating the bogey assembly into its own keyword file

with specific joint and initial velocity definitions may be preferable. The user can call this separate bogey k file into the 00Main file using the *INCLUDE_TRANSFORM option.

Figure A-16. Photograph. Front view of trailer vehicle frame and bogie
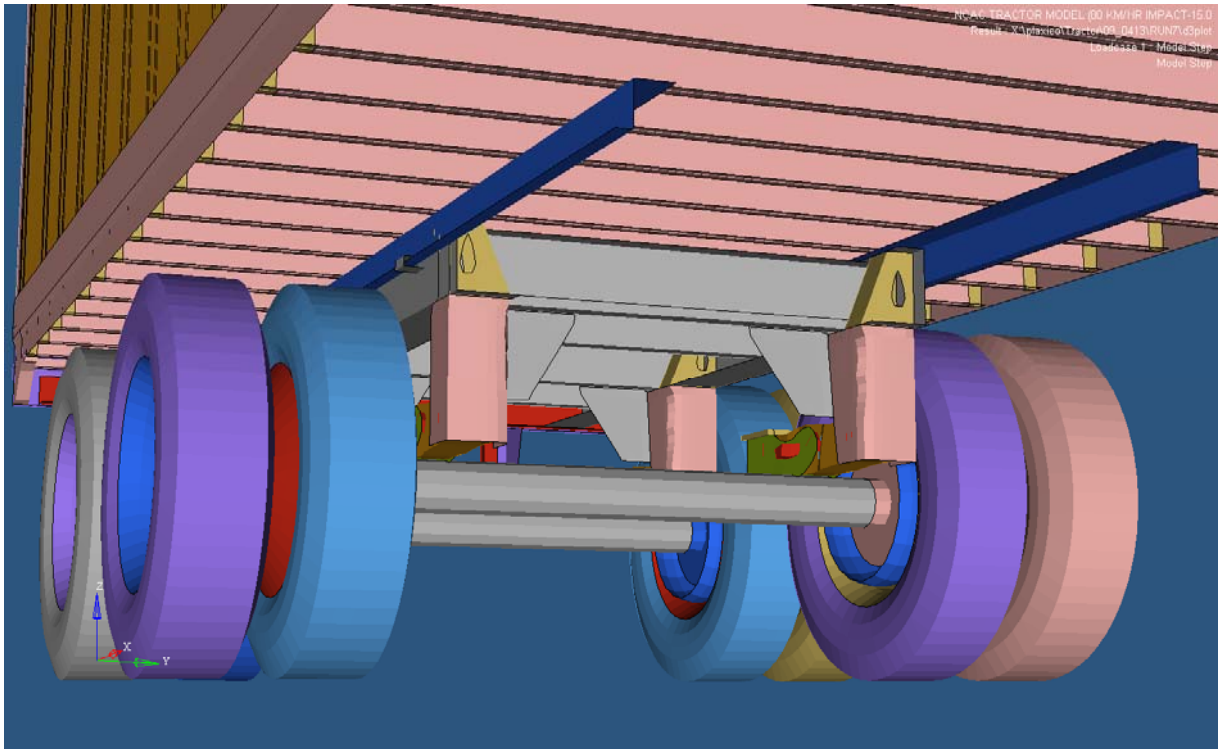
Figure A-17. Illustration. Front view of trailer FE model frame and bogie

Passive Steering Compliance

The response of the tractor during a redirective impact is dependent to a great extent upon the response of all the various components and kinematics of the front suspension system. One of the critical elements in this system is the compliance or stiffness with which the front wheels tend to resist an externally-forced steer. This compliance is dependent upon the overall kinematics and stiffness of the steering linkage mechanism. This compliance must be measured experimentally and input as a discrete spring/damper in the FE model. This measurement has not been done for the current version of the tractor FE model. There is a discrete spring/damper in place for this, but the values of stiffness and damping are "placeholders".

Front Suspension U-Bolt Connections, Contacts and Failure

The main connection that holds the leaf springs together and the leaf spring assembly to the main frame rail is two large "U-Bolts" on the left and on the right front suspensions. These U-Bolts are tightened down during the first 0.001 second of the simulation by thermal contraction. This is accomplished using the *LOAD_THERMAL_VARIABLE and *MAT_ELASTIC_PLASTIC_THERMAL options in LS-Dyna. As shown in Figure A-18 the thermal expansion coefficient for the bolt is set to 1.0, the delta-temperature is set to 1.0, and that

delta-T is scaled by the load curve to increase from 0.0 to -0.4 over 0.001 seconds and hold steady for the entire simulation. This effectively induces a (tensile) strain of 40% in one element in each of the U-Bolts – shortening the bolt and tightening the connection. This particular value of -0.4 will generate an initial tensile force in each bolt, but the actual magnitude of the tensile force is highly dependent upon the initial geometry and orientations of the connected parts.

Some more detailed explanation of the contact between the U-Bolts and the surrounding structure needs to be made. The U-Bolts are represented with beam elements, so the *CONTACT_GENERAL contact option is used. That contact option works well when beam elements need to be in contact with other parts.

The U-Bolt beam elements also have to have geometrically accurate "shell edge" contact with the sides of the leaf springs. LS-Dyna by default adds "thickness" to the edge of shell elements that are involved in contact to eliminate gapping and consequent node-snagging of internal element edges when there is significant bending in a shell structure. To accurately model the geometry of a shell structure, this added thickness at the edge of an element needs to be "turned off" at the free edge of a shell. The LS-Dyna User's Manual states that this added thickness can be turned off at shell free edges by flagging the SHLEDG variable on the *CONTROL_CONTACT card. It turns out that this flag does not work in the recent versions of LS-Dyna 971. Figure A-19 shows the effect that this has on beam/shell edge contact interfaces when initial penetrations are corrected at the start of a simulation. The workaround that is currently used to avoid this in the tractor FE model is to add a set of small-diameter coincident beam elements to the U-Bolt beam elements and make these small-diameter coincident elements be the elements in contact with the leaf spring shell elements rather than the true-diameter beam elements representing the U-bolts.

```
*DEFINE_CURVE
$#     lcid        sidr         sfa         sfo        offa        offo      dattyp
    2200007           0    1.000000    1.000000
$#                     a1                      o1
               0.000                   0.000
           0.0010000              -0.4000000
           5.0000000              -0.4000000


*MAT_ELASTIC_PLASTIC_THERMAL
$#      mid          ro
    2200037 7.8900E-9
$#       t1          t2          t3          t4          t5          t6          t7          t8
        0.000 2000.0000
$#       e1          e2          e3          e4          e5          e6          e7          e8
    2.0000E+5 2.0000E+5
$#      pr1         pr2         pr3         pr4         pr5         pr6         pr7         pr8
     0.300000    0.300000
$#   alpha1      alpha2      alpha3      alpha4      alpha5      alpha6      alpha7      alpha8
     1.000000    1.000000
$#    sigy1       sigy2       sigy3       sigy4       sigy5       sigy6       sigy7       sigy8
   896.00000   896.00000
$#    etan1       etan2       etan3       etan4       etan5       etan6       etan7       etan8
   1380.0000   1380.0000
```

Figure A-18. Illustration. Input for bolt-tightening in LS-Dyna
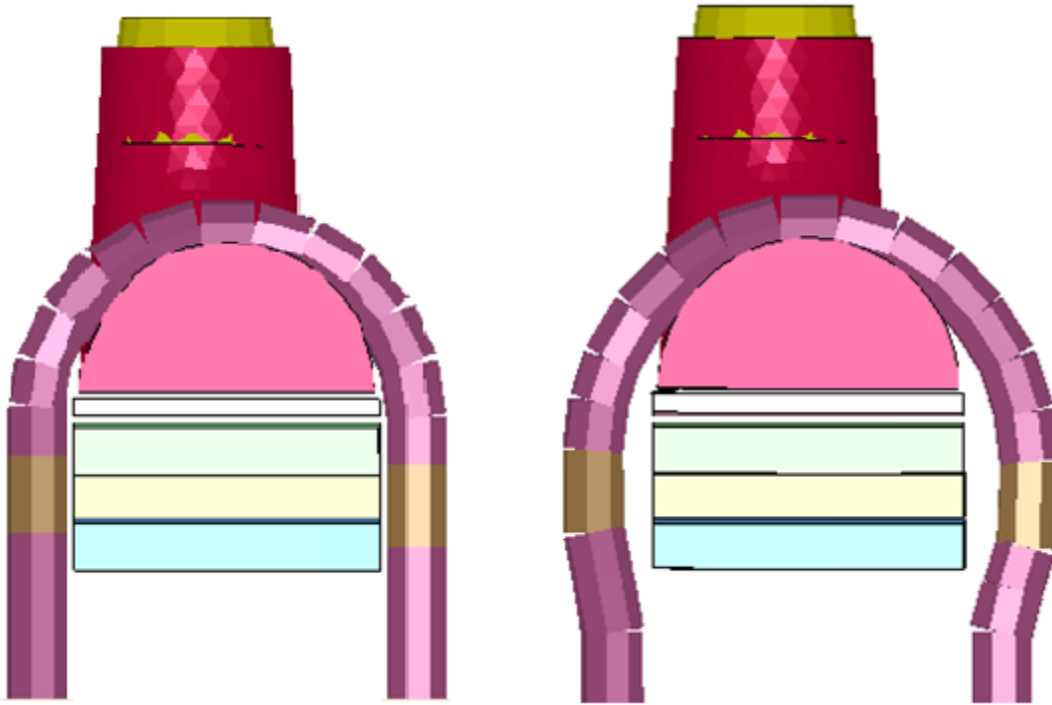
Figure A-19. Illustration. Effect of initial penetrations correction on beam-to-shell-edge contact shown with element dimension display turned on

Use of ADAP Scripts

A set of model modification scripts; Automated Dimensional Adjustment Program (ADAP) was developed that can be used to modify the tractor FE model wheelbase and cab style and the length of the semitrailer FE model to represent more closely the actual tractor-semitrailer models used in crash tests.

The operations executed using these scripts perform a sequence of basic model modifications through stand-alone programs. Each modification step results in a syntactically valid LS-DYNA input file, which allows for easier procedure development and debugging.

Example of Tractor Model Modification Steps

Several basic operations were developed for LS-DYNA model modifications:

1. Elimination of connections of a (list of) part(s) with other parts in the structure
2. Removal of a (list of) part(s)
3. Cutting of a segment from a (list of) part(s)
4. Scaling of the geometry of a (list of) part(s)
5. Rotation of the geometry a (list of) part(s)
6. Translation of a (list of) part(s)
7. Merging of a (list of) part(s)
8. Joining of parts.

All of the above operations can be applied to the specified part region only. These basic operations are combined to yield the desired geometry through a sequence of steps.

Tires and Tire Pressures

The tires of the tractor and the semitrailer are very simplified compared to real tires. The tires are modeled as a homogeneous isotropic elastic material with no beads, plies, cord or belt with a constant thickness of 10 mm. There is no provision for tire failure, de-beading or blowout – that is commonly observed in actual truck crashes.

The air pressure in the tires in the tractor and the semitrailer is simulated using the *AIRBAG_SIMPLE_PRESSURE_VOLUME option. This option allows simple, direct input for pressure inside a volume. The tire pressure set for all tires is 0.69 MPa (100 psi).

Time Step

The target minimum time-step specified on the *CONTROL_TIMESTEP card was set to -1.400 microseconds. This minimum time step was specified with the contingency that mass scaling would be used to maintain it. During a recent simulation, there were only about 40 elements that required a smaller time step. Of these 40 elements, the smallest required time step that LS-Dyna calculated was about 1.19 microseconds. With the mass scaling option invoked, the total mass added to the entire model in this simulation was 8.2 kilograms. The element length that corresponds to the specified 1.4 microsecond time step for steel and aluminum is about 7 to 10 mm. The target element size for structural elements is 25 to 100 mm (1.0 to 4.0 inches). To model the geometry everywhere with reasonable accuracy, the actual element sizes in the model ranged from about 8 mm to about 120 mm.

Computer CPU, Run Time, and Storage

The full tractor-semitrailer FE model with a typical barrier takes roughly 1 day per 1.0 second of simulation time using 8-cpu's in a Linux cluster. A 1.5 second simulation uses 10 – 12 GB disk storage with typical output requests.

The details of the (Linux-based) computer system used are:

- 10-Node Dual-Core (20 cpu) Beowulf Cluster

- Red Hat Enterprise Linux 4 OS

- 64-bit Dual-Core Intel Xeon

- 3.0Ghz Processor

- 4Gb of memory

- Infiniband 4X DDR Network (20Gb)

Figure A-20 shows a printout of a 3-second simulation that was run on 12-cpu's.

```
Problem time        =    3.0000E+00
Problem cycle       =    2083334
Total CPU time      =    141991 seconds (  39 hours 26 minutes 31 seconds)
CPU time per zone cycle  =        296 nanoseconds
Clock time per zone cycle=        294 nanoseconds

Parallel execution with      12 threads
NLQ used/max                 96/    96

 C P U   T i m i n g   i n f o r m a t i o n

                        Processor   Hostname                      CPU(seconds)
       -----------------------------------------------------------------------
                        #    0     m4.EDMS-MEGALODON.battelle.org 1.4199E+05
                        #    1     m4.EDMS-MEGALODON.battelle.org 1.4208E+05
                        #    2     m2.EDMS-MEGALODON.battelle.org 1.4205E+05
                        #    3     m2.EDMS-MEGALODON.battelle.org 1.4203E+05
                        #    4     m5.EDMS-MEGALODON.battelle.org 1.4202E+05
                        #    5     m5.EDMS-MEGALODON.battelle.org 1.4201E+05
                        #    6     m3.EDMS-MEGALODON.battelle.org 1.4215E+05
                        #    7     m3.EDMS-MEGALODON.battelle.org 1.4207E+05
                        #    8     m8.EDMS-MEGALODON.battelle.org 1.4219E+05
                        #    9     m8.EDMS-MEGALODON.battelle.org 1.4225E+05
                        #   10     m10.EDMS-MEGALODON.battelle.or 1.4190E+05
                        #   11     m10.EDMS-MEGALODON.battelle.or 1.4210E+05
       -----------------------------------------------------------------------
 T o t a l s                                                      1.7048E+06


Start time    01/09/2008 11:38:34
End time      01/11/2008 03:26:10
Elapsed time  143256 seconds( 39 hours 47 min. 36 sec.) for 2083334 cycles

 N o r m a l    t e r m i n a t i o n
```

Figure A-20. Illustration. Run-time data for 3-second tractor-semitrailer simulation

**Appendix B – Validation/Verification Report for
Test/Run Number: TL5CMB-2**

APPENDIX B

VALIDATION/VERIFICATION REPORT
FOR

A   **Tractor-Semitrailer Model (36000V)**
(Report 350 Vehicle Type)

Striking a   **42-inch tall "rigid" concrete median barrier**
(roadside hardware type and name)

Report Date: **7/20/2010**

Type of Report (check one)
   ☐ Verification (known numerical solution compared to new numerical solution) or
   ☒ Validation (full-scale crash test compared to a numerical solution).

General Information	Known Solution	Analysis Solution
Performing Organization	MwRSF	Battelle/Roadsafe/ORNL
Test/Run Number:	TL5CMB-2	TT_10-0715 _200ms-approach-SP
Vehicle:	1991 White/GMC Tractor 1988 Pines 48-ft Trailer	01aTrac_Day_2010-0520.k 02_SemiTrailer48_10-0521.k
Accelerometer Location:	trailer floor on the inside of the trailer near the tandem axles of the trailer	trailer floor on the inside of the trailer near the tandem axles of the trailer
Impact Conditions		
Vehicle Mass:	36,154 kg	36,200 kg
Speed:	84.9 km/hr	84.9 km/hr
Angle:	15.5 degrees	15.0 degrees

Composite Validation/Verification Score

	List the Report 350/MASH08 or EN1317 Test Number	
Step I	Did all solution verification criteria in Table A-1 pass?	Y
Step II	Do all the time history evaluation scores from Table A-2 result in a satisfactory comparison (i.e., the comparison passes the criterion)? If all the values in Table A-2 did not pass, did the weighted procedure shown in Table A-3 result in an acceptable comparison. If all the criteria in Table A-2 pass, enter "yes." If all the criteria in Table A-2 did not pass but Table A-3 resulted in a passing score, enter "yes."	Y
Step III	All the criteria in Table A-5 passed	Y
	Are the results of Steps I through III all affirmative (i.e., YES)? If all three steps result in a "YES" answer, the comparison can be considered validated or verified. If one of the steps results in a negative response, the result cannot be considered validated or verified.	Y

The analysis solution (check one) ☒ is ☐ is NOT verified/validated against the known solution.

PART I: BASIC INFORMATION

1. What type of roadside hardware is being evaluated (check one)?
   ☒ Longitudinal barrier or transition
   ☐ Terminal or crash cushion
   ☐ Breakaway support or work zone traffic control device
   ☐ Truck-mounted attenuator
   ☐ Other hardware: _____

2. What test guidelines were used to perform the full-scale crash test (check one)?
   ☒ NCHRP Report 350
   ☐ MASH08
   ☐ EN1317
   ☐ Other: _____

3. Indicate the test level and number being evaluated (fill in the blank). ___5-12____

4. Indicate the vehicle type appropriate for the test level and number indicated in item 3 according to the testing guidelines indicated in item 2.

   <u>NCHRP Report 350/MASH08</u>
   ☐ 700C   ☐ 820C   ☐ 1100C
   ☐ 2000P   ☐ 2270P
   ☐ 8000S   ☐ 10000S
   ☒ 36000V
   ☐ 36000T

   <u>EN1317</u>

   ☐ Car (900 kg)   ☐ Car (1300 kg)   ☐ Car (1500 kg)
   ☐ Rigid HGV (10 ton)   ☐ Rigid HGV (16 ton)   ☐ Rigid HGV (30 ton)
   ☐ Bus (13 ton)
   ☐ Articulated HGV (38 ton)

PART II: ANALYSIS SOLUTION VERIFICATION

Table B-1. Analysis Solution Verification Table

Verification Evaluation Criteria	Change (%)	Pass?
Total Energy of the analysis solution (i.e., kinetic, potential, contact, etc.) must not vary more than 10 percent from the beginning of the run to the end of the run. • *Sliding Interface Energy* was the source of the increase in total energy	0.76	**YES**
Hourglass Energy of the analysis solution at the end of the run is less than 5 percent of the total initial energy at the beginning of the run.	1.6	**YES**
Hourglass Energy of the analysis solution at the end of the run is less than *ten percent* of the total *internal energy* at the *end* of the run.	6.4	**YES**
The part/material with the highest amount of **hourglass energy** at the end of the run is less than ten percent of the total internal energy of the part/material at the end of the run.	*Trailer* 5.0 *Barrier* 2.1	**YES**
Mass added to the total model is less than five percent of the total model mass at the beginning of the run.	0.0	**Yes**
The part/material with the most **mass added** had less than 10 percent of its initial mass added.	400	**NO***
The moving parts/materials in the model have less than five percent of **mass added** to the initial moving mass of the model.	0.0	**YES**
There are no **shooting nodes** in the solution?	No	**YES**
There are no solid elements with **negative volumes**?	No	**YES**

* Part 7803 are weld elements used to connect the trailer's outer side panels to the vertical support posts. These connector elements are relatively "rigid" and the mass added is considered insignificant to the overall mass of the parts to which they connect.

The Analysis Solution (check one) ☒ passes ☐ does NOT pass all the criteria in Table B-1

☒ with ☐ without exceptions noted.

PART III: TIME HISTORY EVALUATION TABLE

Table B-2. Roadside Safety Validation Metrics Rating Table – Time History Comparisons
(single channel option)

Evaluation Criteria										
O **Sprague-Geer Metrics** List all the data channels being compared. Calculate the M and P metrics using RSVVP and enter the results. Values less than or equal to 40 are acceptable.								**Time interval** **[0 sec; 1.54 sec]**		
	RSVVP Curve Preprocessing Options									
			Shift		**Drift**		**M**	**P**	**Pass?**	
	Filter Option	**Sync. Option**	**True Curve**	**Test Curve**	**True Curve**	**Test Curve**				
X acceleration	CFC 180	Min. area of Residuals	N	N	N	N	60.6	48.8	N	
Y acceleration	CFC 180	Min. area of Residuals	N	N	N	N	17.3	35.4	Y	
Z acceleration	CFC 180	Min. area of Residuals	N	N	N	N	18.7	46.3	N	
Resultant acceleration	CFC 180	Min. area of Residuals	N	N	N	N	3.3	20	Y	

	Mean Residual	Standard Deviation of Residuals	Pass?
P **ANOVA Metrics** List all the data channels being compared. Calculate the ANOVA metrics using RSVVP and enter the results. Both of the following criteria must be met: • The mean residual error must be less than five percent of the peak acceleration ($\bar{e} \le 0.05 \cdot a_{Peak}$) and • The standard deviation of the residuals must be less than 35 percent of the peak acceleration ($\sigma \le 0.35 \cdot a_{Peak}$)			
X acceleration/Peak	0.02	0.11	Y
Y acceleration/Peak	0.01	0.09	Y
Z acceleration/Peak	0.0	0.13	Y
Resultant Acceleration	0.03	0.08	Y

The Analysis Solution (check one) ☐ passes   ☒ does NOT pass <u>all</u> the criteria in Table B-2.

Table B-3. Roadside Safety Validation Metrics Rating Table – Time History Comparisons
(multi-channel option using Area II method)

Evaluation Criteria (time interval [0 sec; 1.54 sec])					
Channels (Select which was used)					
☒ **X Acceleration**		☒ **Y Acceleration**		☒ **Z Acceleration**	
☐ **Roll rate**		☐ **Pitch rate**		☐ **Yaw rate**	

Multi-Channel Weights -Area (II) Method-	**X Channel** – 0.111 **Y Channel** – 0.697 **Z Channel** – 0.192	

		M	**P**	**Pass?**
O	*Sprague-Geer Metrics* Values less or equal to 40 are acceptable.	22.4	39	**Y**

		Mean Residual	**Standard Deviation of Residuals**	**Pass?**
P	*ANOVA Metrics* Both of the following criteria must be met: • The mean residual error must be less than five percent of the peak acceleration ($\bar{e} \leq 0.05 \cdot a_{Peak}$) • The standard deviation of the residuals must be less than 35 percent of the peak acceleration ($\sigma \leq 0.35 \cdot a_{Peak}$)	0.01	0.10	**Y**

The Analysis Solution (check one) ☒ passes ☐ does NOT pass <u>all</u> the criteria in Table B-3.

PART IV: PHENOMENA IMPORTANCE RANKING TABLE

Table B-4. Evaluation Criteria Test Applicability Table

Evaluation Factors		Evaluation Criteria			Applicable Tests
Structural Adequacy	A	Test article should contain and redirect the vehicle; the vehicle should not penetrate, under-ride, or override the installation although controlled lateral deflection of the test article is acceptable.			10, 11, 12, 20, 21, 22, 35, 36, 37, 38
	B	The test article should readily activate in a predictable manner by breaking away, fracturing or yielding.			60, 61, 70, 71, 80, 81
	C	Acceptable test article performance may be by redirection, controlled penetration or controlled stopping of the vehicle.			30, 31,, 32, 33, 34, 39, 40, 41, 42, 43, 44, 50, 51, 52, 53
Occupant Risk	D	Detached elements, fragments or other debris from the test article should not penetrate or show potential for penetrating the occupant compartment, or present an undue hazard to other traffic, pedestrians or personnel in a work zone.			All
	E	Detached elements, fragments or other debris from the test article, or vehicular damage should not block the driver's vision or otherwise cause the driver to lose control of the vehicle. (Answer Yes or No)			70, 71
	F	The vehicle should remain upright during and after the collision although moderate roll, pitching and yawing are acceptable.			All except those listed in criterion G
	G	It is preferable, although not essential, that the vehicle remain upright during and after collision.			12, 22 (for test level 1 – 30, 31, 32, 33, 34, 35, 36, 37, 38, 39, 40, 41, 42, 43, 44)
	H	Occupant impact velocities should satisfy the following: **Occupant Impact Velocity Limits (ft/s)** <table><tr><td>Component</td><td>Preferred</td><td>Maximum</td></tr><tr><td>Longitudinal and Lateral</td><td>30</td><td>40</td></tr><tr><td>Longitudinal</td><td>10</td><td>15</td></tr></table>			10, 20, 30,31, 32, 33, 34, 36, 40, 41, 42, 43, 50, 51, 52, 53, 80, 81 60, 61, 70, 71
	I	Occupant ridedown accelerations should satisfy the following: **Occupant Ridedown Acceleration Limits (g's)** <table><tr><td>Component</td><td>Preferred</td><td>Maximum</td></tr><tr><td>Longitudinal and Lateral</td><td>15</td><td>20</td></tr></table>			10, 20, 30,31, 32, 33, 34, 36, 40, 41, 42, 43, 50, 51, 52, 53, 60, 61, 70, 71, 80, 81
Vehicle Trajectory	J	The occupant impact velocity in the longitudinal direction should not exceed 40 ft/sec and the occupant ride-down acceleration in the longitudinal direction should not exceed 20 G's.			11,21, 35, 37, 38, 39
	M	The exit angle from the test article preferable should be less than 60 percent of test impact angle, measured at the time of vehicle loss of contact with test device.			10, 11, 12, 20, 21, 22, 35, 36, 37, 38, 39
	N	Vehicle trajectory behind the test article is acceptable.			30, 31, 32, 33, 34, 39, 42, 43, 44, 60, 61, 70, 71, 80, 81

**Table B-5. Structural Adequacy Phenomena for the Tractor-Semitrailer Test Case**

		Evaluation Criteria	Known Result	Analysis Result	Difference Relative/ Absolute	Agree?
Structural Adequacy	A	Test article should contain and redirect the vehicle; the vehicle should not penetrate, under-ride, or override the installation although controlled lateral deflection of the test article is acceptable. (Answer Yes or No)	Yes	Yes		YES
Occupant Risk	D	Detached elements, fragments or other debris from the test article should not penetrate or show potential for penetrating the occupant compartment, or present an undue hazard to other traffic, pedestrians or personnel in a work zone. (Answer Yes or No)	Pass	Pass		N.M.*
	G · G1	It is preferable, although not essential, that the vehicle remain upright during and after collision. (Answer Yes or No)	Pass	Pass		YES
	G2	The relative difference between the maximum roll of the vehicle is less than 20 percent.	42 deg.	40.8 deg.	2.9% 1.2 deg	YES
	G3	The relative difference between the maximum pitch of the vehicle is less than 20 percent.	Not measured			
	G4	The relative difference between the maximum yaw of the vehicle is less than 20 percent.	15.5	15.5	0	YES
Vehicle Trajectory	M · M1	The exit angle from the test article preferable should be less than 60 percent of test impact angle, measured at the time of vehicle loss of contact with test device.	Yes	Yes		YES
	M2	The relative difference in the yaw angle at loss of contact is less than 20 percent.	15.5 deg	15.5 deg	0	YES
	M3	The relative difference in the exit velocity at loss of contact is less than 20 percent.				
	M4	One or more vehicle tires failed or de-beaded during the collision event (Answer Yes or No).	Yes	N/A		NO**
	M5	One or more tires separated from the vehicle (Answer Yes or No).	No	N/A		YES

In this analysis structural adequacy was not of interest. The barrier was modeled as rigid; therefore criterion D could not be assessed.

** Tire failure/de-beading is not currently modeled. Although tire de-beading can affect crash results, its effects would not likely be of significance until later in the event (e.g., post impact trajectory).

The Analysis Solution (check one) ☒ passes ☐ does NOT pass all the criteria in Table B-5 ☒with exceptions as noted ☐ without exceptions.

Plots of the time histories used to evaluate the comparison metrics at _trailer tandem_ accelerometer
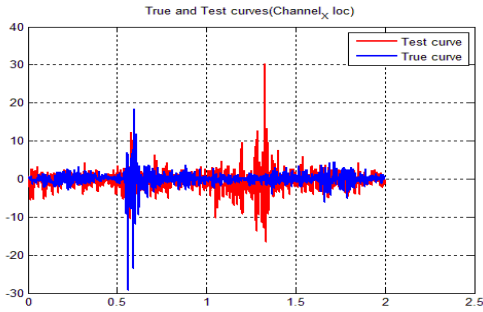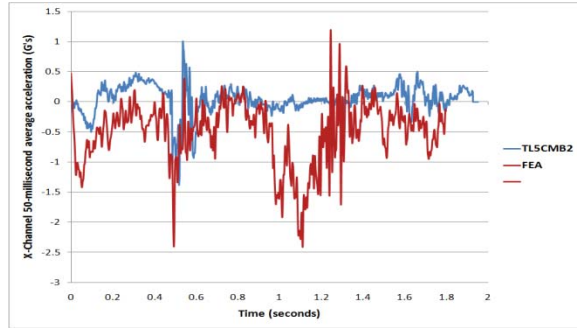
(a) Acceleration (G's)   (b) 50-millisecond moving average acceleration

Figure B-1. X-channel (a) acceleration-time history data used to compute metrics and (b) 50-millisecond moving average x-acceleration -time history
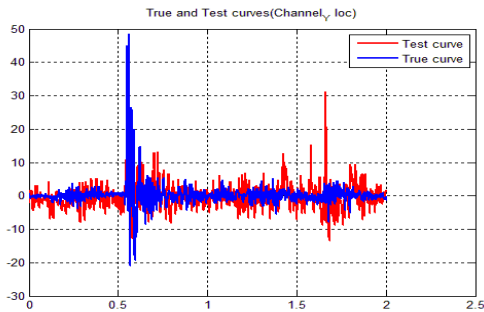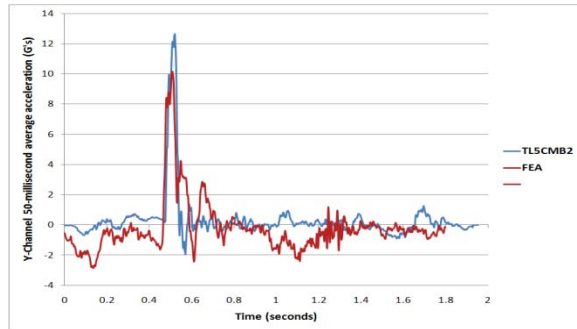
(a) Acceleration (G's)   (b) 50-millisecond moving average acceleration

Figure B-2. Y-channel (a) acceleration-time history data used to compute metrics and (b) 50-millisecond moving average y-acceleration -time history
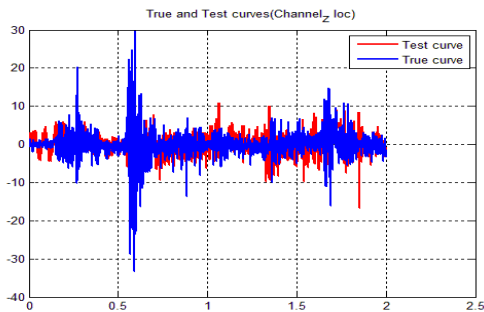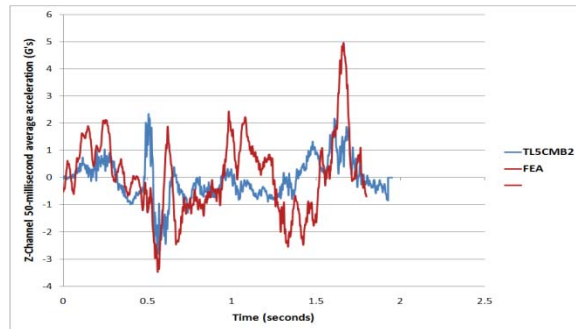
(a) Acceleration (G's)   (b) 50-millisecond moving average acceleration

Figure B-3. Z-channel (a) acceleration-time history data used to compute metrics and (b) 50-millisecond moving average z-acceleration -time history
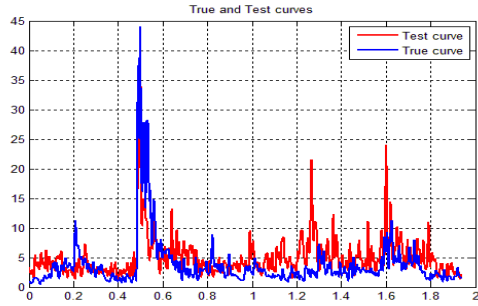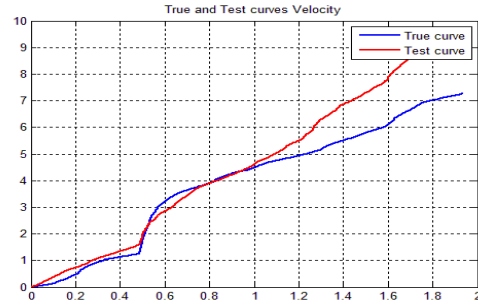
(a) Acceleration (G's)   (b) Integrated Acceleration

Figure B-4. Resultant (a) acceleration-time history data used to compute metrics and (b) Integration of acceleration-time history (resultant change in velocity)

Appendix C – Validation/Verification Report for Test/Run Number: Test7069-13

APPENDIX C

VALIDATION/VERIFICATION REPORT
FOR

A _____Tractor-Semitrailer Model (36000V)_____
(Report 350 Vehicle Type)

Striking a _____42-inch tall concrete parapet_____ _
(roadside hardware type and name)

Report Date: _____7/21/2010_____

Type of Report (check one)
    ☐ Verification (known numerical solution compared to new numerical solution) or
    ☒ Validation (full-scale crash test compared to a numerical solution).

General Information	Known Solution	Analysis Solution
Performing Organization	TTI	Battelle/Roadsafe/ORNL
Test/Run Number:	Test7069-13	TT_7069-13_10-0715-SP
Vehicle:	1991 White/GMC Tractor 1988 Pines 48-ft Trailer	01a_Trac_Day_10-0519_TTI.k 2a_SemiTrailer45_10-0621_TTI7069-13 Gravity initialized in model using dynain file
Accelerometer Locations:	1) Tractor cabin 2) Trailer front near kingpin 3) Trailer rear near tandem	1) Tractor cabin 2) Trailer front near kingpin 3) Trailer rear near tandem
Impact Conditions		
Vehicle Mass:	22,702 kg	23,097 kg
Speed:	82.7 km/hr	82.7 km/hr
Angle:	16.2 degrees	16.2 degrees

Composite Validation/Verification Score

	List the Report 350/MASH08 or EN1317 Test Number	
Step I	Did all solution verification criteria in Table B-1 pass?	Y
Step II	Do all the time history evaluation scores from Tables B-2, B-4 and B-6 result in a satisfactory comparison (i.e., the comparison passes the criterion)? If all the values in those Tables did not pass, did the weighted procedure shown in Tables B-3, B-5 and B-7 result in an acceptable comparison. If all the criteria in Tables B-2, B-4 and B-6 pass, enter "yes." If Tables B-3, B-5 and B-7 resulted in a passing score, enter "yes."	N
Step III	All the criteria in Table B-9 passed	N
	Are the results of Steps I through III all affirmative (i.e., YES)? If all three steps result in a "YES" answer, the comparison can be considered validated or verified. If one of the steps results in a negative response, the result cannot be considered validated or verified.	N

The analysis solution (check one) ☐ is ☒ is NOT verified/validated against the known solution.

PART I: BASIC INFORMATION

1. What type of roadside hardware is being evaluated (check one)?
   ☒ Longitudinal barrier or transition
   ☐ Terminal or crash cushion
   ☐ Breakaway support or work zone traffic control device
   ☐ Truck-mounted attenuator
   ☐ Other hardware: _____

2. What test guidelines were used to perform the full-scale crash test (check one)?
   ☒ NCHRP Report 350
   ☐ MASH08
   ☐ EN1317
   ☐ Other: _____

3. Indicate the test level and number being evaluated (fill in the blank). ___5-12____

4. Indicate the vehicle type appropriate for the test level and number indicated in item 3 according to the testing guidelines indicated in item 2.

   <u>NCHRP Report 350/MASH08</u>
   ☐ 700C   ☐ 820C   ☐ 1100C
   ☐ 2000P   ☐ 2270P
   ☐ 8000S   ☐ 10000S
   ☒ 36000V
   ☐ 36000T

   <u>EN1317</u>

   ☐ Car (900 kg)   ☐ Car (1300 kg)   ☐ Car (1500 kg)
   ☐ Rigid HGV (10 ton)   ☐ Rigid HGV (16 ton)   ☐ Rigid HGV (30 ton)
   ☐ Bus (13 ton)
   ☐ Articulated HGV (38 ton)

PART II: ANALYSIS SOLUTION VERIFICATION

Table C-1. Analysis Solution Verification Table

Verification Evaluation Criteria	Change (%)	Pass?
Total Energy of the analysis solution (i.e., kinetic, potential, contact, etc.) must not vary more than 10 percent from the beginning of the run to the end of the run. • **Sliding Interface Energy** was the source of the increase in total energy	0.77	**YES**
Hourglass Energy of the analysis solution at the end of the run is less than 5 percent of the total initial energy at the beginning of the run.	0.0	**YES**
Hourglass Energy of the analysis solution at the end of the run is less than *ten percent* of the total *internal energy* at the *end* of the run.	1.3	**YES**
The part/material with the highest amount of **hourglass energy** at the end of the run is less than ten percent of the total internal energy of the part/material at the end of the run.	*Tractor* 2.0 *Barrier* 1.2	**YES**
Mass added to the total model is less than five percent of the total model mass at the beginning of the run.	0.0	**Yes**
The part/material with the most **mass added** had less than 10 percent of its initial mass added.	61 (37 lb)	**NO***
The moving parts/materials in the model have less than five percent of **mass added** to the initial moving mass of the model.	0.0	**YES**
There are no **shooting nodes** in the solution?	No	**YES**
There are no solid elements with **negative volumes**?	No	**YES**

* Part 7803 are weld elements used to connect the trailer's outer side panels to the vertical support posts. These connector elements are relatively "rigid" and the mass added is considered insignificant to the overall mass of the parts to which they connect.

The Analysis Solution (check one) ☒ passes ☐ does NOT pass all the criteria in Table C-1.

☒ with ☐ without exceptions noted.

PART III: TIME HISTORY EVALUATION TABLE

Table C-2. Roadside Safety Validation Metrics Rating Table – Time History Comparisons (single channel option) – Tractor Cabin Accelerometer

<table>
<tr><th colspan="8">Evaluation Criteria</th><th></th></tr>
<tr><td rowspan="2">O</td><td colspan="7"><i>Sprague-Geer Metrics</i>
List all the data channels being compared. Calculate the M and P metrics using RSVVP and enter the results. Values less than or equal to 40 are acceptable.</td><td>Time interval
[0 sec; 1.00 sec]</td></tr>
<tr><td colspan="5">RSVVP Curve Preprocessing Options</td><td></td><td></td><td></td></tr>
<tr><td></td><td></td><td></td><td colspan="2">Shift</td><td colspan="2">Drift</td><td>M</td><td>P</td><td>Pass?</td></tr>
<tr><td></td><td>Filter Option</td><td>Sync. Option</td><td>True Curve</td><td>Test Curve</td><td>True Curve</td><td>Test Curve</td><td></td><td></td><td></td></tr>
<tr><td>X acceleration</td><td>CFC 180</td><td>Min. area of Residuals</td><td>N</td><td>N</td><td>N</td><td>N</td><td>135.2</td><td>47</td><td>N</td></tr>
<tr><td>Y acceleration</td><td>CFC 180</td><td>Min. area of Residuals</td><td>N</td><td>N</td><td>N</td><td>N</td><td>176.7</td><td>41.2</td><td>N</td></tr>
<tr><td>Z acceleration</td><td>CFC 180</td><td>Min. area of Residuals</td><td>N</td><td>N</td><td>N</td><td>N</td><td>344.4</td><td>48.8</td><td>N</td></tr>
<tr><td>P</td><td colspan="7"><i>ANOVA Metrics</i>
List all the data channels being compared. Calculate the ANOVA metrics using RSVVP and enter the results. Both of the following criteria must be met:
• The mean residual error must be less than five percent of the peak acceleration ($\bar{e} \leq 0.05 \cdot a_{Peak}$) and
• The standard deviation of the residuals must be less than 35 percent of the peak acceleration ($\sigma \leq 0.35 \cdot a_{Peak}$)</td><td>Mean Residual</td><td>Standard Deviation of Residuals</td><td>Pass?</td></tr>
<tr><td></td><td colspan="7">X acceleration/Peak</td><td>0.0</td><td>0.34</td><td>Y</td></tr>
<tr><td></td><td colspan="7">Y acceleration/Peak</td><td>0.01</td><td>0.38</td><td>N</td></tr>
<tr><td></td><td colspan="7">Z acceleration/Peak</td><td>0.05</td><td>0.93</td><td>N</td></tr>
</table>

The Analysis Solution (check one) ☐ passes   ☒ does NOT pass <u>all</u> the criteria in Table C-2.

**Table C-3. Roadside Safety Validation Metrics Rating Table – Time History Comparisons
(multi-channel option using Area II method) – Tractor Cabin Accelerometer**

Evaluation Criteria (time interval [0 sec; 1.00 sec])		
Channels (Select which was used)		
☒ **X Acceleration**	☒ **Y Acceleration**	☒ **Z Acceleration**
☐ **Roll rate**	☐ **Pitch rate**	☐ **Yaw rate**

Multi-Channel Weights -Area (II) Method-	**X Channel –** 0.423 **Y Channel –** 0.267 **Z Channel –** 0.310	

		M	**P**	**Pass?**
O	*Sprague-Geer Metrics* Values less or equal to 40 are acceptable.	211.1	46	N

		Mean Residual	**Standard Deviation of Residuals**	**Pass?**
P	*ANOVA Metrics* Both of the following criteria must be met: • The mean residual error must be less than five percent of the peak acceleration ($\overline{e} \leq 0.05 \cdot a_{Peak}$) • The standard deviation of the residuals must be less than 35 percent of the peak acceleration ($\sigma \leq 0.35 \cdot a_{Peak}$)			
		.01	0.53	N

The Analysis Solution (check one) ☐ passes ☒ does NOT pass <u>all</u> the criteria in Table C-3.

Table C-4. Roadside Safety Validation Metrics Rating Table – Time History Comparisons (single channel option) – Trailer Kingpin Accelerometer

Evaluation Criteria									
O ***Sprague-Geer Metrics*** List all the data channels being compared. Calculate the M and P metrics using RSVVP and enter the results. Values less than or equal to 40 are acceptable.								**Time interval [0 sec; 1.00 sec]**	
	RSVVP Curve Preprocessing Options						**M**	**P**	**Pass?**
	Filter Option	**Sync. Option**	**Shift**		**Drift**				
			True Curve	**Test Curve**	**True Curve**	**Test Curve**			
X acceleration	CFC 180	Min. area of Residuals	N	N	N	N	130.5	48.6	N
Y acceleration	CFC 180	Min. area of Residuals	N	N	N	N	116.8	40.1	N
P *ANOVA Metrics* List all the data channels being compared. Calculate the ANOVA metrics using RSVVP and enter the results. Both of the following criteria must be met: • The mean residual error must be less than five percent of the peak acceleration ($\bar{e} \leq 0.05 \cdot a_{Peak}$) and • The standard deviation of the residuals must be less than 35 percent of the peak acceleration ($\sigma \leq 0.35 \cdot a_{Peak}$)							**Mean Residual**	**Standard Deviation of Residuals**	**Pass?**
X acceleration/Peak							.07	0.33	Y
Y acceleration/Peak							0.03	0.47	N

The Analysis Solution (check one) ☐ passes ☒ does NOT pass <u>all</u> the criteria in Table C-4.

Table C-5. Roadside Safety Validation Metrics Rating Table – Time History Comparisons (multi-channel option using Area II method) – Trailer Kingpin Accelerometer

Evaluation Criteria (time interval [0 sec; 1.00 sec])		
Channels (Select which was used)		
☒ X Acceleration	☒ Y Acceleration	☐ Z Acceleration
☐ Roll rate	☐ Pitch rate	☐ Yaw rate

Multi-Channel Weights -Area (II) Method-	**X Channel –** 0.298 **Y Channel –** 0.702	

		M	P	Pass?
O	*Sprague-Geer Metrics* Values less or equal to 40 are acceptable.	120.6	42.5	N

		Mean Residual	Standard Deviation of Residuals	
P	*ANOVA Metrics* Both of the following criteria must be met: • The mean residual error must be less than five percent of the peak acceleration ($\overline{e} \le 0.05 \cdot a_{Peak}$) • The standard deviation of the residuals must be less than 35 percent of the peak acceleration ($\sigma \le 0.35 \cdot a_{Peak}$)			Pass?
		.00	0.43	N

The Analysis Solution (check one) ☐ passes ☒ does NOT pass <u>all</u> the criteria in Table C-5.

Table C-6. Roadside Safety Validation Metrics Rating Table – Time History Comparisons (single channel option) – Trailer Rear Tandem Accelerometer

Evaluation Criteria									
O **_Sprague-Geer Metrics_** List all the data channels being compared. Calculate the M and P metrics using RSVVP and enter the results. Values less than or equal to 40 are acceptable.							**Time interval [0 sec; 1.00 sec]**		
	RSVVP Curve Preprocessing Options								
	Filter Option	**Sync. Option**	**Shift**		**Drift**		**M**	**P**	**Pass?**
			True Curve	**Test Curve**	**True Curve**	**Test Curve**			
X acceleration	CFC 180	Min. area of Residuals	N	N	N	N	200.8	45.2	N
Y acceleration	CFC 180	Min. area of Residuals	N	N	N	N	37.4	33	Y

P _ANOVA Metrics_
List all the data channels being compared. Calculate the ANOVA metrics using RSVVP and enter the results. Both of the following criteria must be met:
   • The mean residual error must be less than five percent of the peak acceleration ($\bar{e} \leq 0.05 \cdot a_{Peak}$) and
   • The standard deviation of the residuals must be less than 35 percent of the peak acceleration ($\sigma \leq 0.35 \cdot a_{Peak}$)
							Mean Residual	**Standard Deviation of Residuals**	**Pass?**

X acceleration/Peak							.09	0.44	Y
Y acceleration/Peak							0.00	0.08	Y

The Analysis Solution (check one) ☐ passes ☒ does NOT pass <u>all</u> the criteria in Table C-6.

Table C-7. Roadside Safety Validation Metrics Rating Table – Time History Comparisons (multi-channel option using Area II method) – Trailer Rear Tandem Accelerometer

Evaluation Criteria (time interval [0 sec; 1.00 sec])		
Channels (Select which was used)		
☒ X Acceleration	☒ Y Acceleration	☐ Z Acceleration
☐ Roll rate	☐ Pitch rate	☐ Yaw rate

Multi-Channel Weights -Area (II) Method-	X Channel – 0.298 Y Channel – 0.702	

		M	P	Pass?
O	**Sprague-Geer Metrics** Values less or equal to 40 are acceptable.	86.2	36.7	N

		Mean Residual	Standard Deviation of Residuals	Pass?
P	**ANOVA Metrics** Both of the following criteria must be met: • The mean residual error must be less than five percent of the peak acceleration ($\overline{e} \le 0.05 \cdot a_{Peak}$) • The standard deviation of the residuals must be less than 35 percent of the peak acceleration ($\sigma \le 0.35 \cdot a_{Peak}$)	.00	0.19	Y

The Analysis Solution (check one) ☐ passes ☒ does NOT pass <u>all</u> the criteria in Table C-7.

PART IV: PHENOMENA IMPORTANCE RANKING TABLE

Table C-8. Evaluation Criteria Test Applicability Table

Evaluation Factors		Evaluation Criteria			Applicable Tests
Structural Adequacy	A	Test article should contain and redirect the vehicle; the vehicle should not penetrate, under-ride, or override the installation although controlled lateral deflection of the test article is acceptable.			10, 11, 12, 20, 21, 22, 35, 36, 37, 38
	B	The test article should readily activate in a predictable manner by breaking away, fracturing or yielding.			60, 61, 70, 71, 80, 81
	C	Acceptable test article performance may be by redirection, controlled penetration or controlled stopping of the vehicle.			30, 31,, 32, 33, 34, 39, 40, 41, 42, 43, 44, 50, 51, 52, 53
Occupant Risk	D	Detached elements, fragments or other debris from the test article should not penetrate or show potential for penetrating the occupant compartment, or present an undue hazard to other traffic, pedestrians or personnel in a work zone.			All
	E	Detached elements, fragments or other debris from the test article, or vehicular damage should not block the driver's vision or otherwise cause the driver to lose control of the vehicle. (Answer Yes or No)			70, 71
	F	The vehicle should remain upright during and after the collision although moderate roll, pitching and yawing are acceptable.			All except those listed in criterion G
	G	It is preferable, although not essential, that the vehicle remain upright during and after collision.			12, 22 (for test level 1 – 30, 31, 32, 33, 34, 35, 36, 37, 38, 39, 40, 41, 42, 43, 44)
	H	Occupant impact velocities should satisfy the following: Occupant Impact Velocity Limits (ft/s)			10, 20, 30,31, 32, 33, 34, 36, 40, 41, 42, 43, 50, 51, 52, 53, 80, 81

Occupant impact velocities should satisfy the following:

Occupant Impact Velocity Limits (ft/s)		
Component	Preferred	Maximum
Longitudinal and Lateral	30	40
Longitudinal	10	15

					60, 61, 70, 71
	I	Occupant ridedown accelerations should satisfy the following:			10, 20, 30,31, 32, 33, 34, 36, 40, 41, 42, 43, 50, 51, 52, 53, 60, 61, 70, 71, 80, 81

Occupant Ridedown Acceleration Limits (g's)		
Component	Preferred	Maximum
Longitudinal and Lateral	15	20

Vehicle Trajectory	J	The occupant impact velocity in the longitudinal direction should not exceed 40 ft/sec and the occupant ride-down acceleration in the longitudinal direction should not exceed 20 G's.			11,21, 35, 37, 38, 39
	M	The exit angle from the test article preferable should be less than 60 percent of test impact angle, measured at the time of vehicle loss of contact with test device.			10, 11, 12, 20, 21, 22, 35, 36, 37, 38, 39
	N	Vehicle trajectory behind the test article is acceptable.			30, 31, 32, 33, 34, 39, 42, 43, 44, 60, 61, 70, 71, 80, 81

Table C-9. Structural Adequacy Phenomena for the Tractor-Semitrailer Test Case

		Evaluation Criteria	Known Result	Analysis Result	Difference Relative/ Absolute	Agree?
Structural Adequacy	A	Test article should contain and redirect the vehicle; the vehicle should not penetrate, under-ride, or override the installation although controlled lateral deflection of the test article is acceptable. (Answer Yes or No)	Yes	Yes	✕	YES
Occupant Risk	D	Detached elements, fragments or other debris from the test article should not penetrate or show potential for penetrating the occupant compartment, or present an undue hazard to other traffic, pedestrians or personnel in a work zone. (Answer Yes or No)	Pass	Pass	✕	N.M.*
	G — G1	It is preferable, although not essential, that the vehicle remain upright during and after collision. (Answer Yes or No)	Fail	Pass	✕	NO
	G2	The relative difference between the maximum roll of the vehicle is less than 20 percent.	Unknown**.			NO***
	G3	The relative difference between the maximum pitch of the vehicle is less than 20 percent.	Unknown**			
	G4	The relative difference between the maximum yaw of the vehicle is less than 20 percent.	16.2	16.2	0	YES
Vehicle Trajectory	M — M1	The exit angle from the test article preferable should be less than 60 percent of test impact angle, measured at the time of vehicle loss of contact with test device.	Yes	Yes	✕	YES
	M2	The relative difference in the yaw angle at loss of contact is less than 20 percent.	16.2 deg	16.2 deg	0	YES
	M3	The relative difference in the exit velocity at loss of contact is less than 20 percent.				
	M4	One or more vehicle tires failed or de-beaded during the collision event (Answer Yes or No).	Unknown	N/A	✕	YES
	M5	One or more tires separated from the vehicle (Answer Yes or No).	No	N/A****	✕	YES

In this analysis structural adequacy was not of interest. The barrier was modeled as rigid; therefore criterion D could not be assessed.

** A set of angular-rate gyros were mounted on the vehicle, but their location was not reported. It is assumed that they were mounted at the tractor fifth wheel location (as is typical), but data was not collected at that location in the analysis

**** From visual comparison of FEA results with test video.*

**** Tire failure/de-beading is not currently modeled. Although tire de-beading can affect crash results, its effects would not likely be of significance until later in the event (e.g., post impact trajectory).

The Analysis Solution (check one) ☐ passes ☒ does NOT pass <u>all</u> the criteria in Table C-9 ☐ with exceptions as noted ☐ without exceptions.

Plots of the time histories used to evaluate the comparison metrics at _tractor cabin_ accelerometer
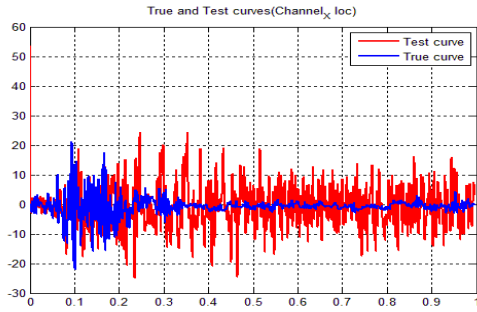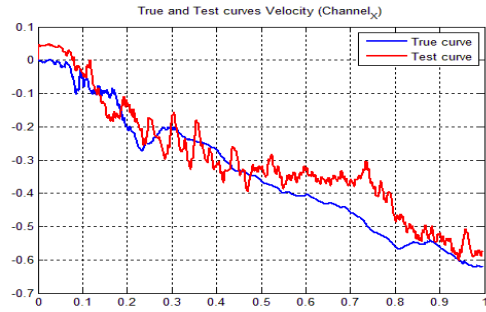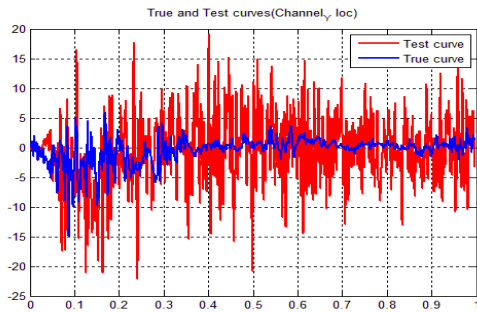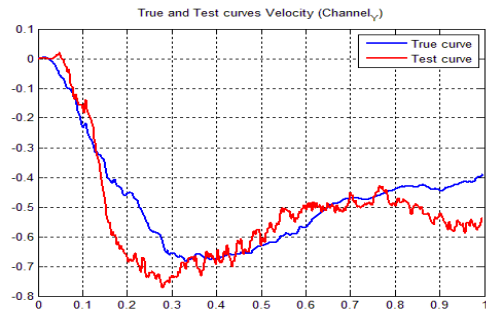

(b) Acceleration (G's)   (b) Acceleration Integrated

Figure C-1. X-channel (a) acceleration-time history data used to compute metrics and (b) x-acceleration -time history data integrated
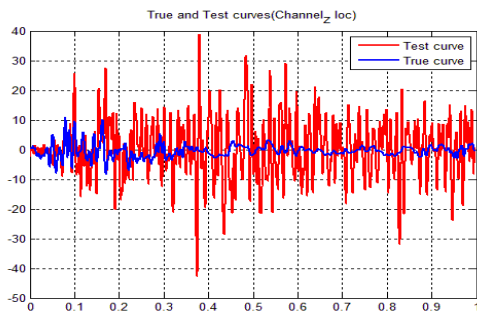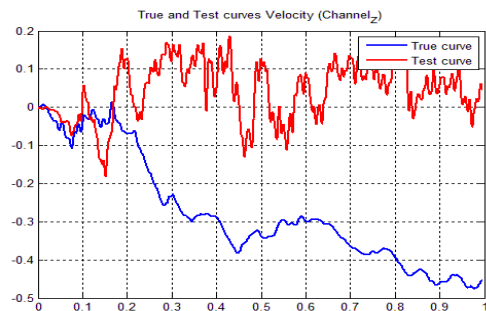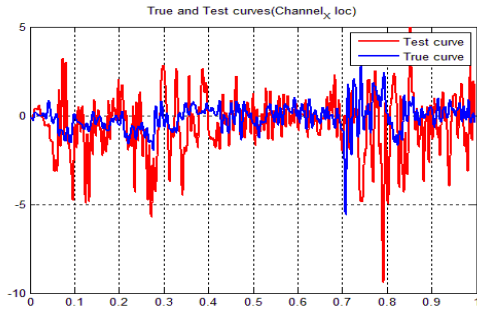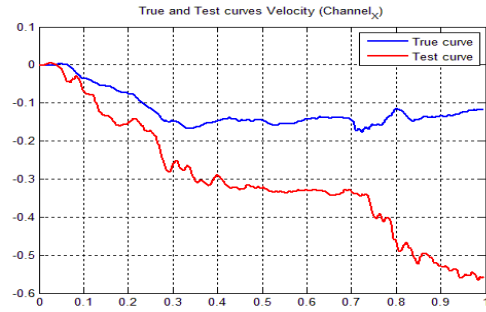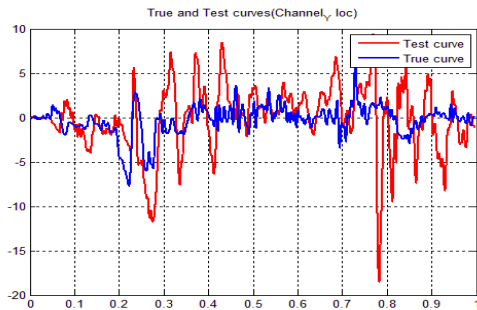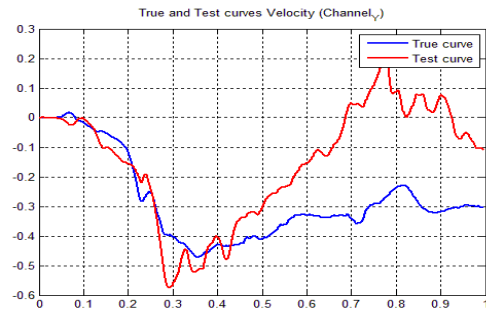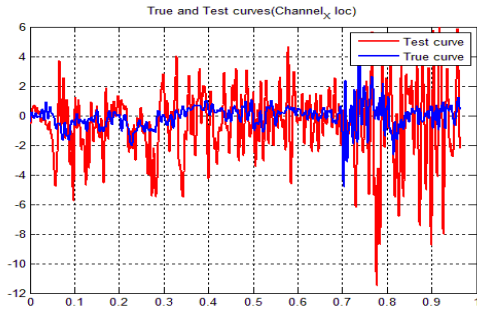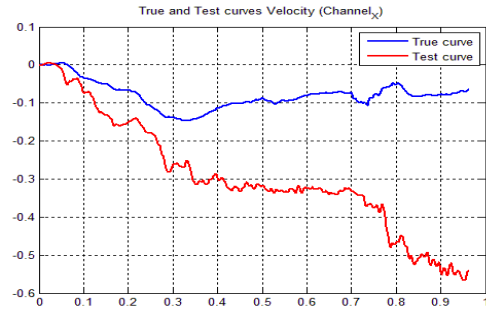

(a) Acceleration (G's)   (b) Acceleration Integrated

Figure C-2. Y-channel (a) acceleration-time history data used to compute metrics and (b) y-acceleration -time history data integrated
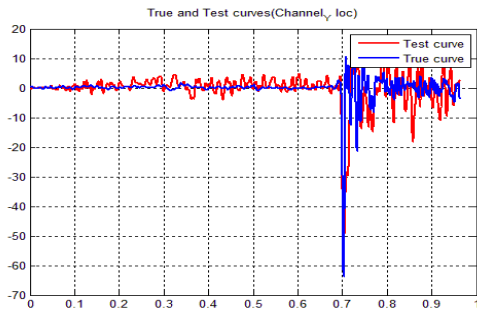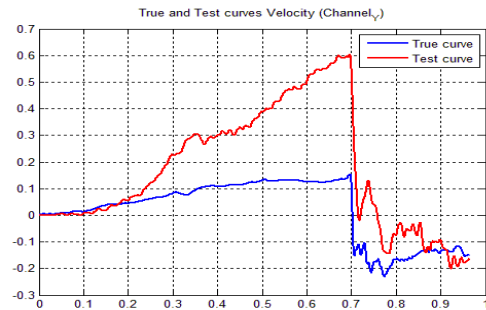
.

(a) Acceleration (G's)   (b) Acceleration Integrated

Figure C-3. Z-channel (a) acceleration-time history data used to compute metrics and (b) z-acceleration -time history data integrated

Plots of the time histories used to evaluate the comparison metrics at _trailer kingpin_ accelerometer

(c) Acceleration (G's)   (b) Acceleration Integrated

Figure C-4. X-channel (a) acceleration-time history data used to compute metrics and (b) x-acceleration -time history data integrated

(b) Acceleration (G's)   (b) Acceleration Integrated

Figure C-5. Y-channel (a) acceleration-time history data used to compute metrics and (b) y-acceleration -time history data integrated

.

Plots of the time histories used to evaluate the comparison metrics at _trailer tandem_ accelerometer

(d) Acceleration (G's)

(b) Acceleration Integrated

Figure C-6. X-channel (a) acceleration-time history data used to compute metrics and (b) x-acceleration -time history data integrated

(c) Acceleration (G's)

(b) Acceleration Integrated

Figure C-7. Y-channel (a) acceleration-time history data used to compute metrics and (b) y-acceleration -time history data integrated

Appendix D – Phenomena Importance Ranking Table (PIRT)

Vehicle PIRT for a 1992 Freightliner FLD120 Tractor

PHENOMENA IMPORTANCE RANKING TABLE FOR A
1992 FREIGHTLINER FLD120 TRACTOR

Developer: NCAC/Battelle/ORNL/University of Tennessee at Knoxville

Date: 8/20/2010

Model: Reduced Element (i.e., bullet model) model of a 1992 Freightliner FLD120 Tractor with integral sleeper-cabin. Wheel-base length measured from center of front axle to the center of the rear tandem assembly is 6.1 m (240 in).

Figure D-1. Photograph / Illustration. Views of FLD 120 Tractor and 48-foot Stoughton semitrailer vehicles and FE corresponding models

NTRCI has funded the research team of Battelle, Oak Ridge National Laboratory (ORNL) and the University of Tennessee at Knoxville (UTK) to conduct a three-phase investigation to enhance and refine an FE model for simulating tractor-trailer crash events involving barriers and roadside safety hardware such as bridge rails and median barriers. This model was originally developed by the National Crash Analysis Center (NCAC) of George Washington University (GWU) and requires refinement and testing before it can be used by the engineering community for infrastructure design.

Table D-1. List of Experiments to be used in the PIRT Development

1. Compression load-displacement test of tractor front leaf-spring.
2. Compression load/unload displacement test of tractor suspension displacement load limiter.
3. Uniaxial sinusoidal displacement test to measure load-velocity time history of the tractor rear shock absorber at various displacement rates.
4. Uniaxial sinusoidal displacement tests to measure load-velocity time history of the tractor front shock absorbers at various displacement rates.
5. Compression/extension tests of the tractor rear "air spring" suspension at various load rates and bag pressures.
6. Failure tests of tractor front suspension u-bolts.
7. Compression/extension tests of the trailer rear "air spring" suspension at various load rates and bag pressures.
8. Uniaxial tension test to measure material stress vs. strain response for characterization/calibration of trailer Kingpin box
9. Uniaxial tension test to measure material stress vs. strain response for characterization/calibration of trailer bogie frame cross member
10. Uniaxial tension test to measure material stress vs. strain response for characterization/calibration of trailer bogie main frame
11. Uniaxial tension test to measure material stress vs. strain response for characterization/calibration of trailer axle tube
12. Uniaxial tension test to measure material stress vs. strain response for characterization/calibration of trailer rear bumper
13. Uniaxial tension test to measure material stress vs. strain response for characterization/calibration of trailer upper rail
14. Uniaxial tension test to measure material stress vs. strain response for characterization/calibration of trailer lower rail
15. Uniaxial tension test to measure material stress vs. strain response for characterization/calibration of trailer pivot support
16. Uniaxial tension test to measure material stress vs. strain response for characterization/calibration of trailer suspension arm
17. Uniaxial tension test to measure material stress vs. strain response for characterization/calibration of trailer bogie slider rails
18. Uniaxial tension test to measure material stress vs. strain response for characterization/calibration of trailer lateral I-beams

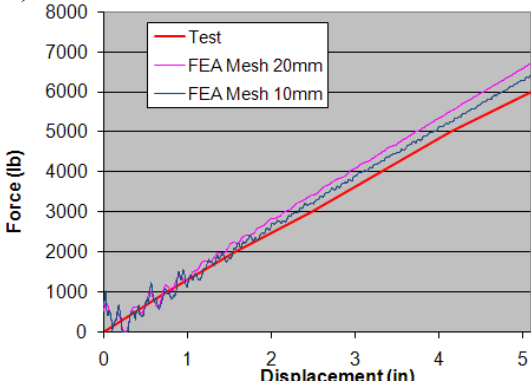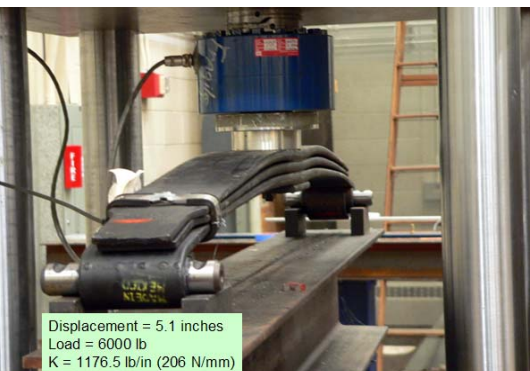**Table D-2. Comparison Metric Evaluation Table. For Phenomena #1**

PHENOMENA #1:	Tractor Front Leaf Suspension		
Sprauge-Geers Metrics List all the data channels to be compared below. Using RSVVP calculate the M and P metrics comparing the experiment and the simulation. Values less than or equal to 20 are acceptable.	**M**	**P**	**Pass?**
• *Force-Displacement History (Element Size 20 mm)* ** Mesh size used in Model*	11.3	0.9	Y
• *Force-Displacement History (Element Size 10 mm)*	5.9	1.1	Y
ANOVA Metrics List all the data channels to compare in the rows below. Use RSVVP to calculate the ANOVA metrics and enter the values below. The following criteria must be met: • The mean residual error must be less than or equal to five percent of the peak acceleration ($\overline{e} \leq 0.05 \cdot a_{Peak}$) • The standard deviation of the residuals must be less than or equal to 25 percent of the peak acceleration ($\sigma \leq 0.25 \cdot a_{Peak}$)	**Mean Residual**	**Standard Deviation of Residuals**	**Pass?**
• *Force-Displacement History (Element Size 20 mm)* ** Mesh size used in Model*	0.06	0.04	N
• *Force-Displacement History (Element Size 10 mm)*	0.03	0.03	Y
General Comparisons	**Test**	**FEA**	**Error**
• Stiffness (lb/in) – Element Size 20 mm ** Mesh size used in Model*	1176	1317	12%
• Stiffness (lb/in) – Element Size 10 mm	1176	1262	7.3%

Front leaf-spring suspension compression test

A leaf spring assembly for a 1992 Freightliner FLD120 tractor was purchased from a local Freightliner dealer. A laboratory test was conducted to measure the force/velocity response of the leaf spring assembly using a MTS uniaxial machine. The FE model of the leaf-spring was modeled with two different mesh densities for comparison: 1) nominal element size =20 mm and 2) nominal element size = 10mm.

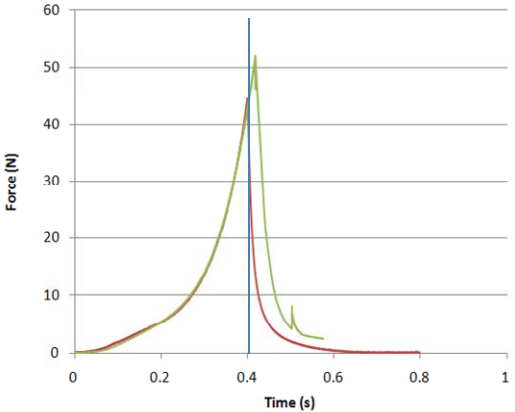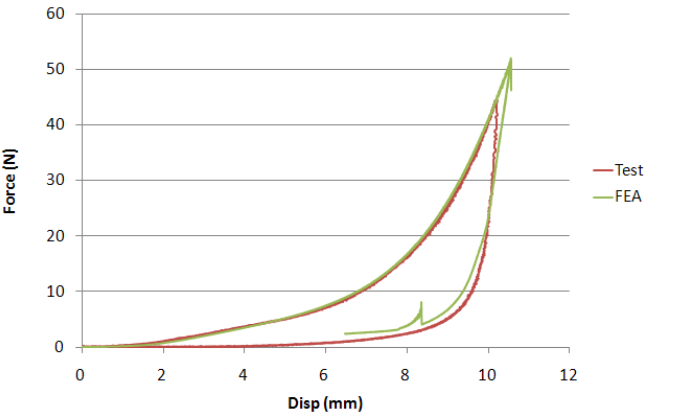**Table D-3. Comparison Metric Evaluation Table for Phenomena #2**

PHENOMENA #2: Tractor Suspension Displacement Limiter			
Sprauge-Geers Metrics List all the data channels to be compared below. Using RSVVP calculate the M and P metrics comparing the experiment and the simulation. Values less than or equal to 20 are acceptable.	**M**	**P**	**Pass?**
• *Uniaxial Force-Time History*	0	0.8	**Y**
ANOVA Metrics List all the data channels to compare in the rows below. Use RSVVP to calculate the ANOVA metrics and enter the values below. The following criteria must be met: • The mean residual error must be less than or equal to five percent of the peak acceleration $(\bar{e} \le 0.05 \cdot a_{Peak})$ • The standard deviation of the residuals must be less than or equal to 25 percent of the peak acceleration ($\sigma \le 0.25 \cdot a_{Peak}$)	**Mean Residual**	**Standard Deviation of Residuals**	**Pass?**
• *Uniaxial Force-Time History*	0	0.01	**Y**

Suspension Displacement Limiter Load/Unload-Displacement Test

The load-deflection response of the rubber tip was measured in the laboratory using displacement control on a uniaxial load machine. The displacement was ramped at a constant velocity from 0 to 0.417 inches in 447 seconds and immediately unloaded at the same rate. *Note: Comparison is made based on the first 0.4 seconds of loading, since the simulation "overshot" the displacement by 1 mm.*

D-4

PHENOMENA #3:	Tractor Rear Shock Absorbers (*Calibration Tests*)

Uniaxial sinusoidal displacement <u>Calibration</u> tests

The shock absorbers (Monroe Gas-Magnum) were tested in a uniaxial loading machine using sinusoidal displacement input with +-0.5 inch maximum displacement. Load-velocity data were collected for loading rates of 0.5, 1, 2, 4, and 8 Hz. The shock absorbers are modeled in the as discrete elements with response characterized using *MAT_DAMPER_NONLINEAR in LS-Dyna. The force-velocity characterization curve for the shock absorber is represented by the bold-red curve in the plot below.
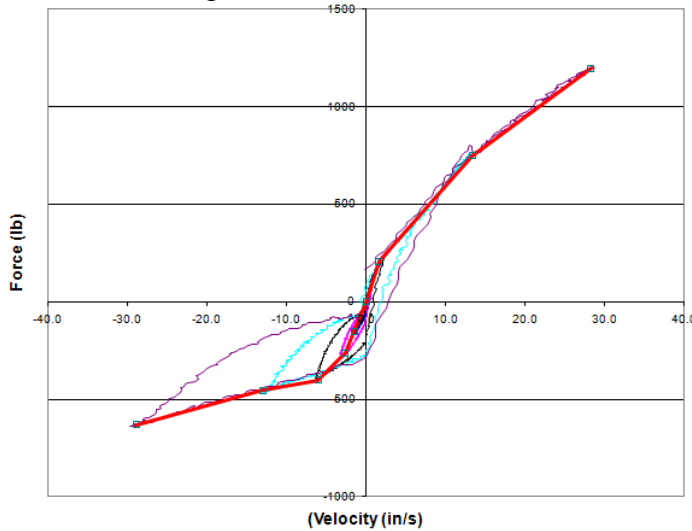
PHENOMENA #4:   Tractor Front Shock Absorbers (*Calibration Tests*)

Uniaxial sinusoidal displacement *Calibration* tests

The shock absorbers (Monroe Gas-Magnum) were tested in a uniaxial loading machine using sinusoidal displacement input with +-0.5 inch maximum displacement. Load-velocity data were collected for loading rates of 0.5, 1, 2, 4, and 8 Hz. The shock absorbers are modeled in the as discrete elements with response characterized using *MAT_DAMPER_NONLINEAR in LS-Dyna. The force-velocity characterization curve for the shock absorber is represented by the bold-red curve in the plot below.
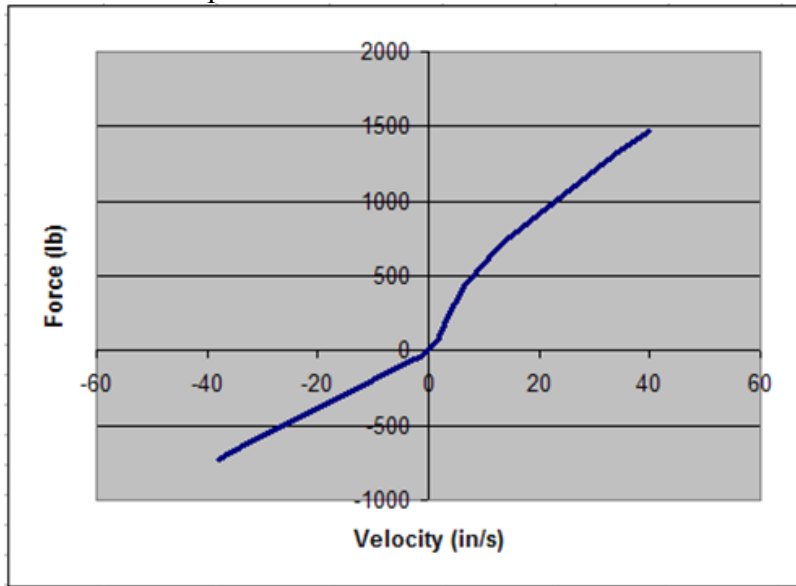
Table D-6. Comparison Metric Evaluation Table for Phenomena #5

PHENOMENA #5: Tractor Rear "Air-Bag" Suspension (20 psig bag pressure, 1.2 in/sec)			
Sprauge-Geers Metrics List all the data channels to be compared below. Using RSVVP calculate the M and P metrics comparing the experiment and the simulation. Values less than or equal to 20 are acceptable.	**M**	**P**	**Pass?**
• *Uniaxial Force-Time History*	**1.1**	**1.6**	**Y**
ANOVA Metrics List all the data channels to compare in the rows below. Use RSVVP to calculate the ANOVA metrics and enter the values below. The following criteria must be met: • The mean residual error must be less than or equal to five percent of the peak acceleration ($\bar{e} \leq 0.05 \cdot a_{Peak}$) • The standard deviation of the residuals must be less than or equal to 25 percent of the peak acceleration ($\sigma \leq 0.25 \cdot a_{Peak}$)	**Mean Residual**	**Standard Deviation of Residuals**	**Pass?**
• *Uniaxial Force-Time History*	**0.01**	**0.02**	**Y**

Tractor "Air-Spring" Suspension: *Compression/extension tests at various load rates and bag pressures*

Firestone AirideTM suspension, Part No. 1T15ZR6. The air spring was modeled using discrete spring and damper elements. Tests were conducted at various bag pressures and deflection rates. For each test, the "zero position" of the Airide component was set to mid-stroke, corresponding to a spring height of 12.5 inches, and held at this position while the internal air pressure in the component was set to the desired value. The tests were conducted under displacement control. Starting from the zero position, the displacement was ramped up 3 inches to a spring height of 15.5 inches, and the displacement was held at this position for 10 seconds to allow for partial relaxation/recovery of the load. The displacement was then ramped down 6 inches to a spring height of 9.5 inches, and again held for 10 seconds. The displacement was then ramped back up 6 inches to a spring height of 15.5 inches and again held.

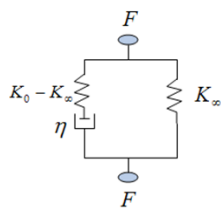**Table D-7. Comparison Metric Evaluation Table for Phenomena #5**

PHENOMENA #5: Tractor Rear "Air-Bag" Suspension (20 psig bag pressure, 6 in/sec)			
Sprauge-Geers Metrics List all the data channels to be compared below. Using RSVVP calculate the M and P metrics comparing the experiment and the simulation. Values less than or equal to 20 are acceptable.	**M**	**P**	**Pass?**
• *Uniaxial Force-Time History*	**1.5**	**1.7**	**Y**
ANOVA Metrics List all the data channels to compare in the rows below. Use RSVVP to calculate the ANOVA metrics and enter the values below. The following criteria must be met: • The mean residual error must be less than or equal to five percent of the peak acceleration ($\bar{e} \leq 0.05 \cdot a_{Peak}$) • The standard deviation of the residuals must be less than or equal to 25 percent of the peak acceleration ($\sigma \leq 0.25 \cdot a_{Peak}$)	**Mean Residual**	**Standard Deviation of Residuals**	**Pass?**
• *Uniaxial Force-Time History*	**0.02**	**0.02**	**Y**

Tractor "Air-Spring" Suspension: *Compression/extension tests at various load rates and bag pressures*

Firestone AirideTM suspension, Part No. 1T15ZR6. The air spring was modeled using discrete spring and damper elements. Tests were conducted at various bag pressures and deflection rates. For each test, the "zero position" of the AirideTM component was set to mid-stroke, corresponding to a spring height of 12.5 inches, and held at this position while the internal air pressure in the component was set to the desired value. The tests were conducted under displacement control. Starting from the zero position, the displacement was ramped up 3 inches to a spring height of 15.5 inches, and the displacement was held at this position for 120 seconds to allow for partial relaxation/recovery of the load. The displacement was then ramped down 6 inches to a spring height of 9.5 inches, and again held for 120 seconds. The displacement was then ramped back up 6 inches to a spring height of 15.5 inches and again held.

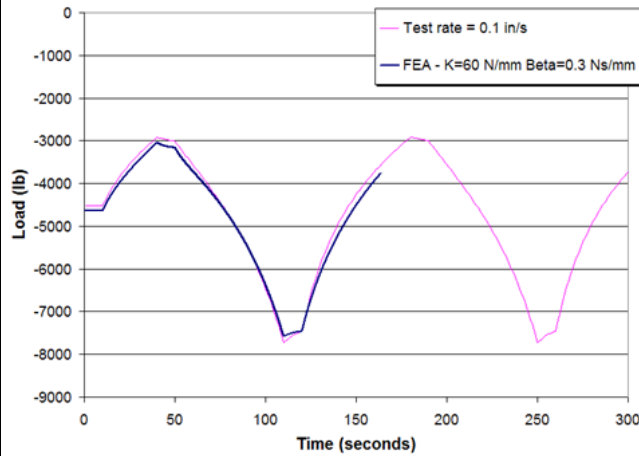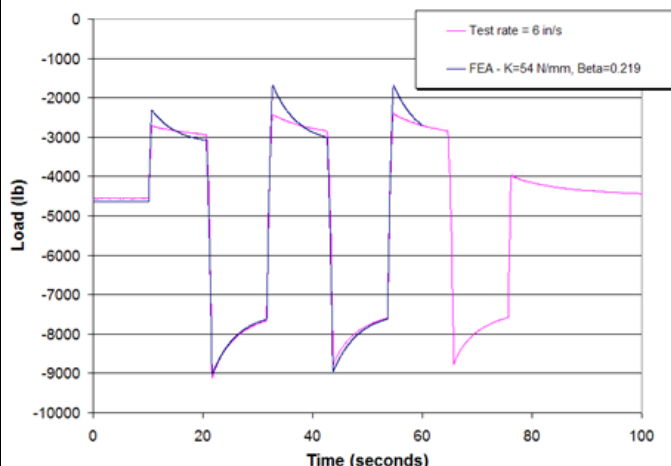**Table D-8. Comparison Metric Evaluation Table for Phenomena #5**

PHENOMENA #5: Tractor Rear "Air-Bag" Suspension (60 psig bag pressure, 0.1 in/sec)			
Sprauge-Geers Metrics List all the data channels to be compared below. Using RSVVP calculate the M and P metrics comparing the experiment and the simulation. Values less than or equal to 20 are acceptable.	**M**	**P**	**Pass?**
• *Uniaxial Force-Time History*	**4.7**	**1.9**	**Y**
ANOVA Metrics List all the data channels to compare in the rows below. Use RSVVP to calculate the ANOVA metrics and enter the values below. The following criteria must be met: • The mean residual error must be less than or equal to five percent of the peak acceleration $(\bar{e} \leq 0.05 \cdot a_{Peak})$ • The standard deviation of the residuals must be less than or equal to 25 percent of the peak acceleration $(\sigma \leq 0.25 \cdot a_{Peak})$	**Mean Residual**	**Standard Deviation of Residuals**	**Pass?**
• *Uniaxial Force-Time History*	**0**	**0.03**	**Y**

Tractor "Air-Spring" Suspension: *Compression/extension tests at various load rates and bag pressures*

Firestone AirideTM suspension, Part No. 1T15ZR6. The air spring was modeled using discrete spring and damper elements. Tests were conducted at various bag pressures and deflection rates. For each test, the "zero position" of the AirideTM component was set to mid-stroke, corresponding to a spring height of 12.5 inches, and held at this position while the internal air pressure in the component was set to the desired value. The tests were conducted under displacement control. Starting from the zero position, the displacement was ramped up 3 inches to a spring height of 15.5 inches, and the displacement was held at this position for 10 seconds to allow for partial relaxation/recovery of the load. The displacement was then ramped down 6 inches to a spring height of 9.5 inches, and again held for 10 seconds. The displacement was then ramped back up 6 inches to a spring height of 15.5 inches and again held.

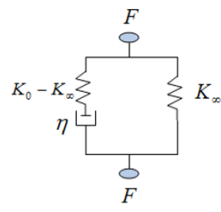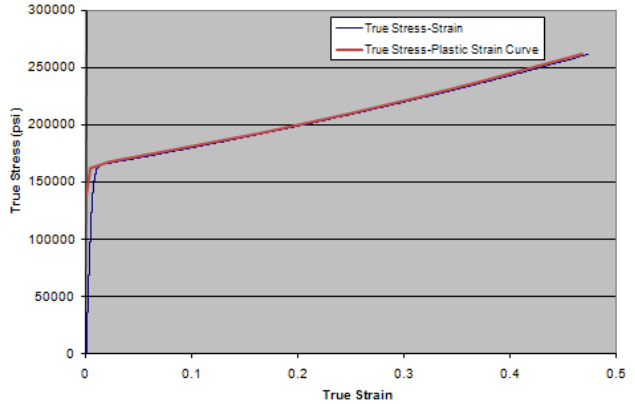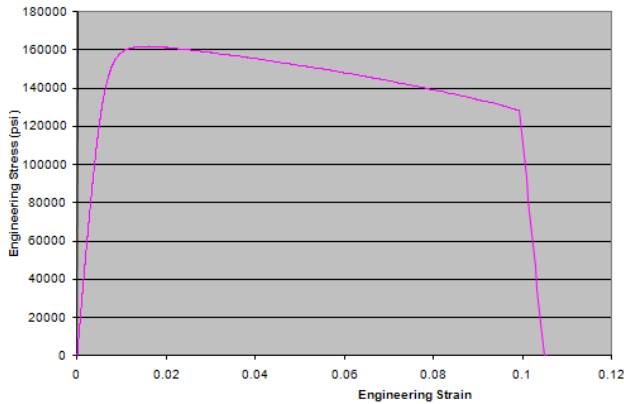**Table D-9. Comparison Metric Evaluation Table for Phenomena #5**

PHENOMENA #5: Tractor Rear "Air-Bag" Suspension (60 psig bag pressure, 6 in/sec)			
Sprauge-Geers Metrics List all the data channels to be compared below. Using RSVVP calculate the M and P metrics comparing the experiment and the simulation. Values less than or equal to 20 are acceptable.	**M**	**P**	**Pass?**
• *Uniaxial Force-Time History*	**2.5**	**2.9**	**Y**

ANOVA Metrics
List all the data channels to compare in the rows below. Use RSVVP to calculate the ANOVA metrics and enter the values below. The following criteria must be met:
   • The mean residual error must be less than or equal to five percent of the peak acceleration ($\bar{e} \leq 0.05 \cdot a_{Peak}$)
   • The standard deviation of the residuals must be less than or equal to 25 percent of the peak acceleration ($\sigma \leq 0.25 \cdot a_{Peak}$)
	Mean Residual	**Standard Deviation of Residuals**	**Pass?**

• *Uniaxial Force-Time History*	**0.02**	**0.04**	**Y**

Tractor "Air-Spring" Suspension: *Compression/extension tests at various load rates and bag pressures*

Firestone AirideTM suspension, Part No. 1T15ZR6. The air spring was modeled using discrete spring and damper elements. Tests were conducted at various bag pressures and deflection rates. For each test, the "zero position" of the AirideTM component was set to mid-stroke, corresponding to a spring height of 12.5 inches, and held at this position while the internal air pressure in the component was set to the desired value. The tests were conducted under displacement control. Starting from the zero position, the displacement was ramped up 3 inches to a spring height of 15.5 inches, and the displacement was held at this position for 10 seconds to allow for partial relaxation/recovery of the load. The displacement was then ramped down 6 inches to a spring height of 9.5 inches, and again held for 10 seconds. The displacement was then ramped back up 6 inches to a spring height of 15.5 inches and again held.

PHENOMENA #6:	Tractor Front Suspension U-Bolt Calibration Tests

Uniaxial Load-to-Failure <u>Calibration</u> Tests

A front suspension u-bolt was cut into a tensile test specimen and a uniaxial tensile test was carried out to failure of the bolt. The data from the test was processed to generate true stress versus true plastic strain data for input to*MAT_24 in LS-Dyna.

Additional Information:
- Yield Strength = 152,009 psi
- Ultimate Strength = 162,933 psi
- A_0 = 0.19737 in^2
- A_f = 0.12285 in^2
- R.A. = 62%
- Elongation = 11%
- Load Rate = 0.01/minute
- Gauge length = 2 in

Table D-11. Comparison Metric Evaluation Table for Phenomena #7

PHENOMENA #7: Trailer Rear "Air-Spring" Suspension (60 psig bag pressure, 6 in/sec)			
Sprauge-Geers Metrics List all the data channels to be compared below. Using RSVVP calculate the M and P metrics comparing the experiment and the simulation. Values less than or equal to 20 are acceptable.	**M**	**P**	**Pass?**
• *Uniaxial Force-Time History*	**0.3**	**0.7**	**Y**
ANOVA Metrics List all the data channels to compare in the rows below. Use RSVVP to calculate the ANOVA metrics and enter the values below. The following criteria must be met: • The mean residual error must be less than or equal to five percent of the peak acceleration ($\bar{e} \leq 0.05 \cdot a_{Peak}$) • The standard deviation of the residuals must be less than or equal to 25 percent of the peak acceleration ($\sigma \leq 0.25 \cdot a_{Peak}$)	**Mean Residual**	**Standard Deviation of Residuals**	**Pass?**
• *Uniaxial Force-Time History*	**0**	**0.009**	**Y**

Trailer "Air-Spring" Suspension: *Compression/extension tests at various load rates and bag pressures*

Firestone AirideTM suspension, Part No. 1T15ZR6. The air spring was modeled using discrete spring and damper elements. Tests were conducted at various bag pressures and deflection rates. For each test, the "zero position" of the AirideTM component was set to mid-stroke, corresponding to a spring height of 12.5 inches, and held at this position while the internal air pressure in the component was set to the desired value. The tests were conducted under displacement control. Starting from the zero position, the displacement was ramped up 3 inches to a spring height of 15.5 inches, and the displacement was held at this position for 120 seconds to allow for partial relaxation/recovery of the load. The displacement was then ramped down 6 inches to a spring height of 9.5 inches, and again held for 120 seconds. The displacement was then ramped back up 6 inches to a spring height of 15.5 inches and again held.
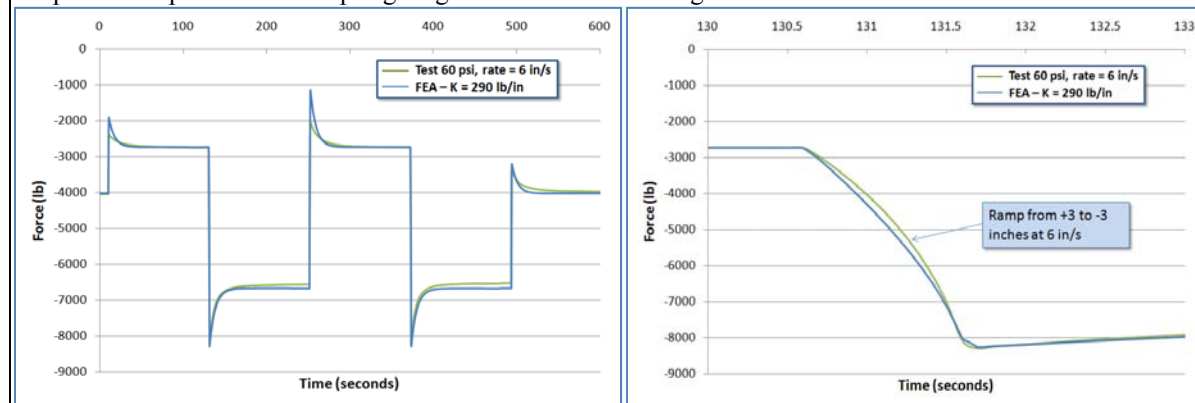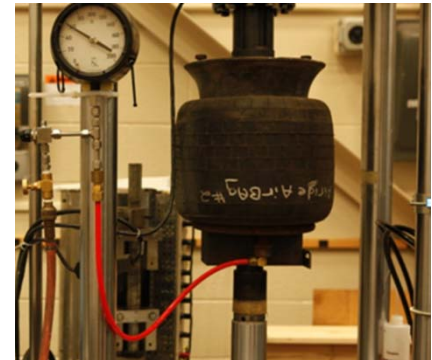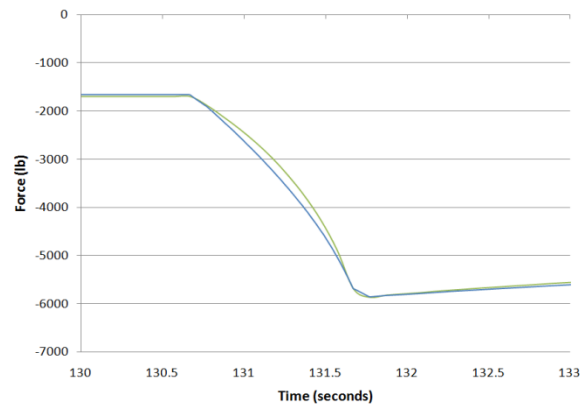
PHENOMENA #7: **Trailer Rear "Air-Spring" Suspension (40 psig bag pressure, 6 in/sec)**			
Sprauge-Geers Metrics List all the data channels to be compared below. Using RSVVP calculate the M and P metrics comparing the experiment and the simulation. Values less than or equal to 20 are acceptable.	**M**	**P**	**Pass?**
• *Uniaxial Force-Time History*	**1**	**1**	**Y**
ANOVA Metrics List all the data channels to compare in the rows below. Use RSVVP to calculate the ANOVA metrics and enter the values below. The following criteria must be met: • The mean residual error must be less than or equal to five percent of the peak acceleration ($\bar{e} \leq 0.05 \cdot a_{Peak}$) • The standard deviation of the residuals must be less than or equal to 25 percent of the peak acceleration ($\sigma \leq 0.25 \cdot a_{Peak}$)	**Mean Residual**	**Standard Deviation of Residuals**	**Pass?**
• *Uniaxial Force-Time History*	**0.006**	**0.011**	**Y**

Trailer "Air-Spring" Suspension: *Compression/extension tests at various load rates and bag pressures*

Firestone AirideTM suspension, Part No. 1T15ZR6. The air spring was modeled using discrete spring and damper elements. Tests were conducted at various bag pressures and deflection rates. For each test, the "zero position" of the AirideTM component was set to mid-stroke, corresponding to a spring height of 12.5 inches, and held at this position while the internal air pressure in the component was set to the desired value. The tests were conducted under displacement control. Starting from the zero position, the displacement was ramped up 3 inches to a spring height of 15.5 inches, and the displacement was held at this position for 120 seconds to allow for partial relaxation/recovery of the load. The displacement was then ramped down 6 inches to a spring height of 9.5 inches, and again held for 120 seconds. The displacement was then ramped back up 6 inches to a spring height of 15.5 inches and again held.
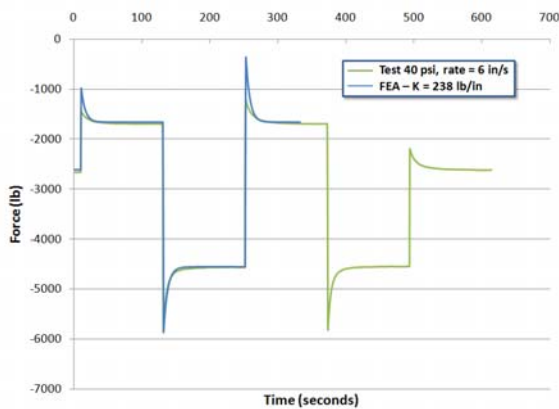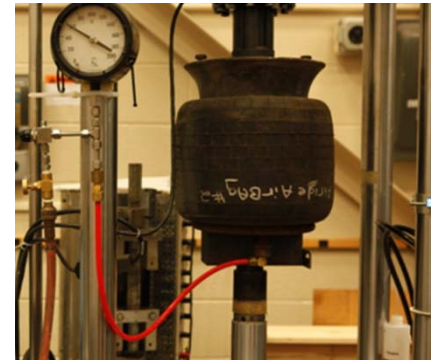
PHENOMENA #7: Trailer Rear "Air-Spring" Suspension (20 psig bag pressure, 6 in/sec)			
Sprauge-Geers Metrics List all the data channels to be compared below. Using RSVVP calculate the M and P metrics comparing the experiment and the simulation. Values less than or equal to 20 are acceptable.	**M**	**P**	**Pass?**
• *Uniaxial Force-Time History*	**0.6**	**0.9**	**Y**
ANOVA Metrics List all the data channels to compare in the rows below. Use RSVVP to calculate the ANOVA metrics and enter the values below. The following criteria must be met: • The mean residual error must be less than or equal to five percent of the peak acceleration ($\bar{e} \leq 0.05 \cdot a_{Peak}$) • The standard deviation of the residuals must be less than or equal to 25 percent of the peak acceleration ($\sigma \leq 0.25 \cdot a_{Peak}$)	**Mean Residual**	**Standard Deviation of Residuals**	**Pass?**
• *Uniaxial Force-Time History*	**0.002**	**0.009**	**Y**

Trailer "Air-Spring" Suspension: *Compression/extension tests at various load rates and bag pressures*

Firestone AirideTM suspension, Part No. 1T15ZR6. The air spring was modeled using discrete spring and damper elements. Tests were conducted at various bag pressures and deflection rates. For each test, the "zero position" of the AirideTM component was set to mid-stroke, corresponding to a spring height of 12.5 inches, and held at this position while the internal air pressure in the component was set to the desired value. The tests were conducted under displacement control. Starting from the zero position, the displacement was ramped up 3 inches to a spring height of 15.5 inches, and the displacement was held at this position for 120 seconds to allow for partial relaxation/recovery of the load. The displacement was then ramped down 6 inches to a spring height of 9.5 inches, and again held for 120 seconds. The displacement was then ramped back up 6 inches to a spring height of 15.5 inches and again held.

Table D-14. Comparison Metric Evaluation Table for Phenomena #8

PHENOMENA #8:	Trailer Kingpin Box Material Calibration Tests

Uniaxial Load-to-Failure <u>Calibration</u> Tests

A tensile test specimen was extracted from the trailer kingpin box and a uniaxial tensile test was carried out to failure. The data from the test was processed to generate true stress versus true plastic strain data for input to*MAT_24 in LS-Dyna.

Additional Information:
- Yield Strength = 73,047 psi
- Ultimate Strength = 76,777 psi
- R.A. = 61%
- Elongation = 27%
- Load Rate = 0.01/minute
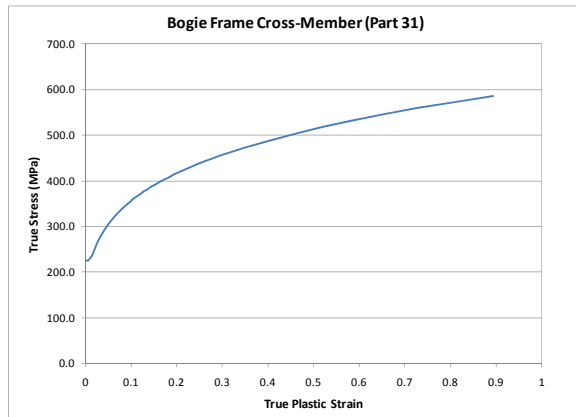- Gauge length = 2 in
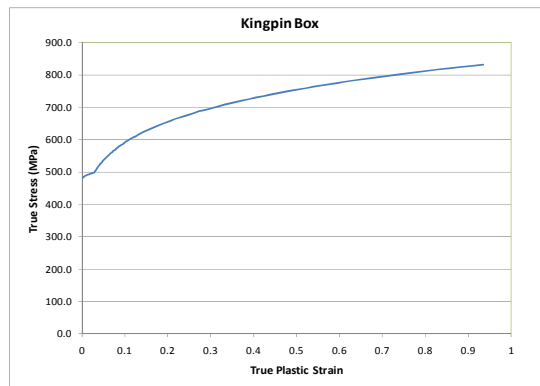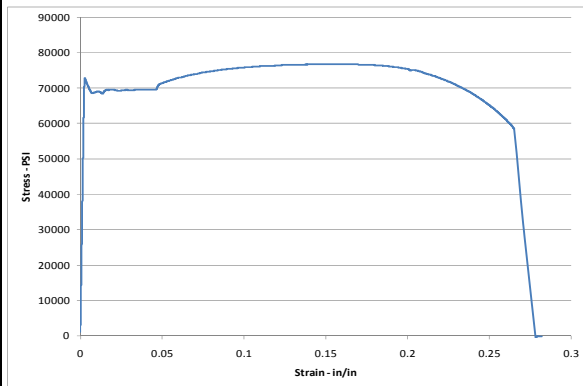
Table D-15. Comparison Metric Evaluation Table for Phenomena #9

PHENOMENA #9:	Trailer Bogie Frame Cross Member Material Calibration Tests

Uniaxial Load-to-Failure <u>Calibration</u> Tests

A tensile test specimen was extracted from the trailer bogie frame cross member and a uniaxial tensile test was carried out to failure. The data from the test was processed to generate true stress versus true plastic strain data for input to*MAT_24 in LS-Dyna.

Additional Information:

- Yield Strength = 34,551 psi
- Ultimate Strength = 49,152 psi
- R.A. = 70%
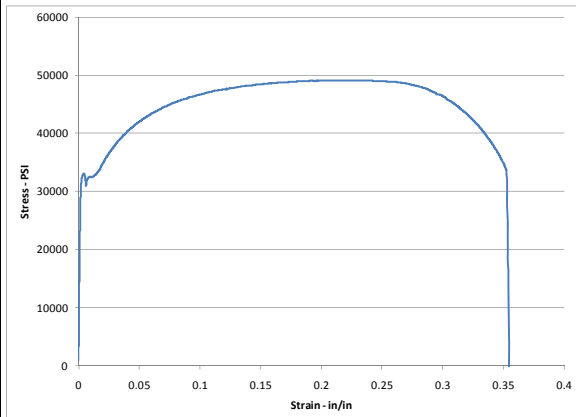- Elongation = 35%
- Load Rate = 0.01/minute
- Gauge length = 2 in

PHENOMENA #10:	Trailer Bogie Main Frame Material Calibration Tests

Uniaxial Load-to-Failure Calibration Tests

A tensile test specimen was extracted from the trailer main frame and a uniaxial tensile test was carried out to failure. The data from the test was processed to generate true stress versus true plastic strain data for input to*MAT_24 in LS-Dyna.

Additional Information:
- Yield Strength = 46,508 psi
- Ultimate Strength = 60,771 psi
- R.A. = 70%
- Elongation = 30%
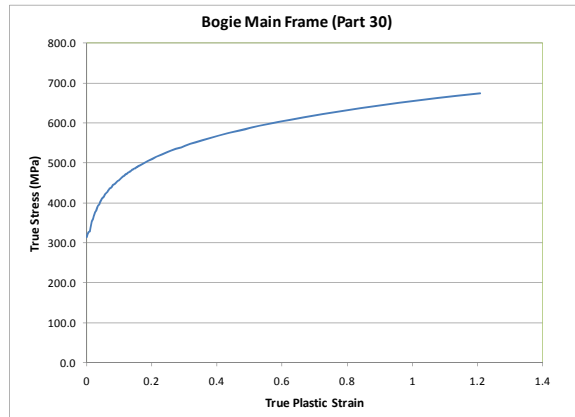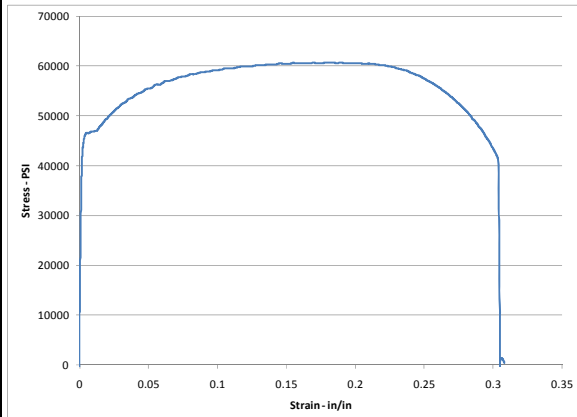- Load Rate = 0.01/minute
- Gauge length = 2 in

Bogie Main Frame (Part 30)

Table D-17. Comparison Metric Evaluation Table for Phenomena #11

PHENOMENA #11:	Trailer Axle Tube Material Calibration Tests

Uniaxial Load-to-Failure <u>Calibration</u> Tests

A tensile test specimen was extracted from the trailer axle tube and a uniaxial tensile test was carried out to failure. The data from the test was processed to generate true stress versus true plastic strain data for input to*MAT_24 in LS-Dyna.

Additional Information:
- Yield Strength = 63,508 psi
- Ultimate Strength = 104,762 psi
- R.A. = 60%
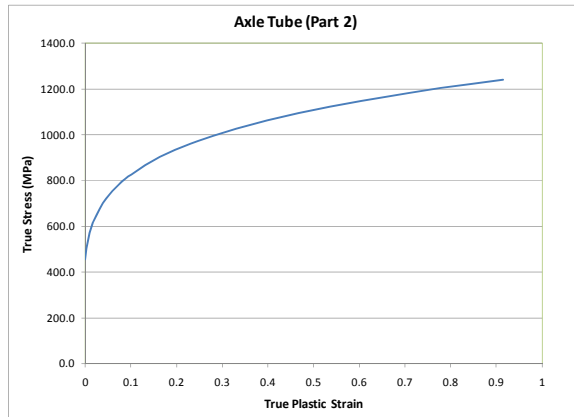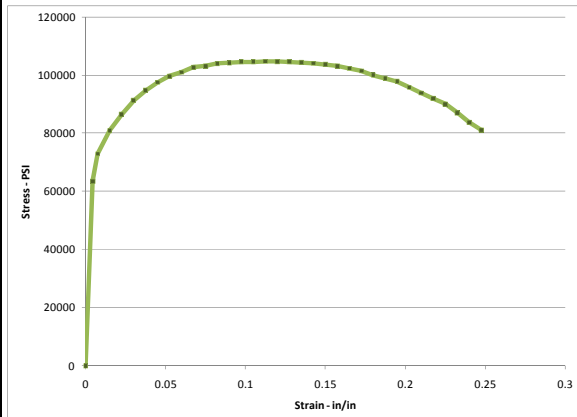- Elongation = 26%
- Load Rate = 0.01/minute
- Gauge length = 2 in

Table D-18. Comparison Metric Evaluation Table for Phenomena #12

PHENOMENA #12:	Trailer Rear Bumper Material Calibration Tests

Uniaxial Load-to-Failure <u>Calibration</u> Tests

A tensile test specimen was extracted from the trailer bumper and a uniaxial tensile test was carried out to failure. The data from the test was processed to generate true stress versus true plastic strain data for input to*MAT_24 in LS-Dyna.

Additional Information:
- Yield Strength = 55,439 psi
- Ultimate Strength = 62,978 psi
- R.A. = 65%
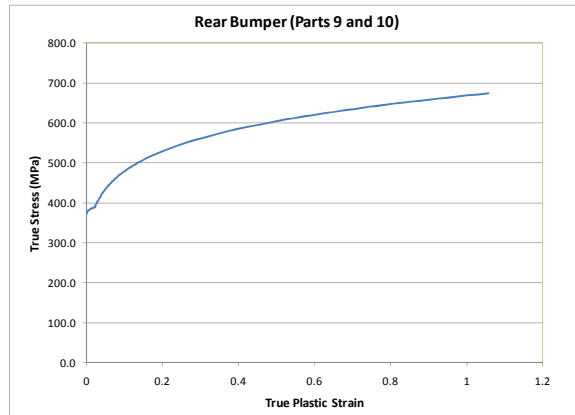- Elongation = 28%
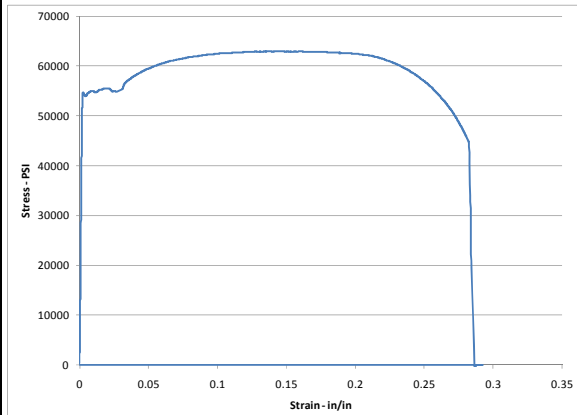- Load Rate = 0.01/minute
- Gauge length = 2 in

PHENOMENA #13:	Trailer Aluminum Upper Rail Material Calibration Tests

Uniaxial Load-to-Failure Calibration Tests

A tensile test specimen was extracted from the trailer upper rail and a uniaxial tensile test was carried out to failure. The data from the test was processed to generate true stress versus true plastic strain data for input to*MAT_24 in LS-Dyna.

Additional Information:
- Yield Strength = 43,712 psi
- Ultimate Strength = 47,334 psi
- R.A. = 33%
- Elongation = 12%
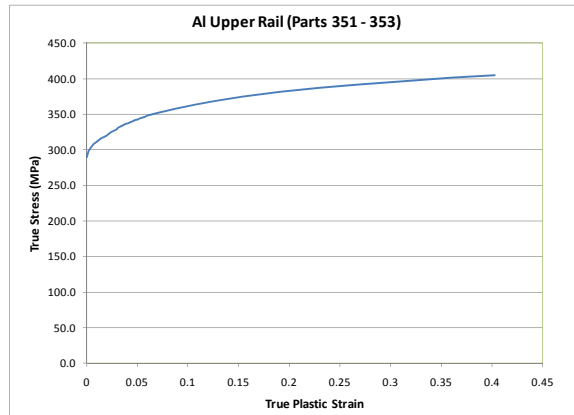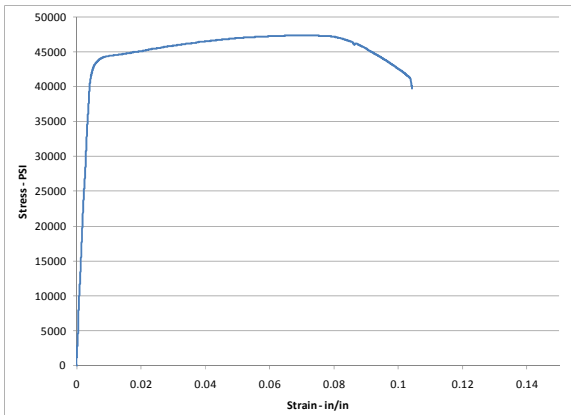- Load Rate = 0.01/minute
- Gauge length = 2 in

PHENOMENA #14:	Trailer Aluminum Lower Rail Material Calibration Tests

Uniaxial Load-to-Failure Calibration Tests

A tensile test specimen was extracted from the trailer lower rail and a uniaxial tensile test was carried out to failure. The data from the test was processed to generate true stress versus true plastic strain data for input to*MAT_24 in LS-Dyna.

Additional Information:

- Yield Strength = 37,900 psi
- Ultimate Strength = 40,856 psi
- R.A. = 23%
- Elongation = 11%
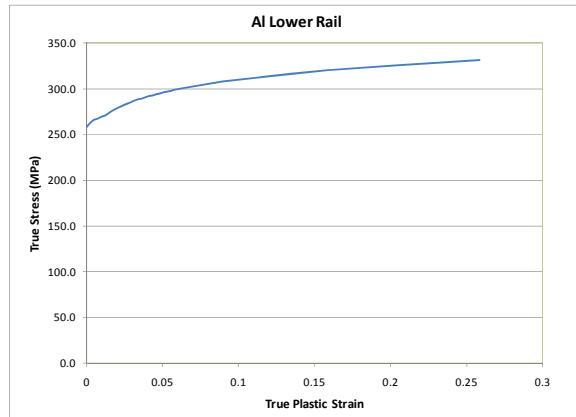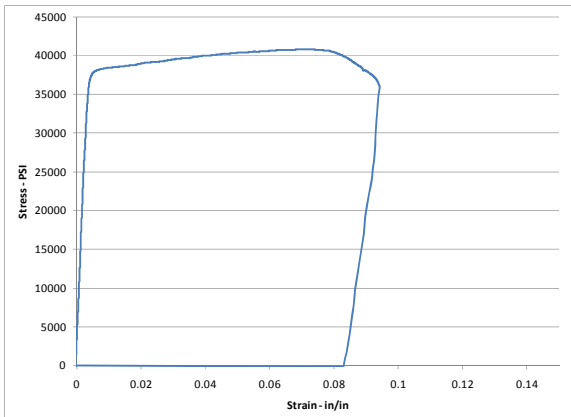- Load Rate = 0.01/minute
- Gauge length = 2 in

PHENOMENA #15:	Trailer Suspension Pivot Support Material Calibration Tests

Uniaxial Load-to-Failure <u>Calibration</u> Tests

A tensile test specimen was extracted from the trailer suspension pivot support and a uniaxial tensile test was carried out to failure. Load vs. deflection data was measured to just beyond yield. The information from the tests was used (e.g., yield and ultimate tensile strength) with information gathered from the literature to determine the most probable material classification of the materials.

Additional Information:
- Yield Strength = 42,260 psi
- Ultimate Strength = 58,072 psi
- R.A. = 66%
- Elongation = 27%
- Load Rate = 0.01/minute
- Gauge length = 1 in
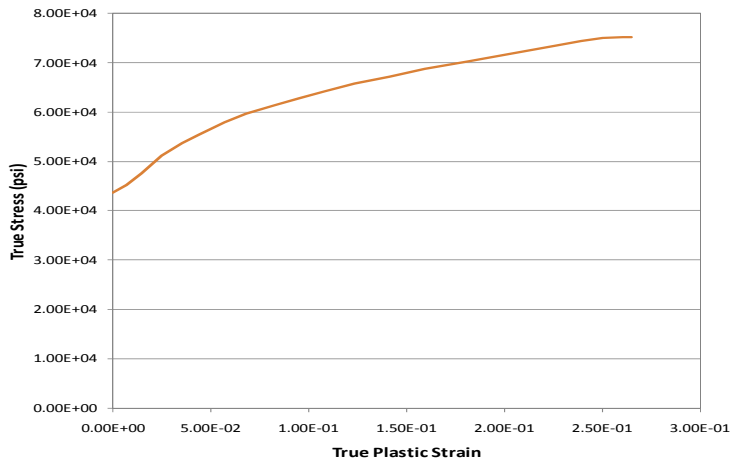
Material Classification: HF 40Y50T

PHENOMENA #16:	Trailer Suspension Pivot Arm Material Calibration Tests

Uniaxial Load-to-Failure <u>Calibration</u> Tests

A tensile test specimen was extracted from the trailer suspension pivot arm and a uniaxial tensile test was carried out to failure. Load vs. deflection data was measured to just beyond yield. The information from the tests was used (e.g., yield and ultimate tensile strength) with information gathered from the literature to determine the most probable material classification of the materials.

Additional Information:
- Yield Strength = 60,000 psi
- Ultimate Strength = 71,429 psi
- R.A. = 70%
- Elongation = 17%
- Load Rate = 0.01/minute
- Gauge length = 1 in
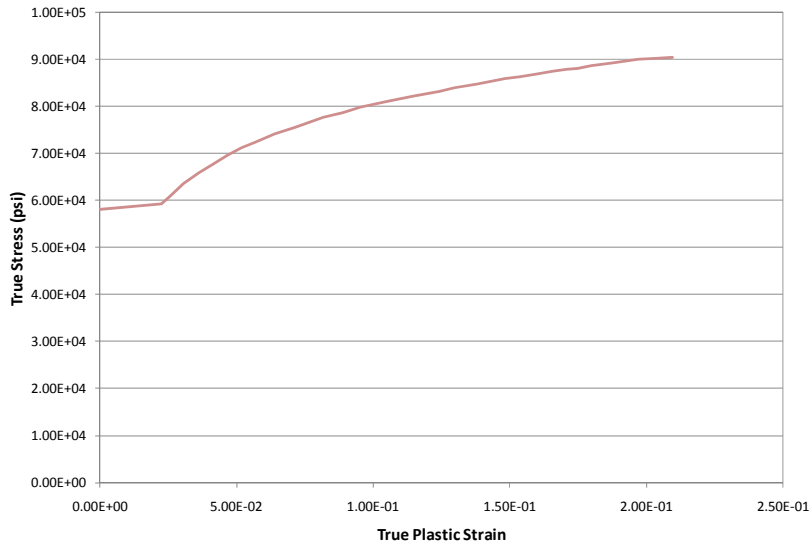
Material Classification: HFY 350

PHENOMENA #17:	Trailer Bogie Slider Rails Material Calibration Tests

Uniaxial Load-to-Failure <u>Calibration</u> Tests

A tensile test specimen was extracted from the trailer bogie slider rail and a uniaxial tensile test was carried out to failure. Load vs. deflection data was measured to just beyond yield. The information from the tests was used (e.g., yield and ultimate tensile strength) with information gathered from the literature to determine the most probable material classification of the materials.

Additional Information:

- Yield Strength = 64,400 psi
- Ultimate Strength = 69,235 psi
- R.A. = 66%
- Elongation = 18%
- Load Rate = 0.01/minute
- Gauge length = 1 in

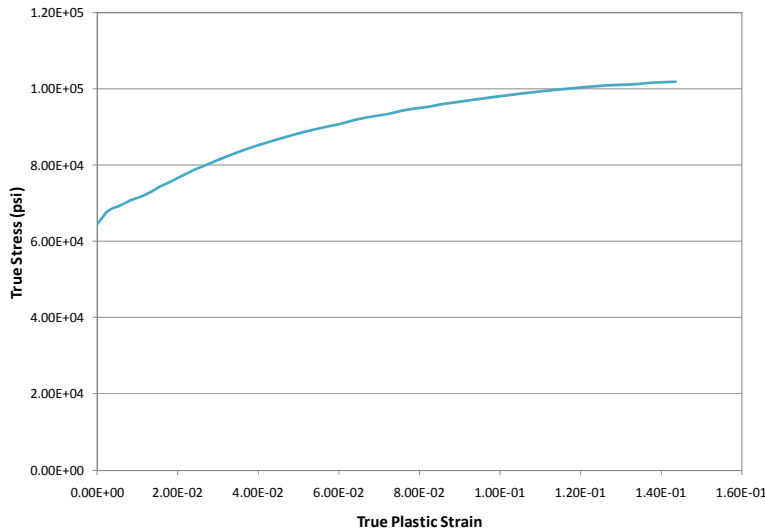Material Classification: HDGA-HFT 590

PHENOMENA #18:	Trailer Lateral I-Beam Material Calibration Tests

Uniaxial Load-to-Failure Calibration Tests

A tensile test specimen was extracted from the trailer lateral I-beam and a uniaxial tensile test was carried out to failure. Load vs. deflection data was measured to just beyond yield. The information from the tests was used (e.g., yield and ultimate tensile strength) with information gathered from the literature to determine the most probable material classification of the materials.

Additional Information:
- Yield Strength = 68,000 psi
- Ultimate Strength = 90,016 psi
- R.A. = 50%
- Elongation = Not Recorded
- Load Rate = 0.01/minute
- Gauge length = 1 in

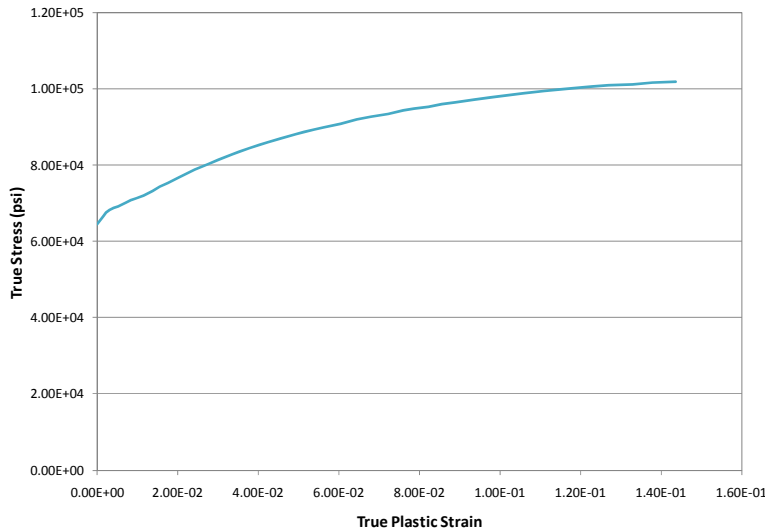Material Classification: HDGA-HFT 590

Table D-25. Phenomenon Importance Ranking Table for Tractor-Semitrailer Model

No.	Phenomenon	Validated? Calibrated?
1.	Tractor Front Leaf-Spring Suspension	Validated
2.	Tractor Suspension Displacement Limiter	Validated
3.	Tractor Rear Shock Absorbers (*Calibration Tests*)	Calibrated
4.	Tractor Front Shock Absorbers (*Calibration Tests*)	Calibrated
5.	Tractor Rear "Air-Spring" Suspension	Validated
6.	Tractor Front Suspension U-Bolts (Calibration Test)	Calibrated
7.	Trailer "Air-Spring" Suspension	Validated
8.	Trailer Kingpin Box Material *(Calibration Tests)*	Calibrated
9.	Trailer Bogie Frame Cross Member Material *(Calibration Tests)*	Calibrated
10.	*Trailer Bogie Main Frame Material (Calibration Tests)*	Calibrated
11.	*Trailer Axle Tube Material (Calibration Tests)*	Calibrated
12.	*Trailer Rear Bumper Material (Calibration Tests)*	Calibrated
13.	*Trailer Aluminum Upper Rail Material (Calibration Tests)*	Calibrated
14.	*Trailer Aluminum Lower rail Material (Calibration Tests)*	Calibrated
15.	*Trailer suspension Pivot Support Material (Calibration Tests)*	Calibrated
16.	*Trailer Suspension Pivot Arm Material (Calibration Tests)*	Calibrated
17.	*Trailer Bogie Slider Rail Material (Calibration Tests)*	Calibrated
18.	*Trailer Lateral I-Beam Material (Calibration Tests)*	Calibrated

Appendix E – References

References

1. Plaxico, C., Kennedy, J., Simunovic, S. and Zisi, N., Enhanced Finite Element Analysis Crash Model of Tractor-Trailers (Phase A), National Transportation Research Center, Inc., Knoxville, TN, 2008.

2. Plaxico, C., Kennedy, J., Simunovic, S. and Zisi, N., Enhanced Finite Element Analysis Crash Model of Tractor-Trailers (Phase B), National Transportation Research Center, Inc., Knoxville, TN, 2008.

3. Ross, H.E., Sicking, D.L., and Perrara, H.S., "Recommended Procedures for the Safety Performance Evaluation of Highway Appurtenances," *National Cooperative Highway Research Program Report No. 350*, Transportation Research Board, Washington, D.C., 1993.

4. Ray, M.H., Mongiardini, M., Atahan, A.O., Plaxico, C.A., and Anghileri, M., "Recommended Procedures for the Verification and Validation of Computer Simulations used for Roadside Safety Applications," Final Report (Draft), Project No. 22-24, National Cooperative Highway Research Program, March 2010.

5. Rosenbaugh, S.K, Sicking, D.L., and Faller, R.K., "Development of a TL-5 Vertical Faced Concrete Median Barrier Incorporating Head Ejection Criteria," Test Report No. TRP-030194-07, Midwest Roadside Safety Facility, University of Nebraska-Lincoln, 12/10/2007. [Test No. TL5CMB-2]

6. Buth, C.E., Hirsch, T.J., and Menges, W.L., "Testing of New Bridge Rail and Transition Designs," Report No. FHWA-RD-93-067, Vol. X Appendix I: 42-in (1.07-m) Concrete Parapet Bridge Railing, Turner-Fairbank Highway Research Center, Federal Highway Administration, McLean, Virginia, (prepared by Texas Transportation Institute, College Station, Texas), 1993. [Test No. 7069-13]

7. LS-Dyna Keyword User's Manual, Version 971, Volume 1, Livermore Software Technology Corporation (LSTC), Livermore, California, May 2007.

8. http://civil-ws2.wpi.edu/Documents/Roadsafe/NCHRP22-24/RevisedInterimReport.pdf

9. Geers, T.L., "An Objective Error Measure for the Comparison of Calculated and Measured Transient Response Histories," The Shock and Vibrations Bulletin, The Shock and Vibration Information Center, Navl Research Laboratory, Washington, D.C., Bulletin 54, Part 2, pp 99:107, June 1984.

10. Sprague, M.A. and Geers, T.L., Spectral elements and field separation for an acoustic fluid subject to cavitations," Journal of Computational Physics, pp. 184:149, Volume 162, 2003.

11. Ray, M.H., "Repeatability of Full-Scale Crash Tests and a Criteria for Validating Finite Element Simulations," Transportation Research Record, Vol. 1528, pp. 155-160, 1996.

12. Road Barrier Upgrade of Standards (ROBUST), "Deliverable 4.1.1 – Full scale test results – An analysis," ROBUST PROJECT, GRD-2002-70021.

13. Ray, M.H., Anghileri, M., Mongiardini, M., "Comparison of Validation Metrics Using Full-Scale Automobile Crash Tests," 8th World Congress on Computational Mechanics, Venice, Italy, June 30 – July 5, 2008.

14. European Committee of Standardization, "European Standard EN 1317-1 and EN 1317-2: Road Restraint Systems," CEN, 1998.

15. *Guide Specifications For Bridge railings, American association of State Highway and Transportation Officials (AASHTO), Washington, DC, 1989.*

16. Ross, H.E., Sicking, D.L., and Perrara, H.S., "Recommended Procedures for the Safety Performance Evaluation of Highway Appurtenances," *National Cooperative Highway Research Program Report No. 350*, Transportation Research Board, Washington, D.C., 1993.

17. Orengo, F., Plaxico, C.A., and Ray, M.H., "Modeling Tire Blow-Out in Roadside Hardware Simulations Using LS-DYNA," In Proceeding of *International Mechanical Engineering Congress & Exposition*, American Society of Mechanical Engineers, Washington, D.C., November 2003.